Catalytic Steam Reforming of Toluene: Study of Reaction Parameters, Reforming Atmosphere and Catalyst Deactivation

Hualun Zhu

Department of Chemical Engineering

Imperial College London

Thesis Submitted for degree of Doctor of Philosophy (PhD) of

Imperial College London

May 2021

Abstract

Lignocellulosic biomass is widely recognized as an effective energy carrier capable of fulfilling the growing demand of clean and everlasting energy source for the sustainable development of the world. Biomass gasification is one of the most promising routes for conversion of biomass into gaseous fuel with tar issue. Among different tar removal methods, catalytic steam reforming is widely considered as one of the most promising and effective techniques for tar elimination in gasification. The main objectives of this work are to obtain a good understanding of the influence of main reforming parameters, reforming atmosphere and catalyst stability of catalytic toluene steam reforming.

A laboratory scale continuous fixed-bed reactor has been used in this project to study the reforming parameters including reforming temperature, steam to carbon (S/C) mole ratio, residence time, and simulated syngas atmosphere (CO, H_2, CO_2, CH_4). Toluene was selected as a tar model compound due to its high content in tar, and it represents a stable aromatic structure. Biomass ash was introduced to the Ni/Al_2O_3 catalytic bed to improve its resistance to deactivation.

The main findings include: (1) 800 °C, gas hourly space velocity (GHSV) 61200 h^{-1} and S/C ratio 3 provide favourable operating conditions for steam reforming of toluene in order to get high toluene conversion (~92%) and hydrogen yield; (2) H_2, even a small amount of CH_4 present in the syngas could deactivate Ni/Al_2O_3 over time by increasing coke deposition; (3) H_2, CO and CO_2 content in the syngas have a strong influence on the selectivity of CO/CO_2. (4) The introduction of biomass ash improved the stability and coke resistance of Ni/Al_2O_3 by acting as a mixture and a guard layer, two-layer biomass ash and Ni/Al_2O_3 catalytic system shows good carbon conversion (~90%) in different atmospheres in 5 hours.

Acknowledgement

First and foremost I am extremely grateful to my supervisor, Dr. Marcos Millán-Agorio, who gave me the opportunity to pursue this PhD. Your immense knowledge, continuous support and patience were invaluable throughout my project, your invaluable advice and plentiful experience have encouraged me in all the time of my academic research and daily life, I am privileged to have been your student.

I would like to express my gratitude to Dr. Laura Pastor-Pérez, you are remarkably amazing to work with. Thank you for helping me with my experiments and sharing your views in support of my project.

I would also like to thank my mentor Dr. Miao Guo for your valuable advice and guidance in the first year of my PhD.

I also thank my colleagues and friends in our research group whom together we have worked in the same labs, motivated each other and helped one another, Dr. Nigel Paterson, Dr. Jose Bermudez Menendez, Dr. Pedro Arcelus Arrillaga, Dr. Jie Yu, Dr. Ziyin Chen, Dr. Xiangyi Long, Dr. Anthony Odongo, Dr. Aderlanio da Silva Cardoso, Dr. Kagiso Bikane, Mr. Arifa Sembiring, Mr. John Ball, Mr. Xudong Yuan, you guys are amazing.

My sincere thanks also go to Ms. Shelagh Markey, Ms. Susi Underwood, Ms. Sarah Payne, Ms Patricia Carry, Mr. Pim Amrit, Dr. Severine Toson, Mr. Ben Kistnah, Mr. Keith Walker, and Mr. James Britz for your sustained support in my PhD career.

I would particularly like to thank my wife, Dr. Yeshui Zhang for all the unconditional support in the very intense academic years, and for providing guidance and a sounding board when required.

Finally, I would like to express my special thanks to my parents, Dr. Jinling Zhu and Ms. Lu Yu, my grandpa Prof. Zhuotang Zhu, my grandma Ms. Changzhi Li. Without their tremendous understanding and encouragement in the past few years, it would be impossible for me to complete my study.

Thank you all for this incredible journey.

Declaration of Originality

I certify that all the work contained in this thesis is my own and all else is appropriately referenced.

Hualun Zhu

Copyright Declaration

Contents

List of Figures

List of Tables

Abbreviations & Nomenclature

Brunauer–Emmett–Teller	BET
Concentration	Conc.
Dimethyl ether	DME
Gas Chromatography-Mass Spectrometry	GC-MS
Gas Hourly Space Velocity	GHSV
Infrared gas analysis	IRGA
Inside diameter	I.D
Methyl tert-butyl ether	MTBE
Multigas Analyser	MGA
Gibbs Reactor	RGIBBS
Gas production in moles per mole toluene	mol $mol_{toluene}^{-1}$
Steam to Carbon in methane and toluene	S/C_{total}
Steam to Carbon	S/C
Standard Error	SE
Thermo-gravimetric Analysis	TGA
Water gas shift	WGS
Weight Hourly Space Velocity	WHSV

X-ray fluorescence	XRF

1. Introduction

Recently, global energy demand is increasing significantly due to population and economic growth, especially in emerging market economies (Studies—Energy 2011). The utilisation of fossil fuels has caused unignorable global warming and air pollution problem by emitting of greenhouse gas, toxic gas, and particulates. The need for world energy consumption to become more sustainable through the threat of global warming and resource depletion is prominent (Foster, Azimov et al. 2021). Abundant and renewable alternative energy resources, such as wind, solar, tide and biomass are stated to be the solution to the growing energy challenges and attracting globe research interests (Asif and Muneer 2007). Figure 1.1 shows the world primary energy consumption by energy source, it can be seen that renewable energy is expected to increase from ~15% to 28% and become the highest primary energy source by 2050. Renewable energy is also proved to be the energy source most resilient to Covid-19 lockdown measures worldwide (Mastropietro, Rodilla et al. 2020).

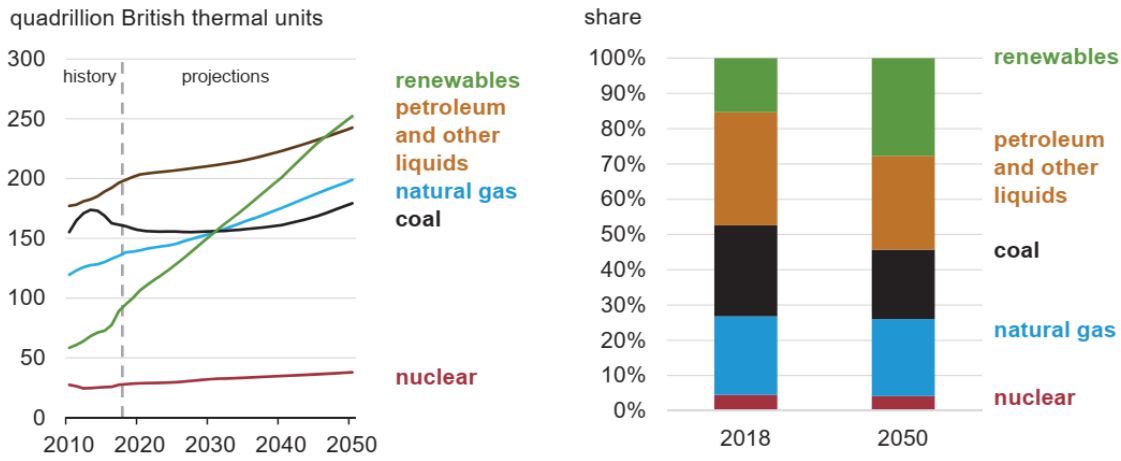

Figure 1.1 World primary energy consumption by energy source. Reproduced from Sieminski (2014).

Biomass is considered as one of the most promising renewable energy sources as energy conversion of burning biomass is a carbon neutral process, and biogenic CO_2 emission could be further effectively reduced by increasing the energy conversion efficiency. It also presents some advantages over other renewable sources. The use of solar energy is limited to the day time; the use of geothermal energy has higher average emissions and may let toxic chemicals under the earth erupt to the atmosphere; the use of wind energy needs strong and stable wind, and also causes noise pollution (Li, Bian et al. 2015, Wang and Wang 2015, Guan, Kaewpanha et al. 2016). Biomass can consistently provide energy and fuels while many other renewable energies should be converted into and stored as the form of electricity (Göransson, Söderlind et al. 2011).

1.1 Biomass resource

The definition of biomass is any organic materials derived from plants or animals. It could be divided to virgin biomass and biomass wastes. Virgin biomass includes terrestrial biomass (grasses, trees, shrubs, cultivated crops, energy plant, etc.) and aquatic biomass (algae, seaweed, aquatic plant, etc.). biomass wastes include forest residues (forest leaves and bark, timber form forest thinning), agricultural solid waste (crop residues, livestock and manures), municipal combustible waste (daily-life trash, market wastes, yard wastes, sewage sludge) and industry wastes (black liquor, demolition wood, waste food, oil and fat).

1.2 Hydrogen

H_2 is considered as a clean energy fuel that has potential to reduce the consumption of fossil fuels to meet sustainable development. Currently, the process to produce hydrogen is extremely expensive, and the storage issue also limits the development of hydrogen energy. There is around 5×10^{11} Nm^3 of hydrogen produced in the world every year, but 96% is produced from fossil fuels. Most is used in processing oil in refineries and producing chemicals (ammonia, methanol), and the demand for hydrogen is also expected to increase (Levin and Chahine 2010). The current hydrogen production methods include methane steam reforming, oil reforming, coal gasification and electrolysis and biomass gasification (Balta, Dincer et al. 2009). Hydrogen production by methane steam reforming used to use natural gas, but there is increasing interest in steam reforming of methane derived from landfill; hydrogen production from electrolysis is of high quality and emission free, but lifecycle emissions are a direct function of the source of the electricity used in the process; biomass gasification utilize renewable feedstocks, but it also generate CO, CO_2, CH_4, and liquid phase co-products (Levin and Chahine 2010).

1.3 Energy from biomass

Biomass as a renewable resource that can be converted into heat, solid, liquid and gaseous fuel by direct combustion, physical conversion, biochemical conversion and thermochemical conversion which are illustrated in Figure 1.2. The aerobic biochemical conversion and anaerobic routes could convert biomass into liquid fuels such as ethanol, acetone and butanol, or the gaseous products including syngas (H_2 and CO) and CH_4 (Pereira, da Silva et al. 2012).

The anaerobic fermentation and thermochemical conversion include of torrefaction, direct liquefaction, pyrolysis and gasification. However, the biochemical conversion is limited to the biomass resources with a high content of starch or sugar, the thermochemical conversion could provide higher conversion rate.

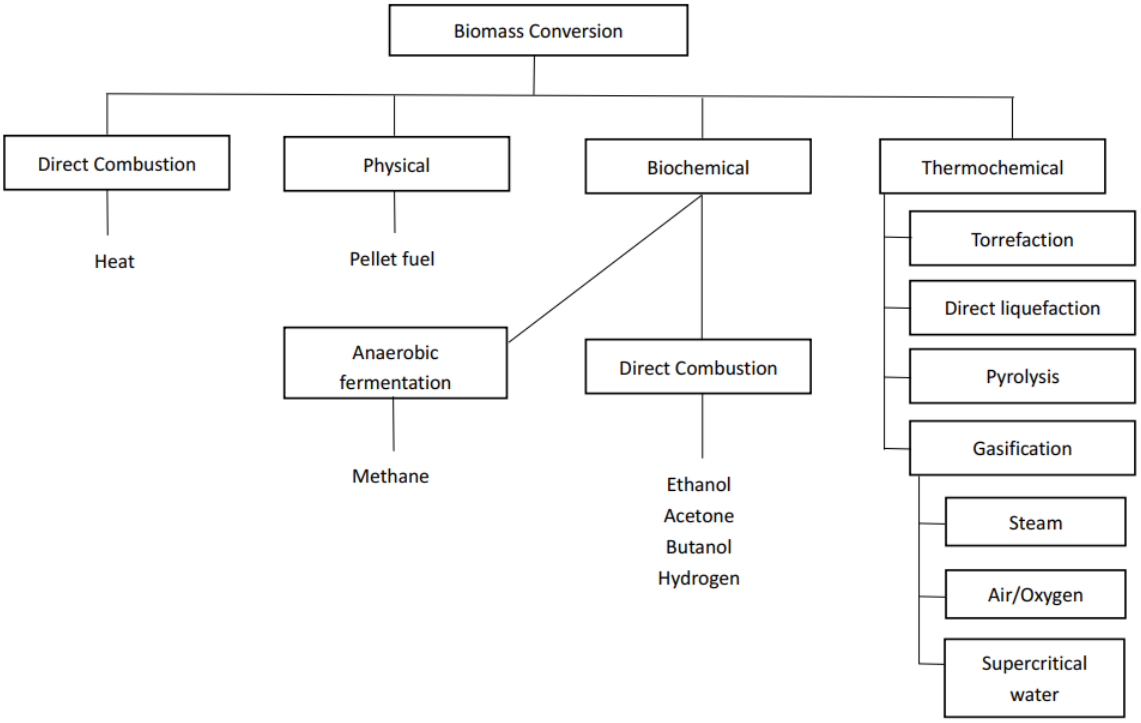

Figure 1.2 Four main routes of biomass conversion to energy. Reproduced from Kirkels and Verbong (2011).

Gasification is one of the promising thermochemical conversion methods to convert biomass into syngas, which is a key intermediate in the chemical industry. It is used in a number of highly selective production of many commercially important chemicals and fuels, such as dimethyl ether (DME), methanol, methyl tert-butyl ether (MTBE), methane and ammonia (Inayat, Sulaiman et al. 2019). It is also used as a source of pure hydrogen and CO, or adopted for heating and power generation purposes in fuel cell, gas turbine or engine. The biomass can also be converted into liquid fuels (Levy, Sanderson

et al. 1981). Biomass gasification requires the presence of gasifying agent includes air, steam, O_2, CO_2 or a mixture at temperature above 700 °C. The products of biomass gasification includes of H_2, CO, CO_2, CH_4, H_2O, solid carbon, ashes and tars (Świerczyński, Libs et al. 2007, Ruiz, Juárez et al. 2013). Biomass gasification process usually undergoes 4 steps, which include drying and heating, pyrolysis, oxidation or partial combustion, reduction or gasification.

Biomass consists of cellulose and hemicellulose, lignin and minerals, all these components have a significantly influence on the product compositions. Aquatic biomass could obtain a higher conversion to gas than terrestrial biomass due to the different chemical compositions and mineral contents (Guan, Kaewpanha et al. 2016). It is concluded that relatively higher ash content and residual alkaline metals in char from aquatic biomass could promote pyrolysis and char gasification. Researchers compared three types of biomass in steam atmospheric gasification in a fixed-bed reactor and suggested that brown seaweed obtained higher gas production yields and H_2 production than other two types of terrestrial biomass since the brown seaweed contains much higher ash content and larger amount of alkali and alkaline earth species (Kaewpanha, Guan et al. 2014). It is also concluded that the carbon conversion to gas and the yields of CO, H_2 and CH_4 were very much affected by the characteristics of the type of biomass (Asadullah, Miyazawa et al. 2004).

Operating conditions also have a great effect on the gaseous composition and carbon conversion. Gasification temperature is the dominant parameter which influences both the amount and compositions of products (Guan, Kaewpanha et al. 2016). Higher gasification temperature can increase hydrogen and CO yield but with small amounts of methane and other heavy hydrocarbons due to the endothermic steam gasification reactions and Boudouard reaction. Moreover, higher temperature can increase the efficiency to convert tar into

lighter gaseous products.

The gasifying agent is another important factor that affects the quantity and quality of the products. Air, O_2, steam, CO_2 or their mixtures are the most used gasifying agents in biomass gasification process. The choice of the agents depends on the target product gas composition/concentration and energy consumption (Shen, Zhao et al. 2014). The most used gasifying agent is air because of its zero cost, but the product gas has a relatively low heating value due to the high content of N_2 in air. The heating value could be improved by changing into O_2 as gasifying agent, while the cost would also increase much more. The introduction of steam to the gasification process could increase the heating value of product gas because it would increase H_2 production, and the product gas could be used in fuel cells and hydrogen engines. Steam gasification of biomass has attracted more attentions in recent years.

There are still several main problems and technical challenges in biomass gasification: the biomass feedstock must be dried before gasification; the cost of equipment to purify and clean the product gas is high; and by-product tar. Tar formation in the biomass gasification process could condense and subsequently block the downstream of the reaction system. The tar could be formed into the type of tar aerosol or polymerized into more complex structures which are harmful to health and correspondingly increase the cost of the downstream equipment maintenance for example of engines or turbines. Therefore, tars should be removed from the effluent stream of biomass gasification (Devi, Ptasinski et al. 2003).

Current tar removal techniques include separation by physical process such as ceramic candle filter or wet scrubber, or thermochemical conversion methods using high temperature thermal or catalytic cracking to convert tar into syngas (Anis and Zainal 2011). Physical separation methods would cause secondary

pollution because the waste stream of tar or oil still needs treatment. On the contrary, thermal cracking has received an increasing interest because tar can be converted into useful gas products and effectively increase the calorific value of the produced gas from gasification (Noichi, Uddin et al. 2010).

Thermal cracking without catalysts operates at high temperature (> 1000 °C) to decompose the tars into smaller non-condensable molecules. The high temperature comes with high energy consumption and makes this process less promising (Devi, Ptasinski et al. 2003). By contrast, catalytic cracking of tars can be carried out at relatively lower temperatures converting tars into syngas in a more efficient manner and is being widely investigated as a more principal method for tar removal (Park, Park et al. 2010)

1.4 Aims and objectives

In this project, a tar steam reforming system was built and modified. It is a fixed-bed reactor which could be applied to hot gas clean up and fuel upgrading to reduce or eliminate tar in a syngas stream and improve the syngas yield. A major emphasis of this project is to study a range of suitable main parameters, and the influence of gasification gas atmosphere on catalytic steam reforming of toluene as a biomass gasification tar model compound. A series of experiments and analysis will be done to complete following objectives:

(1) Assess the effects of different operating conditions on catalytic steam reforming of toluene, which include developing a thermodynamic equilibrium model, conducting experimental tests to explore the effect of reforming temperature, steam to carbon (S/C) ratio and residence time on toluene conversion and gaseous products.

(2) Understand the effect of different components (CO, H_2, CH_4, CO_2) in gasification gas atmosphere during catalytic steam reforming process in terms of carbon conversion, catalyst deactivation and coke deposition on Ni/Al_2O_3 catalyst

(3) Improving the stability, coke resistance of the standard Ni/Al_2O_3 catalyst; test and evaluate the catalytic performance in the steam reforming of toluene; design methods or find optimum catalyst performance in complex gasification gas atmosphere.

1.5 Outline of the thesis

This thesis is divided into seven chapters.

Chapter 2 provides a discussion on literature focusing on catalytic steam reforming of biomass tar and tar model compounds and relevant developments in this field. The rationale for the project objectives is introduced in this chapter.

Chapter 3 provides the experimental setup and details including the materials, the fixed bed reactor, the experimental procedures, analytical methods and sources of errors, uncertainty and accuracy.

Chapter 4 discusses the experimental results from toluene steam reforming under different operating conditions (temperature, S/C ratio, residence time) using a typical Ni/Al_2O_3 catalyst.

Chapter 5 presents the experimental results of toluene steam reforming under varying gasification gas atmospheres (N_2, CO, CO_2, CH_4, H_2) and compare the influence on gas composition/concentration and coke deposition/deactivation on Ni/Al_2O_3 catalyst.

Chapter 6 describes the study of toluene steam reforming using different catalysts and how to improve classic Ni/Al_2O_3 catalyst under complex gas atmosphere.

Chapter 7 summarises the whole research project, presents the main conclusions and gives recommendations for future work.

2 Literature Review

2.1 Tar formation and properties

As discussed in Chapter 1, pyrolysis is defined as a thermochemical deposition process, which produces tar, gas and char from biomass in the absence of oxygen. Lignocellulosic biomass is an ideal feedstock for pyrolysis, which consists of cellulose, hemicellulose and lignin. All the components can be thermally degraded at the temperature between 300 and 500 °C to produce bio-tar, syngas and biochar (Li and Suzuki 2009). Gasification is recognized as a thermochemical process to produce syngas (CO and H_2) from carbonaceous materials, with a considerable amount of oxygen and/or steam. The gasification temperature is higher than 700 °C and the tar yield of gasification is normally lower than the pyrolysis process. Pyrolysis is the precursor mechanism of the gasification of biomass and tar production (Dufour, Masson et al. 2011).

2.1.1 Tar formation

Tar is one of the main byproducts of the pyrolysis and gasification of biomass. The pyrolysis of biomass at a low temperature (300-400 °C) produces oxygenated hydrocarbons, and the oxygenated hydrocarbons can be converted to light hydrocarbons, olefins and aromatics, then further converted to higher hydrocarbons and larger aromatic hydrocarbons at higher temperatures (Bennadji, Smith et al. 2013). Figure 2.1 shows the entire conversion process of oxygenated hydrocarbons in relation to temperature changes. The results indicate that the increase in temperature could convert the organic compounds into more stable components. It can be concluded that reaction temperature

plays an important role in tar distribution.

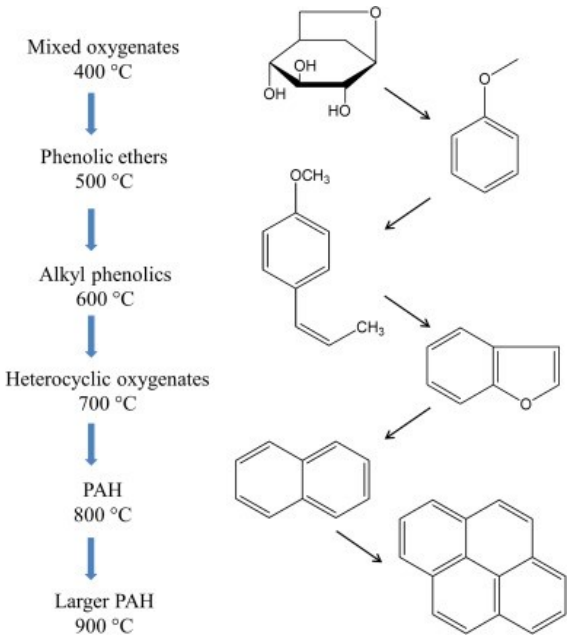

Figure 2.1 Conversion process of oxygenated hydrocarbons in relation to temperature. Reproduced from Guan, Kaewpanha et al. (2016).

There have been various methods to classify tar. Based on the temperature and structure, it can be divided into 3 parts: primary, secondary and tertiary tars. Primary tars are normally produced at the temperature of 300 to 700 °C, which are light oxygenated hydrocarbons including furfural, hydroxyacetaldehyde and levoglucosan. Secondary tars are phenolic and olefin compounds like phenol and xylene, produced at around 700 to 850 °C. Tertiary tars are aromatic compounds such as benzene, naphthalene and toluene which can be formed at temperatures above 850 °C (Guan, Kaewpanha et al. 2016).

2.1.2 Tar properties

The composition of tar is complex. It can consist of over 100 different compounds. There are many factors that influence the composition and concentration of tar produced in biomass gasification, such as feedstock

(composition), gasifier type and design, gasifying agent, and operating conditions including temperature, pressure and residence time. Benzene, toluene and naphthalene are reported to be the most abundant compounds in the tar produced from biomass gasification at high temperatures (> 800 °C). Figure 2.2 shows the typical biomass tar composition from gasification.

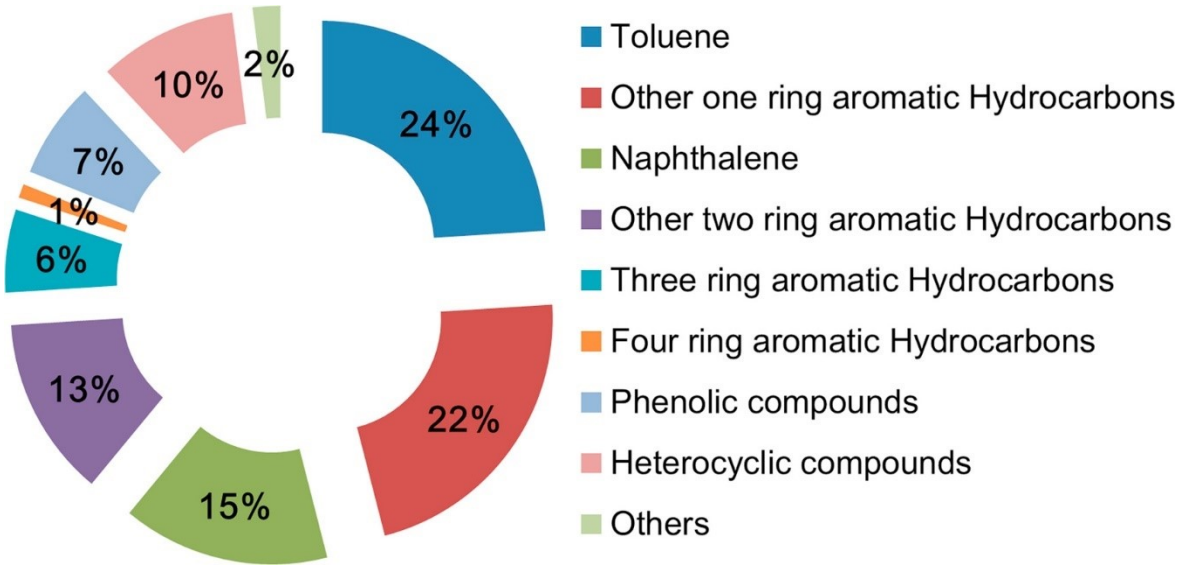

Figure 2.2 The typical biomass tar composition from gasification (Guan, Kaewpanha et al. 2016).

The biomass tar used as feedstock in laboratory-scale steam reforming is normally produced from the low temperature (400 to 600 °C) pyrolysis of biomass. This is because the typical tar yield of an effective gasification process of biomass could be lower than 5 wt.%, and the activity of the tar for further reaction is very limited (Guan, Kaewpanha et al. 2016). The majority compounds of the pyrolysis tar generated at low temperatures are acetic acid, phenol, furfural, levoglucosan and guaiacol. It was reported that acetic acid is formed mainly from hemicellulose, levoglucosan from cellulose, and phenols and guaiacol from lignin.

Levoglucosan is well known as the most abundant sugar compound from pyrolysis of biomass, in particular from cellulose (Fabbri, Torri et al. 2009). It is also reported that the levoglucosan yield could reach to 61 wt.% at 400 °C and reduced to 23 wt.% at 550 °C from the pyrolysis of cellulose, while guaiacol was the main product of lignin pyrolysis at 320, 400, and 550 ºC, and the concentration would increase with the increase in temperature (Wu, Zhao et al. 2009). Other conditions like Reactor type, heating rate, holding time also have an influence on the levoglucosan yield, Li, Wei et al. (2019), Yu, Paterson et al. (2019) found that levoglucosan yield increased from 23.0 to 45.0 wt.% when holing time increased from 300 s to 1200 s at 300 °C, levoglucosan yield increased from 20.8 to 53.3 wt.% when heating rate increased from 1 to 1000 °C s^{-1} at 450 °C.

The most abundant elements in biomass tar from different processes and feedstocks are carbon and hydrogen, which suggest a potential for energy conversion. Tar could not be considered as a suitable fuel like gasoline or diesel, although it is combustible. Due to the high water (15-25 wt.%) and oxygen content (35-45 wt.% on dry basis), the heating value of tar is in the range of 14-15 MJ kg^{-1}, which is similar as the heating value of lignocellulosic biomass feedstock. Besides, tar has high viscosity, low stability and solid content, which are all believed to be the challenges for tar as a future fuel. Tar removal and conversion has become one of the most considerable challenges in biomass gasification.

2.2 Tar removal methods

Many methods for tar elimination have been reported in the literature. In recent years, research emphasis is on the development of effective methods for tar

elimination in an economical and optimized way. Physical, thermal and catalytic tar removal methods have been used during wet or dry cleaning techniques. All these methods can be divided into two types depending on the location where tar reduction take place: either inside the gasifier (primary method) or outside the gasifier (secondary method).

2.2.1 Primary methods

Primary methods can be defined as all the measures taken within the gasification step to prevent tar or convert tar in the gasifier (Devi, Ptasinski et al. 2003). The primary method diagram is shown in Figure 2.3.

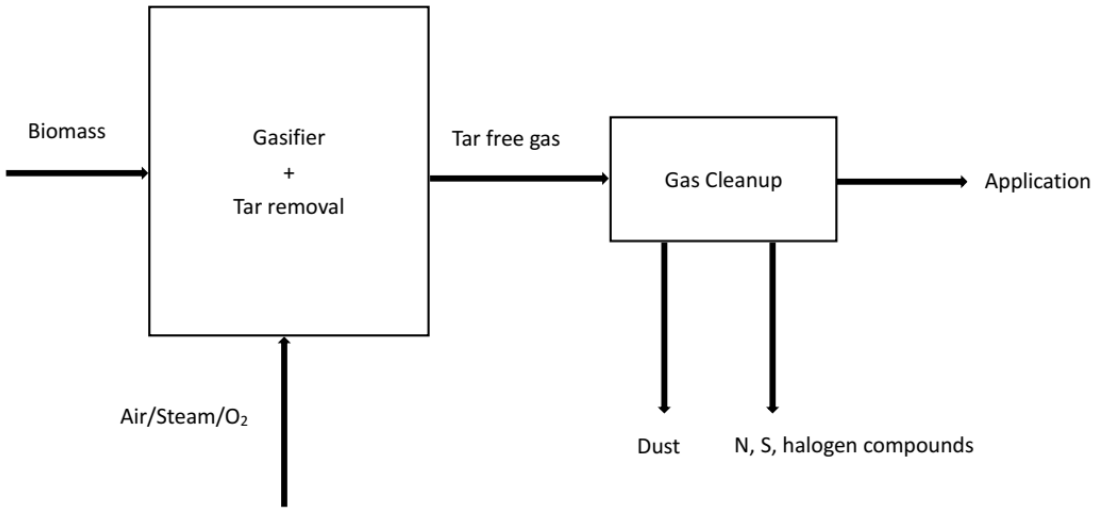

Figure 2.3 Tar removal concept diagram by primary methods.

The primary method requires the gasifier to have an optimized performance and get high quality exit gas. It usually includes the suitable selection of the operating conditions and parameters, the use of proper bed additives or a catalyst (eg. zeolite, olivine.) during gasification, and an optimized gasifier design (Devi, Ptasinski et al. 2003). The gasifier operating conditions, gasifying agent, residence time, feedstock ratio, reaction temperature and pressure

should all be considered in the reforming and decomposition of tar.

2.2.2 Secondary methods

Secondary methods are usually used as treatments to the hot product gas from the gasifier. These methods are carried out in a separate reactor independent of the type of gasifier used, so they could be operated at different conditions from the gasifier. Figure 2.4 shows the concept of secondary methods. These methods include tar cracking thermally or catalytically, mechanical methods such as use of cyclone, baffle filter, ceramic filter, fabric filter, rotating particle separator, electrostatic filter and scrubber. Table 2.1 shows some basic types of physical gas cleaning equipment.

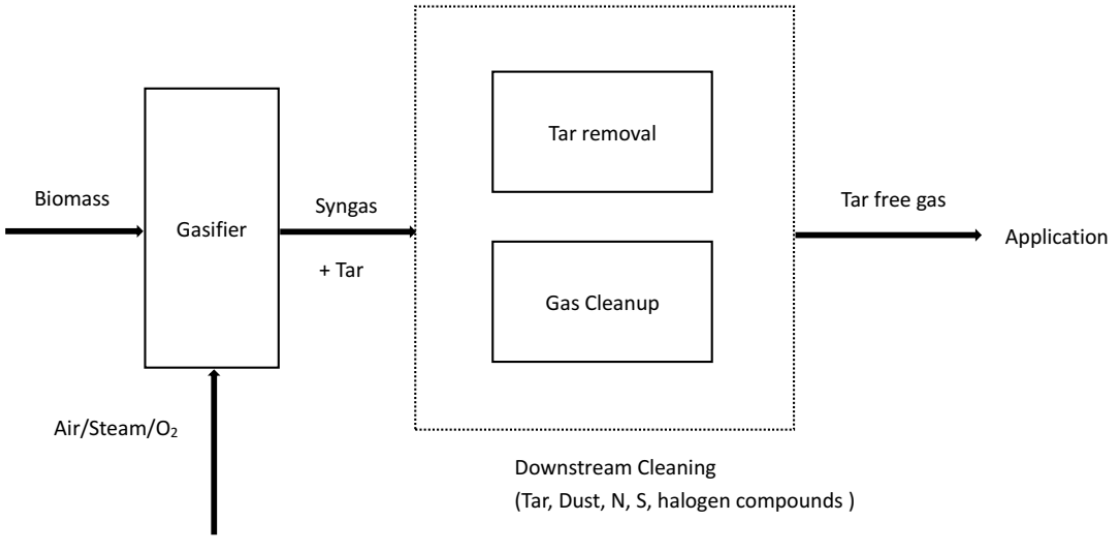

Figure 2.4 Tar removal concept diagram by secondary methods.

Table 2.1 Classification of physical gas cleaning equipment.

Basic type	Basic type
Dry	Cyclone, electrostatic precipitators, fabric/tube filters, baffle filters, sand bed filters, bag filters, ceramic filters, barrier filters, absorbers, rotating particle separators.
Wet	Wet cyclone, wet electrostatic precipitators, venture scrubbers, impingement scrubbers, packed column scrubber and spray towers.

Secondary methods of downstream gas cleaning are considered as very effective way for tar removal, especially in ammonia reduction. However, it is also reported that the production of relatively clean fuel gas from gasification requires a complex process by secondary methods. Narvaez, Corella et al. (1997) reported a three-step process that could produce a very clean gas with very low tar concentration.

2.3 Catalytic steam reforming of tar and model compounds

Current technologies used for fuel gas production from biomass tar include steam reforming, partial oxidation, autothermal, plasma, etc. Partial oxidation by adding air or O_2 could increase CO content in fuel gas at the expense of decrease in conversion efficiency and increase in operational cost (Devi, Ptasinski et al. 2003). Autothermal reforming could also increase the yield of H_2

and prevent coke deposition on catalyst (Tan, Abdullah et al. 2020). However, it requires a costly O_2 purification system for pure O_2 feeding or treats the product gas with a diluent (N_2), and the air would reduce the heating value of the process (Tan, Abdullah et al. 2020). Plasma method easily removes CH_4, SO_2 and NO_x from gaseous pollutants. Plasma cracking is effective for removal of tar from producer gas, while it has some disadvantages including limited lifetime of the pulsed power devices, high costs and high energy demand (Guan, Kaewpanha et al. 2016). Catalytic steam reforming is widely considered as a promising and effective technique for tar elimination in gasification. The catalysts provide a solution not only for the removal of tar but also a method to increase both conversion rate and useful gas (CH_4, CO and H_2) production. The final products of steam reforming are the results of competition and interactions of numerous thermochemical reactions. All the reactions can be summarized below (Coll, Salvado et al. 2001, Josuinkas, Quitete et al. 2014, González-Gil, Chamorro-Burgos et al. 2015):

Thermal cracking:

$$pC_nH_x\ (tar) \leftrightarrow qC_mH_y + rH_2 \qquad (1)$$

Steam reforming:

$$C_nH_x\ (tar) + nH_2O \rightarrow \left(n + \frac{x}{2}\right) H_2 + nCO \qquad (2)$$

Dry reforming:

$$C_nH_x\ (tar) + nCO_2 \rightarrow \left(\frac{x}{2}\right) H_2 + 2nCO \qquad (3)$$

Carbon formation:

$$C_nH_x\ (tar) \rightarrow nC + \left(\frac{x}{2}\right) H_2 \qquad (4)$$

Boudouard reaction:

$$C + CO_2 \leftrightarrow 2CO \quad (5)$$

Steam gasification:

$$C + H_2O \leftrightarrow CO + H_2 \quad (6)$$

Hydrogasification:

$$C + 2H_2 \leftrightarrow CH_4 \quad (7)$$

Oxidation reactions:

$$C + O_2 \rightarrow CO_2 \quad (8)$$

$$CO + 0.5O_2 \rightarrow CO_2 \quad (9)$$

$$CH_4 + 2O_2 \leftrightarrow CO_2 + 2H_2O \quad (10)$$

$$H_2 + 0.5O_2 \rightarrow H_2O \quad (11)$$

Water gas shift reaction:

$$CO + H_2O \leftrightarrow CO_2 + H_2 \quad (12)$$

Methanation reactions:

$$2CO + 2H_2 \rightarrow CH_4 + CO_2 \quad (13)$$

$$CO + 3H_2 \leftrightarrow CH_4 + H_2O \quad (14)$$

$$CO_2 + 4H_2 \rightarrow CH_4 + 2H_2O \quad (15)$$

Steam reforming reactions:

$$CH_4 + H_2O \leftrightarrow CO + 3H_2 \quad (16)$$

$$CH_4 + 0.5O_2 \rightarrow CO + 2H_2 \quad (17)$$

The final gas product of tar steam reforming is expected to be a mixture of light molecules, predominantly H_2 and CO, which could be used as fuel. Excess steam could be introduced to react with CO to produce more H_2 (Lu, Guo et al. 2017). Much research has been carried out to prove the presence of a catalyst could significantly increase carbon conversion, and lower tar yield and coke deposition. Miyazawa, Kimura et al. (2006) investigated Ni/Al_2O_3, Ni/ZrO_2 and Ni/TiO_2 catalysts could decrease tar yield to zero in the steam reforming of tar derived from cedar at 650 °C. Li, Ishikawa et al. (2013) also found that $Co/BaAl_{12}O_{19}$ catalyst could convert over 98% tar in the steam reforming of biomass tar at 550 °C. Kim, Park et al. (2014) reported that 10 wt.% $K_2CO_3/LaMn_{1-x}Cu_xO_3$ could reduce tar content in steam reforming to < 3% at 700 °C.

The mechanism of tar steam reforming has been studied for decades. Since the composition of biomass tar is very complex, the relationship of different thermochemical reactions is difficult to investigate (Luneau, Gianotti et al. 2017). Researchers believe that it is almost impossible to understand the detailed mechanism of the process at present stage. For instances, most researchers used the common model tar compounds to develop the mechanism, including benzene, toluene, naphthalene and phenol. Researchers studied the mechanisms and kinetics of naphthalene, toluene and benzene as the model compounds in thermal conversions with H_2 and steam, and suggested the simplified reaction scheme shown in Figure 2.5.

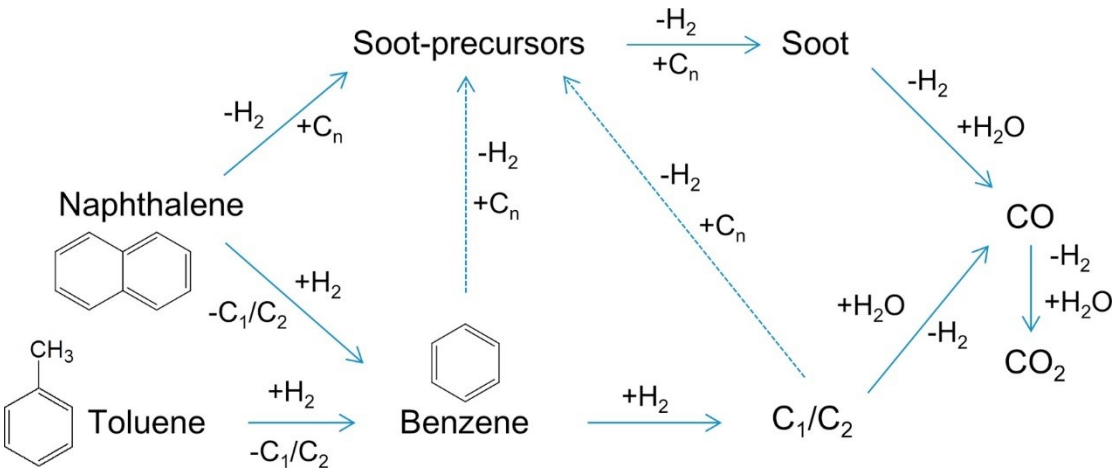

Figure 2.5 Simplified reaction scheme of thermal conversion of aromatic hydrocarbons in the presence of H_2 and steam. Reproduced from Guan, Kaewpanha et al. (2016).

Comparatively, toluene is very popular and more investigated than other tar model compounds. Toluene represents the stable aromatic structure apparent in tar formed in high-temperature processes (Ashok, Dewangan et al. 2020). Trinh, Nguyen et al. (2016) comparatively studied toluene decomposition behavior on Ni (111) catalyst surfaces and described all possible decomposition pathways of toluene and energetics shown in Figure 2.6. Toluene decomposition starts with CH bond activation of the methyl group (CH_3), CH_3 is dehydrogenated into CH_2* in step 1 as this step requires lower reaction energy and activation energy than aromatic CH dissociation(Trinh, Nguyen et al. 2016). Then from step 2 to step 3, CH_2* converts into C* in further dehydrogenation. From step 5 onwards, ring opening via aryl CC bond cleavage and more CC cleavages occurs to generate shorter hydrocarbon chains which become energetically feasible after the ring opening steps (Trinh, Nguyen et al. 2016).

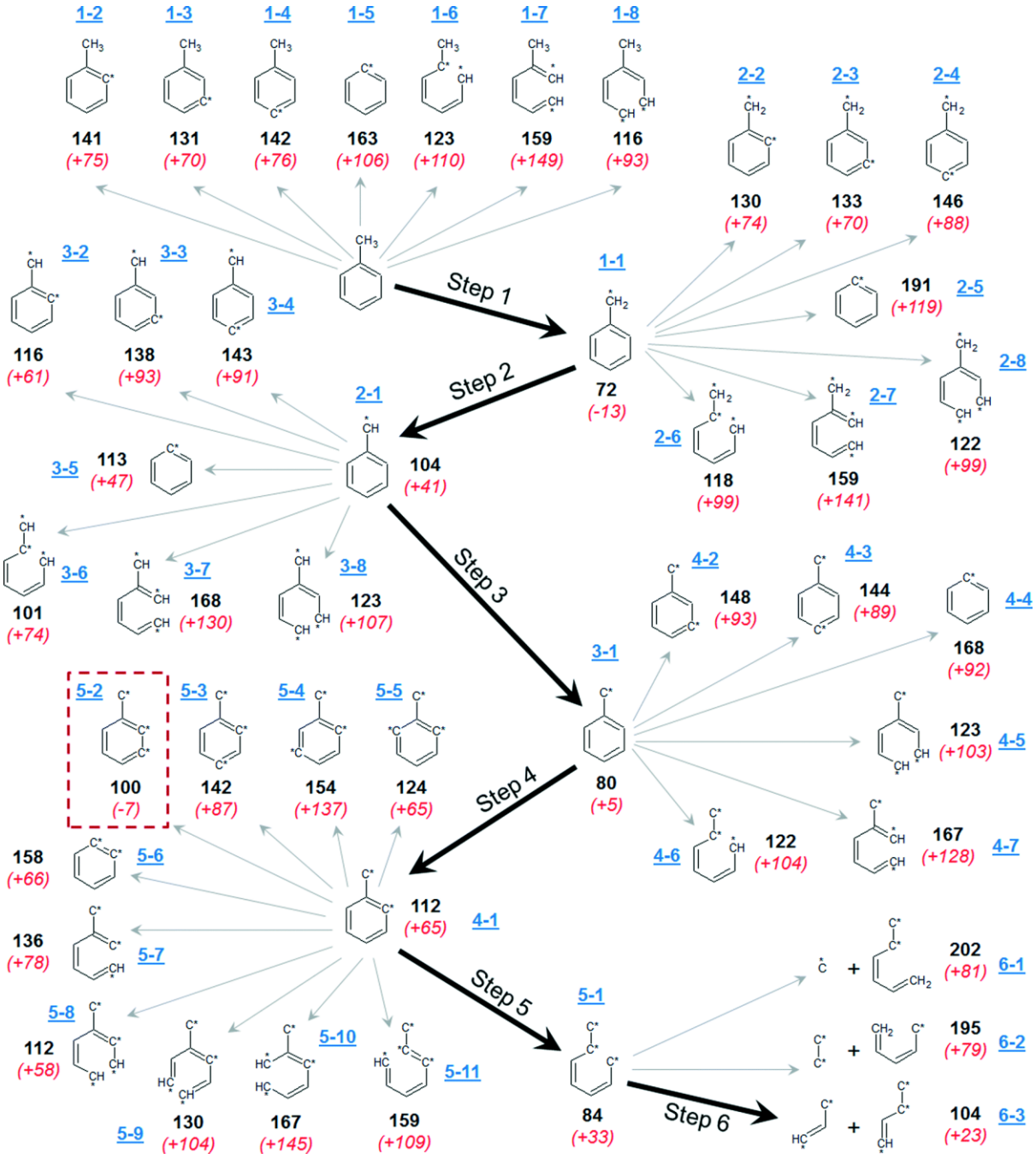

Figure 2.6 Decomposition network of toluene on Ni (111) surface. Bold black arrows denote the most favourable reaction pathway. Reproduced from Trinh, Nguyen et al. (2016).

2.4 Catalyst performance

The catalytic reforming reactions involve adsorption or formation of intermediate compounds and the transfer of ions, electrons, and radicals.

Sutton, Kelleher et al. (2001), Anis and Zainal (2011) suggested that the selection of an ideal catalyst for tar steam reforming should meet the following criteria:

- Catalytic activity in reforming and tar conversion;
- Produce syngas with a suitable ratio for further application;
- Resistance to coke, sintering, and poisoning;
- Regeneration ability;
- Low cost and high availability.

The following sections describe the popular catalysts used in steam reforming of tar and tar model compounds.

2.4.1 Noble metal-based catalysts

Noble metal catalysts are reported to have an outstanding performance in steam reforming of biomass tar. Ru, Rh, and Pt show very high catalytic activity, very good stability with low coke yield (Tomishige, Miyazawa et al. 2003). Rh was reported to be the most effective catalyst in catalytic activity with a selectivity order of Rh > Pt > Pd > Ru = Ni (Tomishige, Miyazawa et al. 2003).

Researchers studied reforming of n-heptane using platinum and platinum-rhenium catalysts on alumina supports (prepared by impregnation and sequential impregnation method). The catalysts were tested in an internal recycle reactor at 500 °C, 1.2 MPa, a liquid hourly space velocity of 3.0 h^{-1}, and a hydrogen/n-heptane ratio of 1000:1. The results showed that platinum-rhenium catalyst had a better stability than platinum catalyst, and had a higher

product distribution. The presence of rhenium had a better performance due to its dispersing carbon on the catalyst (Shozi, Dasireddy et al. 2019). Park et al. (2010) investigated Ni and Ru catalysts in toluene steam reforming and found that both catalysts could achieve a conversion over 90% at 800 °C, but Ru-based catalyst shows a significantly lower coke deposition than Ni-based catalyst.

To promote industrial application of noble metal catalysts, it is very necessary to reduce cost and improve reforming economic efficiency. Low metal loadings (normally <1 wt.%) of noble metal were applied and showed high catalytic activity with some specific supports at low temperatures. The outstanding catalytic performance of noble catalysts increase the possibility to utilize waste heat with a temperature of 400 to 600 °C in industry (Ammendola, Cammisa et al. 2012). However, the expensive cost is still the greatest challenge when comparing with other catalysts.

2.4.2 Nickel-based catalysts

Nickel-based catalysts are believed to be the most widely applied catalysts in the steam reforming of biomass tars. These catalysts have high activity for the rupture of C-C bond and O-H bond, low cost and a relatively good performance in hydrogen production (Chen, Sun et al. 2017). Nickel could be supported on various materials, Ni/Al_2O_3, Ni/olivine, Ni/SiO_2, Ni/MgO, Ni/ZrO_2, Ni/TiO_2 and Ni/CeO_2 have been studied by many researchers in recent decades (Furusawa and Tsutsumi 2005, Świerczyński, Libs et al. 2007, Artetxe, Nahil et al. 2016, Silveira, Rabelo-Neto et al. 2017, Abbas, Tahir et al. 2018, Zhang, Zhang et al. 2020). It is concluded that the catalytic effects of nickel catalysts with single support could be improved with the introduction of other materials (Luneau,

Gianotti et al. 2017).

The effect of CaO and MgO on the catalytic performance of Ni/Al_2O_3 catalysts was investigated by Medrano, Oliva et al. (2011) in steam reforming of the aqueous fraction from bio-oil, which includes acids, alcohols, aldehydes, ketones, and sugars. They suggested that the catalyst with MgO addition showed the best performance (carbon conversion of 81%, H_2 yield of 0.11 g $g_{organic}^{-1}$ at 650 °C, followed by the Ni/Al_2O_3 catalyst (carbon conversion of ~74%, H_2 yield of 0.097 g $g_{organic}^{-1}$), and then the CaO modified Ni/Al_2O_3 catalyst (carbon conversion to gas of 66%, H_2 yield of 0.078 g $g_{organic}^{-1}$) (Medrano, Oliva et al. 2011).

It is also essential to improve the regeneration ability of potential catalysts because frequent catalyst regeneration may be required due to deactivation over time. Nickel-based catalysts tend to have rapid coke formation and deactivation, while many researches have focused on the carbon formation kinetics of nickel (Ortiz-Toral, Satrio et al. 2011). Table 2.2 summarizes Ni-based catalysts with different supports for steam reforming. The coke deposition velocity helps to understand the effect of different support on coke formation rate.

Table 2.2 Summary of Ni catalysts for tar steam reforming.

Catalyst	Preparation method	T(°C); S/C	Conv. (%)	Coke deposition
$Ni/La_{0.8}Ce_{0.2}Al_{11}O_{19}$ (Quitete, Bittencourt et al. 2014)	Co-precipitation route	650; 1.9	70% at $H_2/CO = 1$	58 mg $(g_{cat}\ h)^{-1}$
Ni/CeO_2-ZrO_2 (Zhao, Xue et al. 2017)	Reverse co-precipitation	500; 3	80%	–
$Ni/BaO{\cdot}6Al_2O_3$ (Quitete, Bittencourt et al. 2015)	incipient wetness impregnation method	650; 1.5	82%	6 mg $(g_{cat}\ h)^{-1}$
Ni/LaCeAl (Quitete, Bittencourt et al. 2014)	Co-precipitation method	650; 1.9	80%	3 mg $(g_{cat}\ h)^{-1}$
Ni/MgO-Al_2O_3 (Li, Wang et al. 2011)	Co-precipitation	650; 0.5	100% at $H_2/CO = 1.7$	39 mg $(g_{cat}\ h)^{-1}$

Catalyst	**Preparation method**	**T(°C); S/C**	**Conv. (%)**	**Coke deposition**
Ni/CaO–Al_2O_3 (Ashok, Kathiraser et al. 2015)	Co-precipitation	650; 1	85%	2 mg $(g_{cat}\ h)^{-1}$
Ni/La/SBA-15 (Oemar, Kathiraser et al. 2015)	Incipient wetness impregnation	650; 1	85%	6 mg $(g_{cat}\ h)^{-1}$
Ni/MCM-41 (Karnjanakom, Guan et al. 2015)	Hydrothermal followed by impregnation	750; 1	H_2 gas yield = 92.15 mmol g^{-1}	3 mg $(g_{cat}\ h)^{-1}$
$La_{0.7}Sr_{0.3}AlO_{3-x}$ (Oemar, Ang et al. 2015)	Wetness impregnation	650; 1	67.5%	16 mg $(g_{cat}\ h)^{-1}$
Ni/Al_2O_3 (Artetxe, Alvarez et al. 2017)	Impregnation	750; 3	90%	-
Ni/Al_2O_3, Ni/MgO, Ni/CaO(Vivanpatarakij, Rulerk et al. 2014)	-	450; 5	80-100%	-

Catalyst	Preparation method	T(°C); S/C	Conv. (%)	Coke deposition
Ni/Al_2O_3 (Qian, Zhang et al. 2014)	Al_2O_3sphere: Hydrothermal method Ni/Al_2O_3: impregnation	800; 1	80%	320 mg $(g_{cat}\ h)^{-1}$
Ni–Fe/Hydrochar (Gai, Zhang et al. 2018)	Hydrothermal carbonization (HTC)	500–900	H_2 yield = 113.7 g H_2/g sludge	30-42 mg $(g_{cat}\ h)^{-1}$
Resin char (Li, Morishita et al. 2010)	Ion-exchange method	650	H_2 yield = 45 mmol/g	250 mg $(g_{cat}\ h)^{-1}$
Ni/Biochar (Du, Zhang et al. 2018)	Pyrolytic approach	600; 3	98%, H_2/CO = 4.8	15 mg $(g_{cat}\ h)^{-1}$
Ni/Lignite char (Cao, Ren et al. 2018)	Ion exchange	650; 2	Total gas yield = 116.3%	540 mg $(g_{cat}\ h)^{-1}$
$Ni/\alpha\text{-}Al_2O_3$ (He, Hu et al. 2018)	Wetness Impregnation	700; 3	75%. H_2: 1.0 mol/g·h	365 mg $(g_{cat}\ h)^{-1}$

Catalyst	**Preparation method**	**T(°C); S/C**	**Conv. (%)**	**Coke deposition**
Ni/Activated char (Tan, Abdullah et al. 2020)	Impregnation	800; 2	92%	-
NiCo/NiCo phyllosilicate@CeO_2 hollow core shell (Li, Li et al. 2019)	Hollow spheres: Stober and hydrothermal method CeO_2 shell: Precipitation	700; 1	80% at $H_2/CO = 3.6$	4 mg $(g_{cat}\ h)^{-1}$

Ni/Al_2O_3 catalyst is reported to be very promising in the viewpoint of practical application, and nickel is considered as a good component in many novel catalysts. However, one component in a catalyst could not be suitable for the conversion of all the tar compounds because of the complexity of the biomass tar, and metallic nickel also have drawbacks in some aspects. Nickel is highly active for methanation and relatively lower active for WGS reaction, while the acidity of Al_2O_3 favors dehydration and polymerization reactions. These disadvantages contribute to the deactivation more than the nickel sintering problem does (González-Gil, Chamorro-Burgos et al. 2015). Researchers concluded the effective improvements from numerous previous experiments, including modification by metals with high activity for the WGS and low activity for methanation reactions like Cu and Co, addition of promoters like MgO and CeO_2 to increase the adsorption and activation of steam, neutralize the acidity of catalysts (Göransson, Söderlind et al. 2011, Guan, Kaewpanha et al. 2016). The introduction of effective compounds into the conventional Ni/Al_2O_3 catalyst could increase the catalytic performance comprehensively.

2.4.3 Other metal based catalysts

The other metals like Co, Cu, Fe and Zn also have high catalytic activity in the steam reforming of biomass tar. Furusawa and Tsutsumi (2005) reported that Co/MgO catalyst showed better performance and higher catalytic activity in tar reforming than Ni/MgO catalyst. Recent studies of the metal based catalysts focus on the improvement of catalytic effects by combining several kinds of metal oxides. Wang et al. (2012) modified Co/Al_2O_3 with Fe showed better catalytic performance in terms of the catalytic activity and the suppression of coke deposition than the Co/Al_2O_3.The combination of Co, Cu, Fe and Zn on Al_2O_3 have been widely studied to improve the catalytic activity (Bimbela et al.

2017).

2.4.4 Carbon-supported catalysts

Carbon-supported catalysts widely applied in tar steam reforming consist of activated carbon, biomass char and char derived from coal. The low cost and environment friendly features of carbon support have attracted continuous research interest. The catalytic activity of carbon-support catalysts depends on their surface area, ash or mineral contents. The natural highly porous structure shows a great potential for tar cracking and conversion.

Activated carbon is a non-graphitic, microcrystalline form of carbon (Smisek and Cerny 1970). The porous areas between the crystallites in the activated carbon result in the large surface area. Due to their highly porous structures, activated carbons or charcoals (from biomass or coal) have also been widely used as catalyst supports for tar cracking, because their macropores and mesopores would greatly improve the dispersion of metal ions and the contact of reactant molecules with the internal surfaces of the catalyst (Shen and Yoshikawa 2013).

Many researchers compared the performance of different carbon-support catalysts and other known catalysts. El-Rub, Bramer et al. (2008) stated that biomass chars showed a relatively high naphthalene conversion with an order following nickel > commercial biomass char > biomass char > biomass ash > spent fluid catalytic cracking catalyst > dolomite > olivine > silica sand. Min et al. (2011) found that the Ni-biomass char and Fe-biomass char catalysts showed a significant advantage in catalytic activity over the char catalyst itself. They also found that the char support of Ni-char and Fe-char catalyst also showed significant catalytic activities for tar reforming, which indicated that the

char support was not completely inert. The results showed that coke decreased to negative value when the reforming temperature increased over 800 °C. It is suggested that the iron and nickel might have contributed to the dissociation of tar and steam, and produce reactive intermediates to react with support char, while the coke yield using ilmenite catalyst stayed above zero due to the relatively inert activity of TiO_2 in ilmenite.

Biomass char supported catalysts may share similar reforming reaction pathways. It is believed that the migration of reactive intermediates between the active sites on char and the metal (iron and nickel) is one of the key mechanisms of the catalytic interactions (Chen et al. 2017).

Abu El-Rub, Bramer et al. (2004) compared the performance of a biomass char (produced by pyrolysis of pinewood at 500 °C) to other catalysts for tar reduction including calcined dolomite (21 wt.% MgO, 30 wt.% CaO, 0.2 wt.% Fe_2O_3), olivine (50 wt.% MgO, 42 wt.% SiO_2, and 7 wt.% Fe_2O_3), and a nickel catalyst (70 wt.% NiO, 12 wt.% Al_2O_3 and 7 wt.% SiO_2). Phenol and naphthalene were used as tar model compounds. The catalytic reforming tests were conducted in the presence of CO_2 (6 vol.%), steam (10 vol.%) balanced with nitrogen at 700 and 900 °C. The results showed that all the catalysts had high activities, and phenol was 100% converted at 900 °C. At 700 °C the catalysts a relatively high conversion of phenol with a selectivity order of Ni > biomass char > olivine. The naphthalene reforming tests were conducted at 900 °C. The biomass char catalyst obtained >99% conversion of 90 g Nm^{-3} naphthalene, while the dolomite catalyst achieved only 55 wt.% conversion of 40 g Nm^{-3} naphthalene. Despite slightly inferior to the Ni catalyst, the biomass char was reported to be more active in naphthalene reforming than the other catalysts (olivine and dolomite) tested (El-Rub, Bramer et al. 2008).

2.4.5 Mesoporous catalyst

The support material has a strong influence on the activity, stability and selectivity of steam reforming process. Ordered mesoporous material with large surface areas and well-defined structure has been studied in recent decades (Ma, Zeng et al. 2016). A mesoporous material contains pores with diameters between 2 and 50 nm, it can help to achieve small and anti-sintering metal (nickel) particles. Silica-based SBA-15 and MCM-41 as support, have been widely designed owing to the confinement effect of the ordered channels (Gao, Salisu et al. 2021).

Zhang, Hu et al. (2019) compared Ni support SBA-15 with Ni/Al_2O_3 catalyst for steam reforming of guaiacol. They reported that the deactivation in Ni/Al_2O_3 catalyst is due to the encapsulation of amorphous carbon, while the carbon nanotubes grown on the tip of Ni particle and had less impact on catalyst deactivation for Ni/SBA-15 catalyst (Zhang, Hu et al. 2019). Usman Oemar, Kathiraser et al. (2015) studied the series of La_2O_3 modified Ni/SBA-15 catalysts prepared by organic acid assisted synthesis method. La doped Ni/SBA-15 showed lower coke formation than Ni/SBA-15 catalyst by forming oxy-carbonates thus making the catalyst stable for over 30 h of operation (Oemar, Kathiraser et al. 2015). Ni/MCM-41 can ameliorate the metal dispersion with an elevated interaction between the metal and the support and an effective reusability (Ashok, Dewangan et al. 2020, Tan, Abdullah et al. 2020). Ashok, Dewangan et al. (2020) reported that when nickel was impregnated on MCM-41 using ethylene glycol (EG) assisted co-impregnation method, an enhanced metal dispersion with higher metal support interaction was observed when compared with Ni/MCM-41 prepared by conventional wetness impregnation method. The catalyst reusability remained high and H_2 yield increased by 8% when using 20 wt. % Ni/MCM-41-EG as compared with 20 wt. %

Ni/MCM-41 for the steam reforming of tar (Ashok, Dewangan et al. 2020).

2.4.6 Natural catalysts

Some natural minerals like dolomite, olivine, quicklime and shells show a good activity for tar reforming and they are very abundant and cheap. Hu, Xu et al. (2006) found that olivine and dolomite could produce H_2-rich gas from tar reforming, and the performance could further improve after some pretreatment (eg. calcination at 900 °C for 4 h). Constantinou, Fierro et al. (2010) found that calcined olivine and calcined dolomite both had good performance for tar elimination. Researchers believed that olivine catalyst is more suitable than dolomite catalyst in the application of fluidized bed gasifier due to the higher attrition resistance of olivine.

Further research indicated that the introduction of some metals could increase the catalytic activity to a higher level. Virginie, Courson et al. (2010) reported that Fe/olivine catalyst could improve the conversion and hydrogen production of toluene reforming, the values of conversion and hydrogen production were approximately three times higher when comparing to the olivine catalyst. Similar results were also found when using Ni/olivine catalyst. Świerczyński, Libs et al. (2007) investigated that Ni/olivine catalyst could improve the resistance of coke on catalyst. They also suggested basic MgO oxide and Ni–Fe alloys inhibited the carbon formation in the reforming process. Yang, Xu et al. (2010) modified the structure of olivine with calcium aluminate cement when using Ni/olivine catalyst, stated that the modification could create pore structure and better distribution of Ni particles on the support, the porosity could increase by 30% after treatment.

2.4.7 Zeolite catalyst

Zeolites are defined as the combination of crystalline silicates and aluminosilicates linked by oxygen atoms. The high surface area and aligned pore structure make them an ideal catalyst support. The addition of metals like Ni, Fe, Cu can create suitable catalysts for the conversion of aromatic hydrocarbons, with relatively high tolerance for sulfur poisoning in gasification products.

Dou, Gao et al. (2003) studied the catalytic reforming of tar component and found that Y-zeolite and NiMo/Al_2O_3 catalysts were the most effective catalysts among Y-zeolite, NiMo catalyst, silica, alumina and lime. These two catalysts both eliminated over 98% tar at 550 °C with limited deactivation phenomenon over 10 hours test. They also concluded that the catalytic effects of Y-zeolite depended on the pore size and acidity. Buchireddy, Bricka et al. (2010) investigated the influence of various pore size and acidity on the catalytic activity of zeolites in steam reforming of tar and found that Y-zeolite larger pore size had better catalytic activity compared with ZSM-5, and the impregnation of nickel on zeolites would further increase the activity. They also suggested that the increase of acidity could improve the performance. However, the catalytic performance of Y-zeolite catalysts with or without nickel addition would suffer rapid deactivation in tar reforming due to coke formation.

2.4.8 Alkali catalyst

Alkali catalysts use alkali metals like lithium (Li), sodium (Na), potassium (K), and have been proved to have a good effect on tar steam reforming, especially on gas production. Kuchonthara, Puttasawat et al. (2012) stated that K_2CO_3 had a significant catalytic activity of on the steam gasification of lignin and tar

deposition. They also investigated the catalytic effects on biomass gasification and pyrolysis and found that the biomass conversion could increase over 99% when the temperature was higher than 800 °C. It is also suggested that the alkali components in biomass feedstock could also act as a catalyst in the gasification or pyrolysis process. A study carried out by Hognon, Dupont et al. (2014) confirmed that the inorganic elements in biomass feedstock have strong influence on the reactivity of different biomass. The high concentration of potassium in biomass could increase the reactivity of biomass due to the known catalytic effect of potassium in both char gasification and tar reforming. The major challenge of alkali metal for tar reforming catalyst is the evaporation and recovery problem, as the simple alkali metal catalyst is unstable and difficult to regenerate. However, researchers attempted to develop mixed metal catalysts which may contain alkali metal. The research of Chen, Zhang et al. (2007) investigated the performance of $La_{1-x}K_xM_nO_3$ perovskite-type catalysts in crude bio-oil steam reforming. The $La_{0.8}K_{0.2}M_nO_3$ catalyst showed the best performance with higher carbon conversion and hydrogen yield (up to 72.5 wt.%) than the commercial Ni/ZrO_2 catalyst. However, the formation of $K_2Mn_4O_8$ in the catalyst structure could decrease the catalyst activity, and the catalyst also suffered from coke and deactivation problems.

2.5 Parametric effect on steam reforming

From previous studies, the most significant parameters for tar steam reforming are reforming temperature, S/C ratio, and space velocity or residence time. This section discusses the influence of reforming conditions.

2.5.1 Reforming temperature

The temperature of steam reforming has a significant influence on tar conversion as high temperature could increase syngas yield and conversion from tar to gas products. Josuinkas, Quitete et al. (2014) studied the influence of reforming temperature on the catalytic steam reforming of benzene, toluene, and naphthalene/toluene (ratio=1:9) with Ni/MgO/Al_2O_3 catalyst. The reforming tests were conducted with a S/C ratio 1.5, GHSV = 20,000 h^{-1}. They suggested that the most suitable temperature for complete conversion of both benzene and toluene was 700 °C, while naphthalene was much more difficult to convert even at higher temperatures. In the steam reforming test of naphthalene and toluene mixture, toluene was inhibited by the presence of 10 wt.% naphthalene, and the complete conversion temperature for this mixture was 900 °C.

Park, Oh et al. (2017) investigated the steam reforming of toluene over Ru/αAl_2O_3 and Ni/αAl_2O_3 at different temperatures with a S/C ratio = 3.57 and weight hourly space velocity (WHSV) = 10000 h^{-1}. They reported that Ru/αAl_2O_3 and Ni/αAl_2O_3 catalyst achieved the highest toluene conversions at 98% and 96%, respectively, at 800°C. They also concluded that higher temperature increased the conversion of toluene, and hydrogen and CO production.

2.5.2 Steam to carbon (S/C) ratio

The S/C mole ratio is one of the most important factors in steam reforming of tar and model compounds because it has a significant impact on feedstock/carbon conversion, coke formation, and H_2 yield. Researchers reported that increasing of S/C ratio could prevent coke formation by facilitating the gasification of deposited carbon (Tao, Zhao et al. 2013). Gao, Wang et al. (2016) conducted benzene steam reforming over Ni/ceramic foam catalyst with

a S/C ratio of 0-3 and concluded that too much excess steam could slightly reduce the benzene conversion as excess water molecules competed with tar at adsorptive active sites.

Excess steam also comes with high power consumption for steam generation and requires higher cost of steam separation from the reformate for industrial application. For lab-scale reforming tests, excess steam might cause a fluctuation in the reaction temperature as it absorbs the heat within the reactor (Gao, Liu et al. 2015). Insufficient steam in the reforming test causes that steam reforming and water gas shift (WGS) reactions cannot achieve their state of completion, and results in the low conversion rate and hydrogen yield (Gao, Liu et al. 2015). Therefore, the S/C molar ratio applied to the experiments should be at least higher than the stoichiometric value of the reforming reaction.

Zhang, Wang et al. (2014) studied the effect of S/C ratio on toluene steam reforming over Ni/ olivine catalyst and concluded that H_2 composition increased as S/C ratio increased. They observed the highest conversion of toluene at a S/C ratio of 5 with Ni and Ni/Ce based olivine catalysts, and the highest conversion of toluene at a S/C ratio of 3.5 with Ni/Ce/Mg/olivine catalyst. The addition of Mg to Ni/Ce/olivine enhanced the performance and coke resistance at the S/C ratio of 3.5. This is due to its basicity and the presence of well-stabilized NiO-MgO solid solution. However, Gao, Wang et al. (2016) stated that H_2 composition remained stable at high S/C ratios.

Liang, Wang et al. (2017) studied the influence of different S/C ratios on steam reforming of phenol-ethanol (mixed with different mole ratios) with Ni-Cu/sepiolite catalyst. The results demonstrated that H_2 yield and carbon conversion both increased with the increase of S/C ratios, as sufficient steam drives the tar reforming and high water partial pressure favors the equilibrium of WGS reaction shift toward H_2 production (Liang, Wang et al. 2017, Park, Oh

et al. 2017).

2.5.3 Space velocity and residence time

Space velocity and residence time are used to reflect the contact time of reactant on the active sites of the catalyst. Catalytic steam reforming is much affected by the space velocity and residence time. The suitable value of residence time can significantly avoid wasting catalyst in industrial applications. Residence time, weight hourly space velocity (WHSV) and gas hourly space velocity (GHSV) are the key parameters in steam reforming process to identify and evaluate the reaction rate and efficiency which could be calculated on the following equation:

$$WHSV = \frac{total\ mass\ flow\ rate\ of\ gas\ entering\ the\ reactor(\frac{g_{flow}}{hour})}{mass\ of\ catalyst(g_{catalyst})} \quad (18)$$

$$GHSV = \frac{total\ entering\ reactants_{gas\ phase}(steam + fuel), (\frac{cm^3}{hour})}{catalyst\ bed\ volume\ size, cm^3} \quad (19)$$

$$Residence\ time\left(\frac{\tau}{hour}\right) = \frac{1}{WHSV} \quad (20)$$

Park, Oh et al. (2017) investigated toluene steam reforming test using a Ru/α-Al_2O_3 catalyst and found that toluene conversion dropped from 87.4 to 45.7% as the GHSV increased from 5000 to 30000 h^{-1}. Kim, Chun et al. (2015) studied the steam reforming of toluene over Ni/coal catalyst and found that H_2 yield decreased with increasing GHSV. Koike, Li et al. (2015) investigated the space-time effect on tar steam reforming tests over Ni and Ni-Fe alloy nanoparticles. They concluded that tar conversion increased when increasing residence time, while the H_2/CO ratio at the same time, as the consumption of H_2O was higher

at higher tar conversion and limit the contribution of WGS reaction and H_2 selectivity. Pashchenko (2019) studied the influence of residence time on methane steam reforming using Ni/CaO-MgO-La_2O_3-Al_2O_3 and reported that CH_4 conversion rate increased from 25% to 90% at 926.85 °C when residence time increased from 1 to 5 kg_{cat} (s $mol_{methane}$)$^{-1}$. The contact time of the tar-active sites increases or the active sites of the catalyst increases when residence time is increased, so there is a potential that a suitable residence time could help to optimize both the conversion rate and the conversion speed of tar.

2.5.4 Reforming atmosphere

Catalytic tar steam reforming could be applied in either primary (*in-situ*) or secondary (*ex-situ*) gasification systems. The hot gas stream contains various gas products together with tar, including H_2, CO, CO_2 and CH_4. The typical H_2, CO or CO_2 concentration is >20 vol.%, and CH_4 concentration is 3-6 vol.%. All these gases could affect the tar removal efficiency in catalytic steam reforming. However, there are very few literatures focused on tar reforming atmosphere.

Rönkkönen, Simell et al. (2010) studied the steam reforming of toluene (13.5 g Nm^{-3}) and naphthalene (1.5 g Nm^{-3}) in simulated gas atmosphere which contained 12.5 vol.% CO, 15 vol.% CO_2, 6 vol.% CH_4, 1 vol.% C_2H_4, 11 vol.% H_2, 50 vol.% N_2, 0.01 vol.% H_2S and 0.5% NH_3. They found that Ni/ZrO_2 obtained an overall conversion of 80% at 850 °C, and the deactivation test showed that the carbon conversion dropped from 50% to ~38% in 6 h at 800 °C. Mermelstein, Millan et al. (2011) Mermelstein, Millan et al. (2011) investigated the influence of syngas composition with toluene on the carbon deposition on Ni/CGO catalyst at 765 °C. They compared the influence of the presence of CO, CO_2 and CH_4 in H_2 based syngas. The syngas consisted of 15 vol.% H_2, 10

vol.% CO_2, 25 vol.% CO and 5 vol.% steam. The results showed that CO could slightly increase the coke yield and CO_2 would decrease the coke yield. While 2% CH_4 was introduced into the syngas, the carbon deposition increased five times from 0.672 to 3.5 mg with a catalyst weighing 36 mg. They concluded that CH_4 caused a decrease of steam available for reforming of benzene and contributed to CH_4 decomposition and PAH polymerization, resulting in a rapid increase of amorphous char type carbon formation. They also summarized that the addition of CH_4 decreased benzene conversion and increased carbon formation significantly (Mermelstein, Millan et al. 2011).

2.6 Challenges in tar catalytic steam reforming

Although great efforts have been devoted to steam reforming catalyst research, several challenges still exist, including catalyst deactivation, reactor material selection and engineering economics. The most common catalyst deactivation problems include coke formation, sintering and catalyst poisoning.

2.6.1 Coke formation

The coking problem is almost the main reason for any catalyst deactivation in tar steam reforming. The coke generated from the reactions is deposited on the surface of the catalyst and inhibits the reaction between catalysts and tar compounds, result in deactivation and regeneration problems.

When temperature is lower than 400 °C, the reverse of Boudouard reaction and reverse reaction of carbon gasification contribute to coke formation on catalyst surface (Chen, Tao et al. 2017). During steam reforming, coke can deposit on

catalyst either as amorphous or filamentous carbon. Amorphous carbon tends to the deactivation of catalyst by the hindrance of the active site, while filamentous carbon does not cause significant deactivation but causes reactor blockage and pressure drop (Josuinkas, Quitete et al. 2014, Park, Oh et al. 2017).

Researchers have conducted a variety of tests to inhibit coke formation in catalytic steam reforming. Hu, He et al. (2016) observed that both amorphous (12.8 mg $g_{catalyst}^{-1}$) and filamentous carbon (16.8 mg $g_{catalyst}^{-1}$) existed on spent Ni/Al_2O_3 catalyst after 2 hours in the steam reforming of toluene. Besides, the introduction of Fe to Ni/Al_2O_3 catalyst could decrease the coke formation by increasing the coverage of oxygen species on the catalyst surface. It is also reported that the coke formation on the Ni/MCM-41 catalyst was sequentially increased with the Ni content (Karnjanakom, Guan et al. 2015). The resistance of Ni/MCM-41 to coke deposition could be improved by the ethylene glycol assisted method when comparing to the co-impregnation method (Karnjanakom, Guan et al. 2015). Iida, Fujiyama et al. (2017) investigated steam reforming of toluene with $Ru/SrCO_3$-Al_2O_3 catalyst and found that the amount of coke deposited was remarkably higher with decreasing $SrCO_3/Al_2O_3$ loading ratio, as $SrCO_3$ is the coke suppression agent, which possesses a highly reactive hydroxyl functional group.

2.6.2 Sintering

It is reported that excess steam and high temperature could accelerate the sintering of the active metal in catalysts (Sehested, Larsen et al. 2014). Ni-based catalysts are susceptible to sintering by agglomerating metallic Ni particles in tar steam reforming process, as the typical reforming temperature

(700–900 °C) is higher than Tammann temperature of Ni (691°C), so Ni sintering will happen in tar steam reforming process (Devi, Ptasinski et al. 2003).

Oemar, Ang et al. (2013) reported that the sintering of $LaNiO_3$ catalyst decreased its catalytic activity and increased coke formation, the Ni crystallite size of spent catalyst increased by 34.7% in 8-hour test. Park, Oh et al. (2017) observed the deactivation of Ru/α-A_2O_3 catalysts in tar steam reforming due to Ru sintering, which yielded a bulky crystalline structure that inhibited catalytic reactions. The metal loading could also affect the catalyst sintering. Researchers found that NiO/$CaAl_{12}O_{19}$ and NiO/$LaAl_{11}O_{18}$ with low Ni loading (6 wt.%) experienced a more rapid sintering (Ni crystallite size increased by 150%) than the high Ni loading catalyst (14 wt.%) (Quitete, Bittencourt et al. 2014). Karnjanakom, Guan et al. (2015) mentioned that the high loading of Ni in Ni/MCM-41 catalyst (20-40 wt.%) contributed not only to coke formation but also catalyst sintering.

2.6.3 Catalyst poisoning

The impurities in the biomass-derived syngas such as sulfur-, nitrogen-, and chlorine-containing compounds could poison the catalyst in the downstream tar catalytic reforming process (Dou, Veksha et al. 2019). Sulfur is reported to be the most common poison lead to significant deactivation of reforming catalysts, nitrogen oxides (NO_x) and other nitrogen-containing compounds could also oxidize the active metal and result in the deactivation of catalyst (Ashok, Das et al. 2019). Hydrogen chloride (HCl) could poison the catalyst because the chemisorption of HCl on a metal site could cause metal sintering (Veksha, Giannis et al. 2018, Dou, Veksha et al. 2019)

In the raw syngas produced from biomass gasification, there is usually about

20–200 ppm of sulfur-containing compounds (mainly hydrogen sulphide/H_2S). Metal catalysts, especially Ni catalyst, are susceptible to sulfur poisoning as the strong dissociative chemisorption of sulfur on the metal site. H_2S could react with the Ni site on catalyst and form inactive nickel sulphide, deactivate the catalyst reducing the accessibility of active sites for tar (Tan, Abdullah et al. 2020). Mawdsley and Krause (2008) reported that sulfur poisoning can be inhibited at high pressures (>20 bar) and high temperature (> 900°C).

$$Ni + H_2S \rightarrow NiS + H_2 \qquad (21)$$

2.6.4 Reactor design

Gasification tar constitutionally contains heavy aromatic hydrocarbons with a high thermal stability, and tar catalytic steam reforming usually operates at high temperatures ranging from 700 to 900 °C. However, the process control under high temperatures poses a tough challenge, which increases the operational costs of power consumption, or capital costs of reactor material, engineering, and installation.

Nickel- or iron-based oxide dispersion strengthened alloys can withstand temperature as high as 1100 °C, while the material is relatively expensive (Chapin, Kiffer et al. 2004). Inconel (nickel-chromium-based superalloys) is used extensively for the main reactor tubes in steam reforming (Compagne 2014). The introduction of refractory metals (tungsten and molybdenum) provide endurance capability but poor oxidation resistance at high temperatures (Patra 2017).

The fixed bed reactor is the most commonly used reactor for industrial-scale H_2 production. The drawbacks of the fixed bed reactor consist of significant radial

and axial temperature gradients that lower the bed effective thermal conductivity (Karim, Bravo et al. 2005). Membrane reactors are reported to produce gas with good selectivity and high purity, but its manufacture cost is relatively high (Tan, Abdullah et al. 2020). Thus, the reactor design of tar steam reforming requires a suitable type with good high-temperature resistance material, and a good balance between the safety and economy of the reactor(Tan, Abdullah et al. 2020).

2.7 Summary

Tar is a by-product from gasification or pyrolysis of biomass, coal and other waste feedstocks. It is a complex mixture of condensable hydrocarbons, with one or more carbon rings and other elements including O, N, Cl and S. The majority of biomass originated tars are benzene, toluene and naphthalene.

Catalytic steam reforming is believed to be the most promising and effective technique for the tar elimination in gasification. To summarize the catalysts reviewed above, the popular catalysts used in steam reforming of biomass tar all have obvious disadvantages. Noble metal based catalysts have a good catalytic performance, long-term stability and high resistance to coke deposition, but the high cost limits its industrial application. Nickel-based catalysts are used extensively as the industrial catalysts for the steam reforming of tar because of the high catalytic activity and low cost, but the deactivation due to the rapid carbon formation on the catalyst surface is also the main problem. Other metal-based catalysts like Fe, Co and Cu have a good performance in the steam reforming of tar as well as the coke deposition problem. The alkali catalyst has attracted more and more research interests, because the ash from biomass gasification contains a suitable content of alkali species, which could be used

as the catalyst for steam reforming after treatment, and reduce the stress of ash handling problem of gasification. The industrial application requires disposable catalysts with low cost, therefore natural catalysts win the favor of both industry and research. Their catalytic performance is not as good as some other catalysts, but they are even cheaper and more abundant, only the mechanical properties limit their application to several specific types of reactors. Zeolite and carbon/char are considered as good supports of catalyst used in steam reforming. Currently, researches revealed that the carbon support in the catalysts would be involved in the reforming reactions.

Nickel-based catalysts are widely used for biomass tar reduction because of their good performance in tar destruction and high activity for methane reforming and WGS reaction (Garbarino, Lagazzo et al. 2013). Recent study has been focused on alloying the active nickel metal with other metals, modification of the nickel support with other material and addition of promoters. Many researchers are trying to investigate optimal catalyst design, which modifies the catalyst properties and subsequently improves catalyst performance for tar conversion. However, Al_2O_3 is still the most commonly used support for Ni-based catalysts for tar reduction, Ni/Al_2O_3 catalyst has been the preferred industrial catalyst for reforming as it is cheap and easily synthesized. It is also important to have a better understanding of this state-of-the-art catalyst to reveal the optimum process conditions. This work aims to fill an essential gap in tar reforming literatures via a systematic study of key reaction parameters and conditions.

3 Methodology

This chapter describes the feed materials, detailed procedures followed during experiments and the analytical techniques used in the project.

3.1 Materials

The compressed gas used in the experiments include N_2 (99.995% purity), H_2 (99.99% purity), CH_4 (99.8% purity), CO (99.9% purity), CO_2 (99.9% purity) and span gas was supplied by BOC Ltd. The span gas (for calibrating the online gas analyser described below) contained 20 vol.% H_2, 5 vol.% CO_2, 1 vol.% CH_4 and 20 vol.% CO in N_2. The reactant toluene (99.9% purity) was supplied by Sigma Aldrich. Toluene was chosen as a tar model compound as it has the highest content in biomass tar and less toxic than other single ring aromatic compounds like benzene.

The nickel-based catalyst was prepared following a wet impregnation method. Firstly, the necessary amount of $Ni(NO_3)_2 \cdot 6H_2O$ (≥97.0%, Sigma-Aldrich) to obtain 20 wt.% NiO was dissolved in an excess of acetone (≥99.8%, Sigma Aldrich). Then, the support α- Al_2O_3 (≥98.0% purity, Sasol) was added into the solution. After stirring for 2 h, the solvent was removed under vacuum at 60 °C by a rotating evaporator. The remaining mixture was dried overnight at 110 °C. Finally, the solid was calcined at 600 °C with a ramping rate of 2 °C·min^{-1} for 4 hours, crashed and sieved to particle size in the range 250-500 μm after cooling to room temperature. The Ni content assuming complete reduction from NiO to Ni is 16.4 wt.%. The obtained sample was labelled Ni/Al_2O_3.

3.2 Experimental setup

This section describes the experiment equipment used in this project. The system equipment was classified into four main process stage: material feeding, reaction (fixed-bed reactor), tar collection and gas measurement. Figure 3.1 shows the overall schematic diagram of the experimental setup used for catalytic steam reforming of toluene.

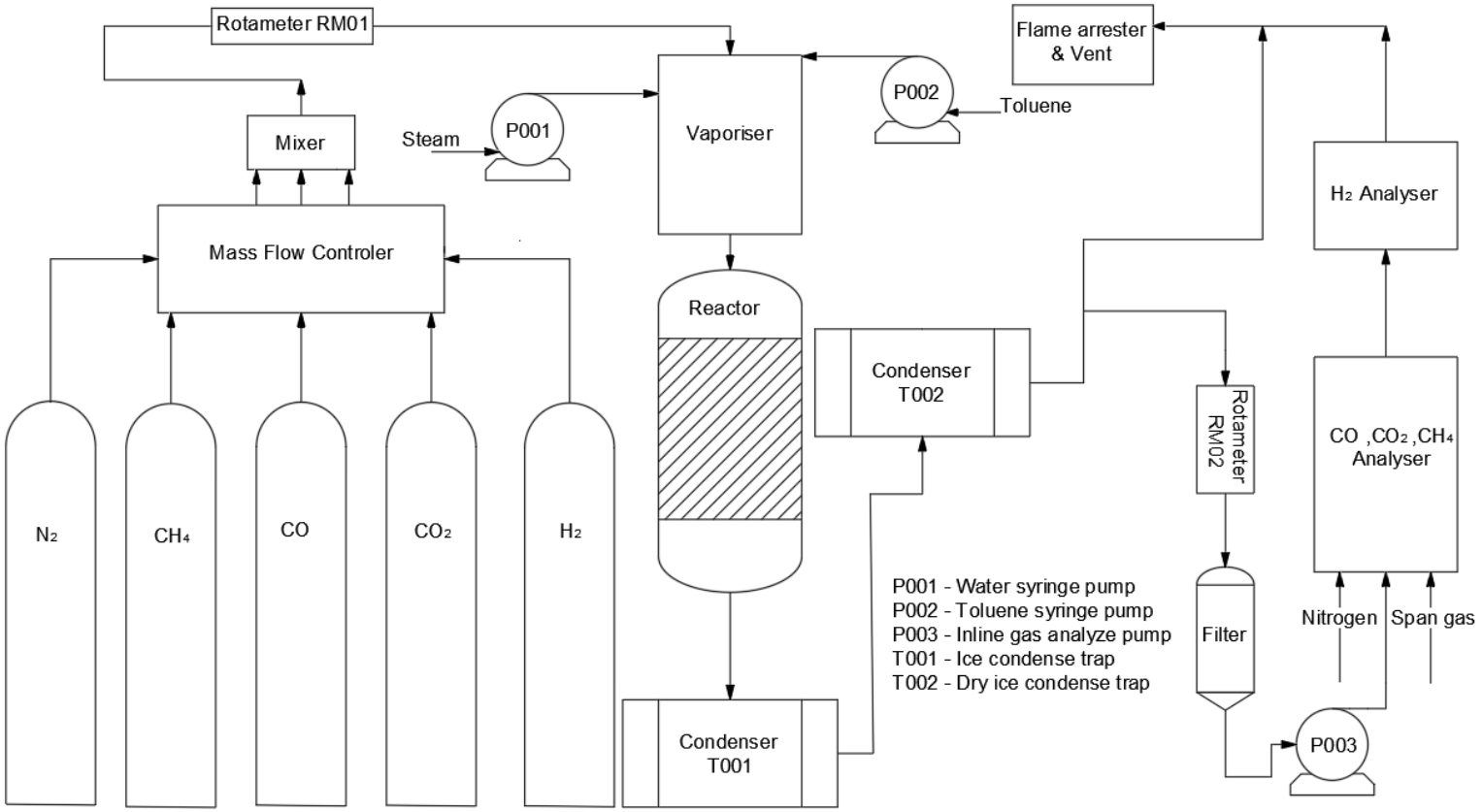

Figure 3.1 Schematic diagram of catalytic toluene steam reforming system.

3.2.1 Material feeding

N_2, H_2, CO, CH_4, CO_2, H_2O and C_7H_8 are mixed and injected from the top of the reactor into the main stream flowing into the preheating zone. All the gases are supplied from gas cylinders at one bar gauge pressure. A flashback arrester was fitted to the mixed gas stream for safety. All the gases pass through a series of valves and a Microprocessor-based Brooks Smart Mass Flow Meter and Controller (supplied by Brooks Instrument) and a controller box to set all the gas channels to desired flow rates. Then the gases are mixed together and enter the reactor with steam and toluene. A flow rotameter was installed to monitor the real time overall inlet gas flow rate before entering the reactor. Toluene, used as tar model compound, steam and carrier gas are all introduced from the top of the reactor. Toluene and steam are injected by two different syringes coupled to Legato 100 syringe pumps (from KD Scientific Inc.) and mixed with carrier gas in the feed section. Then, the mixture flows into the preconditioning chamber to be vaporized.

3.2.2 Fixed-bed reactor

Figure 3.2 shows the structure of the main reaction zone. The Incoloy reactor has an inner diameter of 12 and 2 mm wall thickness with a total length of 253 mm. The detailed chemical composition of this tube material (Incoloy alloy 800) is shown in Table 3.1. A quartz tube of 9 mm inner diameter, 1 mm thick and 300 mm long, is held inside the tube to prevent any catalytic effects of Incoloy material in the reactions. The physical and mechanical properties of quartz provide a suitable reaction environment for the steam reforming reactions. Quartz is inert and has good stiffness, strength and thermal stability. The presence of this quartz tube could further increase its achievable stiffness and

strength to meet the requirements. It could withstand high temperatures as high as 1050 °C and prevent the coke deposition on the tube inner surface to some extent. A high temperature spring is installed in the bottom to hold up the quartz tube to a fixed height.

Table 3.1 Chemical Composition for Incoloy alloys 800 (from Corrotherm International Ltd).

Component	Concentration Range, wt. %
Ni	30.0-35.0
Cr	19.0-23.0
Fe	>39.5.
C	<0.10
Mn	1.5
S	0.015
Si	1.0
Cu	0.75
Al	0.15-0.60
Ti	0.15-0.60

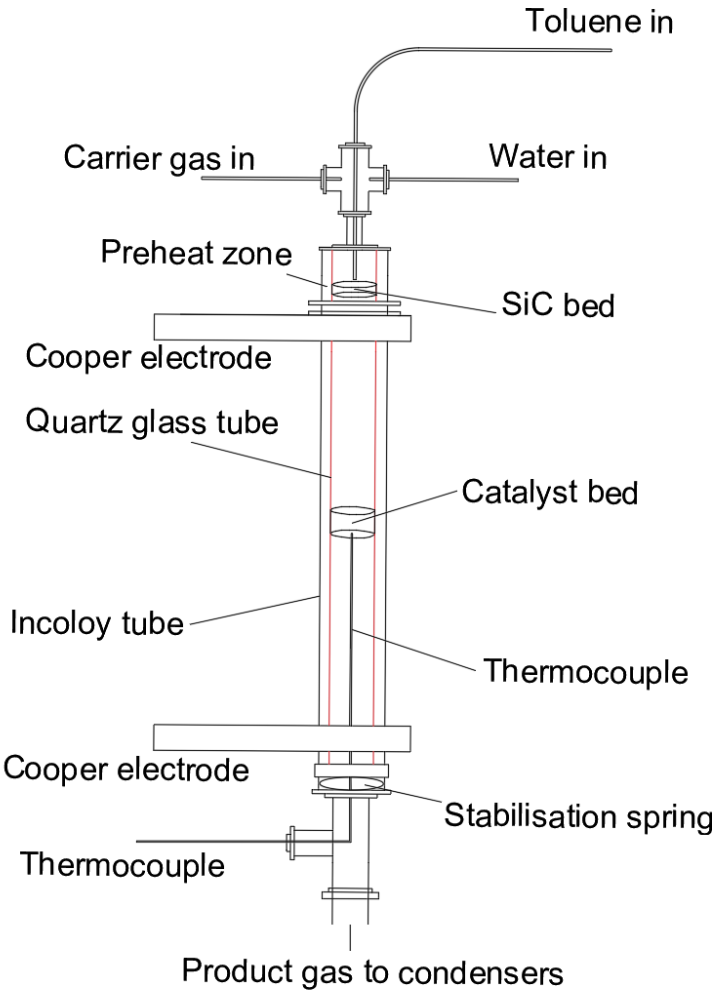

Figure 3.2 Schematic diagram of the reactor used for catalytic toluene steam reforming.

When the main stream entered the reaction zone, it would firstly pass a SiC bed to guarantee a flow uniform distribution and avoid any liquid drop directly into the catalyst bed. Then the reactant flow would enter a quartz liner tube held inside the reactor tube. The temperature along the whole length of the tube was significantly different, so the bottom of the catalyst bed was placed at 120 mm (midway) down the quartz tube, and a thermocouple was introduced into the reactor from the bottom and monitor the real time temperature of the catalyst bed. Another thermocouple was attached to the external surface of the reactor tube to monitor the external surface temperature.

Toluene was injected horizontally to be carried by the main stream into the SiC bed in the preheating zone where it was vaporized at 150 °C. The boiling point of toluene is 110.6 °C, so the temperature of preheating zone toluene could fully vaporize toluene quick and avoid further chemical reactions. A silicon carbide packing weighing 1.0 g is placed in the preconditioning chamber attached to the top of the reactor tube (Figure 3.2) to create an equal distribution of the reactant stream and minimize the risk of tar clots. The catalyst is held by a piece of quartz wool and a stainless-steel wire-mesh plug in the middle of the quartz tube at 120 mm down the reactor tube with a thermocouple sensor to monitor the real-time reaction temperature of the catalyst bed, where the steam reforming reactions take place. The reactor is heated by two copper electrodes which are at the top and the bottom of the tube outer surface. The preconditioning and reaction temperature are controlled by two individual temperature control boxes.

3.2.3 Tar collection

The mixture of products leaving the steam reforming reactor flows continuously into two condensate traps placed in baths containing water-ice (first trap: < −5 °C) and dry-ice (second trap: < −60 °C), as shown in Figure 3.3. This two-stage cooling system aims to separate the liquid products from reforming by their different freezing points. Both traps are U-shaped stainless-steel tubes with an inner diameter of 12 mm. The traps are made of stainless steel 316 because of its corrosion resistance. The first trap, immersed in an ice and water bath, mainly condenses and collects unreacted water, while the second trap condensed by dry ice contains a coiled wire mesh net to filter and retain liquid products. Condensation of the liquid products was directly achieved by immersing the first trap in ice and second trap in dry ice in vacuum flask. The

second trap used a coiled wire mesh net inside as a filter to capture liquid effluent. This coiled wire mesh effectively increased mass and heat transfer along the tap, dispersed the flow and collect liquid products.

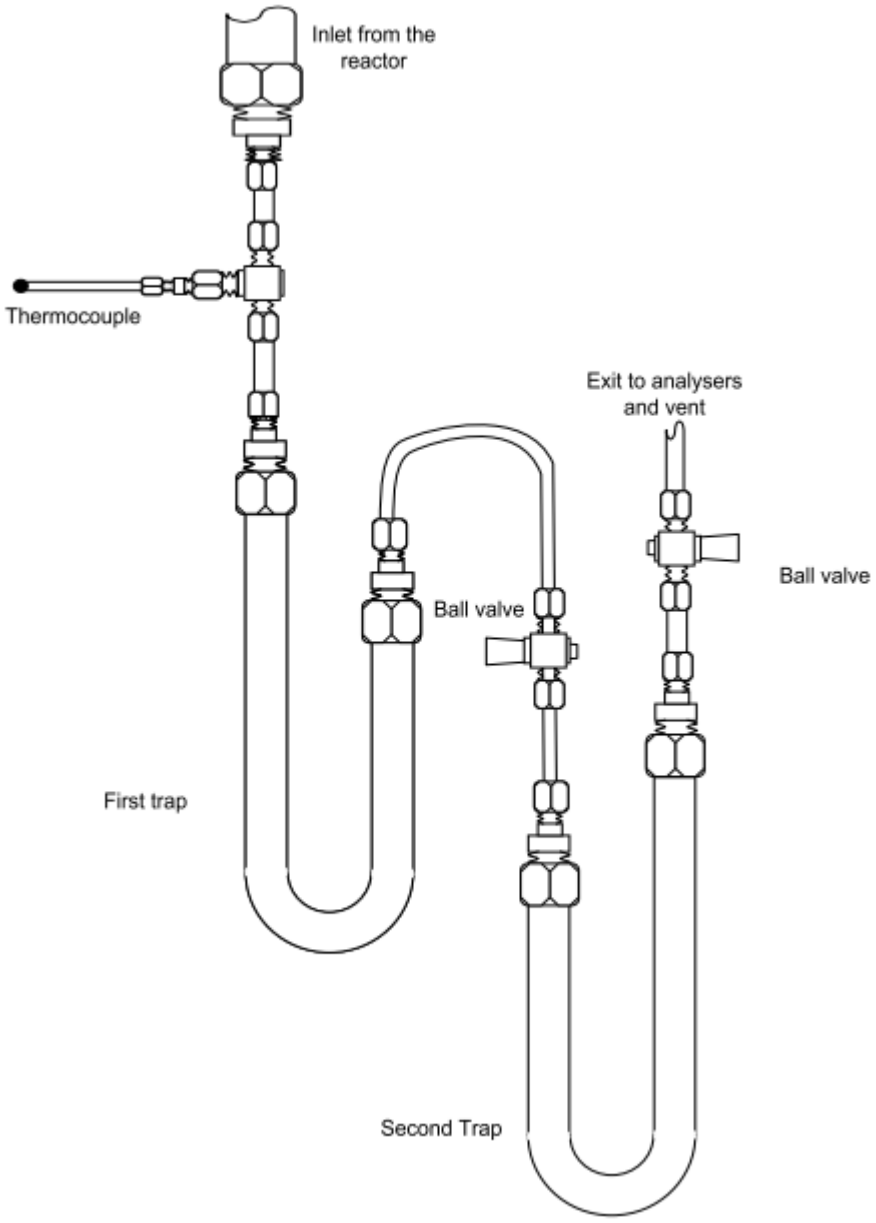

Figure 3.3 Schematic diagram of condensation system.

3.2.4 Gas measurement

The gas leaving the traps and filter was fed through a PTFE hose and

connected to a rotameter. Then the gas flow was split to the gas analysers. The exit of the dry-ice trap is connected to a gas line filter as shown in Figure 3.4 to further remove the water vapor and remaining particles. This filter was filled with the quartz wool and silica gel pellets. The quartz wool was essentially employed to trap any particles. And the silica gel beads were intended to remove any residual moisture before the gas analysers to protect the devices because low moisture and particulate contents would affect the analysis and was harmful to the analysers.

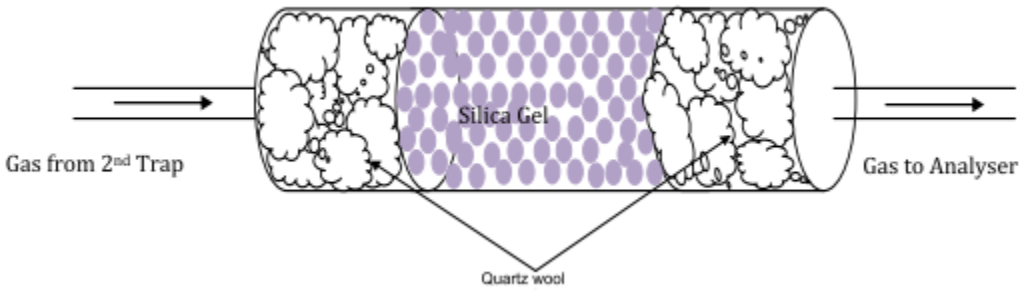

Figure 3.4 Schematic diagram of gas line filter. Reproduced from (Odongo 2015).

The gaseous products after the treatment will be finally analyzed by two online gas analyzers. The gas compositions in production stream can be analyzed after cleaned up by a multi-gas analyzer and a hydrogen analyzer, which was connected to the gas outlet of the reactor.

The concentrations of CO, CO_2 and CH_4 are analyzed online by using an MGA3000 Multi-Gas Analyzer (from ADC Gas Analysis Ltd.) that consists of infrared gas analysis (IRGA) benches. An inline gas analyze pump is built in this analyze to provide a stable and continuous flow of product gas. The generated signal of each type of product gas is proportional to the infrared adsorption of the CO, CO_2 and CH_4. The principles of absorption analyzer system are based all the hetero-atomic gases absorb or transmit light energy

in the infrared region at specific wavelengths are dependent on the chemical structure of each gas. In addition, the absorption level is proportional to the quantity of gas. The absorption level of the produced gas is relevant to the calibration gas concentration.

The MGA3000 was designed specifically for detecting the identified gases within certain ranges with accuracy ± 0.01 vol.%. The detection range 1 for CO is between 0 to 5 vol.%, 0 to 1 vol.% for both of CO_2 and methane. The detection range 2 for CO is 0 to 20 vol.%, 0 to 5 vol.% for both of CO_2 and methane. The gas outlet concentrations are displayed and absorption measurements are recorded by an analogue and digital signal outputs.

Table 3.2 Detection range and accuracy of MGA3000 Multi-gas analyzer.

Gas	Detection range 1	Detection range 2	Accuracy
CO (vol.%)	0 – 5	0 - 40	± 0.01
CO_2 (vol.%)	0 – 5	0 – 40	± 0.01
CH_4 (vol.%)	0 – 1	0 - 5	± 0.01

Figure 3.5 shows the gas flow managements of multi gas analyzer MGA3000. Before the gas can be allocated to various analyzer subunits, it was circulated through a set of polytetrafluoroethylene tubes of the analyzer. An internal fitted diaphragm pump in the analyzer chamber can measure the gas flow rate of the outlet gas production stream. The overall flow rate to the analyser cells was controlled by an adjustable flow meter located after the pump to avoid the influence of the response time on the measurement caused by the overall flow rate inside of the tubes, it could also monitor and adjust the flow rate at infrared sensor. During experiments, the product gas was sampled when the pump

switched on. The flow rate in the gas analysers should stay at 100 mL min^{-1}. When the gas discharged out of the gas analysers, it was directed to the vent together with the by-pass and burnt on a propane burner, a backflow arrestor is connected to the end of the gas line to avoid any backflow from the burning of the fuel gas.

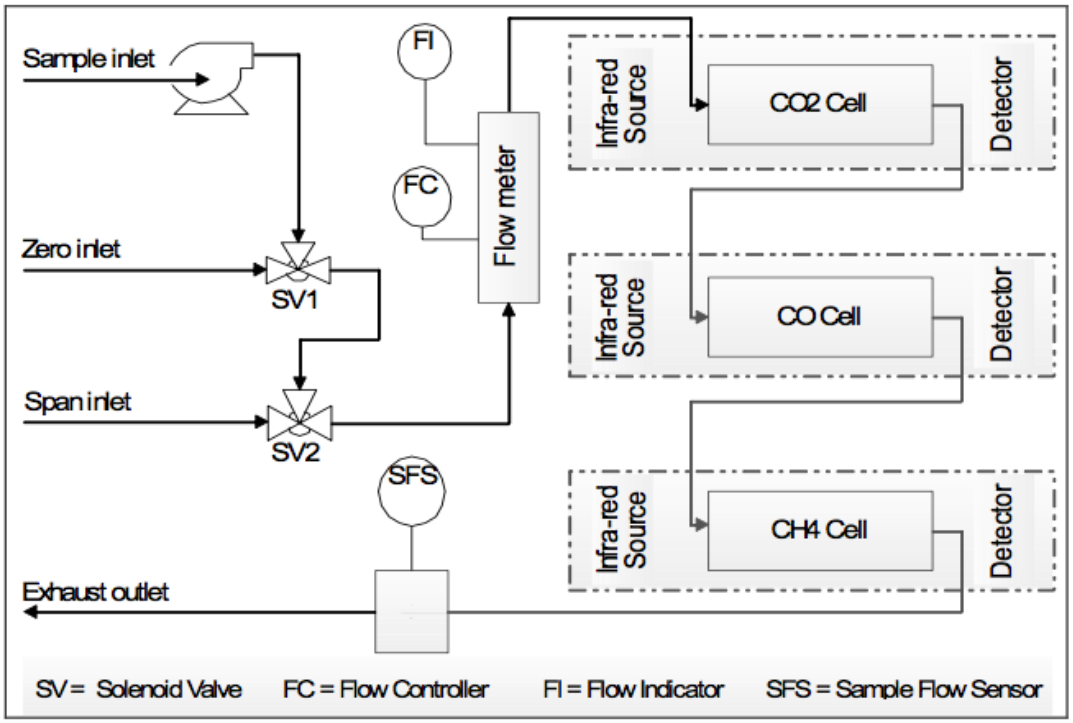

Figure 3.5 The gas flow management of multi gas analyzer MGA3000. Reproduced form MGA 3000 Multi Gas Analyser Operation Manual.

The hydrogen concentration in the gas production stream is analyzed by a K1550 series Hydrogen Analyzer (from Hitech Instruments Ltd.) based on the principle of thermal conductivity. Even though hydrogen in the produced gas stream has higher thermal conductivity when compared with other identified gases, the CO, CO_2 and CH_4 concentrations in the stream could possibly affect the reading of hydrogen concentration.

CO, CH_4 and H_2 gas detectors were placed around the rig, gas cylinders and

the gas analysers. There is also a multi gas detector in the ventilation of the lab. A pressure gage was applied to the top of the reactor, before the reaction stage. Two thermocouples were installed on the outside surface of the reactor and the preheating zone to monitor temperature readings and cut off temperatures at 30 °C above the room temperature.

3.3 Experimental Procedure

This section describes two similar procedures followed during experiments. The procedures could be separated into 5 steps including rig assembly, leakage test, heating up and feeding, reaction and shut down. The first procedure was followed to conduct experiments without catalyst bed, the second procedure was followed to conduct tests with a catalyst bed inside the reactor.

3.3.1 Experiments Without Catalysts

A piece of a circular wire mesh was weighed and placed in the preheating zone to form a bed. The preheating chamber was tightly attached on top of the reactor tube and a weighed quantity (1.0 g) of silicon carbide crystals was placed on the wire mesh. A weighed quartz tube with a piece of wire mesh was placed halfway down inside the metal reactor tube. A high temperature spring was placed at the bottom of the incoloy tube to hold the quartz tube. A thermocouple was applied to maintain a steady and uniform bed temperature with its sensor positioned at the middle of the catalyst bed (right at the mesh plug). The main reactor body (incoloy tube) was then placed between two copper electrodes, and the whole reaction unit was set up with controlled electric power system, and connected to the material feeding system by its top

and cooling traps by its bottom end. The first cooling trap was connected directly below the reactor and its other exit was connected to the second tar trap. The outlet from the second trap was connected to the ventilation and the multi-gas analyser. The tar traps used a water-ice bath and and dry-ice Dewar respectively to collect liquid products.

Before each experiment, the whole experimental lines, reactor, traps were purged with nitrogen for 10 minutes to create an inert atmosphere and remove any remaining air in the system. Then, a leakage test was conducted to prevent any gas escaping to the lab.

After the leakage test, a controlled flow of N_2 (flowrate varied according to the experiment requirement) started to flow into the system and the reactor was heated to the desired temperature. Once a steady setpoint temperature was reached, the two pumps of water for steam generation and toluene injection turned on. Steam and toluene were injected to the preheating zone and got vaporized at 150 °C in the nitrogen environment. The software started to collect data (product gas concentrations) when the reactant injection started. As no catalysts were used and atmospheric pressure was applied, the product gas then left downstream of the reactor and the condensate traps and analysed in the gas analysers. After finishing the experiment, the two syringe pumps for water and toluene injection stopped feeding, the electric heating unit was switched off and the system was allowed to cool to room temperature. The nitrogen flow rate was set to 100 mL min^{-1} through the process and the cooling traps were kept in their coolants until the reactor cooled down to room temperature. Then the rig was disassembled, the traps were removed from the coolants to warm up to room temperature. The two tar traps were rinsed with 4:1 chloroform and methanol solvent to extract products, and the obtained solution was put into a rotary evaporator at atmospheric pressure to remove

access water and solvent. The remained liquid product was then analyzed by gas chromatography/mass spectrometry (GC/MS). The coke and other solid products were recovered from the catalyst bed and the preheating chamber. The liquid product and the remained solid were then weighted to calculate mass balance and carbon balance.

3.3.2 Catalytic Experiment Procedure

When a catalyst bed was used in the experiments, the procedure to set up the process was similar with the tests without catalyst. The main differences are described below.

A weighed piece of circled wire mesh was placed 160 mm from the top the quartz reactor sleeve as a plug to hold the catalyst bed, while a weighed piece of quartz wool was placed below the wire mesh to prevent any small catalyst particles (> 200 μm) from dropping down. The wire mesh plug and quartz wool was held in position by the quartz tube wall and supported by the thermocouple from the bottom. A weighted amount of catalyst was placed on top of the wire mesh plug and the quartz tube was placed inside the reactor incoloy tube. After setup and leakage test, the reactor was purged with N_2 to remove air. The catalyst was reduced under 50 mL min^{-1} of H_2 up to 700 °C for 1 hour before each test. After that, the temperature was set to the desired reforming value. When the temperature reached set point, the inlet gas was then switched to reaction gas. The outlet pressure of each gas channel should be ~1.5 bar. The injection of steam and toluene started simultaneously when the reading of each analyzer stayed stable for at least 5 min. The software started to collect data (product gas concentrations) when the reactant injection started, and the gas concentration was recorded continuously for 5 hours.

After finishing the experiment, the feeding of toluene and water stopped and the controller box of heating copper electrodes were switched off, the carrier gas was switched to 100 mL min^{-1} pure N_2 until the reactor was cooled down to room temperature. The catalyst was recovered; and all other products from the experiment were recovered followed the procedures described in Section 3.3.1.

3.4 Analytical methods

3.4.1 Thermal gravimetric analysis (TGA)

A PerkinElmer Pyris 1 thermal gravimetric analyzer was used to analyze the carbon deposition after each experiment through temperature programmed oxidation. Comparing the different oxidation characteristics between the reacted catalysts obtained from different conditions, the results could identify the amount and different types of carbon deposited. Amorphous carbon is oxidized at lower temperature compared with the filamentous carbon since the filamentous carbon has a higher thermal stability. The weight loss of the reacted catalyst is due to the oxidization of deposited carbon on the catalyst surface.

the First, the spent catalyst was placed in the crucible that was fitted in the furnace of TGA. The furnace of TGA was purged by 40 mL min^{-1} nitrogen flow at 50 °C for 15 mins. Then, the carbon sample needs to be heated up to 900 °C at a ramp rate is 10 °C min^{-1} in air flow rate is 40 mL min^{-1} following with 30 min holding time. Thirdly, the gas flow can be switched to nitrogen again at 40 min^{-1} flow rate for cooling down. Comparing the different oxidation characteristics between the reacted catalysts obtained from different experimental conditions, the results could help identify the different phases of carbon deposition.

3.4.2 Gas chromatography/mass spectrometry (GC/MS)

An Agilent HP6890 gas chromatography/mass spectrometry (GC/MS) coupled with a 30 mm long and 0.25 mm inner diameter BPX5 column. GC/MS analysis could be used to identify the organic compounds of tar production, as it combines the features of gas chromatography and mass spectrometry to identify different substances within a sample component matrix (Daferera, Ziogas et al. 2000). GC/MS can analyze volatile and semi-volatile compounds. Liquid and gas compounds can be analyzed by direct injection into gas chromatography. All the samples are vaporized for identification and quantification. The carrier gas is helium at a constant flow rate of 1 mL min^{-1}. The column oven is heated up from 50 to 300 °C at a ramp rate 10 °C min^{-1} and held at 300 °C for 2 min.

3.4.3 Brunauer–Emmett–Teller (BET) analysis

N_2-adsorption-desorption analysis was conducted in a TriStar 3000 V6.07 A analyzer. BET method was used to calculate the surface area of the catalyst. BET method is based on the physical adsorption of gas molecules (N_2) on a solid material surface, and serves as the basis for the measurement of the specific surface area of the catalyst or the support. It is reported that BET method is a common method for determining the internal and external surface area of the mesoporous materials (Brunauer, Emmett et al. 1938, Bartholomew and Farrauto 2011). The total pore volume of the mesoporous catalysts can be determined from N_2 adsorption isotherms. Before the analysis, the catalyst was degassed at 150 °C for 4 hours in vacuum.

3.4.4 Equilibrium simulation

ASPEN software package (ASPEN v8.4) was used to determine the thermodynamic equilibrium of the toluene reforming reactions over the different reaction conditions. An ideal property method, a RGIBBS reactor (based on Gibbs free energy minimization) was selected to investigate the thermodynamic equilibrium. Material flows into the reactor are identical to those from the related experiments performed in lab scale system.

3.5 Preliminary tests and experimental repeatability

Preliminary tests were conducted to test the stability and reliability of the reactor. A commercial 5% Ni_2O_3/Al_2O_3 catalyst was used in the preliminary experiments to evaluate the ability of the system and the effect of parameters, the total pore volume is 0.50 $cm^3\ g^{-1}$, BET surface area is 196 $m^2\ g^{-1}$, average pore diameter is 8.07 nm. (Odongo 2015).

The performance of catalysts was evaluated by the conversion into gaseous products (based on a carbon balance between the inlet and the outlet stream of the reactor), selectivity to main products (where "i" is CO_2, CO and CH_4 in moles) and hydrogen yield, which were defined as follows:

$$\%\ \text{Carbon Conversion} = \frac{\text{C in the gas product}}{\text{C fed into reactor}} * 100 \qquad (22)$$

$$\%\ \text{"i" selectivity} = \frac{\text{"i" produced in moles}}{\text{C atoms in the gas products}} * 100 \qquad (23)$$

$$\%\ \text{"i" yield} = \frac{\text{"i" produced in moles}}{\text{C atoms in toluene}} * 100 \qquad (24)$$

3.5.1 Preliminary test parameters

It is suggested by previous study of the group that the suitable concentration in N_2 should be 100g Nm^{-3}, as typical biomass tar in gasification product gas is lower than this value (Odongo 2015).

A thermodynamic simulation was performed using ASPEN software package to understand the influence of temperature on toluene steam reforming. The results presenting the concentration of each gas species as a function of reforming temperature between 350 and 1100 °C are shown in Figure 3.6. Toluene was fully converted into gas at all temperatures, CO concentration increased with increasing temperatures, while CH_4 concentration decreased to 0 at 650 °C and remained 0 at higher temperature. H_2 concentration reached the highest also at 650 °C and then descended slightly when temperature increased. The trends of CO, CO_2, H_2O and H_2 concentrations at 650 °C and higher temperatures were mainly dominated by the WGS reaction. According to equilibrium results, the reforming temperature of toluene should be higher than 650 °C to achieve complete CH_4 conversion. Therefore, the most suitable experimental temperature range for toluene steam reforming is found to be between 650 and 900 °C.

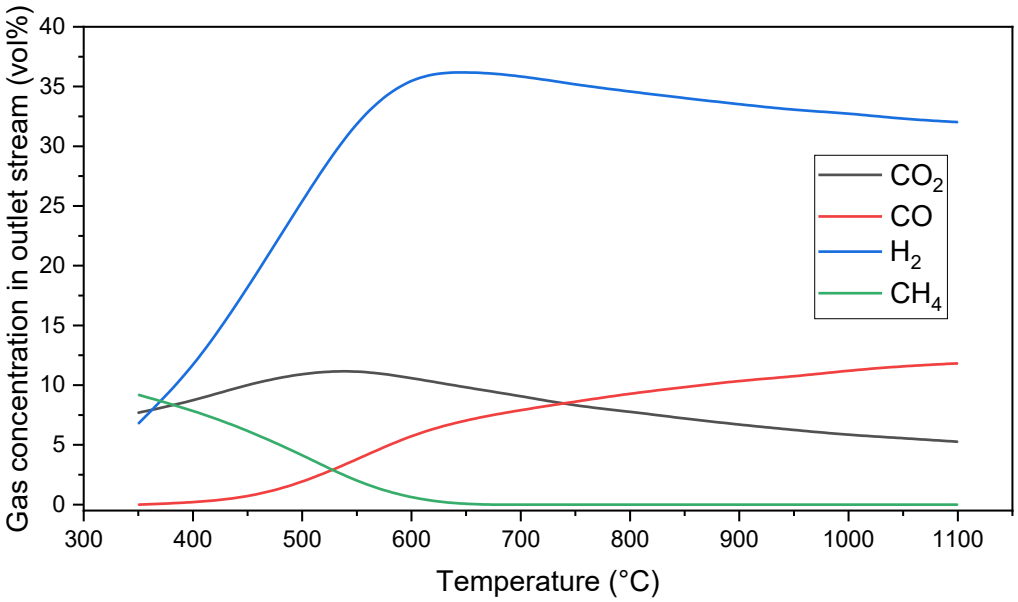

Figure 3.6 Product gas concentration from toluene steam reforming as a function of temperature in thermodynamic equilibrium calculations. (100 g Nm^{-3} toluene in nitrogen, S/C ratio of 3, 1 bar)

A thermodynamic simulation was performed to understand the influence of S/C ratio on toluene steam reforming, the result presented the function of S/C ratio ranging from 0 to 5 as shown in Figure 3.7. Toluene was fully converted into gas when S/C ratio was 1 or higher, CO_2 and H_2 concentration increased with the increasing of S/C ratio, while CO concentration decreased at the same time. According to equilibrium results and literature study, the suitable S/C ratio of toluene steam reforming is between 1 and 3 (Guan, Kaewpanha et al. 2016, Gao, Salisu et al. 2021).

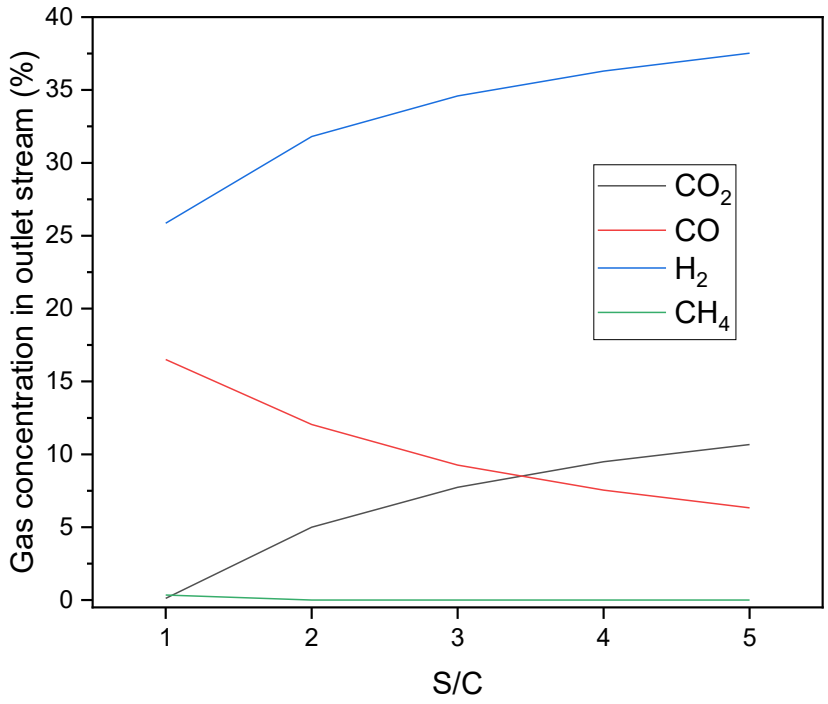

Figure 3.7 Product gas concentration from toluene steam reforming with different S/C ratios in thermodynamic equilibrium calculations. (100 g Nm^{-3} toluene in nitrogen, S/C ratio of 3, 1 bar)

Table 3.3 Parameters of toluene steam reforming for preliminary test

Toluene flow rate	1.38 mL h^{-1}
N_2 flow rate	200 mL min^{-1}
Steam flow rate	4.91 g h^{-1}
Catalyst	1.0 g
GHSV	15,300 h^{-1}
WHSV	16.85 h^{-1}

For the preliminary test, the temperature and S/C ratio was fixed at 800 °C and

3 respectively according to equilibrium simulation. Table 3.3 shows the parameters for preliminary test.

3.5.2 Blank test

A set of preliminary tests was conducted for the blank test conditions (steam reforming test without catalyst), and a series of commercial Ni_2O_3/Al_2O_3 catalyst was used to analyze the reliability and repeatability of the experimental system and evaluate the sufficient process control over the whole experiments. The blank test could also help to understand the performance of catalyst on reforming process when comparing to catalytic reforming results. A continuous flow of feeding materials and steady product trends should be achievable and the results were expected to be reproducible.

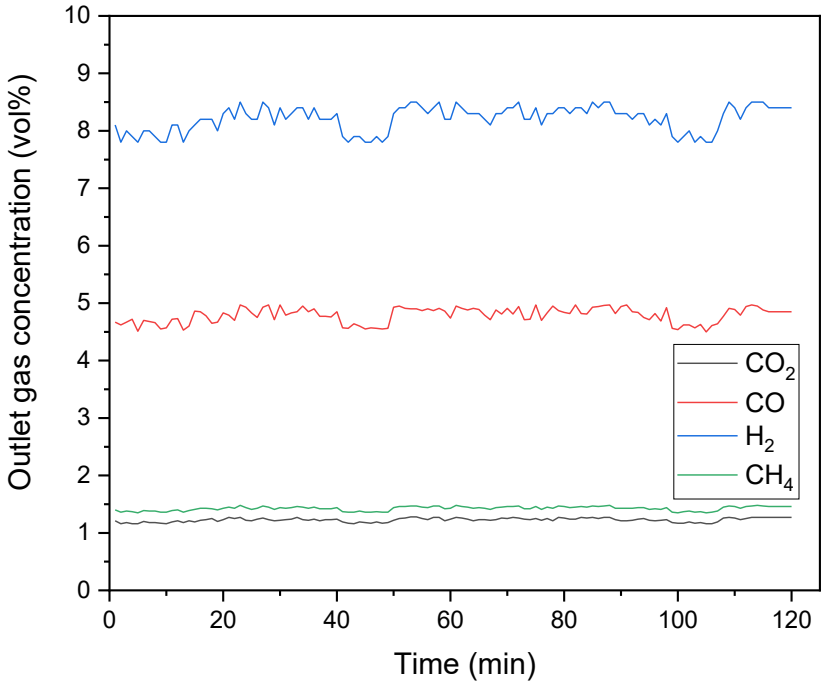

Figure 3.8 Gas product concentration from a blank test of toluene steam reforming (non-catalyst, S/C ratio: 3, 800 °C).

Figure 3.8 presents a test conducted in a blank reactor at a steady temperature of 800 °C for 120 min. The gas concentrations remained mostly steady throughout the 120 min. However, the slight variation of CO and CO_2 concentration in the function of time still makes the trend not easy to understand. These slight variation occurred because the sample cell of the gas analyzers purged every minute automatically and fluctuated the gas concentration data. Figure 3.9 shows the average gas concentration every 20 min, each gas concentration stayed stable in 120 min. This reveals the controllability and reliability of the feed system.

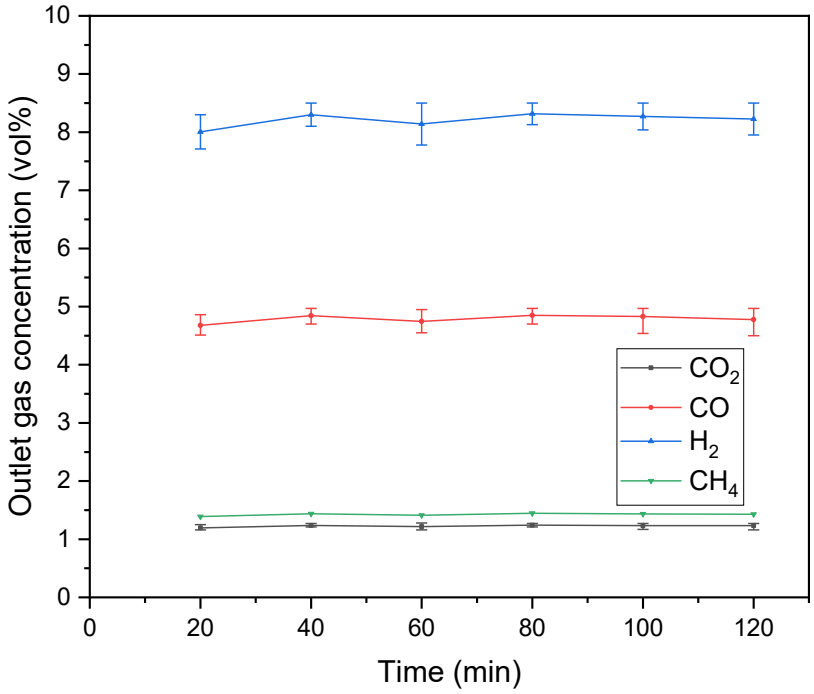

Figure 3.9 Gas product average concentration every 20 min from a blank test of toluene steam reforming (S/C ratio: 3, 800 °C, GHSV: 13440 h^{-1})

The blank test (non-catalyst test) for toluene steam reforming was repeated to further investigate the repeatability and reliability of this experimental system. Table 3.4 shows results of four total runs of the non-catalyst test, CO_2, CO, CH_4

and H_2 was remained steady in all four runs. These results show good control and ability to reproduce data.

Table 3.4 Product gas yields from repeated blank tests (non-catalyst, S/C ratio: 3, 800 °C)

Non-catalyst	CO_2 yield (%)	CO yield (%)	CH_4 yield (%)	H_2 yield (%)
1st run	8.9	34.5	10.3	22.2
2nd run	8.7	34.6	9.8	21.8
3rd run	9.2	33.6	10.5	22.3
4th run	9.1	35.1	10.4	22.4
Average	9.0	34.5	10.3	22.5
Error ±	0.03	0.02	0.03	0.01

3.5.3 Preliminary catalytic test

Figure 3.10 shows the results of product gas concentration from toluene steam reforming using a commercial 5% Ni_2O_3/Al_2O_3 catalyst. The parameters in this catalytic test remained the same to the previous non-catalyst test (S/C ratio: 3, 800 °C, toluene: 100g Nm^{-3} in N_2). The presence of catalyst increased CO, CO_2 and H_2 yield significantly, while CH_4 yield decreased to 0. This commercial Ni_2O_3/Al_2O_3 catalyst could increase syngas production and toluene conversion. The average gas concentration every 20 min results of this catalytic test are shown in Figure 3.11.

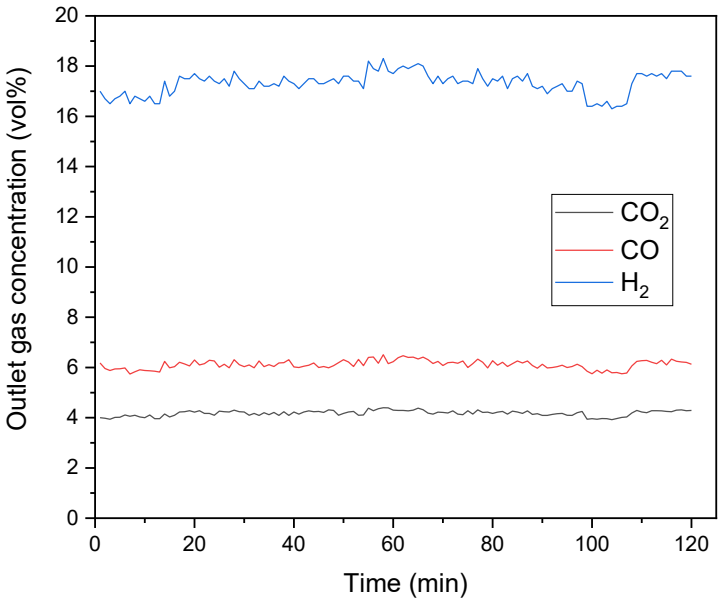

Figure 3.10 Gas product yields from toluene steam reforming using Ni_2O_3/Al_2O_3 catalyst (S/C ratio: 3, 800 °C, GHSV: 13440 h^{-1}).

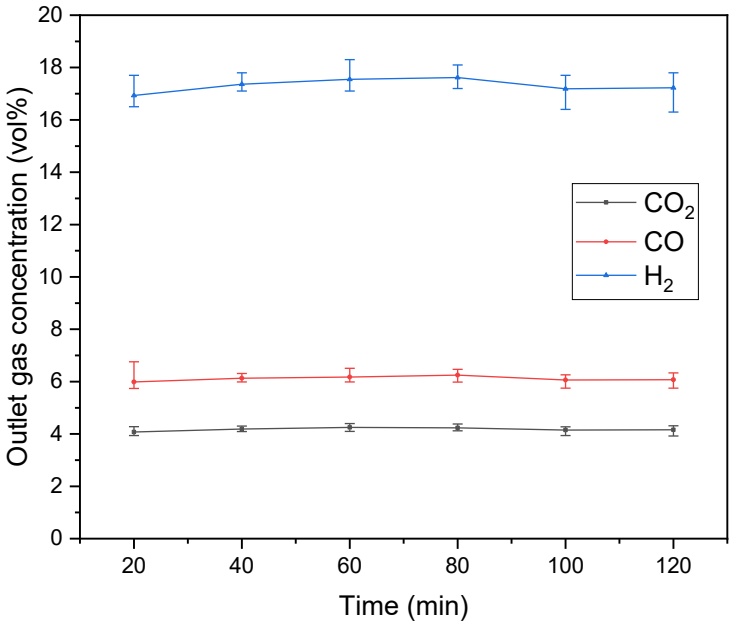

Figure 3.11 Gas product average concentration every 20 min from toluene steam reforming using Ni_2O_3/Al_2O_3 catalyst (S/C ratio: 3, 800 °C, GHSV: 13440 h^{-1}).

The gas yields of the repeated catalytic toluene steam reforming tests are presented in Table 3.5. CO_2, CO, CH_4 and H_2 yield was observed to be stable in all the repeated tests, the catalytic toluene steam reforming test also has a good repeatability and reliability.

Table 3.5 Product gas yields from repeated catalytic tests (Ni_2O_3/Al_2O_3 catalyst S/C ratio: 3, 800 °C, GHSV: 13440 h^{-1}).

Ni_2O_3/Al_2O_3	CO_2 yield (%)	CO yield (%)	CH_4 yield (%)	H_2 yield (%)
1st run	35.9	50.2	0	55.5
2nd run	36.9	49.6	0	56
3rd run	34.2	48.6	0	54.5
4th run	36.2	51.1	0	55.6
Average	45.8	49.8	0	55.4
Error ±	0.03	0.03	0	0.02

3.5.4 Mass balance and gas production

The mass balance and carbon balance were calculated for each experiment to represent the reliability. The overall mass balance was calculated by the equation below:

$$Overall\ mass\ balance = \frac{total\ weight\ of\ gas, liquid\ and\ solid\ product\ (g)}{total\ weight\ of\ materials\ fed\ to\ the\ system\ (g)} * 100\%$$

In most of the conducted experiments, the overall mass balance was less than

100%, which might be due to: (1) A limited amount of unreacted water and other liquid products vaporized and flowed out of the condenser. The experiments lasted for 5 hours, and another 1 hour to cool down and disassemble, the liquid products collected in the cooling trap could have vaporized and flowed out with the carrier gas stream. (2) The total amount of gas might not be that accurate. The gas analysers recorded the data of gas concentrations every 60 seconds, but the gas concentrations sometimes changed sharply in the first 10-20 min. It gave an error when calculating the total amount of gas products. (3) The amount of coke deposition value might be less than it was. Carbon black was found on the internal surface of the quartz tube after the experiments, the amount of this carbon black was very low but it was extremely difficult to remove, collect or measure.

In most of the experiments, the gas product was over 90% of the total product weight. The liquid phase product contains >95% unreacted toluene in all the experiments according to GC/MS result. In this project, the overall mass balance of all the experiments was between 95% and 102 %.

The carbon balance was calculated from the equation below:

$$Carbon\ balance\ = \frac{C\ in\ product\ gas, liquid\ and\ coke}{total\ C\ fed\ to\ the\ system\ (g)} * 100\%$$

A carbon balance of 99% was obtained for the preliminary experiment at 800 °C using nitrogen as carrier gas. To obtain reliable experimental results, the carbon balance of all the experiment results presented in this thesis is 100 ± 2%.

The “i” product yield (where “i” is CO_2, CO and CH_4) in the unit of mol mol $_{toluene}^{-1}$ was calculated from the equation below:

$$\text{"i"}\ yield = \frac{N_2\ fed\ in\ moles}{N_2\ concentration\ in\ outlet\ gas} * \frac{i\ concentration\ in\ outlet\ gas}{toluene\ fed\ in\ moles}$$

In this project, all the experiments in Chapter 4,5 and 6 have been repeated at least once, all the results including CO, CO_2, H_2, CH_4 yield, selectivity, production rate (yield), conversion have a relative error < ± 2%.

3.6 Sources of errors, uncertainty and accuracy of materials

Calibration gas and product gas: contained 20% hydrogen, 5% CO_2, 1% CH_4 and 20% CO in nitrogen, the accuracy of the calibration gas specified by the supplier was ± 2% of the certified values, N_2 (99.995% purity), H_2 (99.99% purity), CH_4 (99.8% purity), CO (99.9% purity), CO_2 (99.9% purity) all the cylinders were kept the same condition with the same regulators throughout the entire project in order to maintain consistency.

Table 3.6 Calibration and Product Gas degree of accuracy.

Cylinder	CO_2 (%)	CO (%)	CH_4 (%)	H_2 (%)
Calibration gas Conc.	5	20	1	20
Accuracy	0.1	0.4	0.02	0.4
product gas Conc.	1	5	1	20
Accuracy	0.02	0.1	0.02	0.4

Mass flow controller: The accuracy of a single mass flow controller unit itself is ± 1%, and some of the mass flow controller units has been calibrated for specific gases, including N_2, H_2, the other mass flow controller units were recalibrated for the gas used in this project. A maximum error was estimated for a mixture

of different gases. The mass flow controller unit was charged with a 0 - 5 V signal with an accuracy of ± 1.2 mV and theoretical resolution of 12 bit. In repeated tests with a bubble column, the controller was found to give an error of approximately 1 mL min^{-1} when set point was higher than 100mL min^{-1}.

Toluene feed and water feed syringe pumps: Calibration on these two pumps by measuring the amount of water against time has conducted and concluded that they both had a same accuracy of ± 0.5%. These two syringe pumps were used throughout this project to prevent any change in accuracy.

Temperature measurement: the preconditioning zone, reactor surface and catalyst bed temperatures were measured by using K-Type thermocouples (from TC Ltd.) with an accuracy of 2%. During the experiment process, the temperatures from the catalyst bed to the top of the reactor and to the bottom of the reactor were shown to have a low temperature difference at lower temperatures and a higher temperature difference at higher temperatures.

Online gas analysers: The precision of each of the analysers used was given as 1%, while it was also affected by the accuracy of the calibration gas. The overall estimated absolute error for each gas is shown in Table 3.7.

Table 3.7 Absolute Gas limits of gas accuracy.

Gas measured	CO_2	CO	CH_4	H_2
Absolute limits of accuracy (concentration %)	± 0.011	± 0.014	± 0.012	± 0.014

4 Influence of Main Reaction Parameters on Toluene Steam Reforming

4.1 Introduction

This chapter presents a series of results from experiments from toluene steam reforming using a conventional Ni/Al_2O_3 catalyst. This benchmark system was investigated in steam reforming of toluene as a biomass gasification tar model compound to explore the effect of reforming temperature, steam to carbon (S/C) ratio and residence time on toluene conversion and gas products.

The steam reforming temperature was concluded to have a significant influence on toluene conversion since higher temperature could increase syngas production and conversion from toluene to gas products (Bona, Guillén et al. 2008). When reforming is envisaged as a downstream tar upgrading unit after gasification, the most interesting temperature interval for atmospheric reforming is between 600 and 900 °C, since the gasification effluent temperature will normally be lower than 900 °C (Quitete, Bittencourt et al. 2014). Research also suggested that high temperature might reduce H_2 yield as the reverse WGS reaction is favored due to its endothermic nature (Stroud, Smith et al. 2018, Yang, Pastor-Pérez et al. 2018, Zhu, Zhang et al. 2019).

Steam as a principal reactant in catalytic steam reforming is widely recognized to have a strong influence on H_2 production. Steam could be involved in most of the reactions in toluene experiments and steam to carbon ratio was chosen as other important key factor to study for this reaction in this project. A high steam partial pressure improves gasification reactions and moves water–gas shift equilibrium towards hydrogen production, while the partial pressure of toluene in the gas stream is lower due to dilution as the S/C ratio rises (Stroud,

Smith et al. 2018). Researchers suggested that suitable S/C ratios to investigate the catalyst performance were mostly between 1 and 4 (Frusteri, Freni et al. 2004, He, Hu et al. 2018). Although steam is a main reactant in the reforming process, in the experiment too much excess water could be condensed into ice in the cooling trap and block the system. It is also reported that the saturation of the catalyst surface by steam at high S/C ratio would not favor the conversion of toluene or H_2 production (Li, Wang et al. 2018).

Residence time is another key factor in catalytic steam reforming process. Literature suggests that suitable GHSVs for steam reforming were mostly between 10000 and 70000 h^{-1} over different catalysts (Frusteri, Freni et al. 2004, He, Hu et al. 2018). For our benchmark catalyst, tests were carried out with 500 mg of catalyst, fixed temperature (800 °C) and S/C ratio of 3 during 5 hours of reaction. The feeding rates of toluene, steam and N_2 were changed according to the desired GHSV.

The results in this chapter were obtained from the reactor described in Chapter 3 and are compared with thermodynamic results to assess how close the experimental reactions are from equilibrium.

4.2 Experimental Conditions

The experimental conditions used for studying the effect of different reforming temperature, S/C ratio and GHSV are shown in Table 4.1, Table 4.2 and Table 4.3, respectively. The toluene steam reforming performance was evaluated by the conversion into gaseous products. Toluene conversion and H_2 production are influenced by experimental conditions and parameters. Reforming temperature, S/C ratio and residence time are reported to be the key factors that would affect the total conversion and H_2 yield (Quitete, Bittencourt et al.

2014, Gao, Liu et al. 2015, Koike, Li et al. 2015). In this chapter, S/C ratios of 1, 2 and 3; temperatures of 700, 800, and 900 °C; and GHSV of 30600, 61200, 91800, and 122400 h^{-1} were investigated.

Table 4.1 Experimental conditions for different reforming temperature.

Reforming parameters	Value
S/C ratio	3
GHSV	61,200 h^{-1}
Carrier gas flow rate	200 mL min^{-1}
Toluene injection rate	1.38 mL h^{-1} (13 mmol h^{-1})
Catalyst	500 mg Ni/Al_2O_3

Table 4.2 Experimental conditions for different reforming S/C ratio.

Reforming parameters	Value
Temperature	800 °C
GHSV	61,200 h^{-1}
Carrier gas flow rate	200 mL min^{-1}
Toluene injection rate	1.38 mL h^{-1} (13 mmol h^{-1})
Catalyst	500 mg Ni/Al_2O_3

Table 4.3 Experimental conditions for different reforming GHSV

Reforming parameters	Value
Temperature	800 °C
S/C ratio	3
Carrier gas flow rate	100 - 400 mL min^{-1}
Toluene injection rate	0.69 - 2.76 mL h^{-1} (6.5 - 26 mmol h^{-1})
Catalyst	500 mg Ni/Al_2O_3

4.3 Textural properties of the synthetized catalyst

The N_2 adsorption-desorption isotherm of calcined Ni/Al_2O_3 catalyst is shown in Figure 4.1, which shows a type IV isotherm with a characteristic hysteresis loop for mesoporous materials. The average pore width was 9.1 nm, the total pore volume was 0.35 cm^3 g^{-1} and BET Surface Area was 153 m^2 g^{-1}. Textural properties are actually governed by the primary support alumina which provides mechanical and thermal stability as well as high surface area.

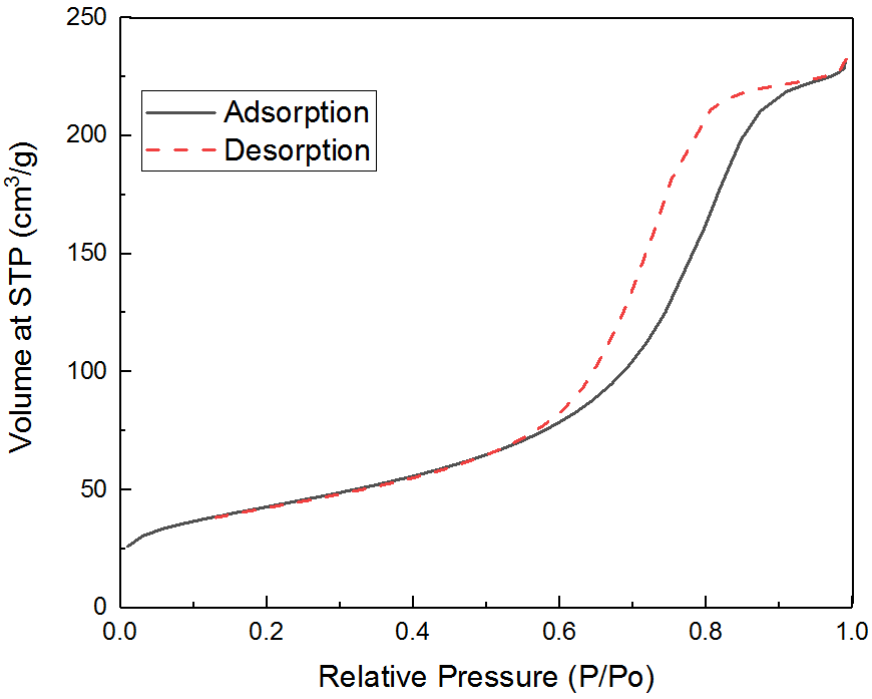

Figure 4.1 Nitrogen adsorption-desorption isotherm of calcined Ni/Al_2O_3 catalyst.

4.4 Influence of reforming temperature on toluene steam reforming

These tests were performed to investigate the effects of reforming temperature on the steam reforming of toluene by analyzing the changes in the product suite. The experiments of the set temperatures were repeated twice and their average was used to represent the data.

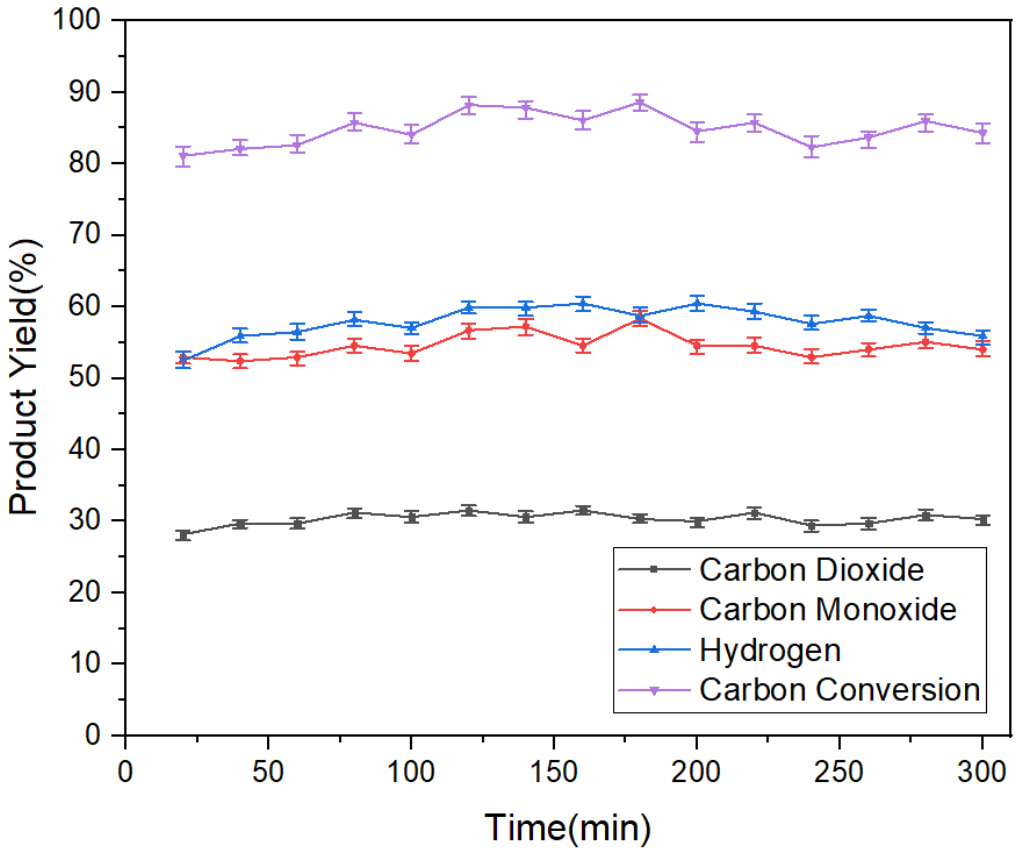

Figure 4.2 Product yield trend of toluene steam reforming at 700 °C in 5-hour test (Ni/Al_2O_3 catalyst, S/C ratio: 3, GHSV: 61200 h^{-1}).

Figure 4.2, Figure 4.3 and Figure 4.4 present the product gas yield trends as a function of time in the 5-hour test of toluene steam reforming at 700, 800 and 900 °C respectively. Very limited amount of CH_4 (yield< 0.1%) was observed in the gas product throughout the 5-hour tests at all temperatures. All these three conditions showed very steady product yields of CO_2, CO and H_2, no obvious drop of any gas product yield throughout the reforming test was observed.

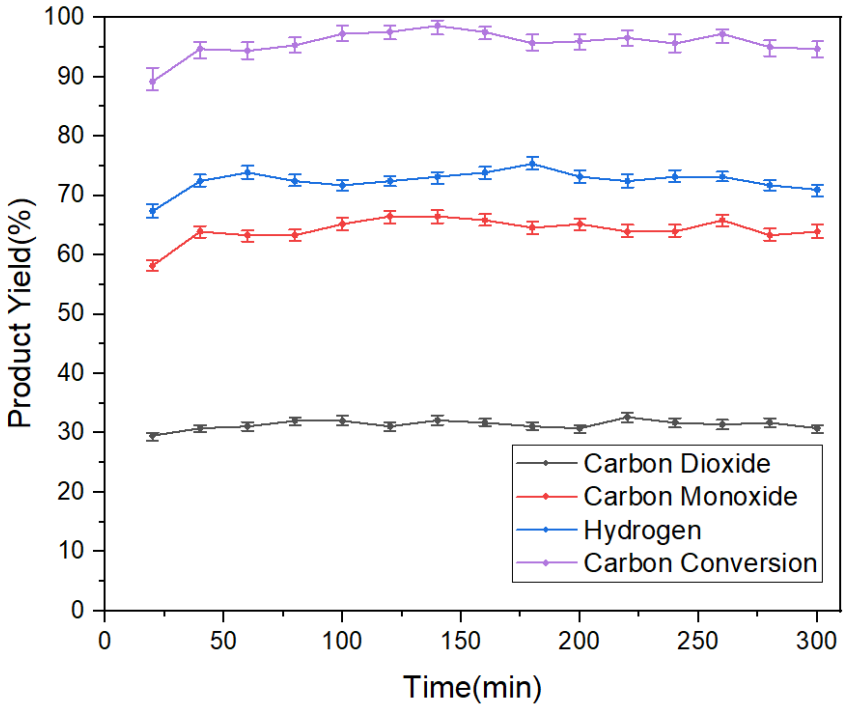

Figure 4.3 Product yield trend of toluene steam reforming at 800 °C in 5-hour test (Ni/Al_2O_3 catalyst, S/C ratio: 3, GHSV: 61200 h^{-1}).

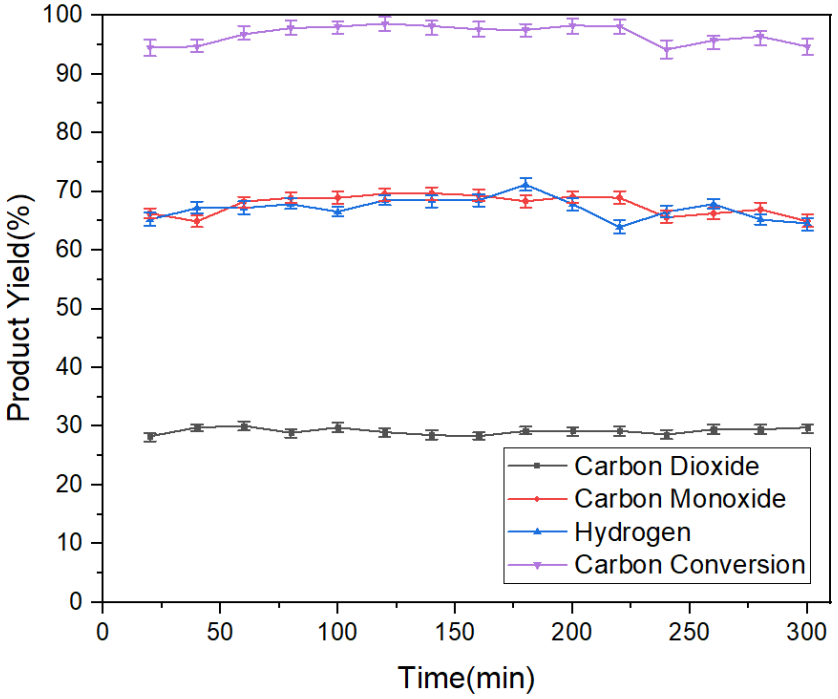

Figure 4.4 Product yield trend of toluene steam reforming at 900 °C in 5-hour test (Ni/Al_2O_3 catalyst, S/C ratio: 3, GHSV: 61200 h^{-1}).

Figure 4.5 concludes the toluene conversion and CO_2, CO yields (based on conversion to C-containing gases) at the three different temperatures in a steady-state within the 5 hours of reaction and compares with equilibrium result. CO and CO_2 were the main gases. The experimental yield of CH_4 at all temperatures was under 0.1%. Conversion and selectivity of the gases approached that of thermodynamic equilibrium as temperature increased. Thermodynamic equilibrium predicts total toluene conversion and no CH_4 production at 700 °C or higher temperatures. At 700 °C thermodynamic equilibrium indicated a CH_4 yield of 1.1%, and for higher temperatures only CO and CO_2 were predicted as C-containing gas products. Experimental toluene conversions ranged from 84% to 96% and approached equilibrium with the temperature increased from 700 to 900 °C. Coke formation only accounted for less than 1% of toluene conversion, the rest being to gas phase products. The high conversions of toluene achieved for the three temperatures highlight once again the good reforming performance of the Ni/Al_2O_3 catalyst. Both experimental and equilibrium selectivity showed that CO/CO_2 ratio increases as temperature increases. This is likely dominated by reverse water-gas shift reaction in the high-temperature area, as the increasing temperature would favor the endothermic direction, and nickel contents would also promote the reaction at high temperatures (Zhao, Zhang et al. 2010).

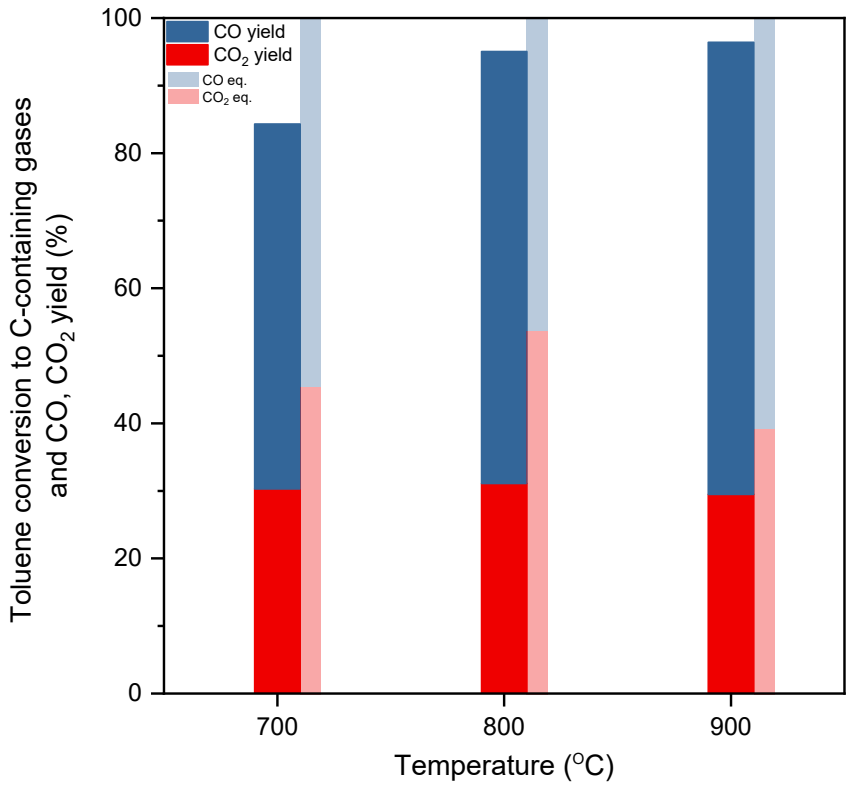

Figure 4.5 Toluene conversion to C-containing gases and CO, CO_2 yield at different temperatures (S/C:3, GHSV:61200 h^{-1}).

Table 4.4 shows the gas production yield including CO, CO_2, H_2 and CH_4. The yields of CO and CO_2 have the similar trends to yield. However, for H_2 yield the maximum was achieved at 800 °C with a H_2 production of 13.0 mol $mol_{toluene}^{-1}$, while the highest H_2 production in equilibrium conditions was predicted at 700 °C. This can be due to that in the experimental test at 700 °C the lowest toluene conversion into gases was obtained. Toluene conversion to gas stayed over 94% at 800 °C or above, while higher temperature would lead to a slight decrease in the content of H_2 in gaseous products due to the presence of the reverse water-gas shift reaction as discussed above. It is interesting to remark that only at 700 °C the undesirable CH_4 side product was obtained and it was only in a small amount. The absence of CH_4 at higher temperatures can be due

to the CH_4 reforming to CO and other parallel processes consuming CH_4 as suggested by the equilibrium results.

Table 4.4 Production rate of the gaseous products at different temperatures (S/C:3, GHSV:61200 h^{-1}).

Temperature (°C)	CO_2 (mol mol $_{toluene}^{-1}$)	CO (mol mol $_{toluene}^{-1}$)	H_2 (mol mol $_{toluene}^{-1}$)	CH_4 (mol mol $_{toluene}^{-1}$)
700	2.1	3.8	10.3	0.1
(equilibrium)	(3.7)	(3.2)	(14.5)	(0.1)
800	2.2	4.5	13.0	0
(equilibrium)	(3.2)	(3.8)	(14.3)	(0)
900	2.1	4.7	11.8	0
(equilibrium)	(2.8)	(4.2)	(13.8)	(0)

Thermal gravimetric analysis was conducted on the catalysts after 5-hour reaction to estimate the coke formation during the reaction tests at the three different temperatures. It has been reported that coke deposition on Ni/Al_2O_3 catalysts is the main cause for deactivation and high nickel contents could also favor coke formation. Although coke deposition is thermodynamically unfavorable at high temperatures (> 600°C) CH_4 decomposition in the high temperature range could lead to the production of solid carbon(Mukai, Tochiya et al. 2013).

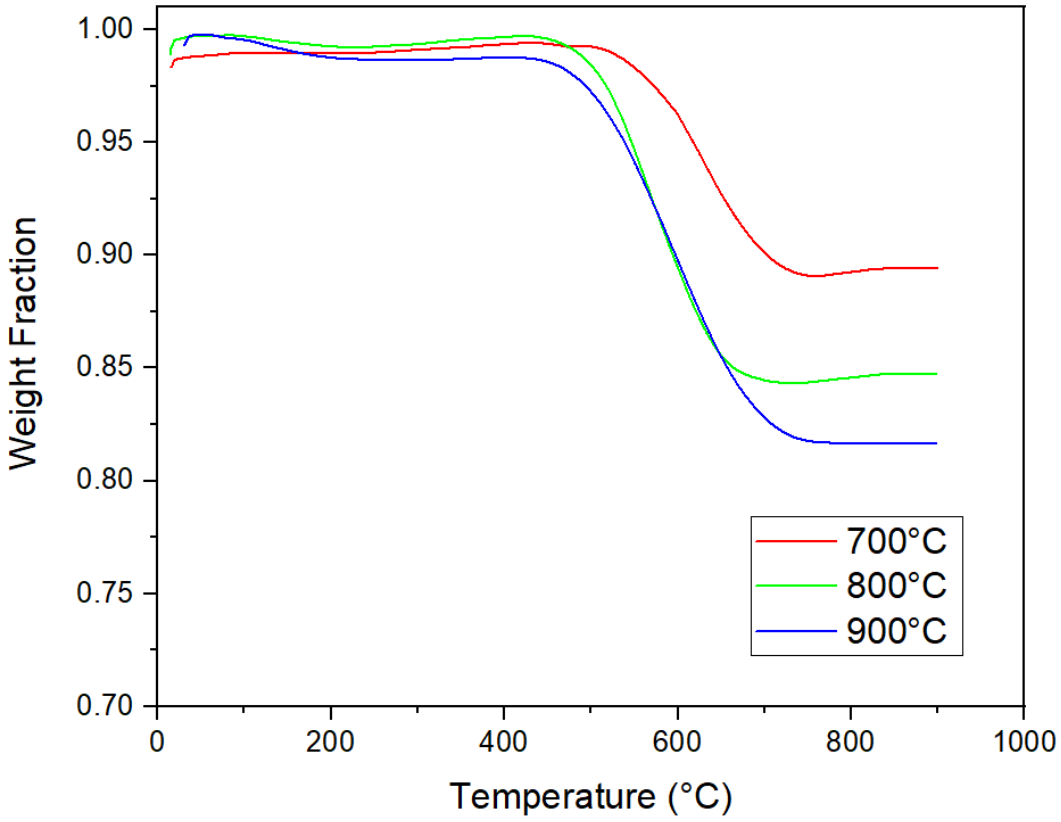

Figure 4.6 Thermal gravimetric analysis for the spent catalysts at different reforming temperatures.

Figure 4.6 shows influence of the three temperatures tested on coke deposition on the catalyst. In addition, Table 4.5 shows the carbon conversion from toluene to coke and the fraction of coke on the catalyst as a function of temperature. As the temperature increased, the conversion to carbon deposits was slightly higher. It is likely that carbon at the higher temperatures was formed from the reforming of CH_4 produced from ,as CH_4 is known to favor coke formation on Ni-based catalysts (Meidanshahi, Bahmanpour et al. 2011). Notwithstanding coke formation at these temperatures, the amount of coke is very low, and the catalyst remains stable during the whole experiments as far as it can be inferred from the product concentrations discussed below.

Table 4.5 Toluene conversion to coke and fraction of coke deposited on the spent catalyst at different reforming temperatures (S/C:3, GHSV:61200 h^{-1}, 5-hour test).

Temperature	700 °C	800 °C	900 °C
Coke/C in toluene	0.43%	0.61%	0.77%
Coke/Catalyst (g_C g_{cat}^{-1})	0.118	0.167	0.211

Based on the results presented above, 800 °C was considered the most suitable reforming temperature due to the highest H_2 production, an excellent overall conversion (94%) and acceptable coke deposition levels. On the contrary, despite the 900 °C experiment showing a slightly higher toluene conversion, lower H_2 production, greater coke deposition and the lower energy efficiency associated with a higher operating temperature made this temperature not preferable against 800 °C for further tests.

4.5 Influence of S/C ratio on toluene steam reforming

In this project, the catalytic performance tests were carried out at S/C ratios of 1, 2, and 3, 800 °C, and GHSV 61200 h^{-1} using 500 mg of catalyst on stream for 5 hours. Figure 4.7, Figure 4.8 and Figure 4.9 present gas product yield trends for CO, CO_2 and H_2 in toluene steam reforming with S/C ratio 1, 2 and 3 respectively.

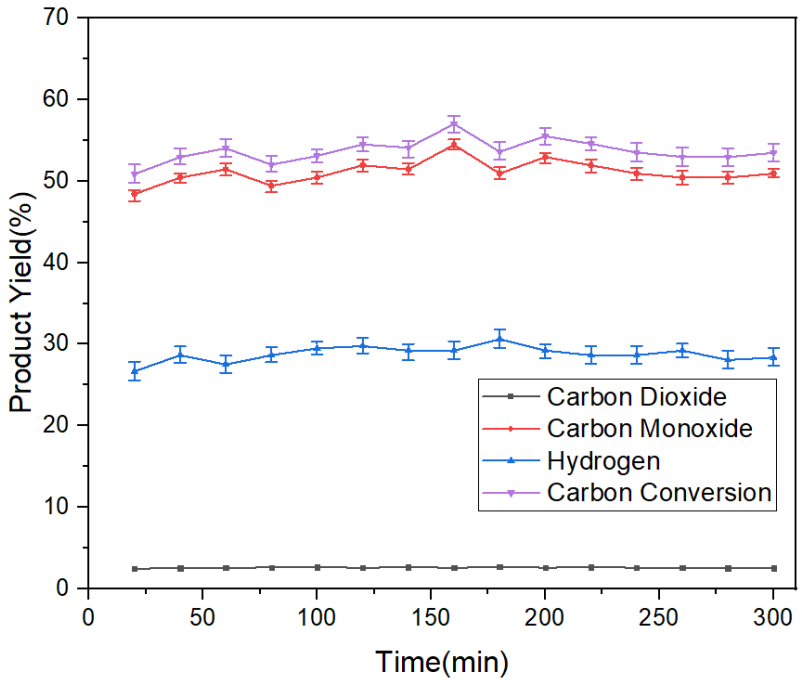

Figure 4.7 Product yield trend of toluene steam reforming with S/C ratio 1 in 5-hour test (Ni/Al_2O_3 catalyst, 800 °C, GHSV: 61200 h^{-1}).

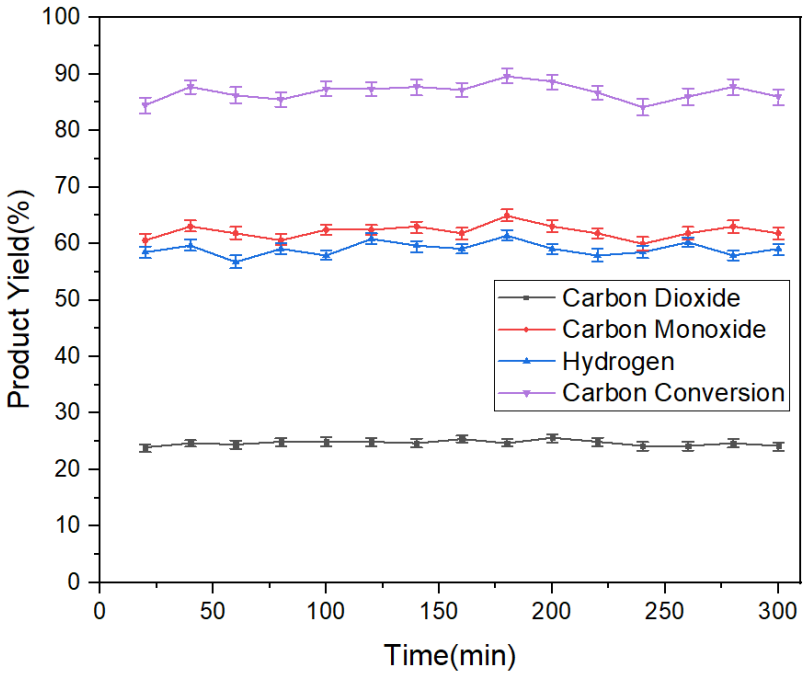

Figure 4.8 Product yield trend of toluene steam reforming with S/C ratio 2 in 5-hour test (Ni/Al_2O_3 catalyst, 800 °C, GHSV: 61200 h^{-1}).

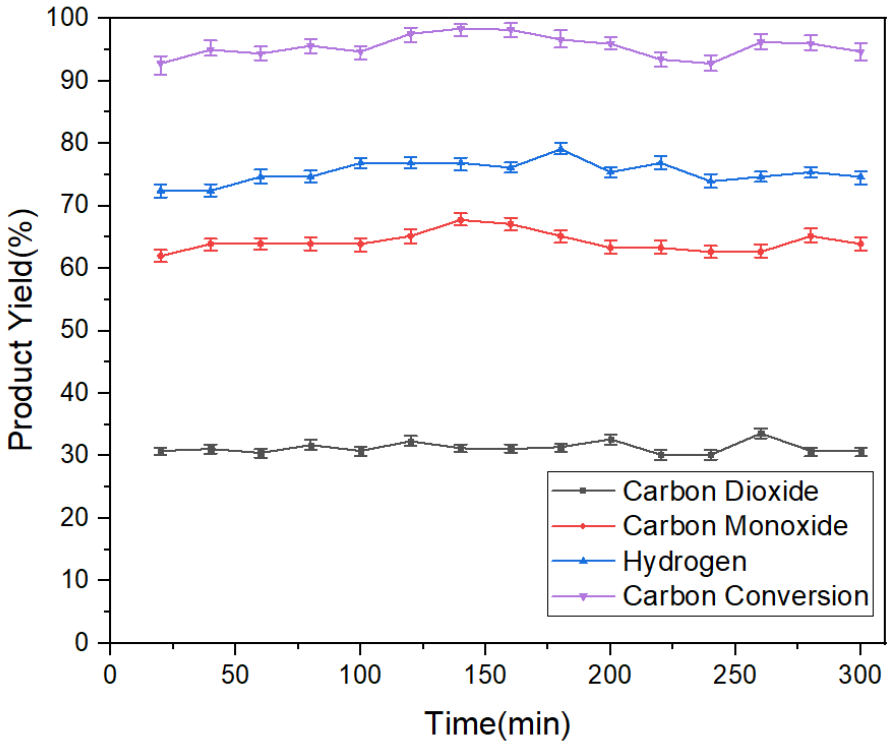

Figure 4.9 Product yield trend of toluene steam reforming with S/C ratio 3 in 5-hour test (Ni/Al_2O_3 catalyst, 800 °C, GHSV: 61200 h^{-1}).

Figure 4.10 summarizes the experimental results and compares the influence of S/C ratio on yield of carbon-containing products with equilibrium results. Both experimental and equilibrium results showed that an increment in S/C ratio results in a large improvement of CO_2 yield/selectivity and toluene conversion. In the experimental tests, toluene to gas conversion increased from 53% to 94% when S/C ratio varied from 1 to 3. Equilibrium results indicated that higher S/C ratio always increase the H_2 production, as the excess steam would promote toluene reforming and the WGS reaction. Some researchers suggested that the most suitable S/C ratio was mostly between 2.5 and 3.5, more excess steam would not increase toluene conversion or H_2 production, because WGS reaction is an exothermic reaction and may be eliminated at 800 °C, causing a drop in toluene partial pressure (Oh, Park et al. 2016).

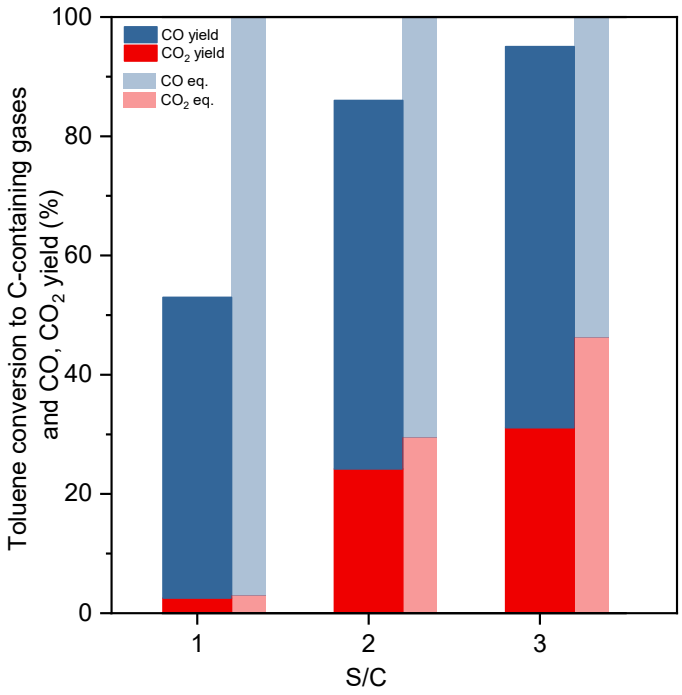

Figure 4.10 Toluene conversion to C-containing gases and CO, CO_2 yields at different S/C ratios (GHSV:61200 h^{-1}, 800 °C).

Table 4.6 Yield of the gaseous products under different S/C ratios (GHSV:61200 h^{-1}, 800 °C).

S/C ratio	CO_2 (mol $mol_{toluene}^{-1}$)	CO (mol $mol_{toluene}^{-1}$)	H_2 (mol $mol_{toluene}^{-1}$)
1	0.2	3.5	5.1
(Equilibrium)	(0.2)	(6.8)	(9.8)
2	1.7	4.3	10.5
(Equilibrium)	(2.1)	(4.9)	(13.0)
3	2.2	4.5	13.0
(Equilibrium)	(3.2)	(3.8)	(14.3)

Table 4.6 compares the production of CO, CO_2 and H_2 with different S/C ratios. Equilibrium simulation and experiments both showed large increases in CO_2 and H_2 production with S/C ratio. Experimental H_2 yield increased from 5.1 to 13.0 mol $mol_{toluene}^{-1}$ when S/C ratio raised from 1 to 3. The opposite trend is expected for CO according to equilibrium calculations, but this was not observed in the experiments. Instead, CO yield was observed to increase with the amount of steam as the trend was dominated by the higher toluene conversion achieved at higher S/C ratios. Despite the experimental CO yield showing a slight increase, in general the CO/CO_2 ratio decreased with the increasing of S/C ratio in line with equilibrium predictions.

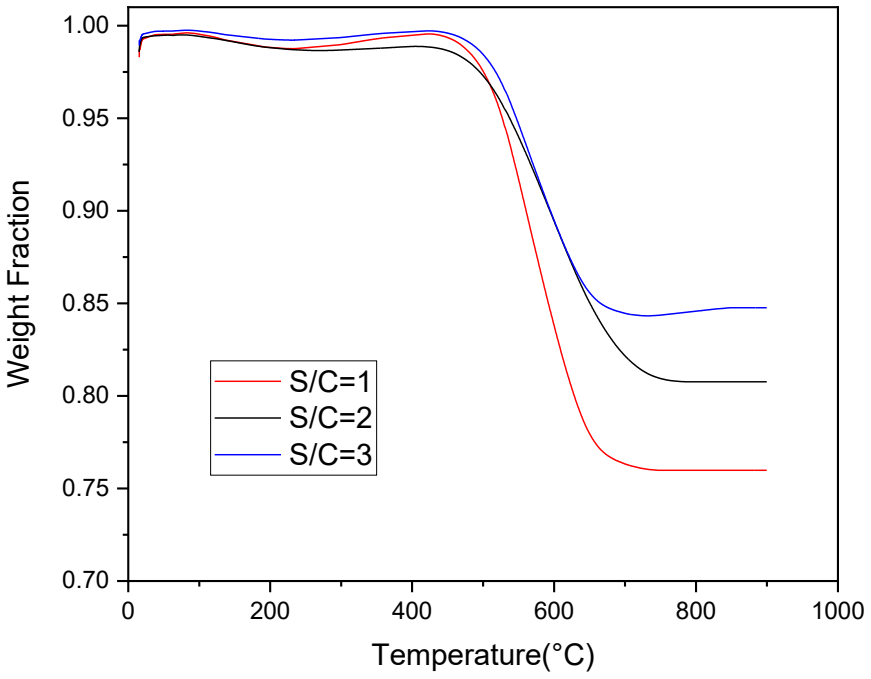

Figure 4.11 Thermo-gravimetric analysis for the spent catalysts at different S/C ratios.

The coke weight on spent catalysts with S/C ratios of 1, 2, and 3 was 0.289, 0.222, 0.167 g_C g_{cat}^{-1}, respectively. As expected, the higher S/C ratio promoted carbon gasification avoiding coke formation (Le Saché, Pastor-Pérez et al.

2019). Table 4.7 shows the carbon conversion from toluene to coke for the three different S/C ratio studied, Figure 4.11 presents the related TGA curves of the spent catalysts. As discussed above, it can be seen that the excess of steam inhibited, but did not suppress, the formation of coke. For all the above, the better choice is to use a S/C ratio of 3 since it permits the highest H_2 production and toluene conversion and the lowest coke amount among the conditions investigated.

Table 4.7 Toluene conversion to coke deposited on catalyst at different S/C ratios (GHSV:61200 h^{-1}, 800 °C, 5-hour test).

S/C ratio	1	2	3
Coke/C in toluene	1.07%	0.82%	0.61%
Coke/Catalyst (g_C g_{cat}^{-1})	0.289	0.222	0.167

4.6 Influence of GHSV on toluene steam reforming

In view of the results obtained in the temperature and S/C ratio screening, a temperature of 800 °C and a S/C ratio 3 were chosen to study the effect of GHSV to elucidate the suitable residence time for a complete conversion of toluene. In principle, high GHSV, or shorter residence time, might inhibit toluene conversion and H_2 production. The GHSV studied were 30600, 61200, 91800 and 122400 h^{-1}. Some of the space velocities selected in this study are indeed over the standard ranges. In fact, high space velocities normally involve smaller reactor volumes, thus decreasing the capital cost of the reformer.

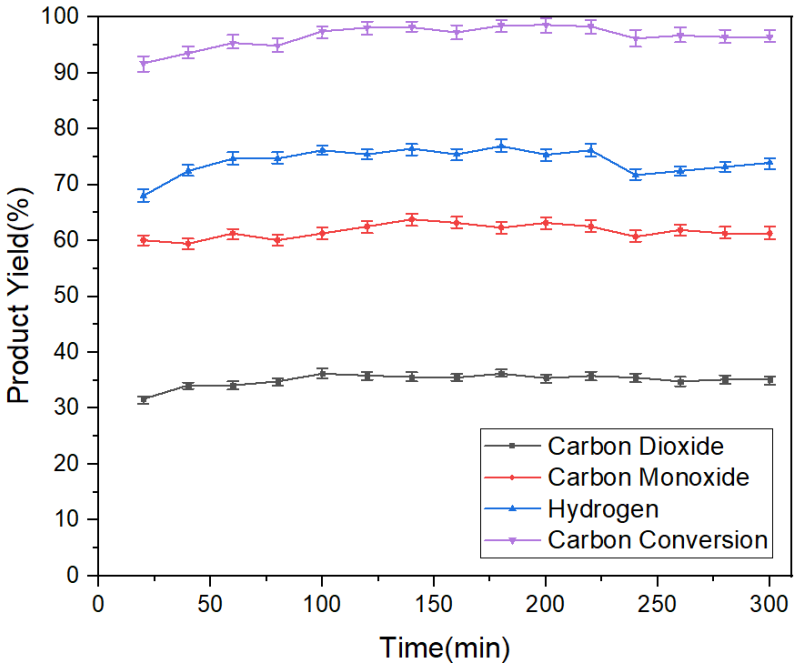

Figure 4.12 Product yield trend of toluene steam reforming with GHSV 30600 h^{-1} in 5-hour test (Ni/Al_2O_3 catalyst, 800 °C, S/C ratio 3)

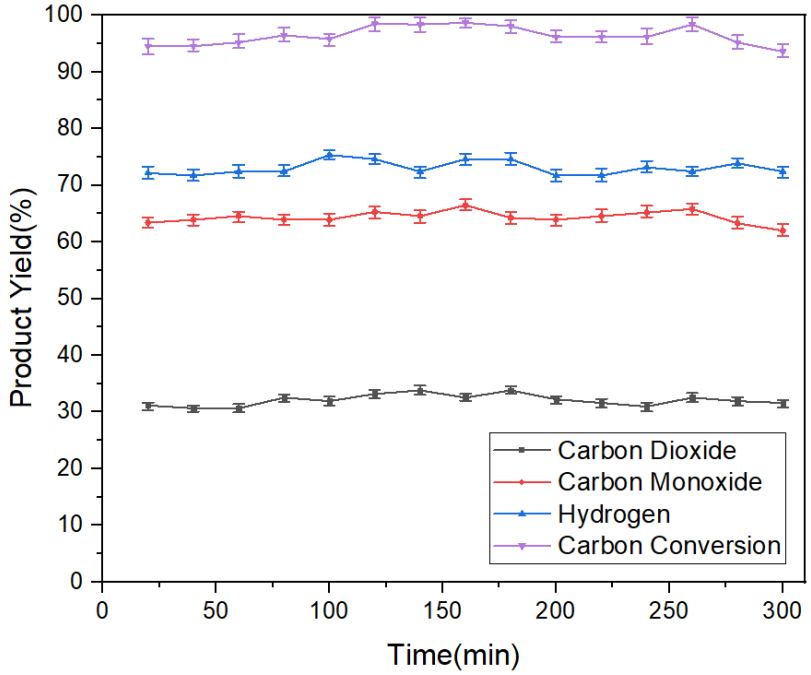

Figure 4.13 Product yield trend of toluene steam reforming with GHSV 61200 h^{-1} in 5-hour test (Ni/Al_2O_3 catalyst, 800 °C, S/C ratio 3)

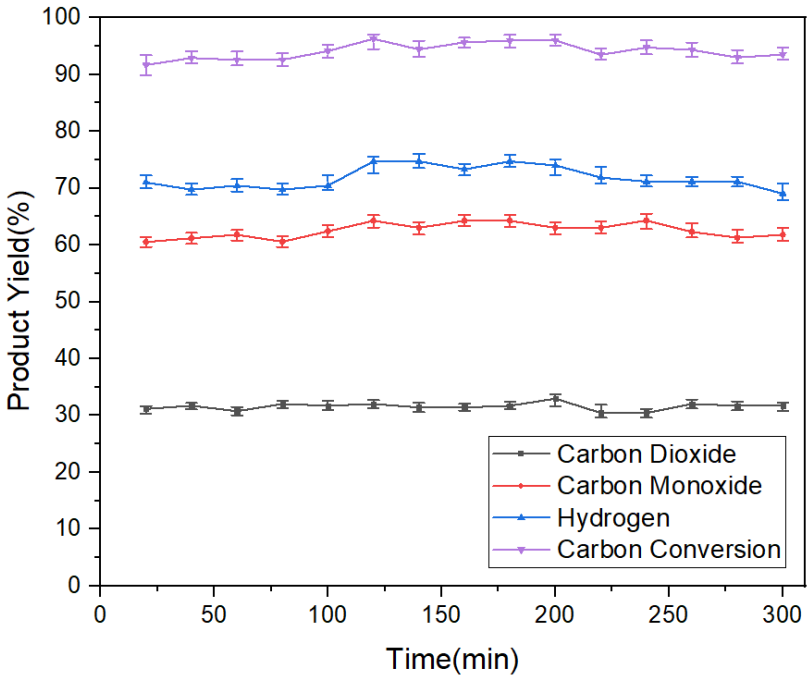

Figure 4.14 Product yield trend of toluene steam reforming with GHSV 91800 h^{-1} in 5-hour test (Ni/Al_2O_3 catalyst, 800 °C, S/C ratio 3)

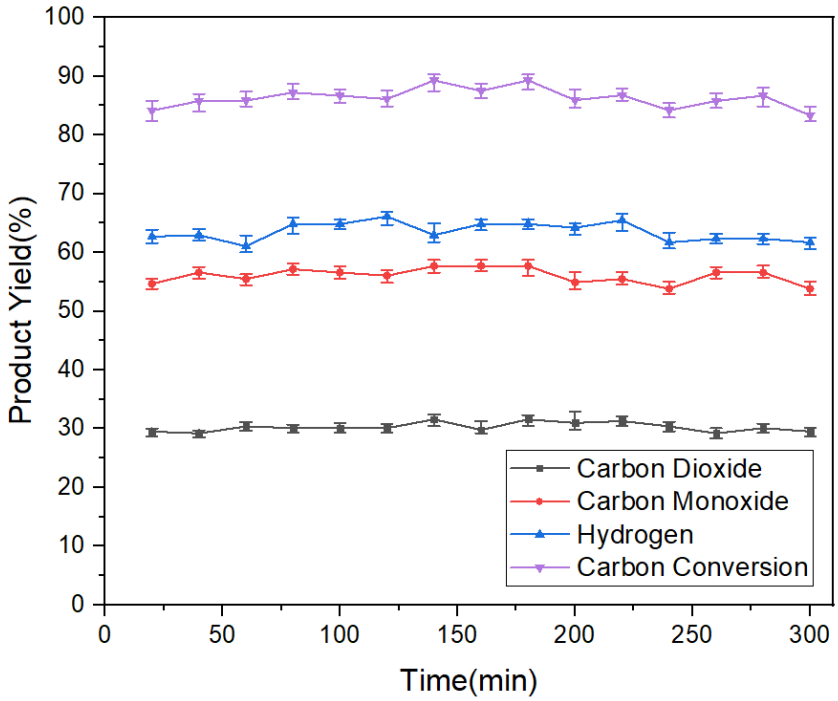

Figure 4.15 Product yield trend of toluene steam reforming with GHSV 122400 h^{-1} in 5-hour test (Ni/Al_2O_3 catalyst, 800 °C, S/C ratio 3).

Figure 4.12, Figure 4.13, Figure 4.14 and Figure 4.15 present the product yield trends of CO, CO_2 and H_2 in 5-hour test of toluene steam reforming with GHSV of 30600, 61200, 91800 and 122400 h^{-1}, respectively. CO, CO_2 and H_2 yield trend under 4 different GHSV remained steady at the same level in 5 h.

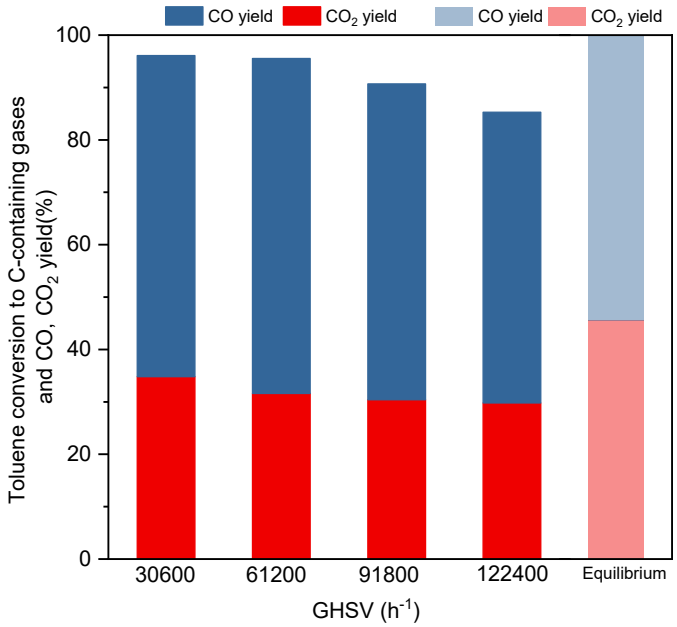

Figure 4.16 Toluene conversion to C-containing gases and CO, CO_2 yields at different GHSV (S/C: 3, 800 °C).

Figure 4.16 shows the toluene conversion and CO_2, CO yield (based on conversion to C-containing gases) at the four different GHSV in a steady-state within the 5 hours of reaction and compares them with equilibrium result. Toluene conversion decreased from 96 to 86% when GHSV increased from 30600 to 122400 h^{-1}. When GHSV was 91800 h^{-1} or lower, toluene conversion to gas remained higher than 90%, without notorious differences for the two lowest GHSV studied (30600 or 61200 h^{-1}), which showed a stabilized conversion at around 95%. The yield of CO and CO_2 approached the equilibrium results slowly when GHSV decreased. It could be seen that toluene conversion and CO_2 yield declined with the increasing of GHSV, as a result of

shorter residence time. It is interesting to note that the selectivity is less affected by the residence time than the conversion. Negligible or no CH_4 was detected in the product gas, in line with literature that suggested that at temperatures higher than 750 °C very small amounts of CH_4 are produced (Zhao, Zhang et al. 2010).

Table 4.8 Production rate for the gaseous products at different GHSV (S/C: 3, 800 °C).

GHSV (h^{-1})	CO_2 (mol $mol_{toluene}^{-1}$)	CO (mol $mol_{toluene}^{-1}$)	H_2 (mol $mol_{toluene}^{-1}$)
30600	2.4	4.3	13.2
61200	2.2	4.5	13.0
91800	2.1	4.2	12.8
122400	2.1	3.9	10.8
(Equilibrium)	(3.2)	(3.8)	(14.3)

The CO_2, CO and H_2 production yields in mol mol $_{toluene}^{-1}$ are shown in Table 4.8. As expected, GHSV 30600 h^{-1} led to the highest H_2 production (13.2 mol mol $_{toluene}^{-1}$). As a trend, CO, CO_2 and H_2 yields dropped when GHSV increased. This decrease in yields for all gas products at high GHSV is linked with the drop in conversion as residence time became shorter. An exception occurred at 61200 h^{-1} GHSV as the reverse water-gas shift reaction could cause a small increase in CO. Previous studies suggest that some tar model compounds (naphthalene) had no apparent trends for the hydrogen yields or selectivity, as the product was affected by the equilibrium of water-gas shift reaction and other side reactions (Li, Wang et al. 2018). In this work, hydrogen yield and total conversion showed a slightly increasing trend in conversion and yields with the

decrease of residence time, but this trend was more remarkable in the conversion of toluene than in selectivities.

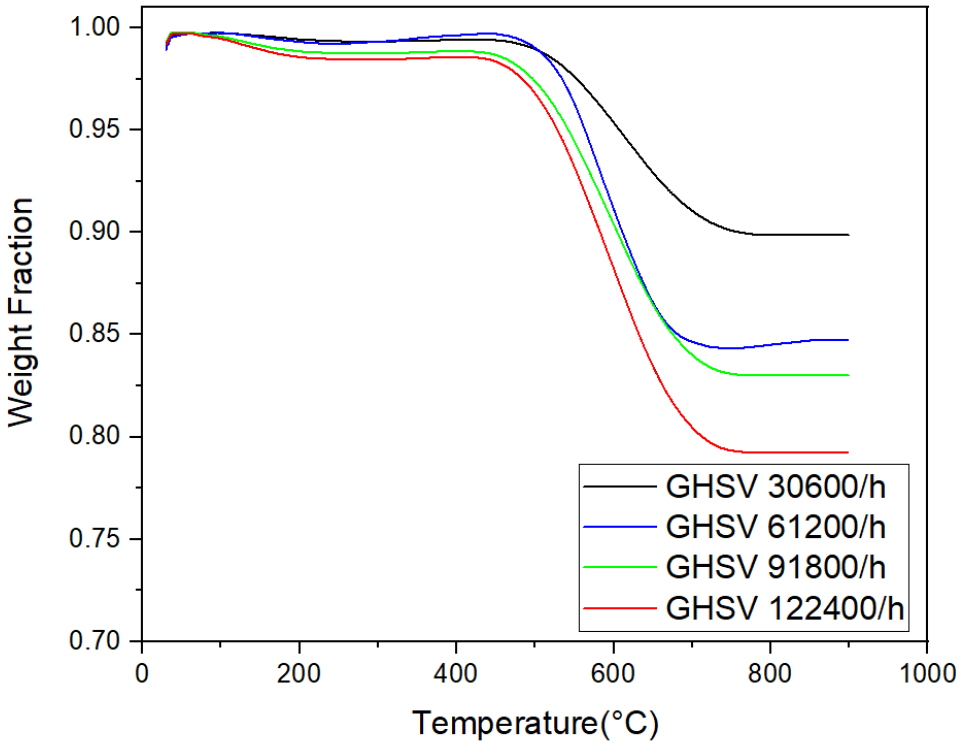

Figure 4.17 Thermal gravimetric analysis for the spent catalysts with different GHSVs.

Table 4.9 shows the carbon conversion from toluene to coke and the amount of coke over the spent Ni/Al_2O_3 catalyst, Figure 4.17 presents the related TGA curves of the spent catalysts. These figures should be analyzed taking into account that GHSV was varied while keeping the toluene concentration in the feed constant in all experiments. Therefore, the throughput of reactive carbon species increased with space velocity, meaning that in experiments at higher GHSV a fixed amount of catalyst (500 mg) was exposed to a larger toluene feed rate. This resulted in the larger coke content observed on spent catalysts. However, in terms of toluene conversion to coke, higher GHSV led to smaller values, as expected from the decrease in residence time. The toluene

conversion to coke was reduced from 0.38 to 0.22% as GHSV increased from 30600 to 122400 h^{-1} accompanied by an increase in toluene and steam feeding rate by a factor of 4. These trends in coke formation are the balance between the higher feed rate of toluene and the decrease in toluene conversion due to the higher GHSV used.

Table 4.9 Toluene conversion to coke deposited on catalyst with different GHSV (S/C: 3, 800 °C, 5-hour test).

GHSV(h^{-1})	30600	61200	91800	122400
Coke/C in toluene	0.38%	0.31%	0.23%	0.22%
Coke/Catalyst ($g_C\ g_{cat}^{-1}$)	0.105	0.167	0.188	0.242

Although the lower space velocity leads to higher conversion, greater yield and lower net amount of carbon deposits, for practical applications (i.e. manufacturing cost savings) higher space velocities are desired. In this sense, 61200 h^{-1} yield very similar conversion and selectivity levels to 30600 h^{-1}, as well as low net coking and lower conversion to coke. Hence, this space velocity (< 91800 h^{-1}) was selected to optimize the next reaction parameter.

4.7 Summary

The effect of reforming temperature, S/C ratio and GHSV on toluene conversion and product distribution was studied in this chapter using a Ni/Al_2O_3 catalyst.

Increasing temperature from 700 to 900 °C increased total conversion, with a potential risk of higher coke deposition. At 800 °C the highest H_2 production was observed, along with high toluene conversion (>94%) and relatively lower coke deposition.

Ni/Al_2O_3 catalyst only requires a very short residence time (GHSV < 91800 h^{-1}) for toluene reforming with this catalyst, and effectively removes low concentration toluene in a mixed gas stream. H_2 yield and toluene conversion increased slightly and approached simulated thermodynamic equilibrium results when GHSV decreased. Coke deposition increased at a lower rate as GHSV increased.

High S/C ratio would greatly increase total conversion, hydrogen production, and reduce the coke formation on catalyst. The presence of excess steam could shift the equilibrium of water-gas shift reaction to produce more H_2.

800 °C, GHSV 61200 h^{-1} and S/C ratio 3 provided the most suitable reaction conditions for toluene conversion and H_2 production in steam reforming of toluene, obtained a steady state of a toluene to gas conversion over 94%, a H_2 production of 13.0 mol $mol_{toluene}^{-1}$ in 5-hour test, with no obvious deactivation observed in 5 hours. Based on these results, this condition would be suitable for tar model compound removal.

5 Influence of Reaction Atmosphere on Toluene Steam Reforming

5.1 Introduction

As shown in Chapter 4, the Ni catalyst proved to be active for toluene reforming and tar cracking, while carbon deposition was considered as an important reason for the deactivation of this catalyst. However, very few works have reported the effects of gas atmosphere in the steam reforming reactions of gasification tars with Ni-based catalysts as part of the treatment to the hot product gas from the gasifier. The gasification gas atmosphere in which tar or toluene steam reforming takes place could affect the process, as H_2, CO or CO_2 in the biomass gasification gas products are normally > 20 vol.% and could shift the equilibrium of WGS reaction. On the other hand, the influence on toluene conversion is not clear, the gas products including H_2, CO or CO_2 may shift the equilibrium towards lower toluene conversion to gas; CH_4 might have a significant influence on carbon deposition on Ni catalyst, and further deactivate the catalyst. This chapter presents an experimental study on the influence of different reaction gas atmosphere on catalytic toluene steam reforming.

5.2 Experimental Conditions

The reaction gas atmosphere was designed to simulate the gas composition from biomass gasification processes. The main products include H_2, CO, CO_2 and CH_4. The typical composition ranges of H_2, CO, CO_2 and CH_4 in biomass gasification gas products are 20% – 50 vol.%, 20% – 40 vol.%, 10% – 30 vol.% and 1 – 8 vol.% respectively(Sutton, Kelleher et al. 2001, Abu El-Rub, Bramer

et al. 2004, Shen and Yoshikawa 2013). To investigate the influence of H_2, CO, CO_2 and CH_4 on catalytic toluene steam reforming, their inlet concentrations were fixed at 30 vol.%, 30 vol.%, 20 vol.% and 3 vol.%, respectively, and balanced with N_2. Table 5.1 shows the detailed reforming atmosphere gas compositions of different catalytic toluene steam reforming test.

Table 5.1 Toluene steam reforming atmospheres used in this work (on dry basis).

Reforming test	Reforming atmosphere
Inert atmosphere	100% N_2
H_2 atmosphere	30% H_2, 70% N_2
CO atmosphere	30% CO, 70% N_2
CO_2 atmosphere	20% CO_2, 80% N_2
CH_4 atmosphere	3% CH_4, 97% N_2
CO and H_2 atmosphere	30% CO, 30% H_2, 40% N_2
CH_4 and H_2 atmosphere	3% CH_4, 30% H_2, 67% N_2
Simulated gas atmosphere	3% CH_4, 30% H_2, 20% CO_2, 30% CO, 17% N_2

Suitable reaction parameters shown in Table 5.2 were chosen according to the results and conclusion from Chapter 4. Each test period (controlled by start/stop reactant injection) was 5 hours. All the results were obtained using the quartz tube reactor detailed in Chapter 3 under atmospheric pressure.

The results from different single gas atmosphere all used N_2 as balance gas, as N_2 is an inert gas and not involved in the reactions. To compare the gas

production from different atmospheres, a catalytic toluene steam reforming test under 100% N_2 (with a S/C ratio 3) was chosen as an inert atmosphere with the same reforming conditions shown in Table 5.2.

Table 5.2 Experimental conditions applied in these reforming tests

Reforming parameters	Value
Reforming temperature	800 °C
$S/C_{toluene}$ (C in toluene only) ratio	3
GHSV	91800 h^{-1}
Carrier gas flow rate	300 mL min^{-1}
Toluene injection rate	2.07 mL h^{-1} (19.5 mmol h^{-1})
Catalyst	500 mg Ni/Al_2O_3
Time on toluene	5 h

As methane steam reforming could also take place in the catalytic test, and might also influence the conversion of toluene, one more set of experiments was planned to understand the influence of adding CH_4 in S/C ratio: in the first experiment only toluene was considered as reactant carbon source to calculate S/C ratio, but in the second experiment CH_4 was considered as a reactant carbon source and taken into account when calculating S/C ratio. This S/C ratio was defined as follow:

$$\mathrm{S/C}_{Total}\ \text{ratio} = \frac{\text{Water input to the reactor in moles}}{\text{C moles in toluene} + \text{C moles in } CH_4}$$

Another CH_4 reforming test was also conducted without the injection of toluene. Table 5.3 summarizes the different conditions in atmosphere reforming tests.

The experimental error in toluene conversion, gas selectivity and gas yield is ± 2%.

The carrier gas mixture was premixed at 1.5 bar and used as the atmosphere of the catalytic reforming test. After 1 hour of catalyst reduction by 100% H_2, the gas channel was then switched to the premixed carrier gas. The injection of steam and toluene started when the reading of each analyzer stayed stable for 5 min. The software started to collect data (product gas concentrations) when the reactant injection started, and the gas concentration was recorded continuously for 5 hours. The thermodynamic equilibrium simulations were performed using a Gibbs free minimization reactor in an Aspen Plus software package, and compared with the experiment result.

Table 5.3 Summary of different conditions in atmosphere reforming tests

Atmosphere	H_2 concentration	CO concentration	CO_2 concentration	CH_4 concentration	N_2 concentration	$S:C_{toluene}$	$S:C_{Total}$
H_2	30% (230 mmol h^{-1})	0	0	0	70% (533 mmol h^{-1})	3	3
CO	0	30% (230 mmol h^{-1})	0	0	70% (533 mmol h^{-1})	3	3
CO_2	0	0	20% (153 mmol h^{-1})	0	80% (611 mmol h^{-1})	3	3
CH_4(1)	0	0	0	3% (23 mmol h^{-1})	97% (741 mmol h^{-1})	3	2.55
CH_4(2)	0	0	0	3% (23 mmol h^{-1})	97% (741 mmol h^{-1})	3.53	3
CO & H_2	30% (230 mmol h^{-1})	30% (230 mmol h^{-1})	0	0	40% (306 mmol h^{-1})	3	3
CH_4 & H_2	30% (230 mmol h^{-1})	0	0	3% (23 mmol h^{-1})	67% (512 mmol h^{-1})	3.53	3
Simulated gas	30% (230 mmol h^{-1})	30% (230 mmol h^{-1})	20% (153 mmol h^{-1})	3% (23 mmol h^{-1})	17% (130 mmol h^{-1})	3.53	3

5.3 Influence of single gas atmosphere on toluene steam reforming

The first group of experiments were conducted to understand the influence of single gas atmosphere on toluene steam reforming and compared with the inert atmosphere (100% N_2). The yields of CO, H_2, CO_2 are defined by the equation below where each term is in moles:

$$\%CO \text{ yield } = \frac{CO \text{ output} - CO \text{ input}}{\text{C in toluene} + \text{C in } CH_4} * 100$$

$$\% \, CO_2 \text{ yield } = \frac{CO_2 \text{output} - CO_2 \text{ input}}{\text{C in toluene} + \text{C in } CH_4} * 100$$

$$\% \, H_2 \text{ yield} = \frac{H_2 \text{ output} - H_2 \text{ input}}{18 * \text{toluene input} + 4 * CH_4 \text{ input}} * 100$$

CO_2 selectivity was also calculated to study the influence of different gas atmospheres on CO/CO_2 selectivity and assess the extent of WGS reaction, as CH_4 stayed < 0.1vol.% in all experiments, CO_2 selectivity is defined by the equation below where each term is in moles:

$$\% \, CO_2 \text{ selectivity } = \frac{CO_2 \text{output } - CO_2 \text{ input}}{CO_2 \text{output } - CO_2 \text{ input } + CO \text{ output} - CO \text{ input}} * 100$$

5.3.1 Influence of the 30 vol.% H_2 on toluene steam reforming

Figure 5.1 presents the trend of product gas distribution of toluene reforming test in 30% H_2 balanced N_2 atmosphere. During the 5-hour test, the carbon conversion from toluene to gas decreased from 94 to 88%, as CO yield was reduced from 67 to 62%, while a steady yield of 26 – 28 % was observed for CO_2 throughout the test. H_2 yield declined slightly from 59% to 55%.

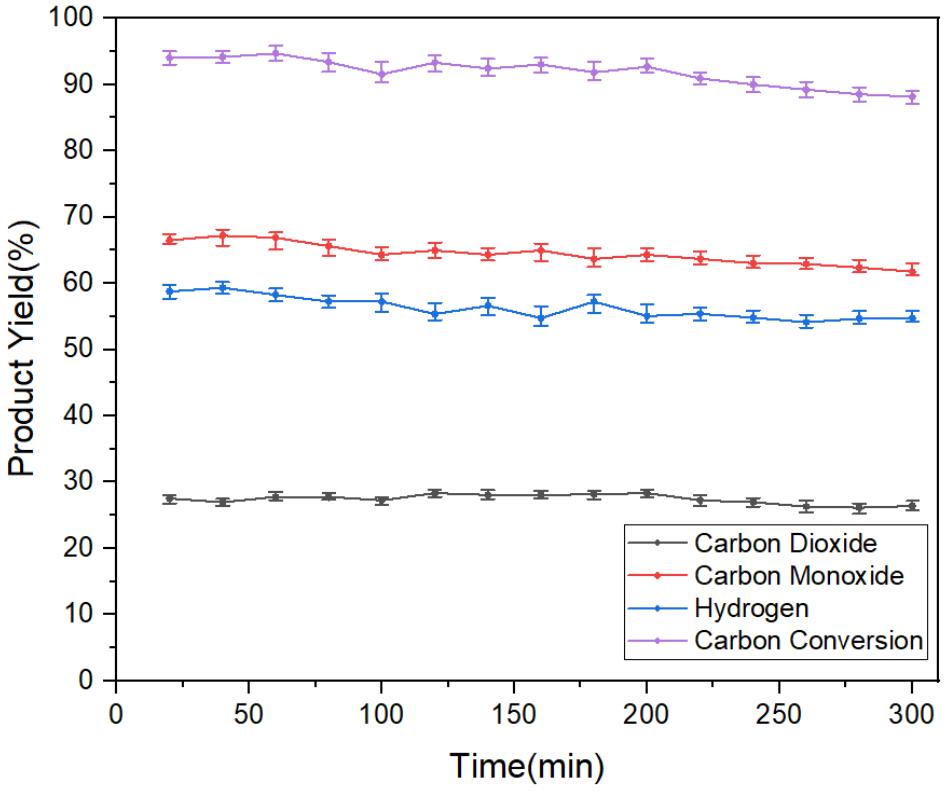

Figure 5.1 Product yield trend and conversion of toluene steam reforming test in 30%H_2 balanced N_2 atmosphere (5-hour test, Ni/Al_2O_3 catalyst, 800 °C, S/C ratio 3, GHSV: 91800 h^{-1}).

5.3.2 Influence of the 30 vol.% CO on toluene steam reforming

Product yield (CO, H_2 and CO_2) and toluene conversion during the reforming test is shown in Figure 5.2. The toluene conversion into gaseous products observed no significant change in 5 hours, and CO, CO_2 yield remained stable at ~33 and ~58%, respectively throughout the experiment. The input CO from carrier gas shifted the WGS reaction to produce more H_2 and CO_2, H_2 yield stayed above 75% in the 5-hour test.

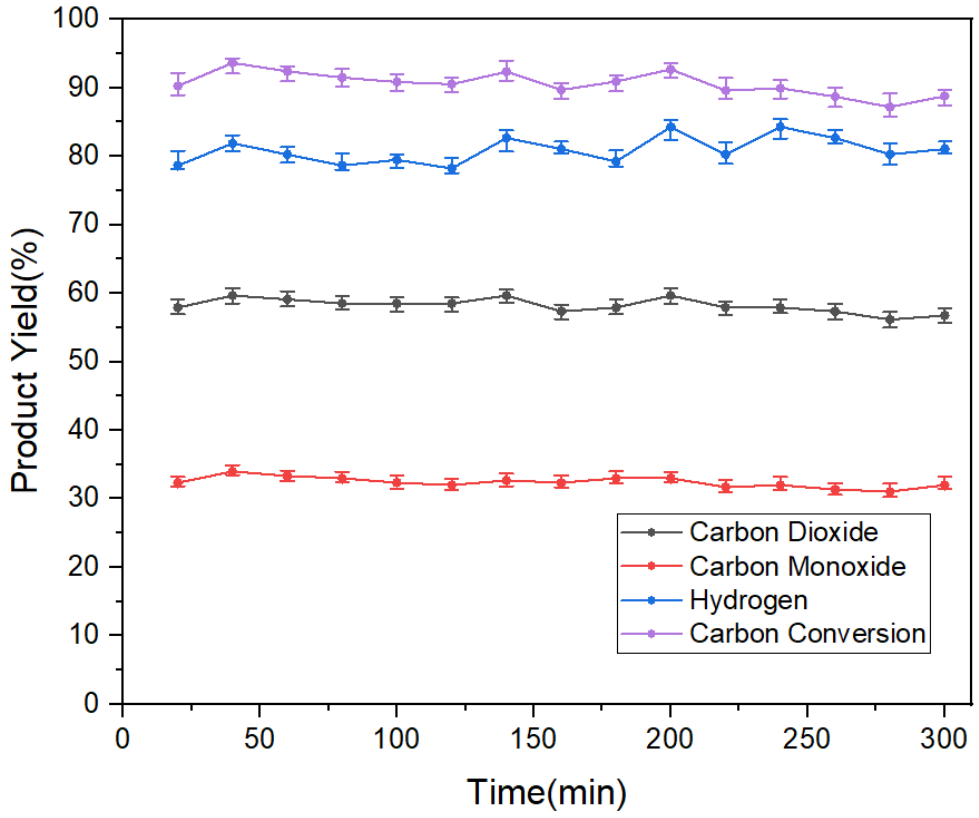

Figure 5.2 Product yield trend and conversion of toluene steam reforming test in 30% CO balanced N_2 atmosphere (5-hour test, Ni/Al_2O_3 catalyst, 800 °C, S/C ratio 3, GHSV: 91800 h^{-1}).

5.3.3 Influence of the 20 vol.% CO_2 on toluene steam reforming

Figure 5.3 exhibits the gas formation and toluene conversion trends over time. The overall conversion of toluene stayed higher than 90% during the 5 hours, CO_2 yield ranged from 17% to 19% and CO yield ranged from 71% to 76%. H_2 yield also remained stable at ~58%.

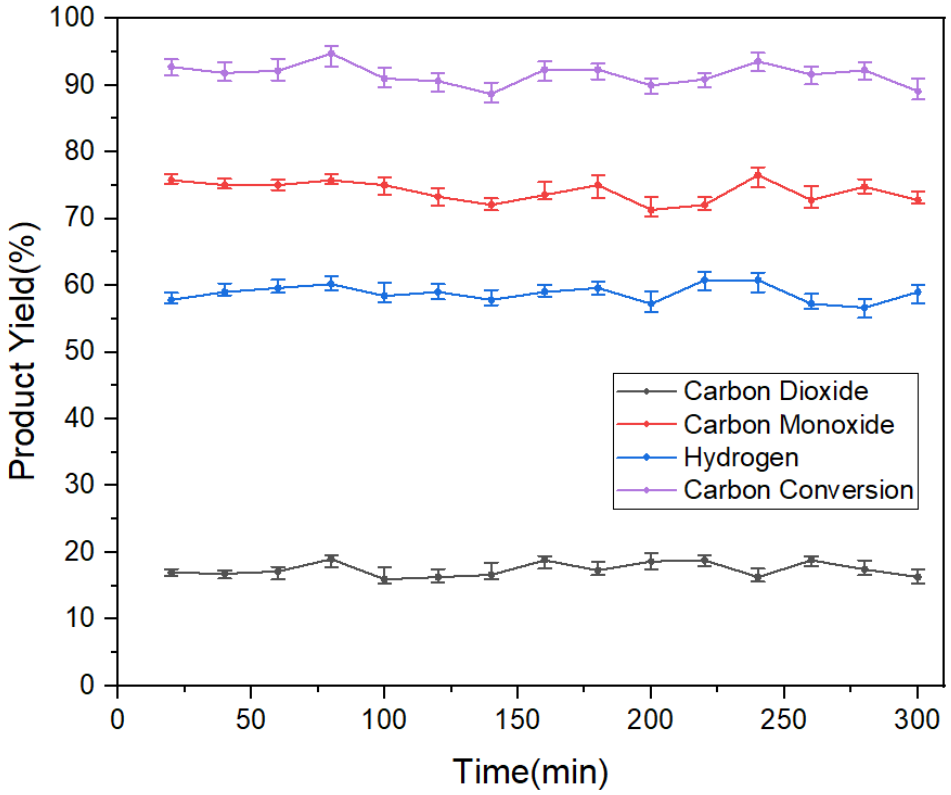

Figure 5.3 Product yield trend and conversion of toluene steam reforming test in 20% CO_2 balanced N_2 atmosphere (5-hour test, Ni/Al_2O_3 catalyst, 800 °C, S/C ratio 3, GHSV: 91800 h^{-1}).

5.3.4 Influence of the 3 vol.% CH_4 on toluene steam reforming

Figure 5.4 presents the toluene conversion and gas yield trends of CH_4 atmosphere test (carbon in CH_4 was not considered when calculating S/C ratio). The overall conversion from toluene to gases decreased from 90% to 79% after 5 hours, and H_2 yield declined from 68% to 60%. CO and CO_2 yields decreased from 65% and 25% to 56% and 22%, respectively. The concentration of CH_4 stayed below 0.1% throughout the experiments, which meant that the injected CH_4 was mostly steam reformed into CO, CO_2 and H_2.

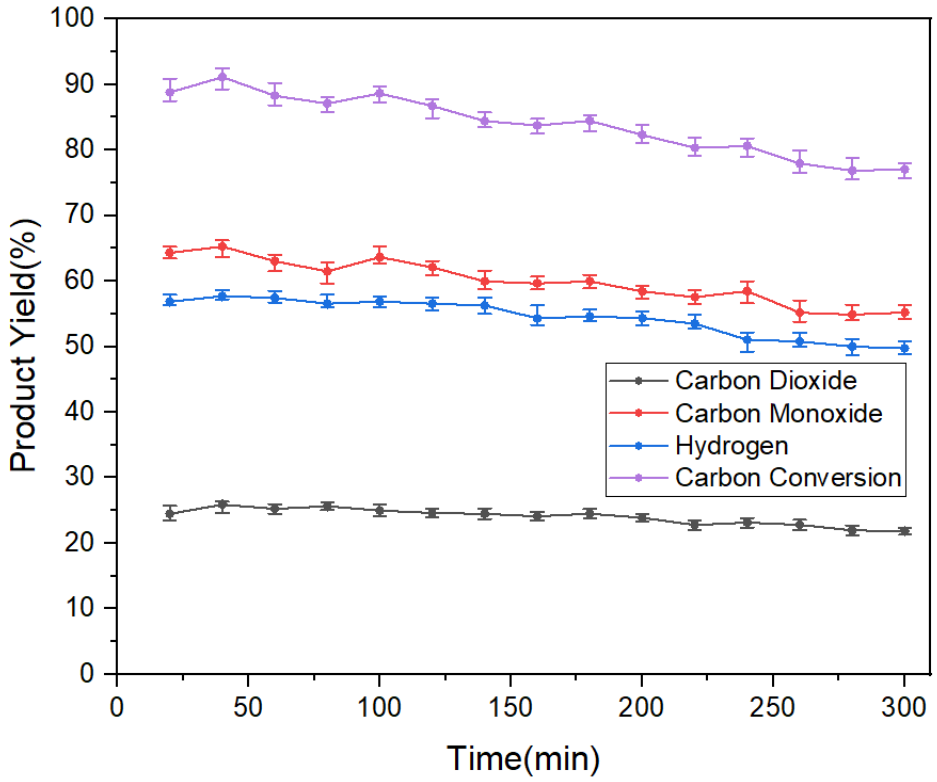

Figure 5.4 Product yield trend and conversion of toluene steam reforming test in 3% CH_4 balanced N_2 atmosphere (5-hour test, Ni/Al_2O_3 catalyst, 800 °C, S/C in toluene CH_4, GHSV: 91800 h^{-1}).

Another experiment was conducted to gain a better understanding on the behavior of the system when there were toluene and methane mixtures. In this experiment the steam feeding rate increased to keep the steam to total carbon in toluene and methane at 3. The product yield and total gas conversion trend are presented in Figure 5.5. The carbon conversion into gases in first hour achieved 93% as a result of the increasing of S/C_{Total} ratio from 2.55 to 3. Then the overall carbo conversion decreased with time smoothly, and finally dropped to 80% during the fifth hour. H_2, CO and CO_2 yields decreased from 72%, 59% and 34% to 64% and 30%, respectively. H_2 yield also increased with the increasing of S/C_{Total} ratio. The degree of reduction of H_2, CO and CO_2 yield in 5 h with these two CH_4 atmosphere experiments was very close.

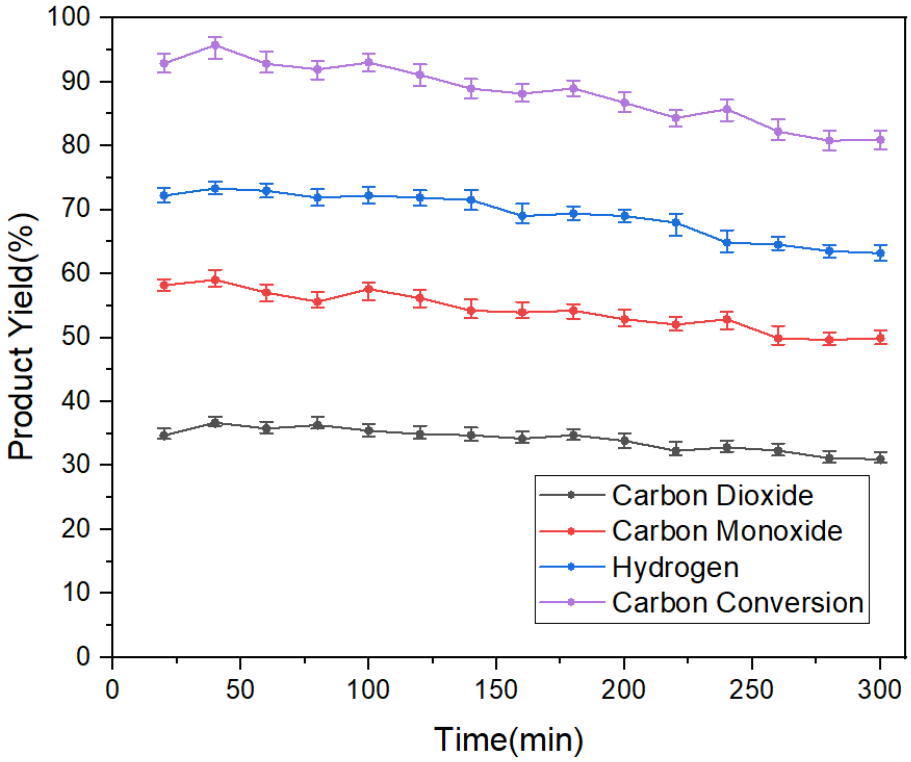

Figure 5.5 Product yield trend and conversion of toluene steam reforming test in 3% CH_4 balanced N_2 atmosphere (5-hour test, Ni/Al_2O_3 catalyst, 800 °C, S/C_{total} ratio 3, GHSV: 91800 h^{-1}).

5.3.5 Comparison of different single gas atmospheres

Figure **5.6** summarizes the CO, CO_2 yield and toluene conversion into C-containing gases under different gas atmospheres at the first and fifth hours of the catalytic tests and compares these values with equilibrium results. The equilibrium simulation shows that all these atmospheres reach 100% toluene conversion into gas, and CH_4 yield stayed lower than 0.1% in all the equilibrium results. The experiment results show that toluene conversion to gas under 100% N_2, 30% CO in N_2, 20% CO_2 in N_2 atmosphere stayed over 90% throughout the 5-hour catalytic reforming tests, with very limited decreases in toluene conversion (< 2.5%) observed in these three atmospheres after 5-hour tests.

100% N_2 atmosphere presents the highest toluene conversion in the whole 5 hours, while 30% CO in N_2, 20% CO_2 in N_2 atmosphere shows lower but stable toluene conversion rate in 5 hours. 30% CO in N_2, 20% CO_2 in N_2 and 30% H_2 in N_2 atmosphere all show slightly lower toluene conversion rate than 100% N_2 atmosphere, while 3% CH_4 presents a similar initial toluene conversion rate with 100% N_2 atmosphere. This indicates that a relatively high contents (>20%) of gasification gas product (CO, H_2, CO_2) can slightly inhibit the reforming reaction of toluene, CH_4 didn't show obvious influence due to its low concentration. Also, the presence of CO in carrier gas favored WGS reaction and produce more CO_2, while feeding CO_2 in N_2 would largely increase CO yield to ~75%, pushing reverse WGS reaction. The experimental CH_4 yield in all atmosphere tests was under 0.1%. The absence of CH_4 under all atmospheres indicated that CH_4 had a very good conversion (>99%) over Ni/Al_2O_3 catalyst even when the deactivation of toluene reforming took place. As there was an excess continuous steam, methane dry reforming didn't seem to have an effect. The CH_4 atmosphere test experienced the largest decrement in toluene conversion (dropped from ~94% to 81% in 5 h), CO and CO_2 yields, followed by H_2 atmosphere test. The ratio of CO/CO_2 stayed almost the same after 5-hour test in all the experiments. Considering that CH_4 only had a concentration of 3 vol.% in carrier gas, it could be suggested that CH_4 showed a vital importance in reforming catalyst deactivation among biomass gasification gas components. Equilibrium results indicated that WGS reaction played an important role in CO/CO_2 selectivity and H_2 production. The injection of H_2, CO, CO_2 had a significant influence on gas product distribution in both experiments and equilibrium simulations. It can also be observed in Figure 5.6 that CO_2 yield was typically much lower than equilibrium calculations except for the CO_2 atmosphere experiment.

Table 5.4 shows the gaseous product yields including CO, CO_2 and H_2 in the unit of mol $mol_{toluene}^{-1}$ at the first hour and the fifth hour of different atmosphere and compares with the related equilibrium results. CO/CO_2 product ratios of different atmospheres also changed towards the equilibrium results. Experimental CO_2 selectivity under all atmospheres is lower than equilibrium predicted except for 20% CO_2 atmosphere, indicating that toluene is reformed to CO first and then CO undergoes WGS reaction to produce CO_2. The injection of CO could promote the production of H_2, while CO_2 inhibited H_2 yield. The addition of H_2 could also reduce H_2 yield, and further decreased in all gas yield with time in 5-hour test. 3% CH_4 in N_2 atmosphere test achieved the highest H_2 at 16.5 mol $mol_{toluene}^{-1}$ during the first hour and observed the highest decrement by 16% at the fifth hour. Meanwhile, H_2 yield of 30% H_2 in N_2 atmosphere test dropped by 7% from 11.2 to 10.4 mol $mol_{toluene}^{-1}$ in the 5-hour test.

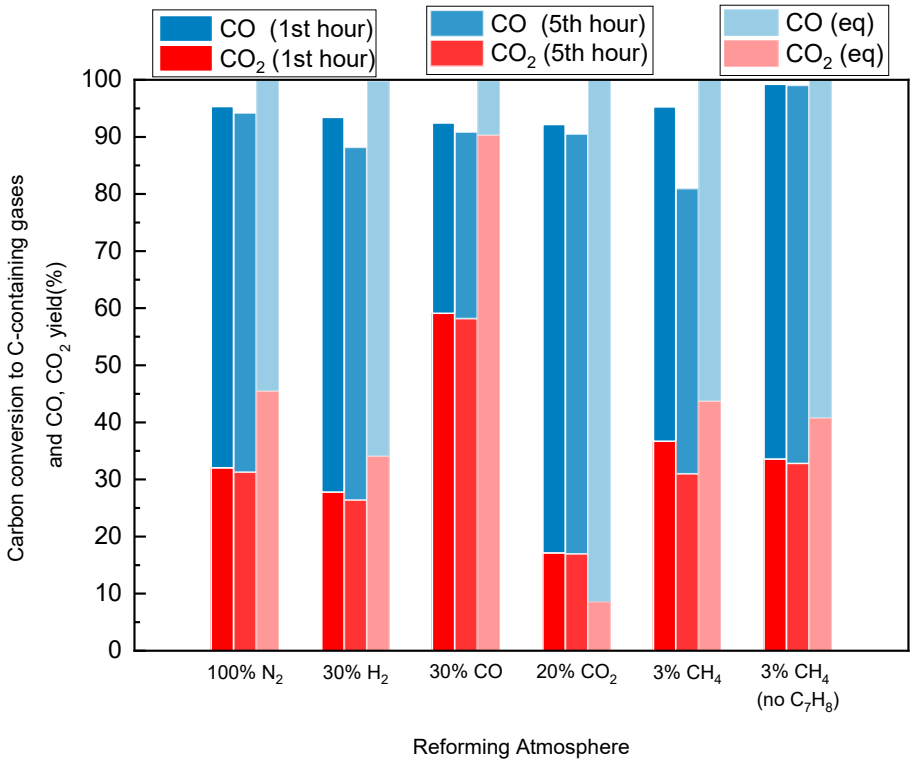

Figure 5.6 Toluene conversion to C-containing gases and CO/CO_2 yield at different single gas atmosphere (S/C ratio 3 GHSV:91800 h^{-1}, reforming temperature 800 °C, all the gas atmosphere balanced with N_2).

Table 5.4 Product yields for the gaseous products in the different reforming atmosphere (S/C ratio 3, GHSV:91800 h^{-1}, reforming temperature 800 °C).

Reforming Atmosphere	CO_2 (mol $mol_{toluene}^{-1}$)	CO (mol $mol_{toluene}^{-1}$)	H_2 (mol $mol_{toluene}^{-1}$)	CO_2 selectivity
N_2 (1st hour)	2.2	4.5	13.0	33%
N_2 (5th hour)	2.2	4.4	13.0	33%
N_2 (Equilibrium)	(3.2)	(3.8)	(14.3)	(46%)
H_2 (1st hour)	1.9	4.6	11.2	29%
H_2 (5th hour)	1.8	4.3	10.4	30%
H_2 (Equilibrium)	(2.4)	(4.6)	(13.3)	(34%)
CO (1st hour)	4.1	2.3	14.7	64%
CO (5th hour)	4.0	2.3	14.5	63%
CO (Equilibrium)	(6.3)	(0.7)	(17.3)	(90%)
CO_2 (1st hour)	1.2	5.3	10.7	18%
CO_2 (5th hour)	1.2	5.1	10.6	19%
CO_2 (Equilibrium)	(0.6)	(6.4)	(11.6)	(9%)
CH_4 (1st hour)	3.0	4.8	16.5	38%
CH_4 (5th hour)	2.5	4.1	13.8	38%
CH_4 (Equilibrium)	(3.5)	(4.6)	(18.0)	(43%)

Thermal gravimetric analysis was conducted on the spent catalysts to investigate the coke deposition in different atmosphere reaction tests. Figure 5.7 presents the influence of the five different reforming atmospheres tested on coke deposition for Ni/Al_2O_3 catalyst. In addition, Table 5.5 shows the carbon conversion from toluene to coke and the fraction of coke on the catalyst under different reforming atmosphere. The conversion to carbon deposits of 100% N_2, 30% CO in N_2 and 20% CO_2 in N_2 atmosphere was very close, which indicates that CO or CO_2 content in reforming atmosphere has very limited influence on carbon deposition on catalyst surface, and the catalyst remains stable during the tests. The presence of 30% H_2 increased the coke weight, which matched the slight deactivation observed in toluene conversion to C-containing gases and the drop in H_2 product yield. The presence of H_2 might prevent coke reaction with steam, and shift the equilibrium towards more coke. A similar phenomenon was discovered by Cao, Ren et al. (2018). They found that H_2 significantly promoted the carbon deposition on Ni/Al_2O_3 and caused the catalyst deactivation, due to the acidity of the carrier (Cao, Ren et al. 2018). CH_4 atmosphere test had the highest coke content and ratio, the high amount of coke on catalyst surface might be the main reason for the catalyst deactivation.

Table 5.5 Toluene conversion to coke and fraction of coke deposited on the catalyst at different reforming atmosphere (800 °C, S/C:3, GHSV:91800 h^{-1}).

Reforming Atmosphere	N_2	H_2	CO	CO_2	CH_4	CH_4(no C_7H_8)
Coke/C in toluene	0.68%	0.90%	0.61%	0.64%	1.54%	-
Coke/Catalyst (g_C g_{cat}^{-1})	0.184	0.245	0.165	0.173	0.417	0.112

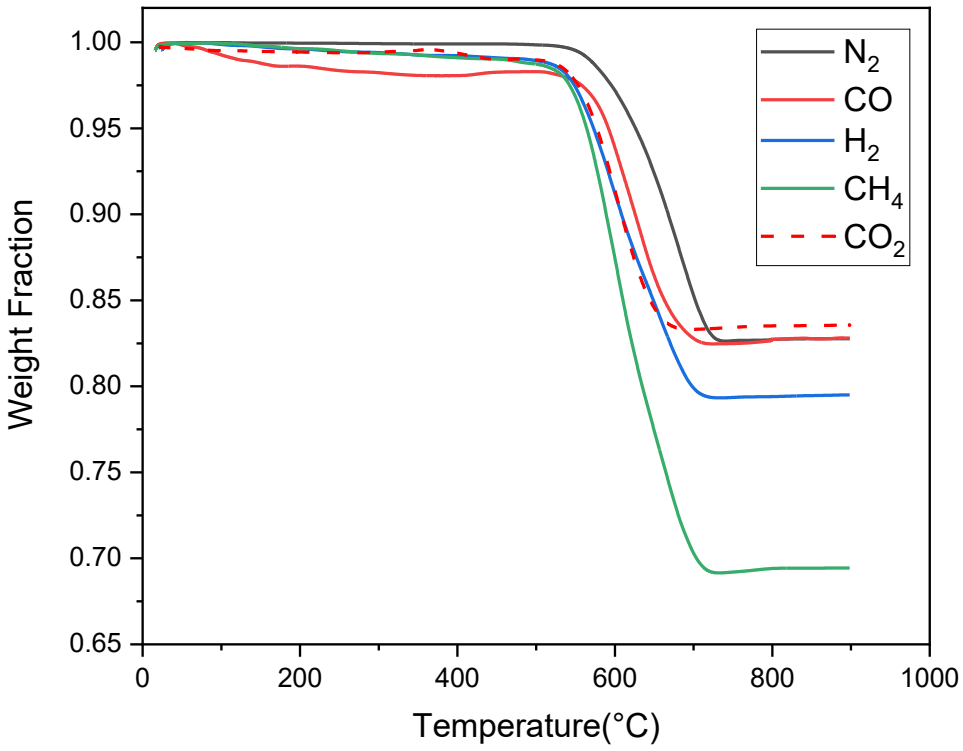

Figure 5.7 Thermal gravimetric analysis for the spent catalysts at different reforming atmosphere (800 °C, S/C:3, GHSV:91800 h^{-1}, 5-hour test. N_2: 100%N_2, H_2: 30% H_2 in N_2, CO: 30% CO in N_2, CO_2: 30% CO_2 in N_2, CH_4: 30% CH_4 in N_2).

5.4 Influence of the multi gas atmosphere on toluene steam reforming

All the above results showed reforming of toluene in a N_2 or single gas in N_2 environment, while the gasification gas is a more complex mixture of CO, CO_2, H_2 and CH_4. The experiments discussed in this section were designed to simulate a syngas rich environment as in a typical gasifier under normal operation conditions. Influence of syngas and other gas mixture atmosphere on toluene steam reforming was studied in this section.

5.4.1 Influence of CO and H_2 mixture on toluene steam reforming

In typical biomass gasification gas or syngas, CO and H_2 were reported to be the two main gases with the highest concentration (Sutton, Kelleher et al. 2001, Abu El-Rub, Bramer et al. 2004). Previous tests focused on the influence of CO and H_2 in reforming respectively, this section studied the impact of CO and H_2 mixture atmosphere. 30% H_2 and 30% CO balanced N_2 was selected as the reaction atmosphere.

Figure 5.8 shows the gas product yield and conversion of toluene steam reforming 5-hour test in 30% H_2 and 30% CO balanced N_2 atmosphere. Product yields of CO and H_2 were very stable in the first 2.5 h, and then started to drop slowly until the end of the tests. The overall conversion from toluene to gases also decreased to lower than 90% at 160 min, and finally achieved a conversion rate of 84%. In addition, Table 5.6 shows the CO_2, CO and H_2 yield in mol mol $_{toluene}^{-1}$. CO and CO_2 yields declined by ~10% in mole production in the 5-hour test.

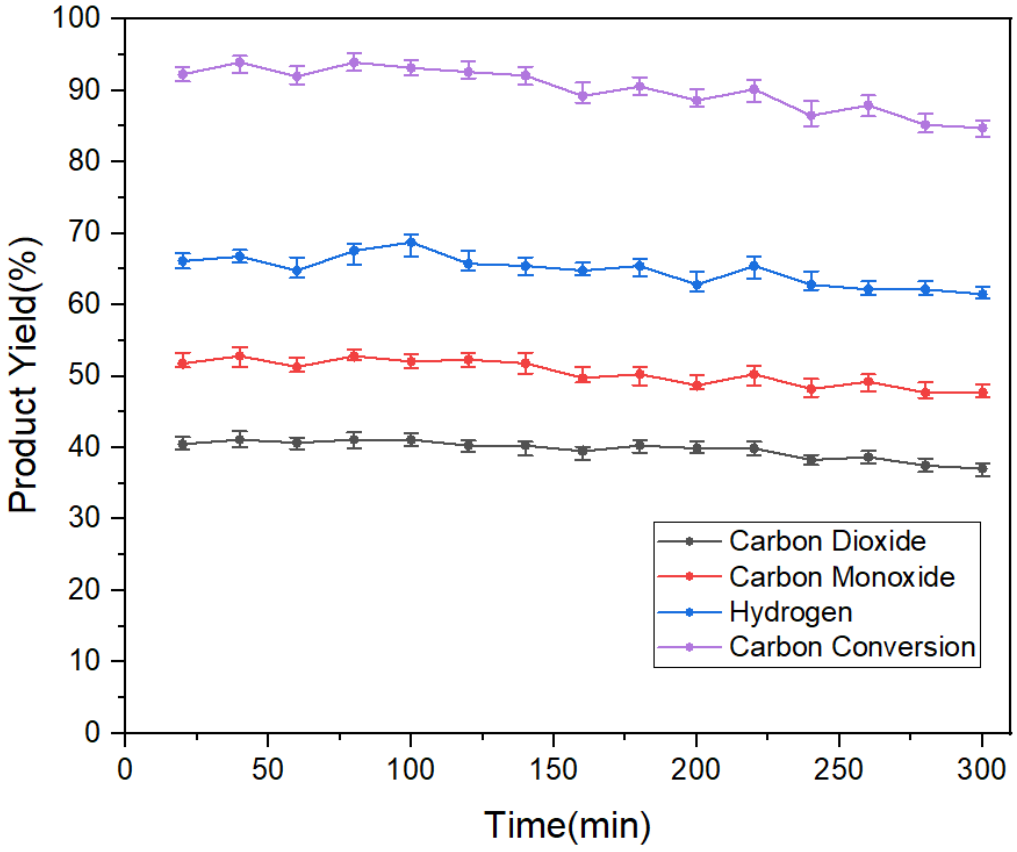

Figure 5.8 Product yield trend and conversion of toluene steam reforming test in 30% H_2 and 30% CO balanced N_2 atmosphere (5-hour test, Ni/Al_2O_3 catalyst, 800 °C, S/C ratio 3, GHSV: 91800 h^{-1}).

Table 5.6 Product yields for the gaseous products in 30% H_2 and 30% CO balanced N_2 atmosphere (5-hour test, Ni/Al_2O_3 catalyst, 800 °C, S/C ratio 3, GHSV: 91800 h^{-1}).

Atmosphere	CO_2 (mol mol $_{toluene}^{-1}$)	CO (mol mol $_{toluene}^{-1}$)	H_2 (mol mol $_{toluene}^{-1}$)	CO_2 selectivity
H_2 & CO (1st hour)	2.8	3.7	11.9	43%
H_2 & CO (5th hour)	2.6	3.3	11.1	44%
(Equilibrium)	(4.3)	(2.7)	(15.3)	(61%)

Figure 5.9 summarizes toluene conversion to C-containing gases and CO, CO_2 yields at H_2, CO and mixture gas atmosphere. CO content in the carrier gas had no obvious effect on catalyst deactivation in multi gas mixture atmosphere. The decrease in toluene conversion was led by the presence of H_2, as the overall toluene conversion showed similar trends in 30% H_2 in N_2 and 30% CO, 30%H_2 in N_2 atmosphere tests. The equilibrium and experimental results both showed that CO had more significant influence on the selectivity of product CO/CO_2 than H_2. When same concentrations of CO and H_2 were introduced to the reaction system, the equilibrium shifted to produce more CO_2 when comparing to inert N_2 atmosphere. Both equilibrium and experimental results showed this phenomenon.

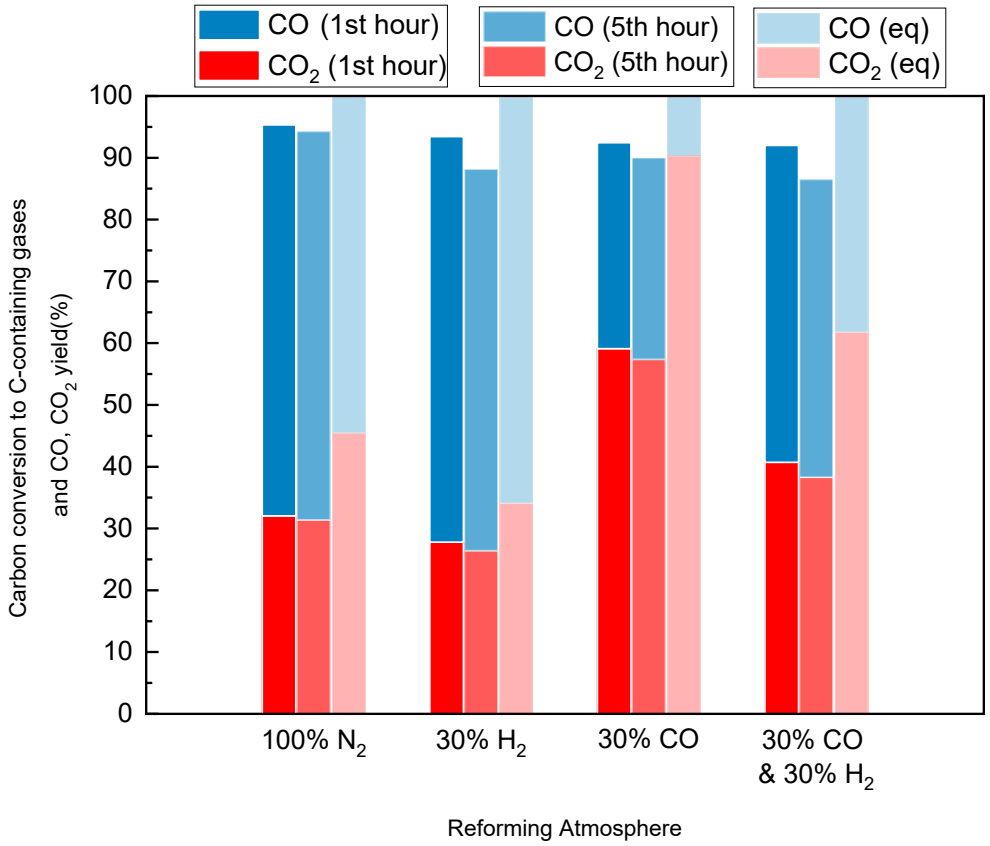

Figure 5.9 Toluene conversion to C-containing gases and CO, CO_2 yields at H_2, CO and mixture gas atmosphere (S/C ratio 3 GHSV:91800 h^{-1}, reforming temperature 800 °C, all the gas atmosphere balanced with N_2).

5.4.2 Influence of CH_4 and H_2 mixture on toluene steam reforming

The above results showed that CH_4 and H_2 atmosphere had relatively more influence on toluene conversion and carbon deposition. This section discusses the impact of CH_4 and H_2 mixture atmosphere on toluene steam reforming. To compare with the previous results, the reforming gas atmosphere was designed as 3% CH_4 and 30% CO in N_2. CH_4 was considered as C-containing reactant and calculated into S/C ratio.

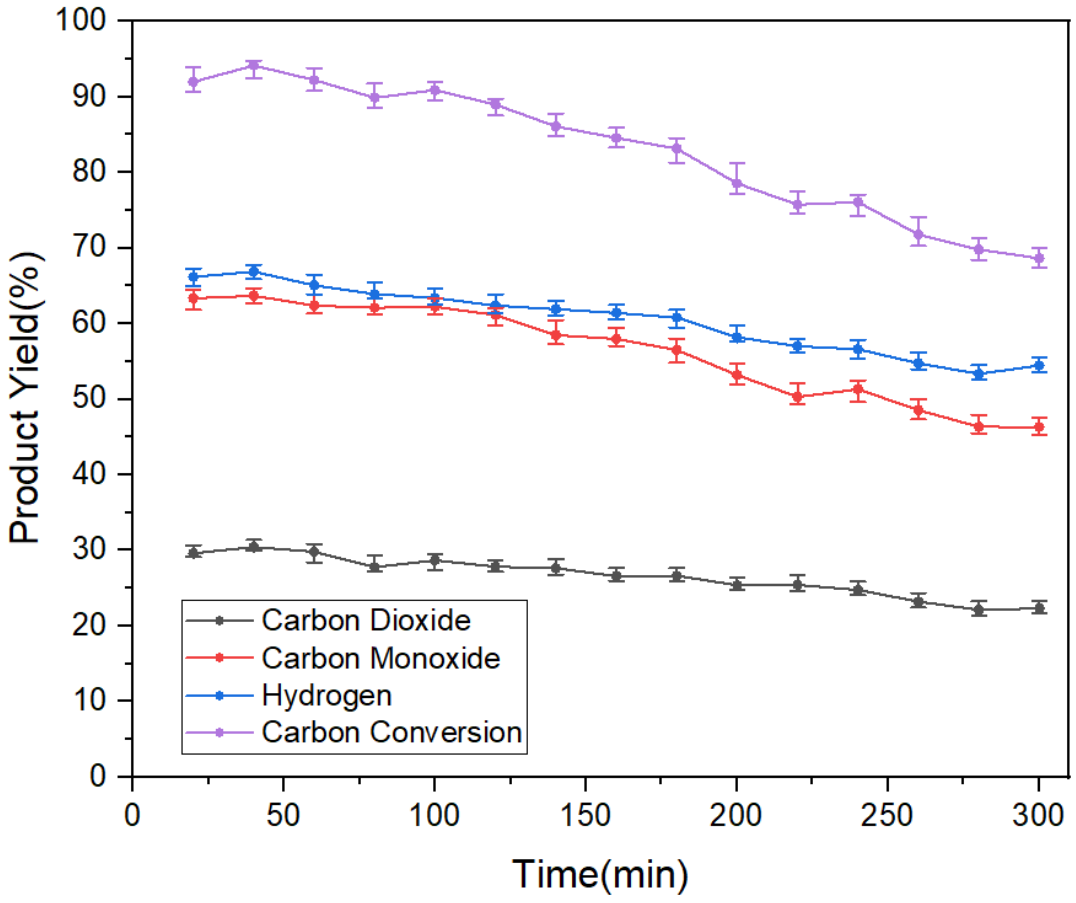

Figure 5.10 Product yield trend and carbon conversion of toluene steam reforming test in 3% CH_4 and 30% H_2 balanced N_2 atmosphere (5-hour test, Ni/Al_2O_3 catalyst, 800 °C, S/C ratio 3, GHSV: 91800 h^{-1}).

Table 5.7 Product yields for the gaseous products in 3% CH_4 and 30% H_2 balanced N_2 atmosphere (5-hour test, Ni/Al_2O_3 catalyst, 800 °C, S/C ratio 3, GHSV: 91800 h^{-1})

Atmosphere	CO_2 (mol mol $_{toluene}^{-1}$)	CO (mol mol $_{toluene}^{-1}$)	H_2 (mol mol $_{toluene}^{-1}$)	CO_2 selectivity
H_2 & CH_4(1st hour)	2.5	5.2	15.1	32%
H_2 & CH_4 (5th hour)	1.8	3.8	10.9	32%
(Equilibrium)	(2.8)	(5.3)	(17.1)	35%

Figure 5.10 shows the gas product yield and toluene conversion into gases in 3% CH_4 and 30% H_2 balanced N_2 atmosphere. The toluene conversion and CO, CO_2 and H_2 yield started to decrease after 100 min and declined steadily until the end of the test. The conversion of toluene, CO yield, H_2 yield and CO_2 yield decreased from 93%, 64%, 66%, 29% to 69%, 46%, 54%, 22% respectively. Figure 5.11 summarizes the toluene conversion to C-containing gases and CO, CO_2 yields in H_2, CH_4 individual and combined atmosphere tests and compares with the experiments in inert N_2 atmosphere. The CH_4 and H_2 combined atmosphere showed more significant decrement in gas production of toluene steam reforming.

Table 5.7 presents CO, CO_2 and H_2 production during the first hour, the fifth hour and compares with equilibrium results. H_2 production yield decreased from 15.1 to 10.9 mol mol $_{toluene}^{-1}$ by 28%, which was larger than expectation. According to Table 5.4, the decrement of H_2 yield in 30% H_2 in N_2 atmosphere and 3% CH_4 in N_2 atmosphere was 7% and 16%, respectively. It could be concluded that the presence of CH_4 and H_2 can deactivate the Ni/Al_2O_3 catalyst much more rapidly than CH_4 or H_2 single gas atmosphere.

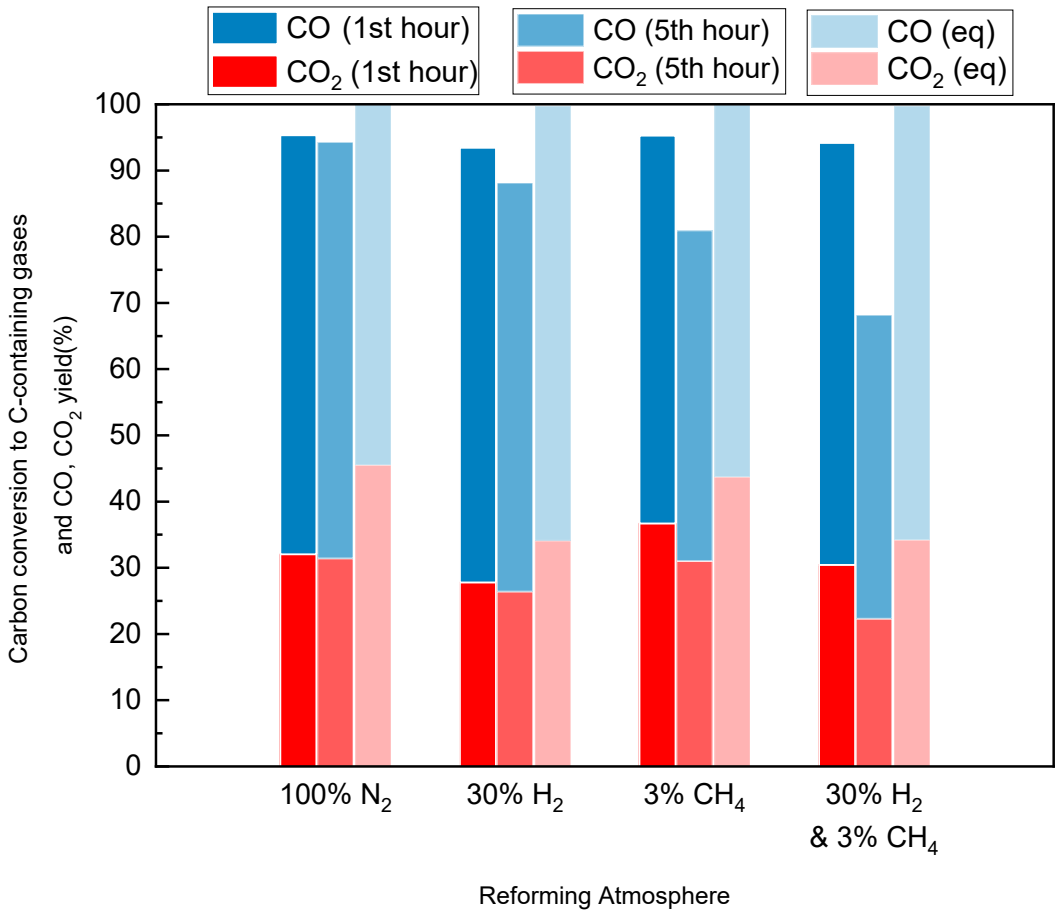

Figure 5.11 Toluene conversion to C-containing gases and CO, CO_2 yield at H_2, CH_4 and mixture gas atmosphere (S/C ratio 3, GHSV:91800 h^{-1}, reforming temperature 800 °C, all the gas atmosphere balanced with N_2).

5.4.3 Influence of all gas mixture toluene steam reforming

In this section, a gas mixture stream of 3% CH_4, 30% H_2, 30% CO and 20% CO_2 in N_2 was chosen to simulate the typical biomass gasification gas product. Figure 5.12 shows the gas product yield and toluene conversion simulated gasification gas atmosphere. Toluene conversion and gas yields started to decline slightly in the second hour, and then decreased significantly in the rest 3 hours. The conversion of toluene dropped from 92% to 66% in the 5-hour test. The trend was similar to the test in 3% CH_4 and 30% H_2 atmosphere, which

indicated that CO and CO_2 had limited influence on the deactivation of the catalyst.

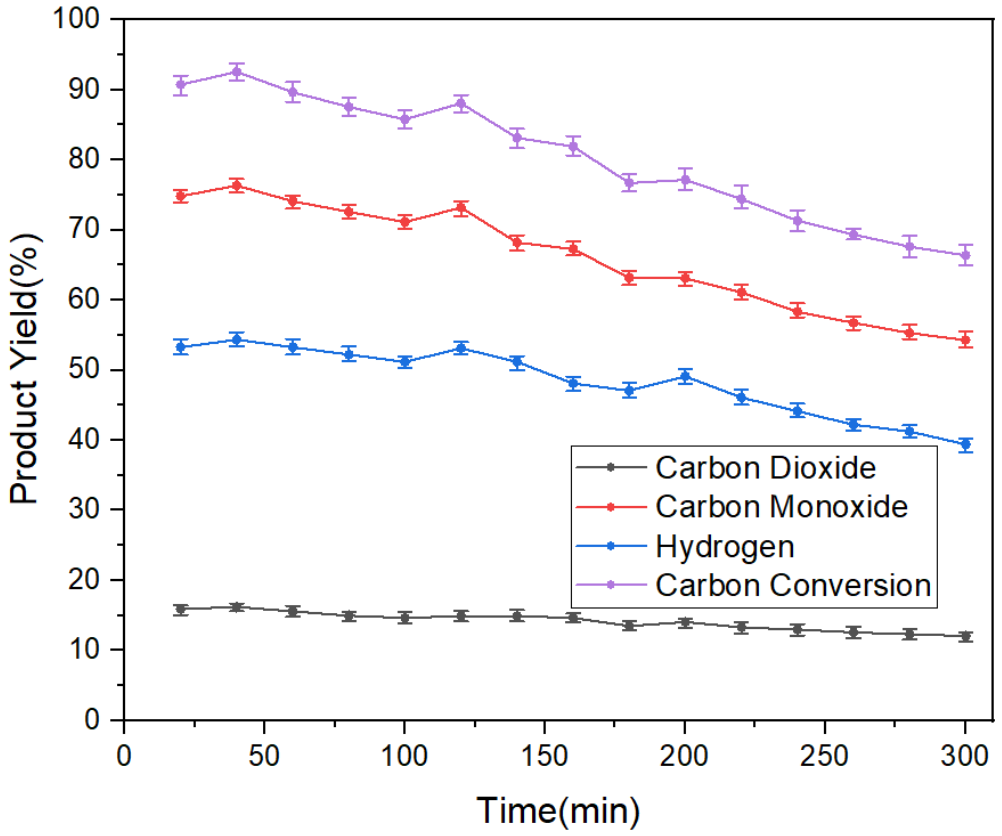

Figure 5.12 Product yield trend and conversion of toluene steam reforming test in 3% CH_4, 30% H_2, 30% CO and 20% CO_2 balanced N_2 atmosphere (5-hour test, Ni/Al_2O_3 catalyst, 800 °C, S/C ratio 3, GHSV: 91800 h^{-1}).

Figure 5.13 summarizes the toluene conversion to C-containing gases and CO, CO_2 yields in all the CH_4 involved atmosphere tests and compares with the experiments in inert N_2 atmosphere. Although the concentration of CH_4 in carrier gas was fixed at 3 vol.%, which was much lower than the concentration of CO, CO_2 and H_2, CH_4 was the main reason for catalyst deactivation. The injected H_2 could largely decrease the toluene conversion to gases with the presence of a small amount of CH_4.

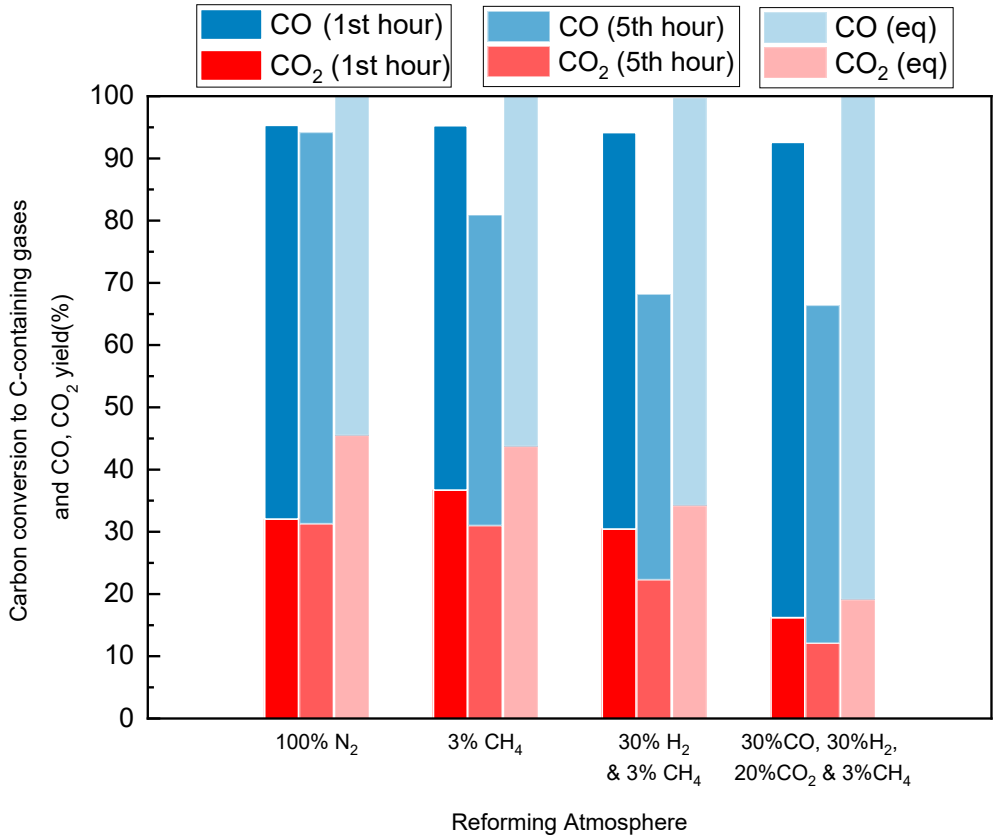

Figure 5.13 Toluene conversion to C-containing gases and CO, CO_2 yield at CO, CO_2, H_2, CH_4 and mixture gas atmosphere (S/C ratio 3 GHSV:91800 h^{-1}, reforming temperature 800 °C, all the gas atmosphere balanced with N_2).

Table 5.8 Product yields for the gaseous products in 3% CH_4, 30% H_2, 30% CO and 20%CO_2 balanced N_2 atmosphere (5-hour test, Ni/Al_2O_3 catalyst, 800 °C, S/C ratio 3, GHSV: 91800 h^{-1}).

Atmosphere	CO_2 (mol mol $_{toluene}^{-1}$)	CO (mol mol $_{toluene}^{-1}$)	H_2 (mol mol $_{toluene}^{-1}$)	CO_2 selectivity
All gas (1st hour)	1.3	6.2	12.0	17%
All gas (5th hour)	1.0	4.8	8.7	17%
(Equilibrium)	(1.6)	(6.5)	(15.5)	(20%)

As shown in Figure 5.14, the coke formation was favored by the complex gas atmosphere. The amount of coke over the Ni/Al_2O_3 catalyst under 30% H_2 and 30% CO balanced N_2, 3% CH_4 and 30% H_2 balanced N_2, 3% CH_4, 30% H_2, 30% CO and 20%CO_2 balanced N_2 was 0.238, 0.684, and 0.676 $g_C\ g_{cat}^{-1}$ respectively. The trend of spent catalyst with CH_4 and H_2 was similar to the trend with CH_4, H_2, CO and CO_2, which also indicated that the presence of CH_4 and H_2 had more significant impact on coke formation on catalyst. CO and CO_2 were observed to have very limited influence on coke formation. Table 5.4 shows the carbon conversion from toluene to coke with different gas mixture reforming atmosphere. Comparing to Table 5.5, the introduction of H_2 to the 3% CH_4 atmosphere could further increase the coke amount greatly, and then deactivated the Ni/Al_2O_3 catalyst.

Table 5.9 Toluene conversion to coke and fraction of coke deposited on the catalyst at different reforming atmosphere (800 °C, S/C:3, GHSV:91800 h^{-1}, 5-hour test. CO & H_2 in N_2: 30% H_2 and 30% CO balanced N_2, CH_4 & H_2 in N_2: 3% CH_4 and 30% H_2 balanced N_2, All gas mixtures: 3% CH_4, 30% H_2, 30% CO and 20%CO_2 balanced N_2).

Reforming Atmosphere	CO & H_2 in N_2	CH_4 & H_2 in N_2	All gas mixture
Coke/C in toluene	0.88%	2.53%	2.49%
Coke/Catalyst ($g_C\ g_{cat}^{-1}$)	0.238	0.684	0.676

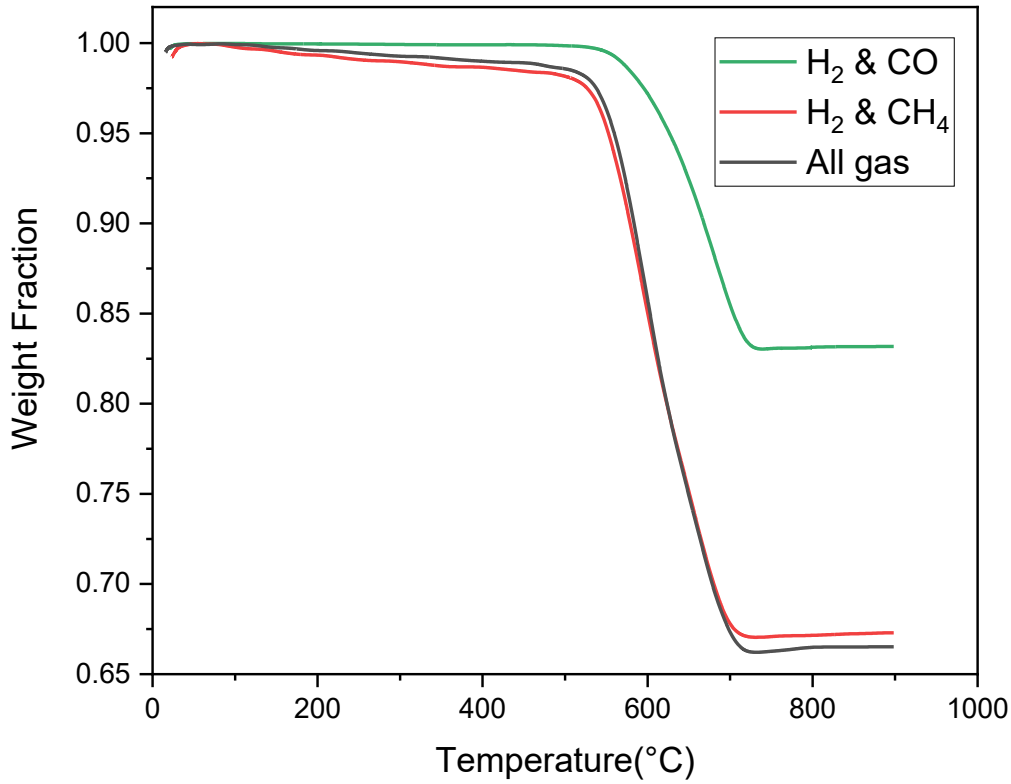

Figure 5.14 Thermal gravimetric analysis for the spent catalysts at different gas mixture atmosphere (800 °C, S/C:3, GHSV:91800 h^{-1}, 5-hour test. CO & H_2 in N_2: 30% H_2 and 30% CO balanced N_2, CH_4 & H_2 in N_2: 3% CH_4 and 30% H_2 balanced N_2, All gas mixture: 3% CH_4, 30% H_2, 30% CO and 20%CO_2 balanced N_2).

5.5 Summary

Ni/Al_2O_3 is a conventional catalyst with serious coke and deactivation problems in steam reforming of tar and tar model compounds. The effect of reforming gas atmosphere was studied using Ni/Al_2O_3 catalyst. The compositions of input H_2, CO, CO_2 and CH_4 (balanced with N_2) was fixed at 30, 30, 20 and 3 vol.%, the

influence of single gas, multi gas and simulated gasification gas atmosphere was studied in this chapter.

CO, CO_2 and H_2 with a relatively high contents (>20%) in reforming atmosphere could slightly inhibit the toluene conversion into gas, but still show a relatively high initial toluene conversion rate >90 % in first hour. However, the presence of both CO and H_2 did not show an additive effect to prevent initial toluene conversion further, toluene conversion still stayed above 90% in first hour.

CO and CO_2 in reaction atmosphere showed limited impact on the catalyst deactivation, while the high content of CO and CO_2 in reforming atmosphere would affect the selectivity of product CO/CO_2 mainly due to (reverse) WGS reaction. Also, CO had more significant influence on the selectivity of product CO/CO_2 than H_2. Experimental CO_2 selectivity under all atmospheres is lower than equilibrium predicted except for 20% CO_2 atmosphere, indicating that toluene is reformed to CO first and then CO undergoes WGS reaction to produce CO_2.

H_2 content in reforming atmosphere could slightly deactivate the catalyst and promote the coke formation on Ni/Al_2O_3 catalyst and decrease the H_2 production yield from toluene steam reforming, one possible reason is that H_2 shift the equilibrium to produce more coke. A relatively low content of CH_4 had a significant influence on coke formation on catalyst and catalyst deactivation. Moreover, the addition of H_2 to the reforming atmosphere with the presence of CH_4 could increase the coke amount greatly, further decrease the gas yield and deactivate the Ni/Al_2O_3 catalyst.

6 Improving Catalyst Stability under Different Atmosphere in Toluene Steam Reforming

6.1 Introduction

Recently, much research has been focused on the modification of conventional Ni-based catalyst in several approaches, such as change in the synthesis method to establish interactions between metal and basic oxide supports (Nabgan, Abdullah et al. 2016), doping with base metal oxides (Ashok, Dewangan et al. 2020). The most explored method is doping the metal and/or support with base metal oxides. It is reported that adding alkali (K, Na) (Mitsuoka, Hayashi et al. 2011, Hognon, Dupont et al. 2014) and alkaline earth metals (Mg, Ca) (Li, Koike et al. 2014, Lertwittayanon, Youravong et al. 2017) can promote the stability of the catalyst by increasing the water adsorption on the surface.

Gasification ash is one of the main solid wastes produced from the gasification process of coal and biomass. It usually contains many oxides such as SiO_2, Al_2O_3, Fe_2O_3, CaO, MgO, K_2O, Na_2O, etc. Although some of these metallic oxides in ash can promote the gasification rate, the extremely high amount of ash may cause some disadvantages. Gasification ash (coal ash, biomass ash) has been studied as a catalyst support for steam reforming of tar for years since it can reduce the problem of ash-handling during biomass gasification. Lu, Xiong et al. (2020) reported that Mo-Ni/coal gangue ash catalyst showed a good steam reforming performance in terms of the toluene conversion (~92%) and H_2 yield (~64%) with a S/C ratio 2, at 800 °C. Gu, Wang et al. (2020) studied waste peat ash supported Ca catalyst and found that this catalyst showed a > 91% toluene conversion and > 67% yield at 800 °C, 0.7 s residence time and S/C ratio 3. Although ash was reported to be a suitable support for toluene

steam reforming, little research has focused on the effects of ash as direct catalyst or a guard layer. Ash itself showed a relatively low activity as direct catalyst even at high temperatures, Chen, Schmid et al. (2020) studied the catalytic effect of straw char containing fly ash in toluene steam reforming and found that the highest toluene conversion (21%) was achieved at 900 °C, which is much lower than other catalysts.

As mentioned in Chapters 4 and 5, Ni/Al_2O_3 showed good activity and stability in an inert atmosphere, while the complicated gasification gas atmosphere could rapidly deactivate the catalyst due to the presence of H_2 and CH_4. It is very necessary to improve the stability of Nickel catalysts in the gasification gas atmosphere. In this chapter, a biomass ash was investigated to try to improve the stability of Ni catalyst under simulated gas reforming atmosphere. However, this biomass ash was not introduced as catalyst support, the effect of this biomass ash acting as a guard layer (a pre-treating/protection layer set before Ni/Al_2O_3 layer) and a spacer (physically mixed with Ni/Al_2O_3) was investigated.

6.2 Experimental conditions

All the experiments in this chapter were carried out at 800 °C using toluene as feedstock. S/C (Injected steam to Carbon in fed toluene and methane) mole ratio was kept at 3, GHSV 91800 h^{-1}. The feeding rate of carrier gas (atmosphere gas) was fixed at 0.3 L min^{-1}, toluene injection rate was 1.8 g h^{-1} (2.05 ml h^{-1} on syringe pump). The conventional Ni/Al_2O_3 catalyst was used for all the tests, and each test period (controlled by start/stop reactant injection) was 5 hours. All the results were obtained from the quartz tube reactor described in Chapter 3 under atmospheric pressure.

Table 6.1 Compositions of metal elements in biomass ash detected by X-ray Fluorescence analysis.

Compound	Concentration (wt.%)
Mg	0.43
Al	0.95
Si	21.70
P	0.55
S	0.34
Cl	0.34
K	7.39
Ca	37.61
Ti	0.45
Cr	3.46
Mn	3.84
Fe	14.34
Ni	7.53
Zn	0.27

Biomass fly ash was generated from the steam gasification of beech-wood and polyethylene at 850 °C, 1 atm in a fluidized-bed reactor (Zhu, Zhang et al. 2019). After the biomass ash was obtained from those tests, it was calcined at 800 °C with a ramping rate of 2 °C min^{-1} for 4 hours. After cooling, the biomass ash was crushed and sieved to a size of 0.2 to 0.5 mm. Table 6.1 shows the metal element compositions in the biomass ash. In the biomass ash, Ca is the most

abundant metal element, followed by Si, Fe, K and Ni.

To investigate the influence of adding biomass ash as a spacer or a guard layer for the Ni/Al_2O_3, there were four different toluene reforming catalyst bed configurations applied in the experiments as shown in Table 6.2. The 5-hour experimental results of Ni/Al_2O_3 are shown in Chapter 5. Three catalyst bed configurations employed a one-layer setup and the fourth used two layers, as shown in Figure 6.1. The total weight of the catalyst bed remained at 500 mg to keep a constant GHSV/residence time. All the catalyst beds were activated by 50 mL min^{-1} 100% H_2 at 800°C for 1 hour. The distance of the ash layer and the catalyst layer of the two-layer reforming system was kept at 10 mm. Five different reforming atmospheres were chosen to investigate the effect of different catalyst beds in toluene steam reforming: inert atmosphere (100% N_2), H_2 atmosphere (30% H_2, balance N_2), CH_4 atmosphere (3% CH_4, balance N_2), H_2 and CH_4 atmosphere (3% CH_4, 30% H_2, balance N_2), simulated gasification gas atmosphere (3% CH_4, 30% H_2, 20% CO_2, 30% CO, balance N_2). The gas product yield and carbon conversion were calculated by the equations stated in Chapter 5. CH_4 product yields under all conditions are low than 5%, and the absolute error is $< \pm 0.15\%$, so the error bars of CH_4 product yield are not shown in the figures.

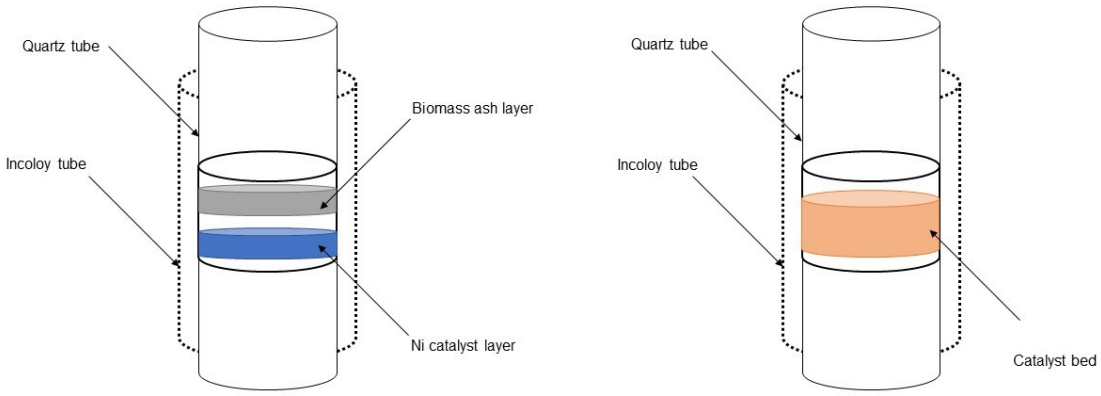

Figure 6.1 Two-layer and one-layer toluene reforming test setup.

Table 6.2 Different catalyst beds for toluene steam reforming.

Reforming tests	Catalyst bed
Biomass ash activity test	500 mg ash
Ni/Al_2O_3 catalyst activity test	500 mg Ni/Al_2O_3
Biomass ash and Ni/Al_2O_3 mixture activity test	250 mg Ni/Al_2O_3 mixed with 250 mg ash
Two-layer biomass ash-Ni/Al_2O_3 reforming test	First layer: 250 mg ash Second layer: 250 mg Ni/Al_2O_3

6.3 Catalytic tests under inert atmosphere

This section compares the influence of different catalyst beds on steam reforming of toluene under 100% N_2 atmosphere.

6.3.1 Biomass ash activity test in inert atmosphere

The steam reforming test of this biomass ash only under 100% N_2 atmosphere was conducted as shown in Figure 6.2. The results showed that the biomass ash itself could promote the conversion of toluene into gaseous products, the overall carbon conversion was stable at ~43% throughout the 5-hour test. The main gas products included H_2, CO_2, CO and CH_4. The product yield of H_2, CO_2, CO and CH_4 remained stable at ~24%, 7.5%, ~29% and 5% respectively. The total conversion from toluene into gas product and all the gas yields were much lower than Ni/Al_2O_3 catalyst (shown in Section 4.5), and most toluene fed to the reactor remained unreacted after the 5-hour catalytic test.

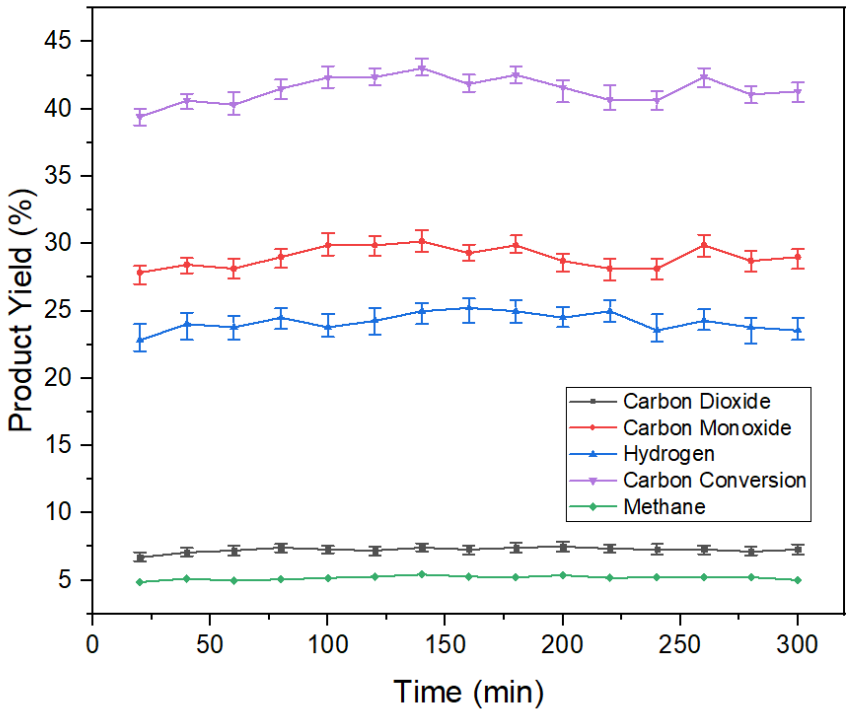

Figure 6.2 Product yield trend and carbon conversion of toluene steam reforming test in N_2 atmosphere (5-hour test, 500 mg biomass ash catalyst, 800 °C, S/C ratio 3, GHSV: 91800 h^{-1}).

6.3.2 Ni/Al_2O_3 and biomass ash mixture activity test in inert atmosphere

Figure 6.3 presents the trend of product gas distribution of toluene reforming test using biomass ash and Ni/Al_2O_3 mixture as catalyst bed. The introduction of Ni/Al_2O_3 increased the overall conversion to 83% and remained > 80% throughout the 5-hour test. The product yield of H_2, CO_2, CO and CH_4 stayed at ~54%, 25%, ~57% and 2% respectively in 5 hours. Although the addition of Ni/Al_2O_3 improved the performance of ash, the overall conversion and H_2 yield were still lower than most metal catalyst in toluene steam reforming (Guan, Kaewpanha et al. 2016).

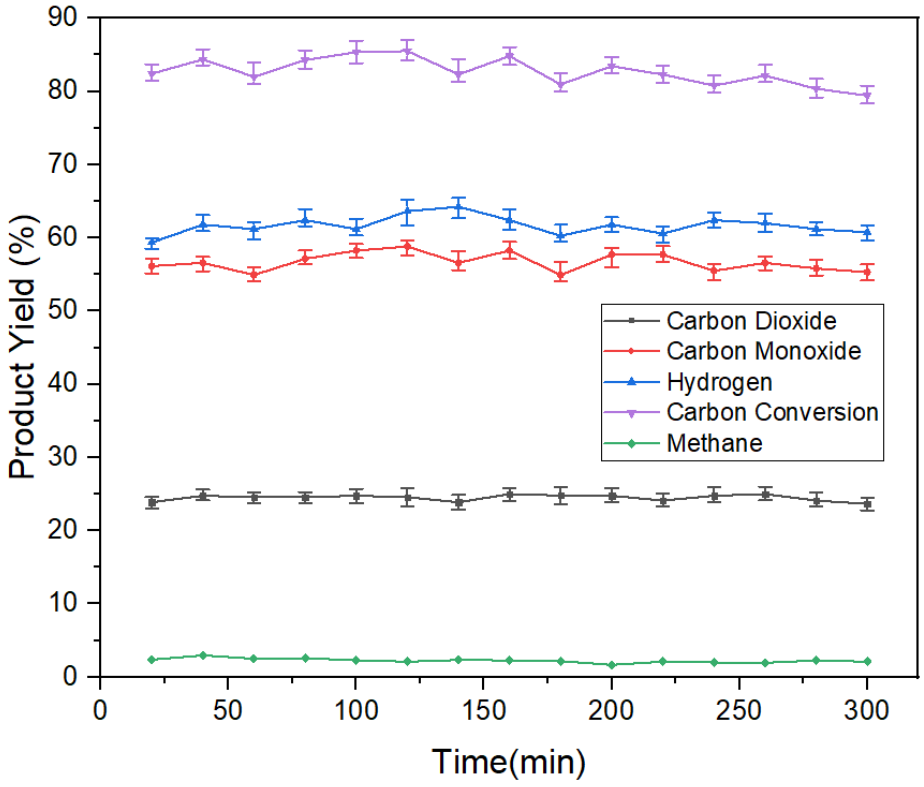

Figure 6.3 Product yield trend and carbon conversion of toluene steam reforming test in N_2 atmosphere (5-hour test, biomass ash and Ni/Al_2O_3 mixture catalyst, 800 °C, S/C ratio 3, GHSV: 91800 h^{-1}).

6.3.3 Two-layer biomass ash and Ni/Al_2O_3 reforming test in inert atmosphere

Product yield (CO, H_2 and CO_2), toluene conversion trend of the two-layer catalyst bed reforming test is shown in Figure 6.4. Toluene conversion into gases stayed at 94% in the 5-hour test, and CH_4 yield remained lower than 0.1%. H_2 yield also increased to ~75% in the 5-hour test, while CO_2 and CO yield stayed at 28% and 64%, respectively.

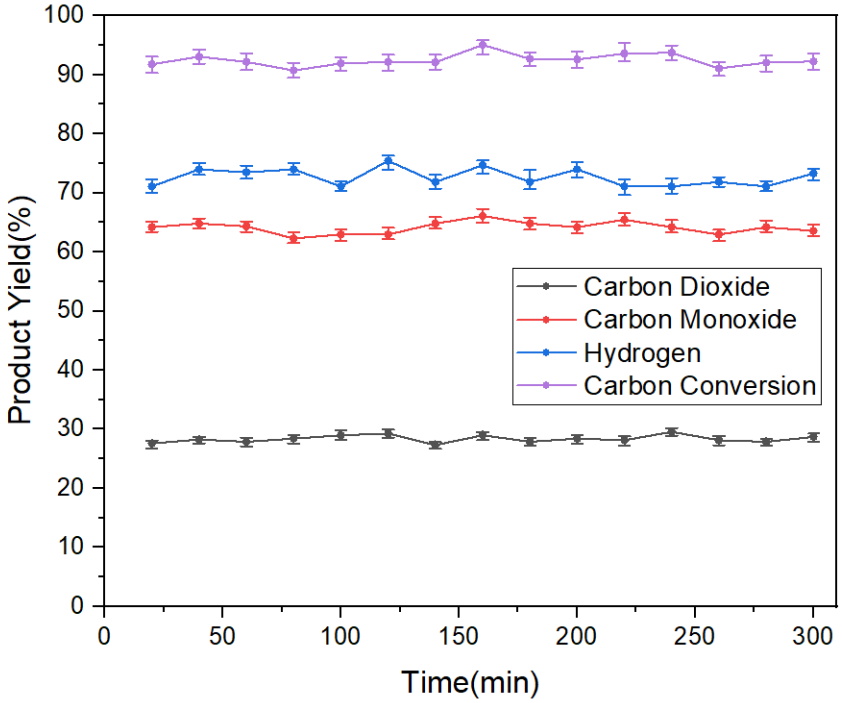

Figure 6.4 Product yield trend and carbon conversion of toluene steam reforming test in N_2 atmosphere (5-hour test, Two-layer biomass ash and Ni/Al_2O_3 catalyst, 800 °C, S/C ratio 3, GHSV: 91800 h^{-1}).

6.3.4 Inert atmosphere comparison

The catalytic performance of different catalyst beds was tested under 100% N_2 atmosphere, as N_2 is an inert gas and not involved in the reactions. To compare the gas production from catalyst beds, Figure 6.5 summarizes the toluene

conversion into C-containing gases and CO, CO_2, CH_4 yields using different catalyst beds at first hour and fifth hour of the catalytic tests and compares with equilibrium results. The thermodynamic equilibrium simulations were performed using a Gibbs free minimization reactor to help to understand the catalytic performance of different catalyst beds. Ni/Al_2O_3 catalyst performance test results were collected from Chapter 4. Table 6.3 shows the gaseous product yields including CO, CO_2, CH_4 and H_2 in the unit of mol mol $_{toluene}^{-1}$ at the first hour and the fifth hour using different catalyst bed and compares with equilibrium results. No obvious decrease in overall conversion of toluene was observed in all catalyst beds, so all these four catalyst beds have a good stability in toluene steam reforming test. Ni/Al_2O_3 catalyst bed and 2-layer biomass ash-Ni/Al_2O_3 catalyst bed show very similar distribution of CO/CO_2, and they both have high conversions of toluene (> 92%).

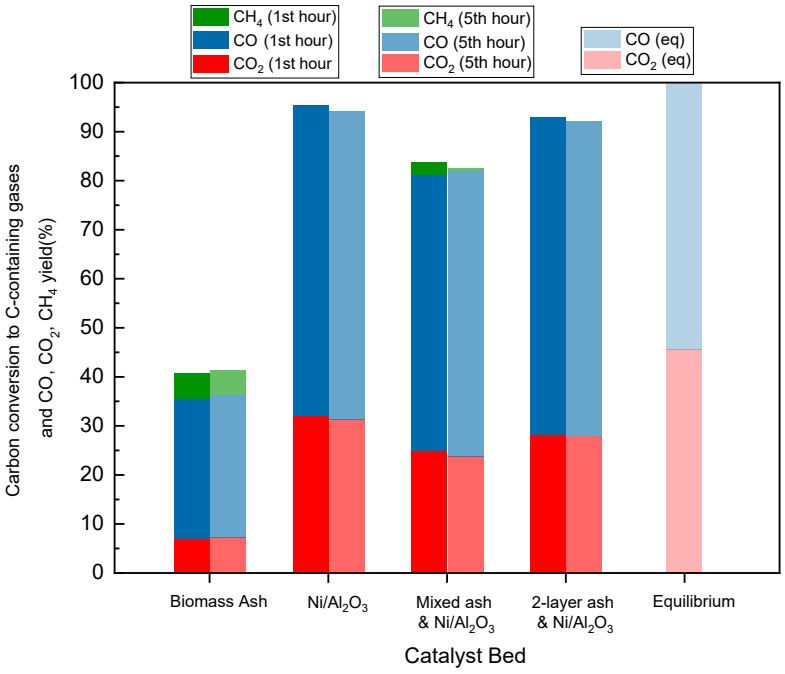

Figure 6.5 Carbon conversion to C-containing gases and CO, CO_2, CH_4 yield under 100% N_2 atmosphere using different catalyst beds (S/C ratio 3 GHSV:91800 h^{-1}, reforming temperature 800 °C).

Table 6.3 shows the gaseous product yields of CO, CO_2, H_2 and CH_4 in the unit

of mol mol $_{toluene}^{-1}$ at the first hour and the fifth hour of different catalyst bed and compares with the equilibrium result. Ni/Al_2O_3 catalyst bed and 2-layer biomass ash-Ni/Al_2O_3 catalyst bed have similar H_2 yield and the highest H_2 production yield is ~13.0 mol mol $_{toluene}^{-1}$. It could also be seen that presence of biomass ash decreased CO_2 selectivity. CO_2 selectivity follows the order: Ni/Al_2O_3 > 2-layer > ash and Ni/Al_2O_3 mixture > ash. Alkali and alkaline earth metal contents in biomass ash could reduce the production of CO_2 and increase CO yield. CO_2 selectivity of 2-layer (31%) and mixture (29%) catalyst bed is very close, but 2-layer system is slightly higher, which indicates that the second Ni/Al_2O_3 layer could promote reverse WGS reaction when comparing to ash layer.

Table 6.3 Product yields for the gaseous products in the catalyst beds (S/C ratio: 3, GHSV:91800 h^{-1}, reforming temperature 800 °C).

Catalyst bed	CO_2 (mol mol $_{toluene}^{-1}$)	CO (mol mol $_{toluene}^{-1}$)	H_2 (mol mol $_{toluene}^{-1}$)	CH_4 (mol mol $_{toluene}^{-1}$)	CO_2 selectivity
Ash (1st hour)	0.6	2.0	4.2	0.4	22%
Ash (5th hour)	0.6	2.0	4.3	0.4	22%
Ni/Al_2O_3 (1st hour)	2.2	4.5	13.0	0	33%
Ni/Al_2O_3 (5th hour)	2.2	4.4	13.0	0	33%
Mixture (1st hour)	1.8	4.4	11.0	0.1	29%
Mixture (5th hour)	1.8	4.4	10.9	0.1	29%
2-layer (1st hour)	2.0	4.5	12.8	0	31%
2-layer (5th hour)	2.0	4.5	12.9	0	31%
(Equilibrium)	(3.2)	(3.8)	(14.3)	(0)	(46%)

Figure 6.6 presents the influence of the different catalyst beds tested on coke deposition for Ni/Al_2O_3 catalyst using thermos-gravimetric analysis. The detailed data of coke fraction is shown in Table 6.4. There are two catalyst results from the 2-layer Ni/Al_2O_3-biomass ash catalytic test: first layer of biomass ash and second layer of Ni/Al_2O_3. The order of coke faction and weight was Ni/Al_2O_3 > 2-layer: Ni/Al_2O_3 layer > Ash and Ni/Al_2O_3 mixture > 2-layer: Ash layer > Ash. The biomass ash showed a good resistance to coke deposition when comparing to Ni/Al_2O_3, and the guardian layer of ash helped to reduce the coke deposition of Ni/Al_2O_3 from 0.184 to 0.146 g g_{cat}^{-1} by 20%

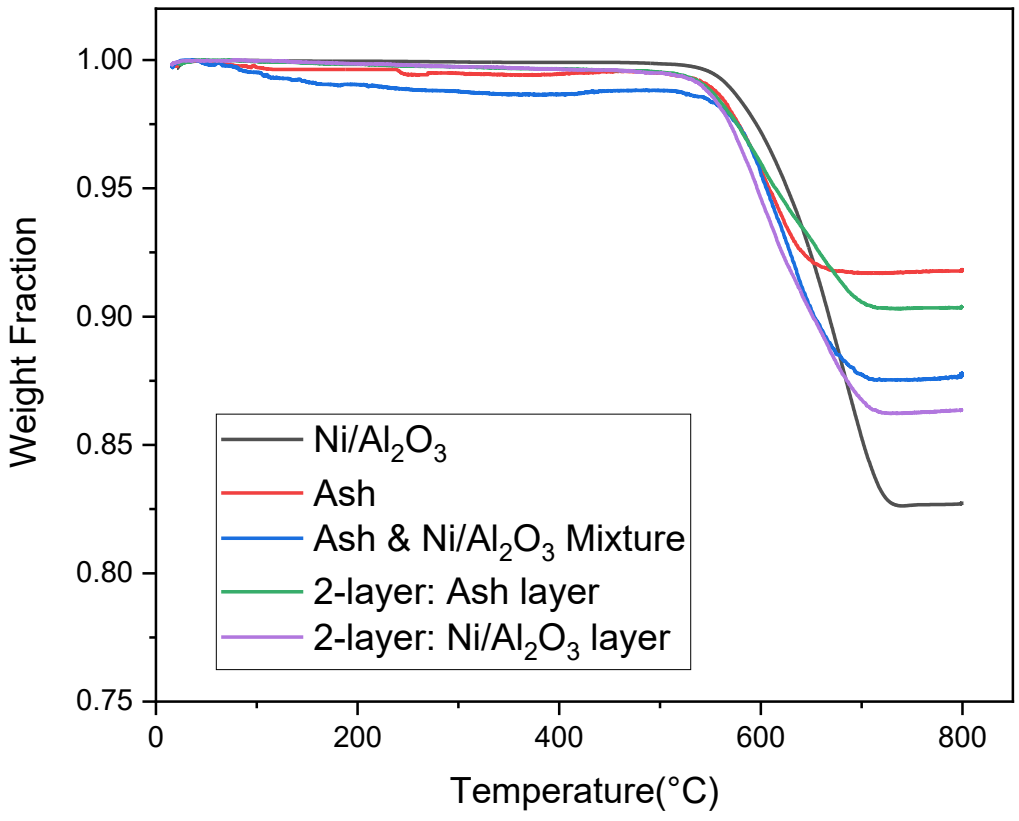

Figure 6.6 Thermal gravimetric analysis for the different spent catalysts in 100% N_2 atmosphere (800 °C, S/C:3, GHSV:91800 h^{-1}, 5-hour test).

Table 6.4 Toluene conversion to coke and fraction of coke deposited on the different catalysts in 100% N_2 (800 °C, S/C:3, GHSV:91800 h-1, 5-hour test).

Catalyst bed	Ni/Al_2O_3	Ash	Ni/Al_2O_3 and Ash mixture	2-layer: Ash layer	2-layer: Ni/Al_2O_3 layer
Coke/C in toluene	0.68%	0.29%	0.47%	0.35%	0.54%
Coke/Catalyst bed ($g_C\ g_{cat}^{-1}$)	0.184	0.078	0.128	0.095	0.146

6.4 Catalytic tests under 30% H_2 atmosphere

In this set of experiments, 30% H_2 in balanced N_2 was used as reforming atmosphere for toluene steam reforming test using different catalyst beds.

6.4.1 Biomass ash activity test under 30% H_2 atmosphere

The reforming activity results of biomass ash itself is shown in Figure 6.7. Carbon conversion reached to the highest at 42.8% at second hour and stayed above 40% in the 5-hour test. The overall conversion was slightly lower than in 100% N_2 atmosphere. H_2 yield stayed at ~18%, which was much lower than in N_2 atmosphere (24%). CO, CO_2 and CH_4 stayed at 29%, 5%, 6%, respectively in the 5-hour test.

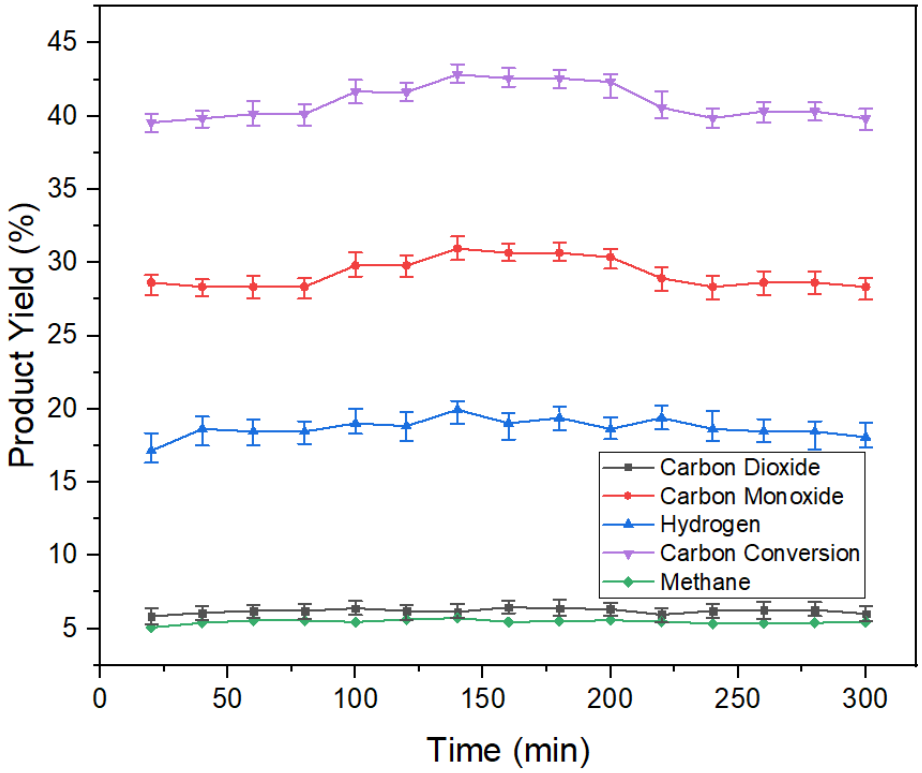

Figure 6.7 Product yield trend and carbon conversion of toluene steam reforming test in 30% H_2 atmosphere (5-hour test, 500 mg biomass ash catalyst, 800 °C, S/C ratio 3, GHSV: 91800 h^{-1}).

6.4.2 Ni/Al_2O_3 and biomass ash mixture activity test under 30% H_2 atmosphere

Figure 6.8 shows the gas product yield and conversion of toluene steam reforming test using Ni/Al_2O_3 and biomass ash mixture catalsyt bed in 30% H_2 balanced N_2 atmosphere. Product yields of CO_2, CO and H_2 were very stable in the 5 hours, stayed at 21%, 49% and 62%, respectively. The overall conversion from toluene to gases stayed at ~ 84%, only CH_4 decreased from 3% to 0.2% after 5 hours.

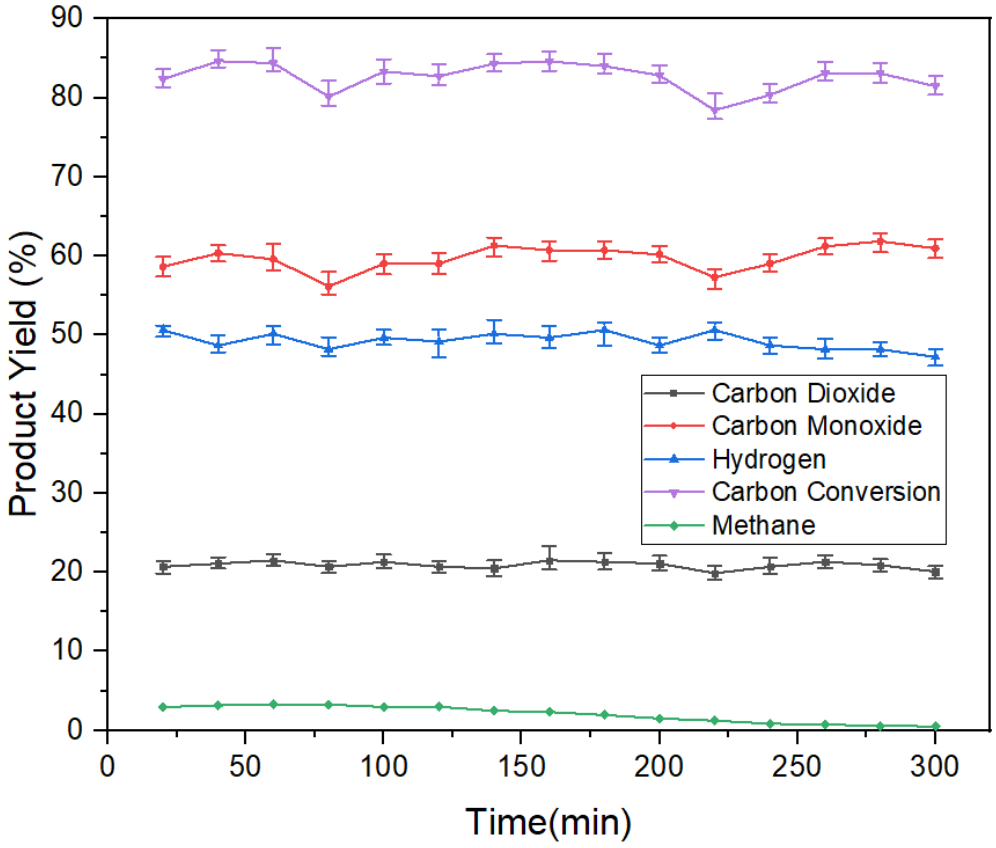

Figure 6.8 Product yield trend and carbon conversion of toluene steam reforming test in 30% H_2 atmosphere (5-hour test, biomass ash and Ni/Al_2O_3 mixture catalyst, 800 °C, S/C ratio 3, GHSV: 91800 h^{-1}).

6.4.3 Two-layer biomass ash and Ni/Al_2O_3 reforming test under 30% H_2 atmosphere

Figure 6.9 shows the the gas product yield and conversion of toluene steam reforming test using two-layer catalsyt bed in 30% H_2 atmosphere. Toluene conversion into gases stayed at ~92% in the 5-hour test, and no CH_4 was detected in the experiment. H_2, CO_2 and CO yield stayed at ~61%, 28% and ~64%, respectively.

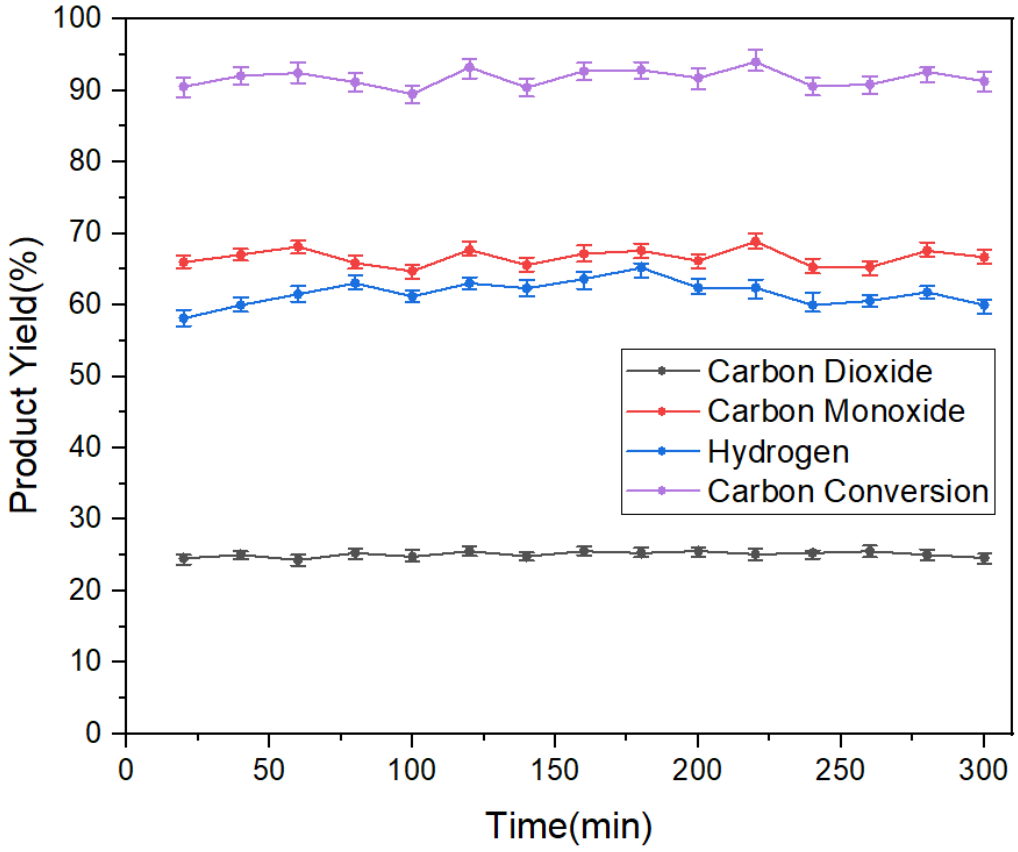

Figure 6.9 Product yield trend and carbon conversion of toluene steam reforming test in 30% H_2 atmosphere (5-hour test, Two-layer biomass ash and Ni/Al_2O_3 catalyst, 800 °C, S/C ratio 3, GHSV: 91800 h^{-1}).

6.4.4 30% H_2 atmosphere comparison

Figure 6.10 summarizes the toluene conversion to Carbon-containing gases (CO, CO_2, CH_4) of different catalyst beds in 30% H_2 atmosphere. The mixture of Ni/Al_2O_3 and biomass ash has a stable toluene conversion of 84%, the 2-layer Ni/Al_2O_3-biomass ash catalytic test shows the highest and the most stable conversion of toluene, the conversion rate stayed > 90% after 5 hours, while Ni/Al_2O_3 catalytic test observes a decrease of conversion from 92% to 85%. Table 6.5 shows the gaseous product yields including CO, CO_2, CH_4 and H_2 in

the unit of mol mol $_{toluene}^{-1}$. The H_2 production of Ni/Al_2O_3 decreased from 11.2 to 10. mol mol $_{toluene}^{-1}$ in 5 hours, while the 2-layer catalyst bed achieved a relatively stable H_2 production at around 10.8 mol mol $_{toluene}^{-1}$. The biomass ash still showed a good performance in stabilize the toluene conversion and gas production. CO_2 selectivity follows the order: Ni/Al_2O_3 > 2-layer > ash and Ni/Al_2O_3 mixture > ash.

Table 6.5 Product yields for the gaseous products in the catalyst beds under 30% H_2 atmosphere (S/C ratio: 3, GHSV:91800 h^{-1}, reforming temperature 800 °C).

Catalyst bed	CO_2 (mol mol $_{toluene}^{-1}$)	CO (mol mol $_{toluene}^{-1}$)	H_2 (mol mol $_{toluene}^{-1}$)	CH_4 (mol mol $_{toluene}^{-1}$)	CO_2 selectivity
Ash (1st hour)	0.5	2.0	3.3	0.4	17%
Ash (5th hour)	0.5	2.0	3.3	0.4	17%
Ni/Al_2O_3 (1st hour)	1.9	4.6	11.2	0	29%
Ni/Al_2O_3 (5th hour)	1.8	4.3	10.4	0	29%
Mixture (1st hour)	1.4	4.2	9.2	0.2	24%
Mixture (5th hour)	1.4	4.3	9.3	0	25%
2-layer (1st hour)	1.7	4.8	10.8	0	27%
2-layer (5th hour)	1.8	4.7	11.0	0	27%
(Equilibrium)	(2.4)	(4.6)	(13.3)	(0)	(34%)

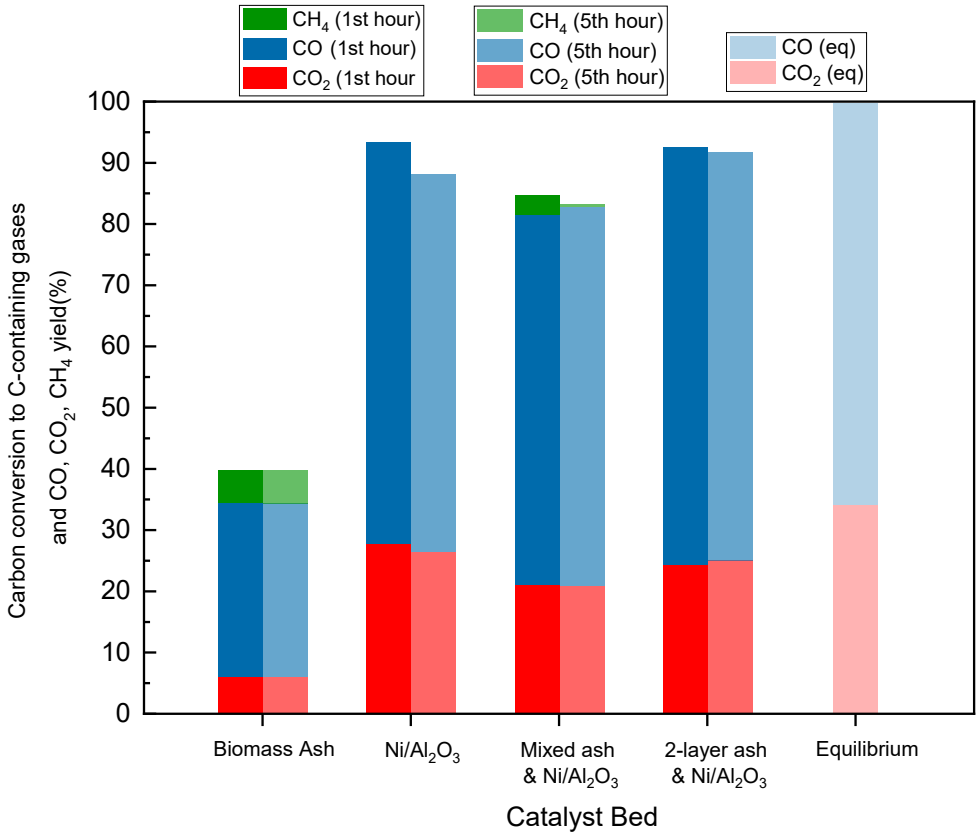

Figure 6.10 Carbon conversion to C-containing gases and CO, CO_2, CH_4 yield under 30% H_2 atmosphere using different catalyst beds (S/C ratio 3 GHSV:91800 h^{-1}, reforming temperature 800 °C).

Figure 6.11 shows the thermogravimetric analysis results for the different spent catalyst beds. Toluene conversion to coke and fraction of coke deposited on the different catalyst beds/layers is shown in Table 6.6. The biomass ash has a good resistance towards coke deposition on catalyst bed, and it also decreased the coke deposited on Ni/Al_2O_3 when acting as a guardian layer or mixing with Ni/Al_2O_3. The coke faction and weight followed the order as Ni/Al_2O_3 > 2-layer: Ni/Al_2O_3 layer > Ash and Ni/Al_2O_3 mixture > 2-layer: Ash layer > Ash. The mixture and the second layer of Ni/Al_2O_3 decreased the coke amount on catalyst by 42% and 28% respectively. The presence of H_2 could promote coke formation by producing more CH_4 as intermediate (Cao, Ren et al. 2018, Chen, Schmid et al. 2020), and CH_4 can promote coke formation on Nickel catalyst

according to Chapter 5, while biomass ash have a relatively good conversion of CH_4 with good resistance to coke formation. The presence of biomass ash could protect Ni/Al_2O_3 from coke deposition as both guardian layer and mixture. This also explain that biomass ash could help to increase the stability of Ni/Al_2O_3 and remain active in terms of toluene conversion due to lower coke deposition.

Table 6.6 Toluene conversion to coke and fraction of coke deposited on the different catalysts in 30 % H_2 atmosphere (800 °C, S/C:3, GHSV:91800 h^{-1}, 5-hour test).

Catalyst bed	Ni/Al_2O_3	Ash	Ni/Al_2O_3 and Ash mixture	2-layer: Ash layer	2-layer: Ni/Al_2O_3 layer
Coke/C in toluene	0.90%	0.33%	0.52%	0.38%	0.65%
Coke/Catalyst bed (g_C g_{cat}^{-1})	0.245	0.089	0.142	0.102	0.177

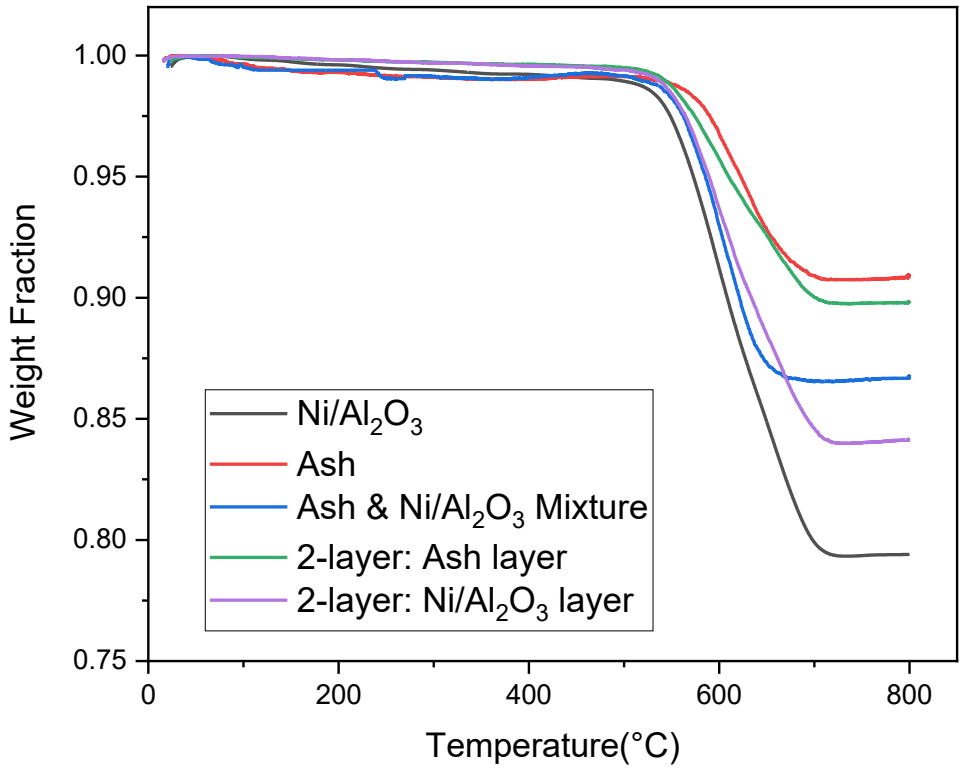

Figure 6.11 Thermo-gravimetric analysis for the different spent catalysts in 30% H_2 atmosphere (800 °C, S/C:3, GHSV:91800 h^{-1}, 5-hour test).

6.5 Catalytic tests under 3% CH_4 atmosphere

This section compares the influence of different catalyst beds on steam reforming of toluene under 3% CH_4 in balanced N_2 atmosphere.

6.5.1 Biomass ash activity test under 3% CH_4 atmosphere

Figure 6.12 shows the gas product yield and toluene conversion into gases in 3% CH_4 balanced N_2 atmosphere using ash catalyst bed. The toluene

conversion, CO, H_2 and CO_2 yields were stable at ~42%, 28%, 25% and 10% respectively. CH_4 yield was relatively lower (3.5%) due to the presence of CH_4 in reaction atmosphere.

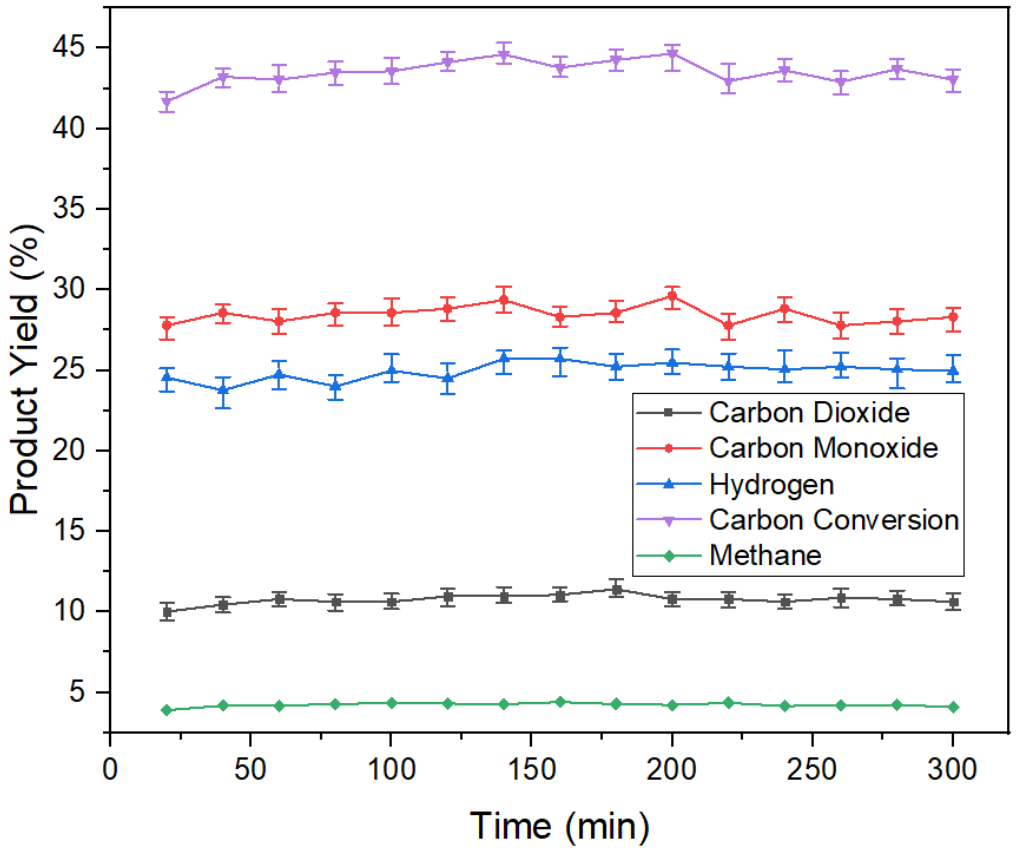

Figure 6.12 Product yield trend and carbon conversion of toluene steam reforming test in 3% CH_4 atmosphere (5-hour test, 500 mg biomass ash catalyst, 800 °C, S/C ratio 3, GHSV: 91800 h^{-1}).

6.5.2 Ni/Al_2O_3 and biomass ash mixture activity test under 3% CH_4 atmosphere

The reforming activity results of biomass ash and Ni/Al_2O_3 mixture catalyst were shown in Figure 6.13. Product yields of CO_2, CO and H_2 were very stable in the 5 hours, stayed at 27%, 54% and 71% respectively. The overall conversion from

toluene to gases stayed at ~ 85%, only CH_4 decreased from 4% to 2% after 5 hours.

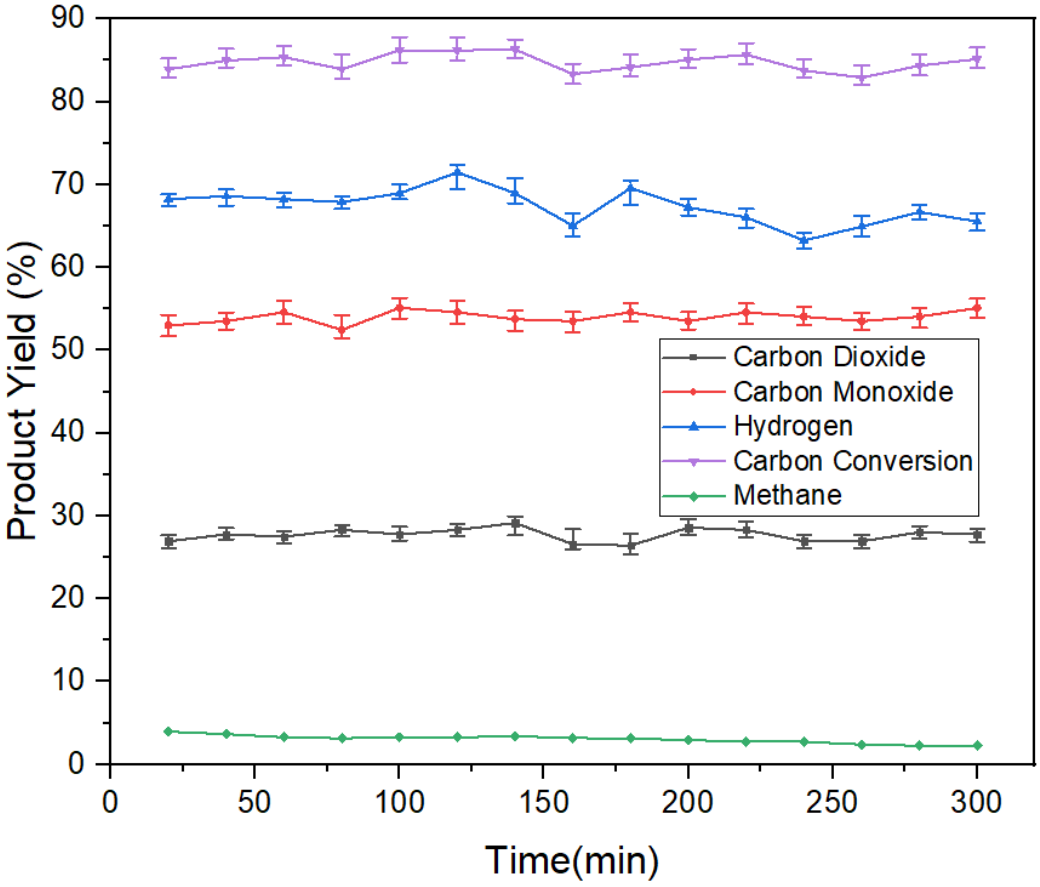

Figure 6.13 Product yield trend and carbon conversion of toluene steam reforming test in 3% CH_4 atmosphere (5-hour test, biomass ash and Ni/Al_2O_3 mixture catalyst, 800 °C, S/C ratio 3, GHSV: 91800 h^{-1}).

6.5.3 Two-layer biomass ash and Ni/Al_2O_3 reforming test 3% CH_4 atmosphere

Product yield (CO, H_2 and CO_2), toluene conversion trend of the 2-layer catalyst bed toluene reforming test is shown in Figure 6.14. No methane was observed throughout the experiment period. All the CH_4 in the reaction atmosphere was converted to CO and CO_2. The toluene conversion, CO, H_2 and CO_2 yields were

stable at ~93%, 62%, ~73% and 31%, respectively.

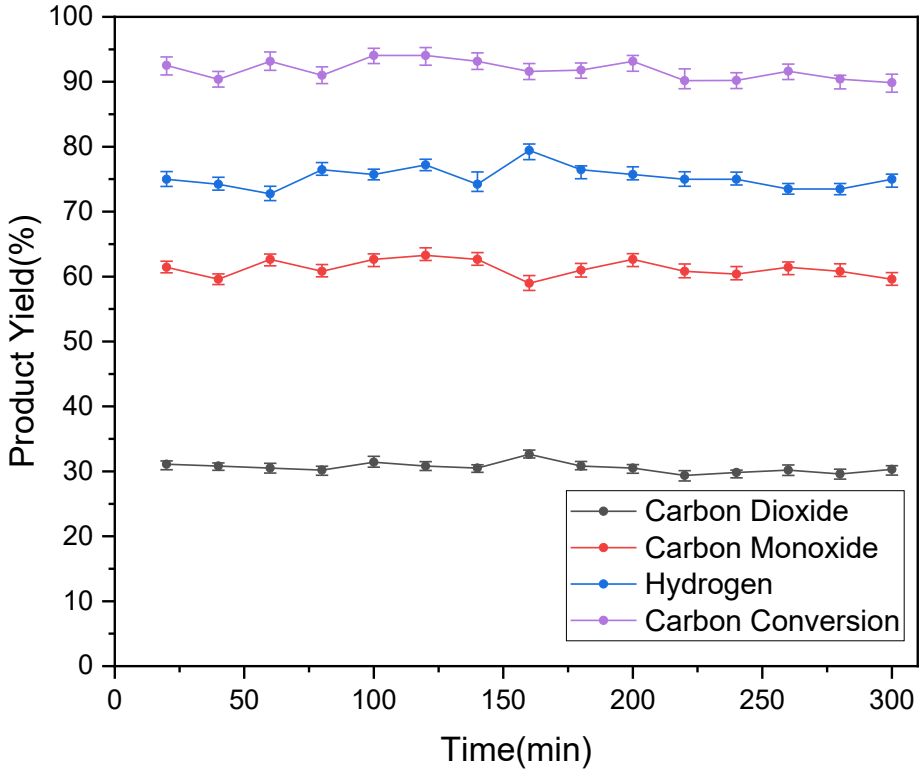

Figure 6.14 Product yield trend and carbon conversion of toluene steam reforming test in 3% CH_4 atmosphere (5-hour test, Two-layer biomass ash and Ni/Al_2O_3 catalyst, 800 °C, S/C ratio 3, GHSV: 91800 h^{-1}).

6.5.4 3% CH_4 atmosphere comparison

Figure 6.15 summarizes the toluene conversion to CO, CO_2 and CH_4 of different catalyst beds in 3% CH_4 atmosphere and compares with equilibrium. Table 6.7 presents H_2, CO, CO_2 and CH_4 gas production yields in the unit of mol mol $_{toluene}^{-1}$. Ni/Al_2O_3 achieved the highest initial toluene conversion in first hour at 95%, but decreased to 82% after 5 hours. The toluene conversion of ash, Ni/Al_2O_3 mixture and the 2-layer ash-Ni/Al_2O_3 stayed at 92% and 85%

respectively in the 5-hour tests. the 2-layer ash-Ni/Al_2O_3 also observed the highest H_2 production of 16.6 mol mol $_{toluene}^{-1}$ and stabilized in 5 hours, while the H_2 production of Ni/Al_2O_3 decreased from 16.5 to 13.8 mol mol $_{toluene}^{-1}$.

Table 6.7 Product yields for the gaseous products in the catalyst beds under 3% CH_4 atmosphere (S/C ratio: 3, GHSV:91800 h^{-1}, reforming temperature 800 °C).

Catalyst bed	CO_2 (mol mol $_{toluene}^{-1}$)	CO (mol mol $_{toluene}^{-1}$)	H_2 (mol mol $_{toluene}^{-1}$)	CH_4 (mol mol $_{toluene}^{-1}$)	CO_2 selectivity
Ash (1st hour)	0.8	2.3	4.6	0.4	23%
Ash (5th hour)	0.8	2.2	4.5	0.4	24%
Ni/Al_2O_3 (1st hour)	3.0	4.8	16.5	0	38%
Ni/Al_2O_3 (5th hour)	2.5	4.1	13.8	0	38%
Mixture (1st hour)	2.2	4.4	14.1	0.2	32%
Mixture (5th hour)	2.3	4.4	13.9	0	33%
2-layer (1st hour)	2.5	5.0	16.7	0	33%
2-layer (5th hour)	2.5	4.9	16.6	0	34%
(Equilibrium)	(3.6)	(4.6)	(18.0)	(0)	(44%)

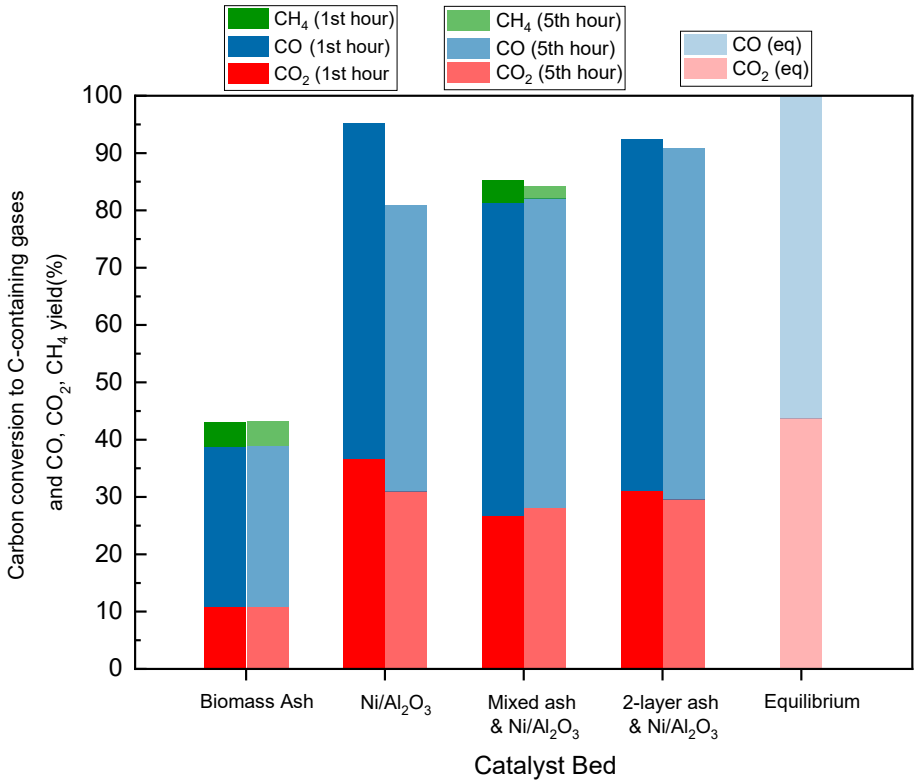

Figure 6.15 Carbon conversion to C-containing gases and CO, CO_2, CH_4 yield under 3% CH_4 atmosphere using different catalyst beds (S/C ratio 3 GHSV:91800 h^{-1}, reforming temperature 800 °C).

Figure 6.16 shows the thermos-gravimetric analysis results for the different spent catalysts after 5-hour catalytic tests, and the coke deposition fractions are presented in Table 6.8. The trend in terms of coke weight and fraction was Ni/Al_2O_3 > 2-layer: Ni/Al_2O_3 layer > Ash and Ni/Al_2O_3 mixture = 2-layer: Ash layer > Ash. The presence of biomass ash could reduce the coke deposition on Ni/Al_2O_3 no matter in mixture or as a guardian layer, which further help the catalyst beds to have a stable catalytic performance on toluene conversion.

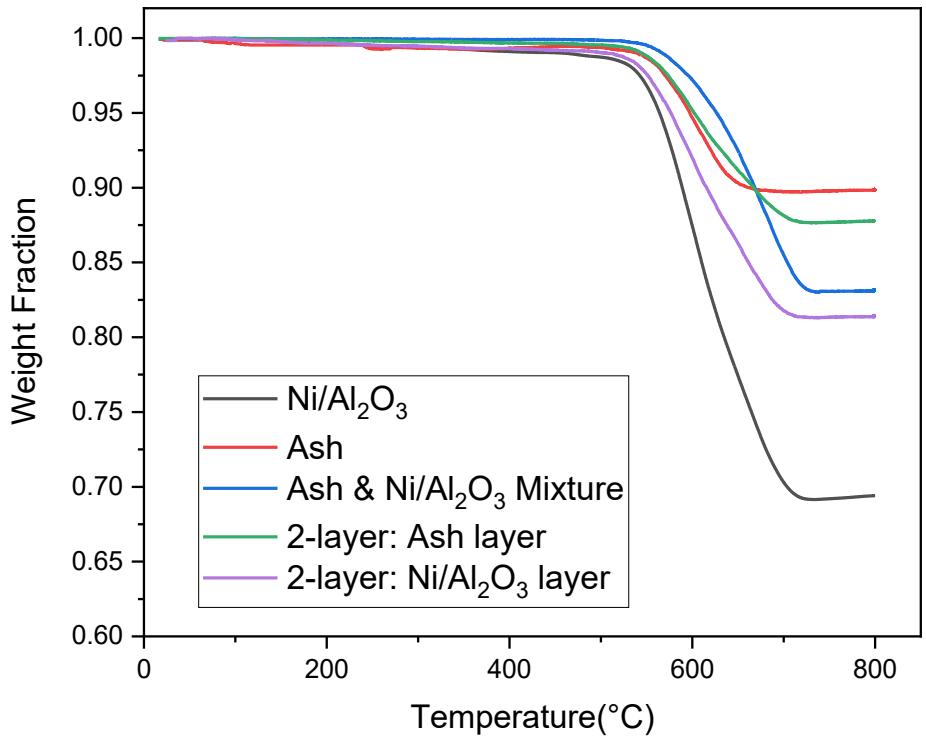

Figure 6.16 Thermogravimetric analysis for the different spent catalysts in 3% CH_4 atmosphere (800 °C, S/C:3, GHSV:91800 h^{-1}, 5-hour test).

Table 6.8 Toluene conversion to coke and fraction of coke deposited on the different catalysts in 3% CH_4 atmosphere (800 °C, S/C:3, GHSV:91800 h^{-1}, 5-hour test).

Catalyst bed	Ni/Al_2O_3	Ash	Ni/Al_2O_3 and Ash mixture	2-layer: Ash layer	2-layer: Ni/Al_2O_3 layer
Coke/C in toluene	1.54%	0.42%	0.70%	0.47%	0.80%
Coke/Catalyst bed (g_C g_{cat}^{-1})	0.417	0.113	0.190	0.128	0.216

6.6 Catalytic tests under 3% CH_4, 30% H_2 atmosphere

This section compares the influence of different catalyst beds on steam reforming of toluene under 3% CH_4, 30% H_2 in balanced N_2 atmosphere.

6.6.1 Biomass ash activity test under 3% CH_4, 30% H_2 atmosphere

Figure 6.17 shows the gas product yield and toluene conversion into gases in 3% CH_4 balanced N_2 atmosphere using ash catalyst bed. The presence of CH_4 and H_2 reduced toluene conversion to 38%. CO, H_2, CO_2 and CH_4 yields were stable at ~27%, 24%, 7% and 3%, respectively.

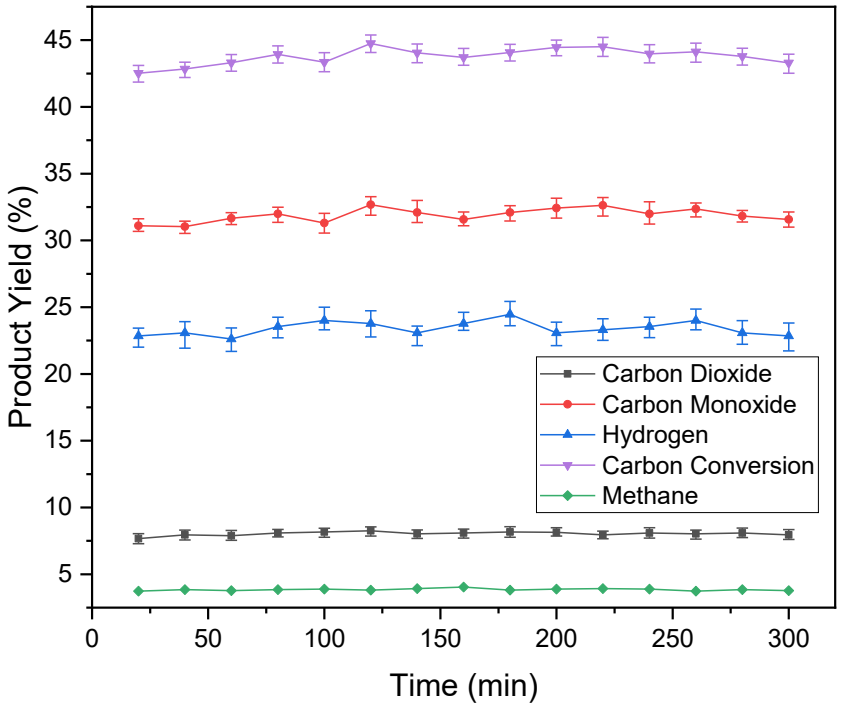

Figure 6.17 Product yield trend and carbon conversion of toluene steam reforming test in 3% CH_4, 30% H_2 atmosphere (5-hour test, 500 mg biomass ash catalyst, 800 °C, S/C ratio 3, GHSV: 91800 h^{-1}).

6.6.2 Ni/Al_2O_3 and biomass ash mixture activity test under 3% CH_4, 30% H_2 atmosphere

The reforming activity results of biomass ash and Ni/Al_2O_3 mixture catalyst are shown in Figure 6.18. Product yields of CO_2, CO and H_2 were very stable in the 5 hours, stayed at 23%, 58% and 63% respectively. The overall conversion from toluene to gases stayed at ~ 83%, only CH_4 decreased slightly from 3.5% to 1% after 5 hours.

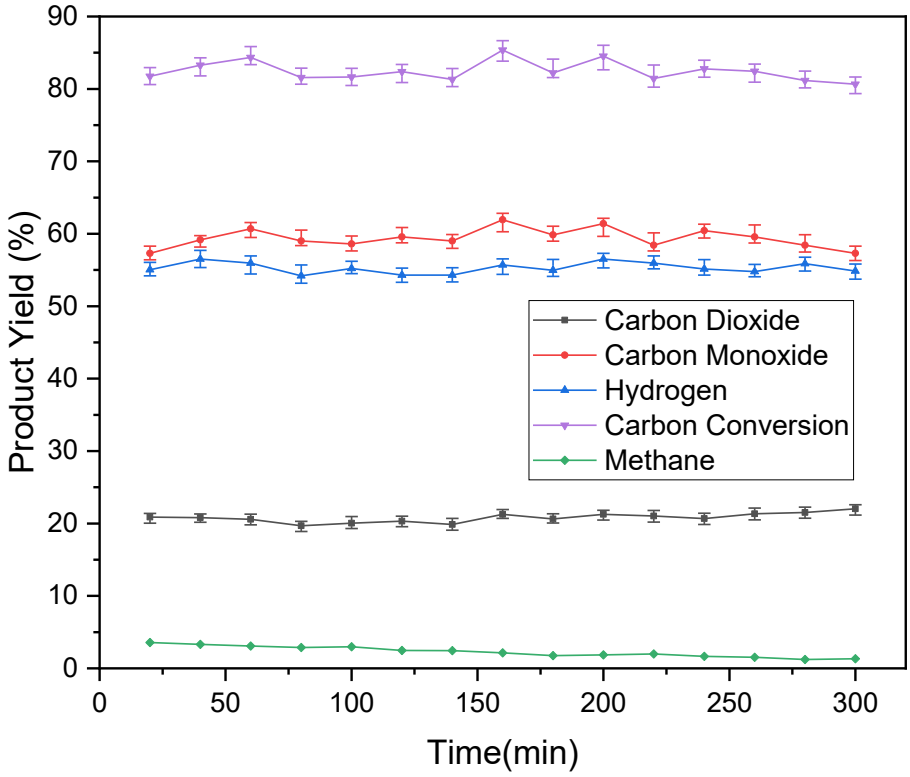

Figure 6.18 Product yield trend and carbon conversion of toluene steam reforming test in 3% CH_4, 30% H_2 atmosphere (5-hour test, biomass ash and Ni/Al_2O_3 mixture catalyst, 800 °C, S/C ratio 3, GHSV: 91800 h^{-1}).

6.6.3 Two-layer biomass ash and Ni/Al_2O_3 reforming test under 3% CH_4, 30% H_2 atmosphere

Product yield (CO, H_2 and CO_2), toluene conversion trend of the 2-layer catalyst bed toluene reforming test is shown in Figure 6.19. No methane was observed throughout the experiment period. The toluene conversion, CO, H_2 and CO_2 yields were stable at ~92%, 65%, ~70% and 27%, respectively.

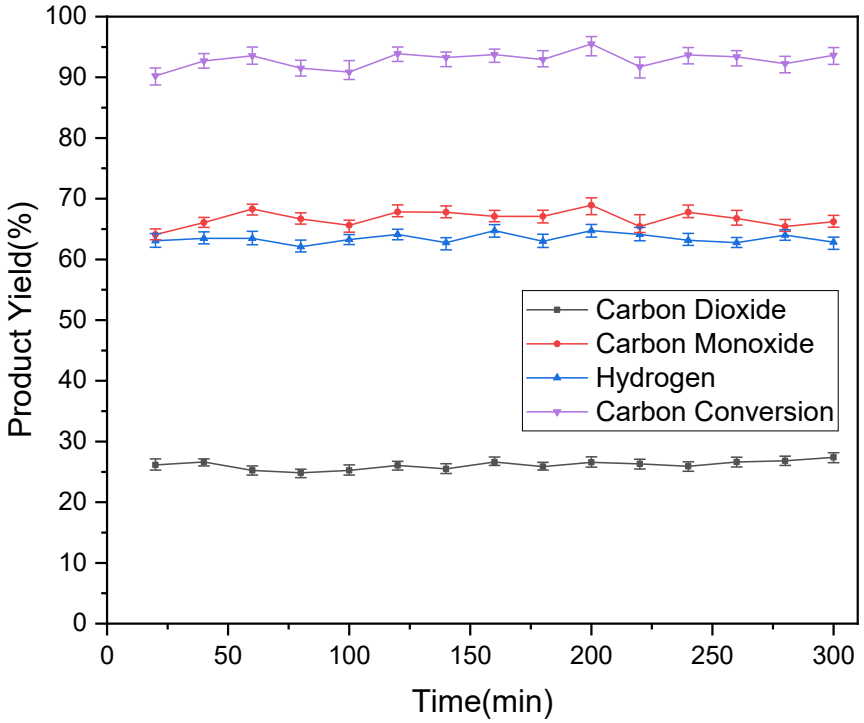

Figure 6.19 Product yield trend and carbon conversion of toluene steam reforming test in 3% CH_4, 30% H_2 atmosphere (5-hour test, Two-layer biomass ash and Ni/Al_2O_3 catalyst, 800 °C, S/C ratio 3, GHSV: 91800 h^{-1})

6.6.4 3% CH_4, 30% H_2 atmosphere comparison

Figure 6.20 summarizes the toluene conversion to CO, CO_2 and CH_4 of different

catalyst beds in 30% H_2 and 3% CH_4 atmosphere and compares with equilibrium. The overall conversion of Ni/Al_2O_3 decreased significantly in 5 hours, while the 2-layer ash-Ni/Al_2O_3 was the only achieved a toluene conversion > 90% in both first and fifth hour. Table 6.9 shows the gaseous product yields including CO, CO_2, CH_4 and H_2 in the unit of mol mol $_{toluene}^{-1}$ at the first hour and the fifth hour using different catalyst beds. Ni/Al_2O_3 showed a good gas production yields in first hour but decreased by 28% after 5 hours, the carbon conversion also decreases from 93% to 69%. Biomass ash, ash and Ni/Al_2O_3 mixture, the 2-layer ash-Ni/Al_2O_3 all observed stable product yields of CO, CO_2 and H_2 after 5-hour tests, as the 2-layer ash-Ni/Al_2O_3 presented the average highest production of CO, CO_2 and H_2 at 5.5, 2.2, 15.2 mol mol $_{toluene}^{-1}$, respectively. CO_2 selectivity follows the order: Ni/Al_2O_3 > 2-layer > ash and Ni/Al_2O_3 mixture > ash, which is similar to the order at inert gas atmosphere.

Table 6.9 Product yields for the gaseous products in the catalyst beds under 3% CH_4, 30% H_2 atmosphere (S/C ratio: 3, GHSV:91800 h^{-1}, reforming temperature 800 °C).

Catalyst bed	CO_2 (mol mol $_{toluene}^{-1}$)	CO (mol mol $_{toluene}^{-1}$)	H_2 (mol mol $_{toluene}^{-1}$)	CH_4 (mol mol $_{toluene}^{-1}$)	CO_2 selectivity
Ash (1st hour)	0.7	2.4	5.4	0.3	20%
Ash (5th hour)	0.7	2.4	5.4	0.3	20%
Ni/Al_2O_3 (1st hour)	2.5	5.2	15.1	0	33%
Ni/Al_2O_3 (5th hour)	1.8	3.8	10.9	0	32%
Mixture (1st hour)	1.7	4.9	12.8	0.2	25%
Mixture (5th hour)	1.7	5.0	12.9	0	24%
2-layer (1st hour)	2.1	5.6	14.9	0	27%
2-layer (5th hour)	2.2	5.5	15.2	0	28%
(Equilibrium)	(2.8)	(5.4)	(17.1)	(0)	(39%)

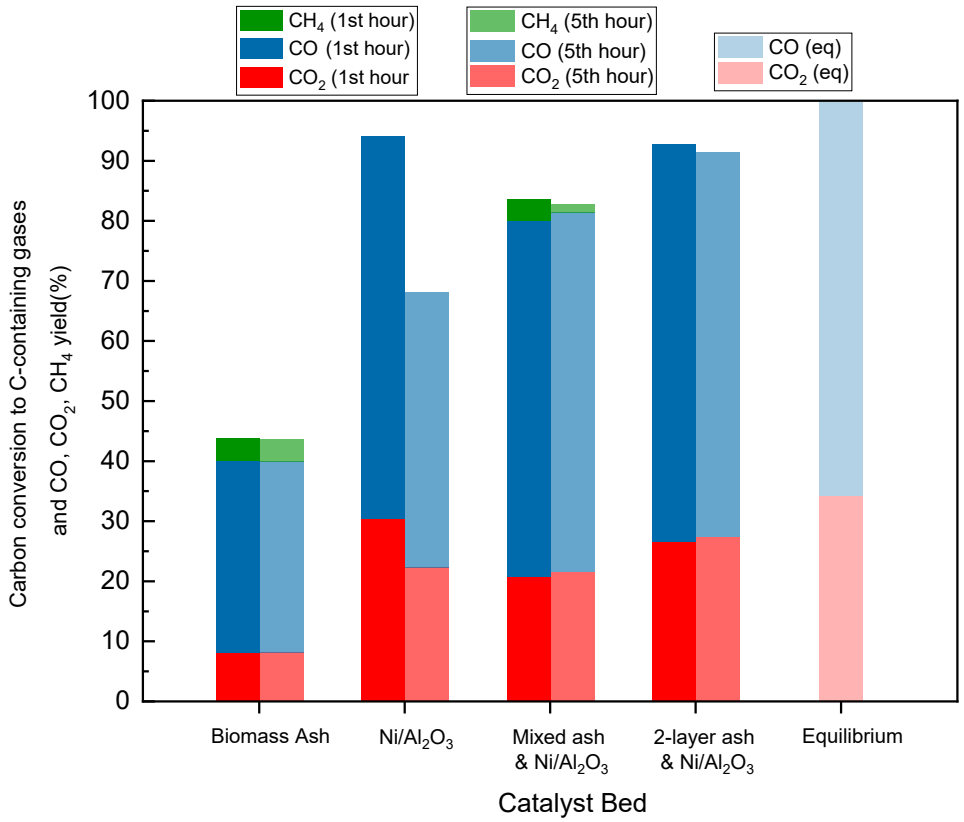

Figure 6.20 Carbon conversion to C-containing gases and CO, CO_2, CH_4 yield under 3% CH_4, 30% H_2 atmosphere using different catalyst beds (S/C ratio 3 GHSV:91800 h^{-1}, reforming temperature 800 °C).

Figure 6.21 presents the influence of the different catalyst beds tested on coke deposition for biomass ash and Ni/Al_2O_3 catalyst using thermogravimetric analysis. The detailed data of coke amount and fraction is shown in Table 6.10. Biomass ash still helped to reduce the coke deposition on Ni/Al_2O_3 catalyst. The order of coke weight on spent catalyst was Ni/Al_2O_3 > 2-layer: Ni/Al_2O_3 layer > Ash and Ni/Al_2O_3 mixture > 2-layer: Ash layer > Ash.

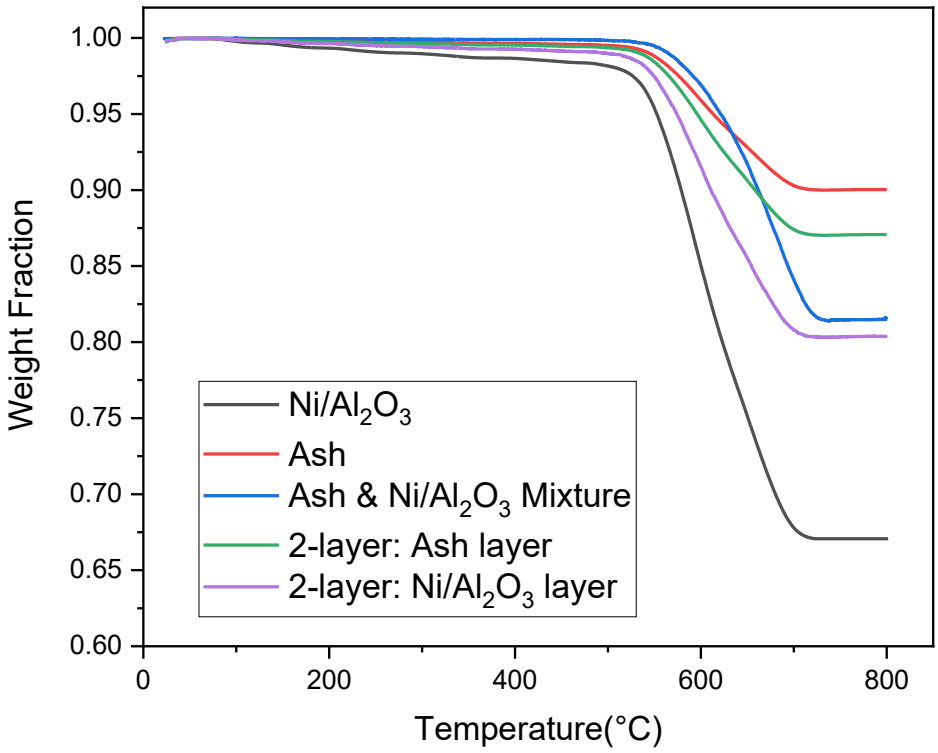

Figure 6.21 Thermal gravimetric analysis for the different spent catalysts in 30 % H_2 and 3 % CH_4 atmosphere (800 °C, S/C:3, GHSV:91800 h^{-1}, 5-hour test).

Table 6.10 Toluene conversion to coke and fraction of coke deposited on the different catalysts in 30 % H_2 and 3 % CH_4 atmosphere (800 °C, S/C:3, GHSV:91800 h-1, 5-hour test).

Catalyst bed	Ni/Al_2O_3	Ash	Ni/Al_2O_3 and Ash mixture	2-layer: Ash layer	2-layer: Ni/Al_2O_3 layer
Coke/C in toluene	2.53%	0.41%	0.84%	0.55%	0.90%
Coke/Catalyst bed (g_C g_{cat}^{-1})	0.684	0.111	0.227	0.148	0.244

6.7 Catalytic tests under simulated syngas atmosphere

This section compares the influence of different catalyst beds on steam reforming of toluene under simulated syngas atmosphere (3% CH_4, 30% H_2, 20% CO_2, 30% CO in balanced N_2).

6.7.1 Biomass ash activity test under simulated syngas atmosphere

Figure 6.22 shows the gas product yield and toluene conversion into gases in simulated syngas atmosphere using ash catalyst bed. Carbon conversion of toluene came back to ~42%, which was only slightly lower than in 100% N_2 atmosphere. H_2, CO, CO_2 and CH_4 yield stayed at 33%, 25%, 7% and 4% respectively in the 5-hour test.

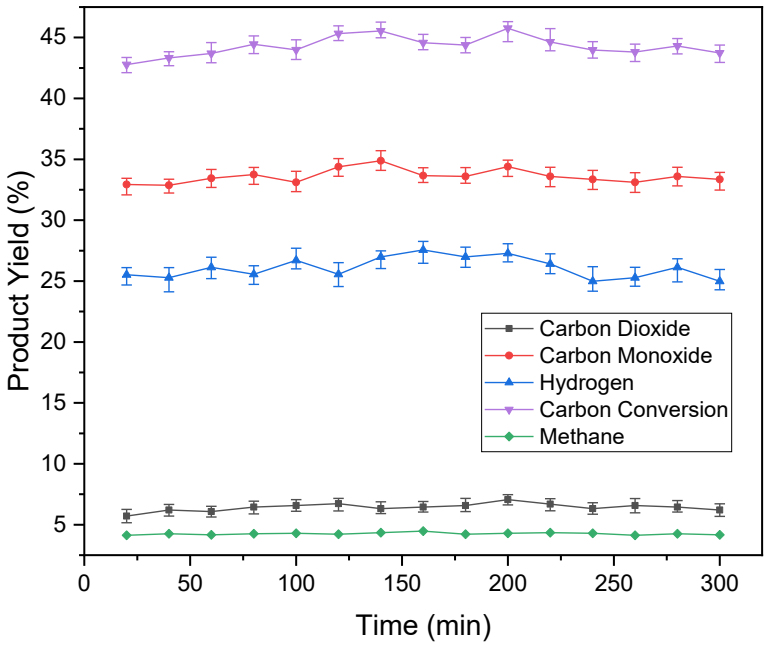

Figure 6.22 Product yield trend and carbon conversion of toluene steam reforming test in simulated syngas atmosphere (5-hour test, 500 mg biomass as catalyst, 800 °C, S/C ratio 3, GHSV: 91800 h^{-1}).

6.7.2 Ni/Al_2O_3 and biomass ash mixture activity test under simulated syngas atmosphere

The reforming activity results of biomass ash and Ni/Al_2O_3 mixture catalyst were shown in Figure 6.23. Product yields of CO_2, CO and H_2 were very stable throughout the 5-hour test, stayed at 19%, 61% and 55% respectively. The overall conversion from toluene to gases stayed at 83%, while CH_4 decreased from 4% to 1% after 5 hours.

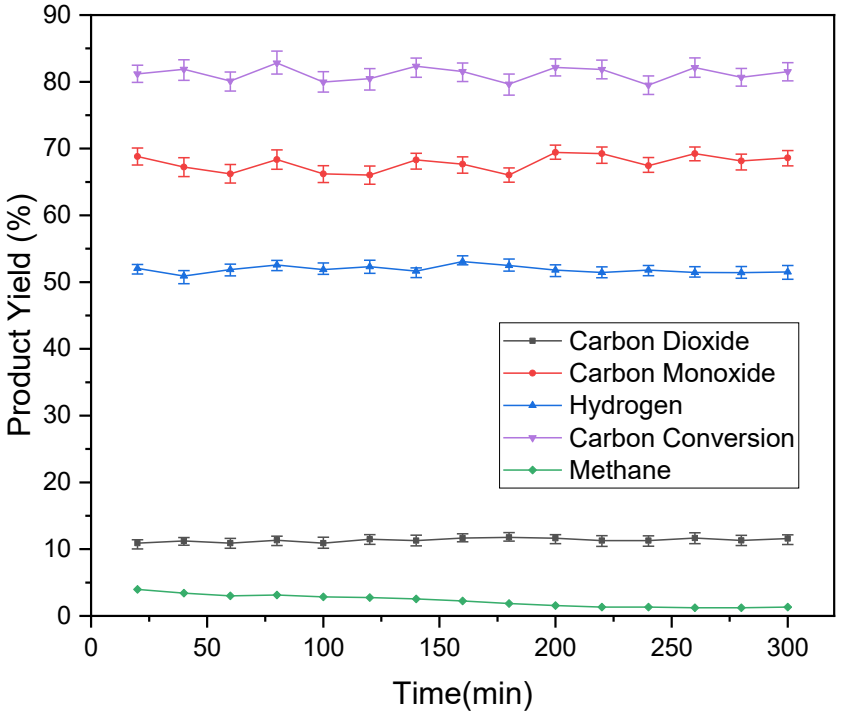

Figure 6.23 Product yield trend and carbon conversion of toluene steam reforming test in simulated syngas atmosphere (5-hour test, biomass ash and Ni/Al_2O_3 mixture catalyst, 800 °C, S/C ratio 3, GHSV: 91800 h^{-1}).

To compare the CH_4 yield using Ni/Al_2O_3 and biomass ash mixture catalyst bed under different reforming atmosphere, the CH_4 yields all declined on different

degrees in the 5-hour test except for inert atmosphere. Similar results have been reported, Quitete, Bittencourt et al. (2014) studied NiO–LaCeAl catalyst in toluene steam reforming at 650 °C, S/C = 1.9 and found that methane composition increased from 10% to 15% in the first 4 hours, and declined to 9% in the next 10 hours. They suggested that the competition between many parallel and consecutive reactions resulted in the change of different gas concentrations (Quitete, Bittencourt et al. 2014). Cao, Ren et al. (2018) found that CH_4 yield decreased slightly with time in the presence of H_2 at 650 °C in 5-hour toluene steam reforming test using Ni/lignite char catalyst, while CH_4 yield using Ni/Al_2O_3 catalyst was maintained stable. The production of CH_4 in toluene steam reforming mainly due to the hydrodealkylation of toluene and reaction of carbon (coke) with H_2. Considering that the decreasing of CH_4 yield has not been observed under inert atmosphere, it is possible that the decreasing is more affected by the reaction of carbon (coke) with H_2. However, this phenomenon only occurs in the biomass ash and Ni/Al_2O_3 mixture catalyst reforming system in this project, which indicates that the biomass ash and Ni/Al_2O_3 mixture might inhibit the reaction of carbon with H_2 over time.

6.7.3 Two-layer biomass ash and Ni/Al_2O_3 reforming test under simulated syngas atmosphere

Product yield (CO, H_2 and CO_2), toluene conversion trend of the 2-layer catalyst bed toluene reforming test is shown in Figure 6.24. No methane was observed in the 5-hour test. The toluene conversion, CO, H_2 and CO_2 yields were stable at ~90%, 76%, ~67% and 15%, respectively.

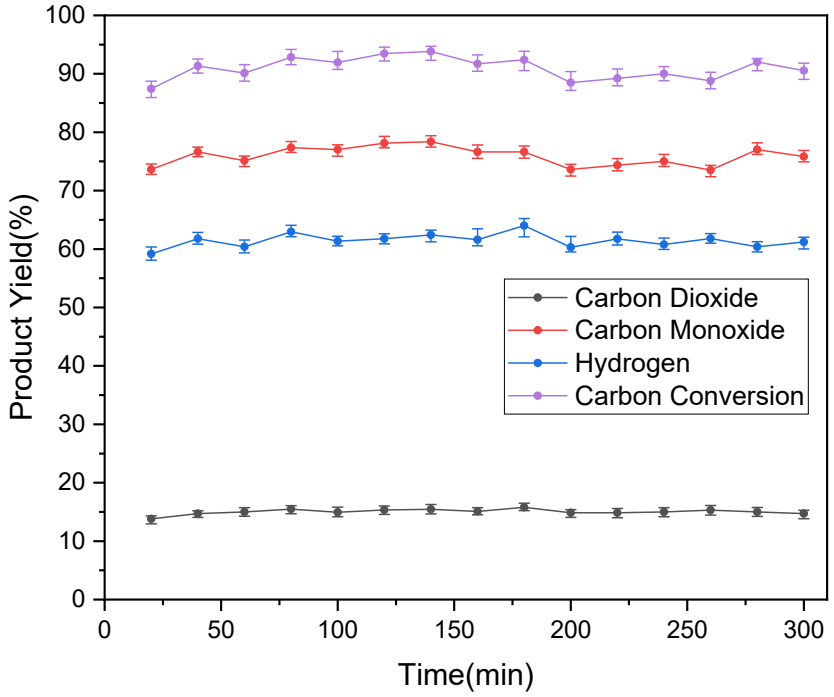

Figure 6.24 Product yield trend and carbon conversion of toluene steam reforming test in simulated syngas atmosphere (5-hour test, Two-layer biomass ash and Ni/Al_2O_3 catalyst, 800 °C, S/C ratio 3, GHSV: 91800 h^{-1}).

6.7.4 Simulated syngas atmosphere comparison

Figure 6.25 summarizes the toluene conversion to Carbon-containing gases of different catalyst beds in simulated syngas atmosphere. The mixture of Ni/Al_2O_3 and biomass ash has a stable toluene conversion of 84%, the 2-layer Ni/Al_2O_3-biomass ash catalytic test shows the highest and the most stable conversion of toluene, the carbon conversion rate stayed ~90% in 5 hours, while Ni/Al_2O_3 catalytic test observes a decrease of conversion from 93% to 67%. Table 6.11 shows the gaseous product yields of CO, CO_2, CH_4 and H_2 in the unit of mol mol $_{toluene}^{-1}$ and compares with equilibrium. The H_2 production of Ni/Al_2O_3 decreased from 12.0 to 8.7 mol mol $_{toluene}^{-1}$ in 5 hours, while the 2-layer catalyst

bed achieved a relatively stable H_2 production at 12.3 mol mol $_{toluene}^{-1}$. CO_2 selectivity follows the order: Ni/Al_2O_3 > 2-layer = ash and Ni/Al_2O_3 mixture > ash. In all these five atmospheres, CO_2 selectivity follows the order as Ni/Al_2O_3 > 2-layer ≥ ash and Ni/Al_2O_3 mixture > ash, shows that CO_2 selectivity is also significantly affected by the catalyst bed. It is reported that presence of alkali or alkaline earth metals increases the production of CO (Mg > Ca = K) and CO_2 yield is observed to decrease in the order of initial > K > Ca > Mg (Zhang, Ou et al. 2019). They also claimed that the presence of K, Ca, and Mg results in a better coke resistance (a reduction of over 60%).

Although Ni/Al_2O_3 showed the best initial catalytic performance in terms of carbon conversion and H_2 production in the first hour under all five atmospheres, Ni/Al_2O_3 experienced big drops under CH_4-containing atmospheres. The 2-layer catalyst bed shows a good conversion and stability in toluene conversion under simulated syngas atmosphere, the guardian layer of biomass ash could improve Ni/Al_2O_3 catalyst stability in 5-hour tests. The mixture of Ni/Al_2O_3 and biomass ash always shows a lower carbon conversion and H_2 yield than 2-layer Ni/Al_2O_3-biomass ash catalyst bed under all five reforming atmospheres in 5 hours, similar or lower CO_2 selectivity. The reasons that the guard column works better than the mixed ash/Ni/Al_2O_3 bed could be: 1. 2-layer catalyst bed observes no CH_4, while the mixed bed shows a low CH_4 production, the CH_4 yield represent the degree of reforming reaction; 2. The gap (~5 mm, filled by quartz wool and wire mesh) between guardian layer (ash) and Ni/Al_2O_3 slightly increase the residence time of the catalyst bed by forming a small residence reaction chamber; 3. The second layer of Ni/Al_2O_3 plays an important role in overall carbon conversion by having fully contact with the main gas stream, while the conversion of mixed ash/Ni/Al_2O_3 bed is much affected by the ash content.

Considering the residence time in 2-layer Ni/Al_2O_3-biomass ash catalyst bed,

GHSV of Ni/Al_2O_3 layer is 183,600 h^{-1}, comparing to the GHSV study in Section 4.6, the carbon conversion of this layer is expected to be lower than 90%. The CH_4 atmosphere result using ash catalyst in Section 6.5.1 shows that ~90% of the injected CH_4 is converted to CO and CO_2, while toluene conversion is ~ 40%. It could be concluded that the first layer of ash mainly converts the injected CH_4, and part of toluene (expected to be less than 40%), and the second layer of Ni/Al_2O_3 mainly converts the rest toluene (expected to be less than 56%), results in an overall carbon conversion of ~90%.

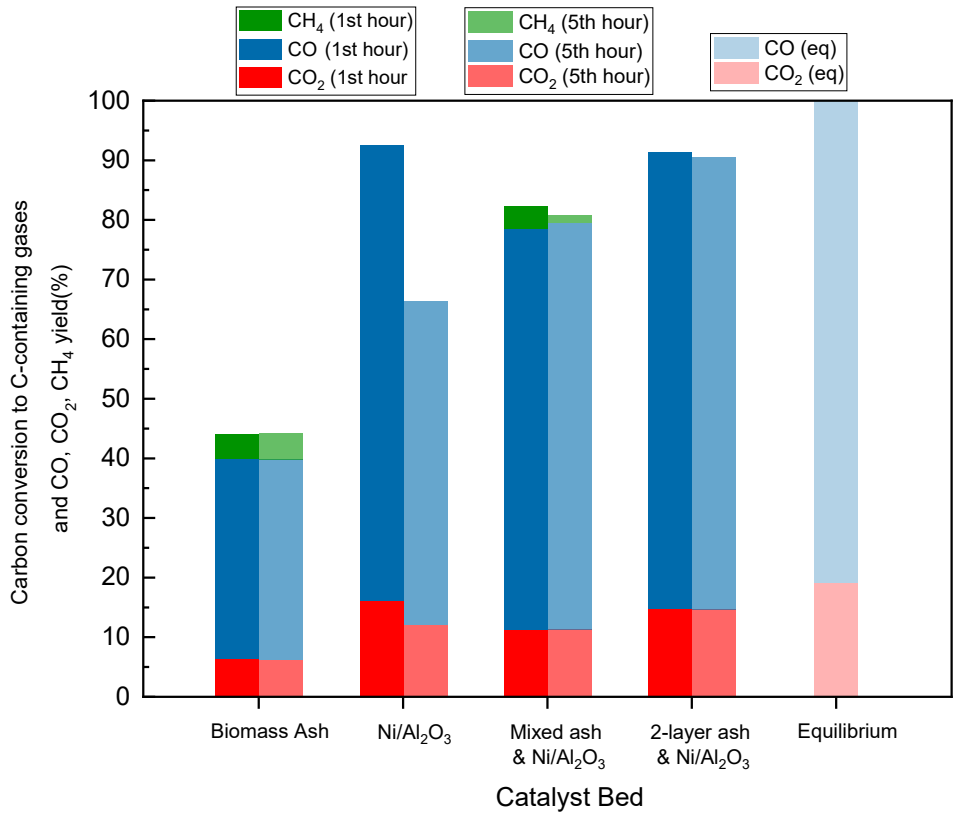

Figure 6.25 Carbon conversion to C-containing gases and CO, CO_2, CH_4 yield under simulated syngas atmosphere using different catalyst beds (S/C ratio 3 GHSV:91800 h^{-1}, reforming temperature 800 °C).

Table 6.11 Product yields for the gaseous products in the catalyst beds under simulated syngas atmosphere (S/C ratio: 3, GHSV:91800 h^{-1}, reforming temperature 800 °C).

Catalyst bed	CO_2 (mol mol $_{toluene}^{-1}$)	CO (mol mol $_{toluene}^{-1}$)	H_2 (mol mol $_{toluene}^{-1}$)	CH_4 (mol mol $_{toluene}^{-1}$)	CO_2 selectivity
Ash (1st hour)	0.5	2.8	5.6	0.3	15%
Ash (5th hour)	0.6	2.7	5.5	0.3	16%
Ni/Al_2O_3 (1st hour)	1.3	6.2	12.0	0	17%
Ni/Al_2O_3 (5th hour)	1.0	4.8	8.7	0	17%
Mixture (1st hour)	1.0	5.4	10.0	0.2	15%
Mixture (5th hour)	1.0	5.5	10.2	0	16%
2-layer (1st hour)	1.2	6.3	12.1	0	16%
2-layer (5th hour)	1.2	6.2	12.3	0	15%
(Equilibrium)	(1.6)	(6.5)	(15.5)	(0)	(20%)

Figure 6.26 shows the thermogravimetric analysis results for the different spent catalyst beds. Toluene conversion to coke and the fraction of coke deposited on the different catalyst beds/layers are shown in Table 6.6. The coke weight on spent catalysts follows the order as Ni/Al_2O_3 > 2-layer: Ni/Al_2O_3 layer > Ash and Ni/Al_2O_3 mixture > 2-layer: Ash layer > Ash. The biomass ash layer protected Ni/Al_2O_3 layer from coke deposition and help to achieve a relatively high and stable conversion of toluene.

The coke weight and fraction on spent catalysts under these five different

reforming atmospheres follows the same order as Ni/Al_2O_3 > 2-layer: Ni/Al_2O_3 layer > Ash and Ni/Al_2O_3 mixture > 2-layer: Ash layer > Ash, which indicated that: 1. Biomass ash showed a good coke resistance in all reforming atmospheres; 2. Ni/Al_2O_3 favors coke formation, while the introduction of biomass ash could inhibit the coke deposition on Ni/Al_2O_3 surface in the forms of mixture and guardian layer; 3. Ash and Ni/Al_2O_3 mixture shows a lower coke content than 2-layer: Ni/Al_2O_3 layer, while the average coke deposition of 2-layer catalyst system was lower than ash and Ni/Al_2O_3 mixture.

Table 6.12 Toluene conversion to coke and fraction of coke deposited on the different catalysts in simulated gas atmosphere (800 °C, S/C:3, GHSV:91800 h^{-1}, 5-hour test).

Catalyst bed	Ni/Al_2O_3	Ash	Ni/Al_2O_3 and Ash mixture	2-layer: Ash layer	2-layer: Ni/Al_2O_3 layer
Coke/C in toluene	2.49%	0.41%	0.88%	0.54%	0.92%
Coke/Catalyst bed (g_C g_{cat}^{-1})	0.676	0.113	0.240	0.146	0.248

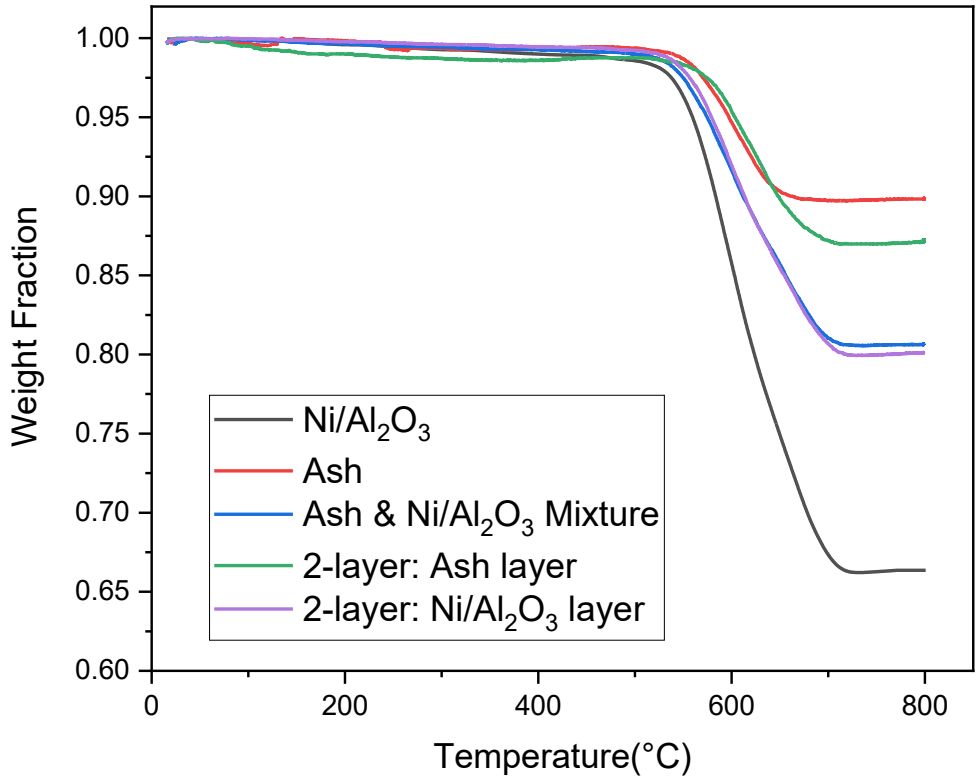

Figure 6.26 Thermogravimetric analysis for the different spent catalysts in simulated gas atmosphere (800 °C, S/C:3, GHSV:91800 h^{-1}, 5-hour test).

6.8 Summary

Biomass ash has a potential to use as catalyst as it is cheap and abundant. However, biomass ash itself has a relatively low catalytic performance, most researches have been focused on biomass ash support. This chapter discussed the possibility of biomass ash as catalyst by physical blend/mixture and acting as guard layer for Ni/Al_2O_3 catalyst. Inert atmosphere (100% N_2), H_2 atmosphere (30% H_2 in balanced N_2), CH_4 atmosphere (3% CH_4 in balanced N_2), H_2 and CH_4 atmosphere (3% CH_4, 30% H_2 in balanced N_2), simulated gasification gas atmosphere (3% CH_4, 30% H_2, 20% CO_2, 30% CO in balanced

N_2) has been used to study the performance of different catalyst beds.

Biomass ash has a very good resistance to coke deposition in toluene steam reforming, but the catalytic performance is very limited, the toluene conversion is usually lower than 50% in all conditions. The 1:1 biomass ash-Ni/Al_2O_3 mixture also has a good resistance to coke deposition, and it has a stable conversion of toluene to gas between 80% and 85% under different atmospheres in 5-hour tests.

The coke weight and fraction on spent catalysts under these five different reforming atmospheres follows the same order as Ni/Al_2O_3 > 2-layer: Ni/Al_2O_3 layer > Ash and Ni/Al_2O_3 mixture > 2-layer: Ash layer > Ash. Two-layer biomass ash and Ni/Al_2O_3 catalytic system shows a very good performance in different atmospheres. The ash layer has a relatively low coke formation, but still helps to prevent the coke deposition on the Ni/Al_2O_3 layer. Under all five reforming atmospheres, the 2-layer catalyst bed achieves a conversion of toluene to gases ~90% throughout 5-hour tests. As the coke deposition rate on Ni/Al_2O_3 layer is significantly reduced by the biomass ash layer, the stability of Ni/Al_2O_3 is largely improved.

7 Summary, Conclusions and Recommendation for Future Work

7.1 Summary

A laboratory continuous fixed bed reactor has been used in this project to study toluene catalytic steam reforming. Preliminary tests showed that this reactor had good repeatability and reliability, it could be heated up to 950 °C with steady and continuous feeding/injection of steam and model compounds.

To reveal the optimum process conditions, the effects of reforming temperature, steam to carbon (S/C) ratio and residence time (GHSV) on toluene conversion and gas products have been investigated using Ni/Al_2O_3 catalyst. A S/C molar ratio range from one to three and temperature range from 700 to 900 °C were selected according to thermodynamic equilibrium calculations, and gas hourly space velocity (GHSV) was varied from 30,600 to 122,400 h^{-1} according to previous work. The composition, production yields of gas products (H_2, CO, CO_2 and CH_4) have been acquired. The toluene conversions have been calculated and all these results have been compared with equilibrium results. The influence of reforming temperature, S/C ratio and GHSV on catalyst coke deposition has been analyzed by TGA. This study helped to investigate the optimal parameters on fixed bed reactor for toluene steam reforming, 800 °C, S/C ratio 3, GHSV 61200 h^{-1} was observed to be the most suitable reforming conditions.

To understand the influence of syngas atmosphere in catalytic steam reforming of toluene/tar model compound, the effects of different reforming atmosphere toluene conversion, gas products and coke deposition have been investigated using Ni/Al_2O_3 catalyst. The gas concentration in the atmosphere was decided

by the typical biomass gasification gas products. The concentration of H_2, CO, CO_2 and CH_4 was fixed at 30%, 30%, 20% and 3% respectively, single gas and multi gas atmosphere were tested. The catalytic tests were conducted at 800 °C, S/C ratio 3, GHSV 61200 h^{-1}. The toluene conversion, the composition and production yields of gas products (H_2, CO, CO_2 and CH_4) have been recorded and calculated. The potential reasons for the observed drop in toluene conversion in H_2 and CH_4 containing atmosphere have been analyzed.

To improve the catalytic performance and stability of Ni/Al_2O_3 catalyst, biomass ash was introduced as a spacer/guardian layer to Ni/Al_2O_3 catalyst. Four different catalyst beds including biomass ash, Ni/Al_2O_3, biomass ash and Ni/Al_2O_3 mixture, Two-layer biomass ash-Ni/Al_2O_3 were tested under different reforming atmosphere (100% N_2, 30% H_2 atmosphere, 3% CH_4 atmosphere, 30% CO, 30% H_2 atmosphere, simulated gasification gas atmosphere).

7.2 Conclusions

The main conclusions of this project are:

(1) **Toluene catalytic steam reforming parameters:** Increasing temperature from 700 to 900 °C increased toluene conversion into gases, with a potential risk of higher coke deposition. 800 °C presented the highest H_2 production, a high toluene conversion (>94%) and relatively lower coke deposition. Ni/Al_2O_3 catalyst only requires a relatively short residence time (GHSV < 91800 h^{-1}) for toluene reforming, and effectively removes low concentrations toluene (100 g Nm^{-3}) in a hot gas stream (>90%). H_2 yield and toluene conversion increased slightly and approached simulated thermodynamic equilibrium results when GHSV decreased. Coke deposition increased at a lower rate as GHSV increased. High S/C ratio

would greatly increase total conversion, hydrogen production, and reduce the coke formation on catalyst. The presence of excess steam could shift the equilibrium of water-gas shift reaction to produce more H_2. 800 °C, GHSV 61200 h^{-1} and S/C ratio 3 provided the most suitable reaction conditions for toluene conversion and H_2 production in steam reforming of toluene, obtained a steady state of a toluene to gas conversion over 94%, a H_2 production of 13 mol mol $_{toluene}^{-1}$ in 5-hour test, with no obvious deactivation observed in 5 hours. Based on these results, this condition would be suitable for tar model compound removal.

(2) **Steam reforming atmosphere:** CO and CO_2 in reaction atmosphere showed limited impact on the toluene conversion or catalyst deactivation, while the high content of CO and CO_2 in reforming atmosphere would affect the selectivity of product CO/CO_2 mainly due to (reverse) WGS reaction. Also, CO had more significant influence on the selectivity of product CO/CO_2 than H_2. H_2 content in reforming atmosphere could slightly deactivate the catalyst and promote the coke formation on Ni/Al_2O_3 catalyst due to the acidity of H_2. The presence of H_2 could also decrease the H_2 production yield from toluene steam reforming. A relatively low content of CH_4 had a significant influence on coke formation on catalyst and catalyst deactivation. Moreover, the addition of H_2 to the reforming atmosphere with the presence of CH_4 could increase the coke amount greatly, further decrease the gas yield and deactivate the Ni/Al_2O_3 catalyst.

(3) **Improving Ni/Al_2O_3 catalyst**: Biomass ash has a very good resistance to coke deposition in toluene steam reforming, but the catalytic performance is very limited, the toluene conversion is usually lower than 50% in all conditions. The 1:1 biomass ash-Ni/Al_2O_3 mixture also has a good resistance to coke deposition, and it has a stable conversion of toluene to

gas between 80% and 85% under different atmospheres in 5-hour tests. Two-layer biomass ash and Ni/Al_2O_3 catalytic system shows a very good performance in different atmospheres. The ash layer has a relatively low coke formation, but still helps to prevent the coke deposition on the Ni/Al_2O_3 layer. Under all five reforming atmospheres, the 2-layer catalyst bed achieves a conversion of toluene to gases higher than 90% throughout 5-hour tests. As the coke deposition rate on Ni/Al_2O_3 layer is significantly reduced by the biomass ash layer, the stability of Ni/Al_2O_3 is largely improved.

7.3 Recommendation for Future Work

Based on the conclusions of this project, the following work recommended for the future:

(1) Biomass ash could also be used as catalyst support for Ni and compares the effects in toluene steam reforming, coke deposition, catalyst deactivation with 2-layer catalyst system in this work.

(2) A kinetic model could be developed to understand the involved reactions and help to optimize the process parameters/conditions.

(3) A more complex model tar mixture or real tar from biomass gasification could be used as feedstock in different reforming atmosphere condition study. The aim of reforming atmosphere study is to improve the tar removal efficiency in biomass gasification gas, a more complex tar mixture or real tar could be applied as the feedstock to the catalytic reforming test, to further investigate the influence of reforming atmosphere on tar catalytic

removal.

(4) A better determination of the pore size and porosity of the catalysts, study the effect of pore size and porosity on the mass transfer and determine if the intraparticle resistance plays a role on the reaction kinetics.

(5) Different experiment periods could be investigated. This could give a more detail process of coke deposition on catalyst surface and reveal the relationship between catalyst deactivation and coke deposition rate.

(6) The regeneration/repeatability of the spent catalysts could be studied. The coke deposition on spent catalysts prevents the conversion of toluene, the coke could be removed by burning in air, it is important to test the ability to regenerate/reactivate the catalyst and its catalytic performance after regeneration, the effect of the sintering of the catalysts could be performed.

ReferencesUncategorized References

Abbas, T., M. Tahir and N. A. Saidina Amin (2018). "Enhanced metal–support interaction in Ni/Co3O4/TiO2 nanorods toward stable and dynamic hydrogen production from phenol steam reforming." Industrial & Engineering Chemistry Research **58**(2): 517-530.

Abu El-Rub, Z., E. A. Bramer and G. Brem (2004). "Review of catalysts for tar elimination in biomass gasification processes." Industrial & engineering chemistry research **43**(22): 6911-6919.

Ammendola, P., E. Cammisa, R. Chirone, L. Lisi and G. Ruoppolo (2012). "Effect of sulphur on the performance of Rh–LaCoO3 based catalyst for tar conversion to syngas." Applied Catalysis B: Environmental **113**: 11-18.

Anis, S. and Z. Zainal (2011). "Tar reduction in biomass producer gas via mechanical, catalytic and thermal methods: A review." Renewable and sustainable energy reviews **15**(5): 2355-2377.

Artetxe, M., J. Alvarez, M. A. Nahil, M. Olazar and P. T. Williams (2017). "Steam reforming of different biomass tar model compounds over Ni/Al2O3 catalysts." Energy Conversion and Management **136**: 119-126.

Artetxe, M., M. A. Nahil, M. Olazar and P. T. Williams (2016). "Steam reforming of phenol as biomass tar model compound over Ni/Al2O3 catalyst." Fuel **184**: 629-636.

Asadullah, M., T. Miyazawa, S.-i. Ito, K. Kunimori, M. Yamada and K. Tomishige (2004). "Gasification of different biomasses in a dual-bed gasifier system combined with novel catalysts with high energy efficiency." Applied Catalysis A: General **267**(1-2): 95-102.

Ashok, J., S. Das, N. Dewangan and S. Kawi (2019). "H2S and NOx tolerance capability of CeO2 doped La1− xCexCo0. 5Ti0. 5O3− δ perovskites for steam reforming of biomass tar model reaction." Energy Conversion and Management: X **1**: 100003.

Ashok, J., N. Dewangan, S. Das, P. Hongmanorom, M. H. Wai, K. Tomishige and S. Kawi (2020). "Recent progress in the development of catalysts for steam reforming of biomass tar model reaction." Fuel Processing Technology **199**: 106252.

Ashok, J., Y. Kathiraser, M. Ang and S. Kawi (2015). "Bi-functional hydrotalcite-derived NiO–CaO–Al2O3 catalysts for steam reforming of biomass and/or tar model compound at low steam-to-carbon conditions." Applied Catalysis B: Environmental **172**: 116-128.

Asif, M. and T. Muneer (2007). "Energy supply, its demand and security issues for developed and emerging economies." Renewable and sustainable energy reviews **11**(7): 1388-1413.

Balta, M. T., I. Dincer and A. Hepbasli (2009). "Thermodynamic assessment of geothermal energy use in hydrogen production." International Journal of hydrogen

energy **34**(7): 2925-2939.
Bartholomew, C. H. and R. J. Farrauto (2011). Fundamentals of industrial catalytic processes, John Wiley & Sons.
Bennadji, H., K. Smith, S. Shabangu and E. M. Fisher (2013). "Low-temperature pyrolysis of woody biomass in the thermally thick regime." Energy & fuels **27**(3): 1453-1459.
Bona, S., P. Guillén, J. G. Alcalde, L. García and R. Bilbao (2008). "Toluene steam reforming using coprecipitated Ni/Al catalysts modified with lanthanum or cobalt." Chemical Engineering Journal **137**(3): 587-597.
Brunauer, S., P. H. Emmett and E. Teller (1938). "Adsorption of gases in multimolecular layers." Journal of the American chemical society **60**(2): 309-319.
Buchireddy, P. R., R. M. Bricka, J. Rodriguez and W. Holmes (2010). "Biomass gasification: catalytic removal of tars over zeolites and nickel supported zeolites." Energy & Fuels **24**(4): 2707-2715.
Cao, J.-P., J. Ren, X.-Y. Zhao, X.-Y. Wei and T. Takarada (2018). "Effect of atmosphere on carbon deposition of Ni/Al2O3 and Ni-loaded on lignite char during reforming of toluene as a biomass tar model compound." Fuel **217**: 515-521.
Chapin, D., S. Kiffer and J. Nestell (2004). "The very high temperature reactor: a technical summary." MPR Associates, Alexandria, VA.
Chen, G.-m., X.-w. Zhang and Z.-t. MI (2007). "Effects of pressure on coke and formation of its precursors during catalytic cracking of toluene over USY catalyst." Journal of Fuel Chemistry and Technology **35**(2): 211-216.
Chen, G., J. Tao, C. Liu, B. Yan, W. Li and X. Li (2017). "Hydrogen production via acetic acid steam reforming: a critical review on catalysts." Renewable and Sustainable Energy Reviews **79**: 1091-1098.
Chen, J., J. Sun and Y. Wang (2017). "Catalysts for steam reforming of bio-oil: a review." Industrial & Engineering Chemistry Research **56**(16): 4627-4637.
Chen, Y.-H., M. Schmid, T. Kertthong and G. Scheffknecht (2020). "Reforming of toluene as a tar model compound over straw char containing fly ash." Biomass and Bioenergy **141**: 105657.
Coll, R., J. Salvado, X. Farriol and D. Montane (2001). "Steam reforming model compounds of biomass gasification tars: conversion at different operating conditions and tendency towards coke formation." Fuel Processing Technology **74**(1): 19-31.
Compagne, P. A. (2014). Multi-tubular steam reformer and process for catalytic steam reforming of a hydrocarbonaceous feedstock, Google Patents.
Constantinou, D. A., J. L. G. Fierro and A. M. Efstathiou (2010). "A comparative study of the steam reforming of phenol towards H2 production over natural calcite, dolomite and olivine materials." Applied Catalysis B: Environmental **95**(3-4): 255-269.
Daferera, D. J., B. N. Ziogas and M. G. Polissiou (2000). "GC-MS analysis of essential oils from some Greek aromatic plants and their fungitoxicity on Penicillium

digitatum." Journal of agricultural and food chemistry **48**(6): 2576-2581.
Devi, L., K. J. Ptasinski and F. J. Janssen (2003). "A review of the primary measures for tar elimination in biomass gasification processes." Biomass and bioenergy **24**(2): 125-140.
Dou, B., J. Gao, X. Sha and S. W. Baek (2003). "Catalytic cracking of tar component from high-temperature fuel gas." Applied Thermal Engineering **23**(17): 2229-2239.
Dou, X., A. Veksha, W. P. Chan, W.-D. Oh, Y. N. Liang, F. Teoh, D. K. B. Mohamed, A. Giannis, G. Lisak and T.-T. Lim (2019). "Poisoning effects of H2S and HCl on the naphthalene steam reforming and water-gas shift activities of Ni and Fe catalysts." Fuel **241**: 1008-1018.
Du, Z.-Y., Z.-H. Zhang, C. Xu, X.-B. Wang and W.-Y. Li (2018). "Low-temperature steam reforming of toluene and biomass tar over biochar-supported Ni nanoparticles." ACS Sustainable Chemistry & Engineering **7**(3): 3111-3119.
Dufour, A., E. Masson, P. Girods, Y. Rogaume and A. Zoulalian (2011). "Evolution of Aromatic Tar Composition in Relation to Methane and Ethylene from Biomass Pyrolysis-Gasification." Energy & Fuels **25**(9): 4182-4189.
El-Rub, Z. A., E. A. Bramer and G. Brem (2008). "Experimental comparison of biomass chars with other catalysts for tar reduction." Fuel **87**(10-11): 2243-2252.
Fabbri, D., C. Torri, B. R. Simoneit, L. Marynowski, A. I. Rushdi and M. J. Fabiańska (2009). "Levoglucosan and other cellulose and lignin markers in emissions from burning of Miocene lignites." Atmospheric Environment **43**(14): 2286-2295.
Foster, W., U. Azimov, P. Gauthier-Maradei, L. C. Molano, M. Combrinck, J. Munoz, J. J. Esteves and L. Patino (2021). "Waste-to-energy conversion technologies in the UK: Processes and barriers–A review." Renewable and Sustainable Energy Reviews **135**: 110226.
Frusteri, F., S. Freni, L. Spadaro, V. Chiodo, G. Bonura, S. Donato and S. Cavallaro (2004). "H2 production for MC fuel cell by steam reforming of ethanol over MgO supported Pd, Rh, Ni and Co catalysts." Catalysis Communications **5**(10): 611-615.
Furusawa, T. and A. Tsutsumi (2005). "Comparison of Co/MgO and Ni/MgO catalysts for the steam reforming of naphthalene as a model compound of tar derived from biomass gasification." Applied Catalysis A: General **278**(2): 207-212.
Gai, C., F. Zhang, T. Yang, Z. Liu, W. Jiao, N. Peng, T. Liu, Q. Lang and Y. Xia (2018). "Hydrochar supported bimetallic Ni–Fe nanocatalysts with tailored composition, size and shape for improved biomass steam reforming performance." Green Chemistry **20**(12): 2788-2800.
Gao, N., S. Liu, Y. Han, C. Xing and A. Li (2015). "Steam reforming of biomass tar for hydrogen production over NiO/ceramic foam catalyst." international journal of hydrogen energy **40**(25): 7983-7990.
Gao, N., J. Salisu, C. Quan and P. Williams (2021). "Modified nickel-based catalysts for improved steam reforming of biomass tar: A critical review." Renewable and Sustainable Energy Reviews **145**: 111023.

Gao, N., X. Wang, A. Li, C. Wu and Z. Yin (2016). "Hydrogen production from catalytic steam reforming of benzene as tar model compound of biomass gasification." Fuel Processing Technology **148**: 380-387.
Garbarino, G., A. Lagazzo, P. Riani and G. Busca (2013). "Steam reforming of ethanol–phenol mixture on Ni/Al2O3: effect of Ni loading and sulphur deactivation." Applied Catalysis B: Environmental **129**: 460-472.
González-Gil, R., I. Chamorro-Burgos, C. Herrera, M. Larrubia, M. Laborde, F. Marino and L. Alemany (2015). "Production of hydrogen by catalytic steam reforming of oxygenated model compounds on Ni-modified supported catalysts. Simulation and experimental study." International Journal of Hydrogen Energy **40**(34): 11217-11227.
Göransson, K., U. Söderlind, J. He and W. Zhang (2011). "Review of syngas production via biomass DFBGs." Renewable and Sustainable Energy Reviews **15**(1): 482-492.
Gu, J., S. Wang, T. Lu, Y. Wu, H. Yuan and Y. Chen (2020). "Synthesis and evaluation of pyrolysis waste peat char supported catalyst for steam reforming of toluene." Renewable Energy **160**: 964-973.
Guan, G., M. Kaewpanha, X. Hao and A. Abudula (2016). "Catalytic steam reforming of biomass tar: Prospects and challenges." Renewable and sustainable energy reviews **58**: 450-461.
He, L., S. Hu, L. Jiang, G. Liao, X. Chen, H. Han, L. Xiao, Q. Ren, Y. Wang and S. Su (2018). "Carbon nanotubes formation and its influence on steam reforming of toluene over Ni/Al2O3 catalysts: Roles of catalyst supports." Fuel Processing Technology **176**: 7-14.
Hognon, C., C. Dupont, M. Grateau and F. Delrue (2014). "Comparison of steam gasification reactivity of algal and lignocellulosic biomass: influence of inorganic elements." Bioresource technology **164**: 347-353.
Hu, G., S. Xu, S. Li, C. Xiao and S. Liu (2006). "Steam gasification of apricot stones with olivine and dolomite as downstream catalysts." Fuel Processing Technology **87**(5): 375-382.
Hu, S., L. He, Y. Wang, S. Su, L. Jiang, Q. Chen, Q. Liu, H. Chi, J. Xiang and L. Sun (2016). "Effects of oxygen species from Fe addition on promoting steam reforming of toluene over Fe–Ni/Al2O3 catalysts." International Journal of Hydrogen Energy **41**(40): 17967-17975.
Iida, H., A. Fujiyama, A. Igarashi and K. Okumura (2017). "Steam reforming of toluene over Ru/SrCO3-Al2O3 catalysts." Fuel Processing Technology **168**: 50-57.
Inayat, M., S. A. Sulaiman, J. C. Kurnia and M. Shahbaz (2019). "Effect of various blended fuels on syngas quality and performance in catalytic co-gasification: A review." Renewable and Sustainable Energy Reviews **105**: 252-267.
Josuinkas, F. M., C. P. Quitete, N. F. Ribeiro and M. M. Souza (2014). "Steam reforming of model gasification tar compounds over nickel catalysts prepared from hydrotalcite precursors." Fuel processing technology **121**: 76-82.

Kaewpanha, M., G. Guan, X. Hao, Z. Wang, Y. Kasai, K. Kusakabe and A. Abudula (2014). "Steam co-gasification of brown seaweed and land-based biomass." Fuel Processing Technology **120**: 106-112.

Karim, A., J. Bravo, D. Gorm, T. Conant and A. Datye (2005). "Comparison of wall-coated and packed-bed reactors for steam reforming of methanol." Catalysis Today **110**(1-2): 86-91.

Karnjanakom, S., G. Guan, B. Asep, X. Du, X. Hao, C. Samart and A. Abudula (2015). "Catalytic steam reforming of tar derived from steam gasification of sunflower stalk over ethylene glycol assisting prepared Ni/MCM-41." Energy Conversion and Management **98**: 359-368.

Kim, S., D. Chun, Y. Rhim, J. Lim, S. Kim, H. Choi, S. Lee and J. Yoo (2015). "Catalytic reforming of toluene using a nickel ion-exchanged coal catalyst." International Journal of Hydrogen Energy **40**(35): 11855-11862.

Kim, Y.-K., J.-I. Park, D. Jung, J. Miyawaki, S.-H. Yoon and I. Mochida (2014). "Low-temperature catalytic conversion of lignite: 3. Tar reforming using the supported potassium carbonate." Journal of Industrial and Engineering Chemistry **20**(1): 9-12.

Kirkels, A. F. and G. P. Verbong (2011). "Biomass gasification: Still promising? A 30-year global overview." Renewable and Sustainable Energy Reviews **15**(1): 471-481.

Koike, M., D. Li, H. Watanabe, Y. Nakagawa and K. Tomishige (2015). "Comparative study on steam reforming of model aromatic compounds of biomass tar over Ni and Ni–Fe alloy nanoparticles." Applied Catalysis A: General **506**: 151-162.

Kuchonthara, P., B. Puttasawat, P. Piumsomboon, L. Mekasut and T. Vitidsant (2012). "Catalytic steam reforming of biomass-derived tar for hydrogen production with K2CO3/NiO/γ-Al2O3 catalyst." Korean Journal of Chemical Engineering **29**(11): 1525-1530.

Le Saché, E., L. Pastor-Pérez, V. Garcilaso, D. J. Watson, M. Centeno, J. A. Odriozola and T. Reina (2019). "Flexible syngas production using a La2Zr2-xNixO7-δ pyrochlore-double perovskite catalyst: Towards a direct route for gas phase CO2 recycling." Catalysis Today.

Lertwittayanon, K., W. Youravong and W. J. Lau (2017). "Enhanced catalytic performance of Ni/α-Al2O3 catalyst modified with CaZrO3 nanoparticles in steam-methane reforming." International Journal of Hydrogen Energy **42**(47): 28254-28265.

Levin, D. B. and R. Chahine (2010). "Challenges for renewable hydrogen production from biomass." International Journal of Hydrogen Energy **35**(10): 4962-4969.

Levy, P., J. Sanderson, R. Kispert and D. Wise (1981). "Biorefining of biomass to liquid fuels and organic chemicals." Enzyme and Microbial Technology **3**(3): 207-215.

Li, C. and K. Suzuki (2009). "Tar property, analysis, reforming mechanism and model for biomass gasification—An overview." Renewable and Sustainable Energy

Reviews **13**(3): 594-604.
Li, D., C. Ishikawa, M. Koike, L. Wang, Y. Nakagawa and K. Tomishige (2013). "Production of renewable hydrogen by steam reforming of tar from biomass pyrolysis over supported Co catalysts." International Journal of hydrogen energy **38**(9): 3572-3581.
Li, D., M. Koike, L. Wang, Y. Nakagawa, Y. Xu and K. Tomishige (2014). "Regenerability of hydrotalcite-derived nickel–iron alloy nanoparticles for syngas production from biomass tar." ChemSusChem **7**(2): 510-522.
Li, D., L. Wang, M. Koike, Y. Nakagawa and K. Tomishige (2011). "Steam reforming of tar from pyrolysis of biomass over Ni/Mg/Al catalysts prepared from hydrotalcite-like precursors." Applied Catalysis B: Environmental **102**(3-4): 528-538.
Li, K., H. Bian, C. Liu, D. Zhang and Y. Yang (2015). "Comparison of geothermal with solar and wind power generation systems." Renewable and Sustainable Energy Reviews **42**: 1464-1474.
Li, L., K. Morishita, H. Mogi, K. Yamasaki and T. Takarada (2010). "Low-temperature gasification of a woody biomass under a nickel-loaded brown coal char." Fuel Processing Technology **91**(8): 889-894.
Li, Q., Q. Wang, A. Kayamori and J. Zhang (2018). "Experimental study and modeling of heavy tar steam reforming." Fuel Processing Technology **178**: 180-188.
Li, W.-P., M.-M. Wei, Y.-Q. Liu, S.-R. Li, Y.-Y. Ye, M. Wang and D. Wang (2019). "Interaction of Ce-char catalyst and partial oxidation on changes in biomass syngas composition." Journal of Renewable and Sustainable Energy **11**(2): 023101.
Li, Z., M. Li, J. Ashok and S. Kawi (2019). "NiCo@ NiCo phyllosilicate@ CeO2 hollow core shell catalysts for steam reforming of toluene as biomass tar model compound." Energy Conversion and Management **180**: 822-830.
Liang, T., Y. Wang, M. Chen, Z. Yang, S. Liu, Z. Zhou and X. Li (2017). "Steam reforming of phenol-ethanol to produce hydrogen over bimetallic NiCu catalysts supported on sepiolite." International Journal of Hydrogen Energy **42**(47): 28233-28246.
Lu, J., S. Guo, Y. Fu and J. Chang (2017). "Catalytic upgrading of bio-oil by simultaneous esterification and alkylation with azeotropic water removal." Fuel Processing Technology **161**: 193-198.
Lu, M., Z. Xiong, K. Fang, X. Li, J. Li and T. Li (2020). "Steam reforming of toluene over nickel catalysts supported on coal gangue ash." Renewable Energy **160**: 385-395.
Luneau, M., E. Gianotti, F. C. Meunier, C. Mirodatos, E. Puzenat, Y. Schuurman and N. Guilhaume (2017). "Deactivation mechanism of Ni supported on Mg-Al spinel during autothermal reforming of model biogas." Applied Catalysis B: Environmental **203**: 289-299.
Ma, H., L. Zeng, H. Tian, D. Li, X. Wang, X. Li and J. Gong (2016). "Efficient hydrogen

production from ethanol steam reforming over La-modified ordered mesoporous Ni-based catalysts." Applied Catalysis B: Environmental **181**: 321-331.
Mastropietro, P., P. Rodilla and C. Batlle (2020). "Emergency measures to protect energy consumers during the Covid-19 pandemic: A global review and critical analysis." Energy Research & Social Science **68**: 101678.
Mawdsley, J. R. and T. R. Krause (2008). "Rare earth-first-row transition metal perovskites as catalysts for the autothermal reforming of hydrocarbon fuels to generate hydrogen." Applied Catalysis A: General **334**(1-2): 311-320.
Medrano, J., M. Oliva, J. Ruiz, L. García and J. Arauzo (2011). "Hydrogen from aqueous fraction of biomass pyrolysis liquids by catalytic steam reforming in fluidized bed." Energy **36**(4): 2215-2224.
Meidanshahi, V., A. M. Bahmanpour, D. Iranshahi and M. R. Rahimpour (2011). "Theoretical investigation of aromatics production enhancement in thermal coupling of naphtha reforming and hydrodealkylation of toluene." Chemical Engineering and Processing: Process Intensification **50**(9): 893-903.
Mermelstein, J., M. Millan and N. Brandon (2011). "The interaction of biomass gasification syngas components with tar in a solid oxide fuel cell and operational conditions to mitigate carbon deposition on nickel-gadolinium doped ceria anodes." Journal of power sources **196**(11): 5027-5034.
Mitsuoka, K., S. Hayashi, H. Amano, K. Kayahara, E. Sasaoaka and M. A. Uddin (2011). "Gasification of woody biomass char with CO2: The catalytic effects of K and Ca species on char gasification reactivity." Fuel Processing Technology **92**(1): 26-31.
Miyazawa, T., T. Kimura, J. Nishikawa, S. Kado, K. Kunimori and K. Tomishige (2006). "Catalytic performance of supported Ni catalysts in partial oxidation and steam reforming of tar derived from the pyrolysis of wood biomass." Catalysis Today **115**(1-4): 254-262.
Mukai, D., S. Tochiya, Y. Murai, M. Imori, T. Hashimoto, Y. Sugiura and Y. Sekine (2013). "Role of support lattice oxygen on steam reforming of toluene for hydrogen production over Ni/La0. 7Sr0. 3AlO3− δ catalyst." Applied Catalysis A: General **453**: 60-70.
Nabgan, W., T. A. T. Abdullah, R. Mat, B. Nabgan, Y. Gambo and S. Triwahyono (2016). "Influence of Ni to Co ratio supported on ZrO2 catalysts in phenol steam reforming for hydrogen production." International Journal of Hydrogen Energy **41**(48): 22922-22931.
Narvaez, I., J. Corella and A. Orio (1997). "Fresh tar (from a biomass gasifier) elimination over a commercial steam-reforming catalyst. Kinetics and effect of different variables of operation." Industrial & Engineering Chemistry Research **36**(2): 317-327.
Noichi, H., A. Uddin and E. Sasaoka (2010). "Steam reforming of naphthalene as model biomass tar over iron–aluminum and iron–zirconium oxide catalyst catalysts." Fuel processing technology **91**(11): 1609-1616.

Odongo, A. (2015). "Tar removal in hot gas streams."
Oemar, U., M. L. Ang, Y. C. Chin, K. Hidajat and S. Kawi (2015). "Role of lattice oxygen in oxidative steam reforming of toluene as a tar model compound over Ni/La 0.8 Sr 0.2 AlO 3 catalyst." Catalysis Science & Technology **5**(7): 3585-3597.
Oemar, U., P. Ang, K. Hidajat and S. Kawi (2013). "Promotional effect of Fe on perovskite LaNixFe1− xO3 catalyst for hydrogen production via steam reforming of toluene." International journal of hydrogen energy **38**(14): 5525-5534.
Oemar, U., Y. Kathiraser, M. L. Ang, K. Hidajat and S. Kawi (2015). "Catalytic biomass gasification to syngas over highly dispersed lanthanum-doped nickel on SBA-15." ChemCatChem **7**(20): 3376-3385.
Oh, G., S. Y. Park, M. W. Seo, Y. K. Kim, H. W. Ra, J.-G. Lee and S. J. Yoon (2016). "Ni/Ru–Mn/Al2O3 catalysts for steam reforming of toluene as model biomass tar." Renewable energy **86**: 841-847.
Ortiz-Toral, P. J., J. Satrio, R. C. Brown and B. H. Shanks (2011). "Steam reforming of bio-oil fractions: effect of composition and stability." Energy & fuels **25**(7): 3289-3297.
Park, H. J., S. H. Park, J. M. Sohn, J. Park, J.-K. Jeon, S.-S. Kim and Y.-K. Park (2010). "Steam reforming of biomass gasification tar using benzene as a model compound over various Ni supported metal oxide catalysts." Bioresource technology **101**(1): S101-S103.
Park, S. Y., G. Oh, K. Kim, M. W. Seo, H. W. Ra, T. Y. Mun, J. G. Lee and S. J. Yoon (2017). "Deactivation characteristics of Ni and Ru catalysts in tar steam reforming." Renewable Energy **105**: 76-83.
Pashchenko, D. (2019). "Numerical study of steam methane reforming over a pre-heated Ni-based catalyst with detailed fluid dynamics." Fuel **236**: 686-694.
Patra, A. (2017). "Oxide dispersion strengthened high temperature alloys." Journal of Masterials Science and Nanomaterials **1**(1): e101.
Pereira, E. G., J. N. da Silva, J. L. de Oliveira and C. S. Machado (2012). "Sustainable energy: a review of gasification technologies." Renewable and sustainable energy reviews **16**(7): 4753-4762.
Qian, N., L. Zhang, W. Ma, X. Zhao, L. Han and W. Lu (2014). "Core–shell Al 2 O 3-supported Ni for high-performance catalytic reforming of toluene as a model compound of tar." Arabian Journal for Science and Engineering **39**(9): 6671-6678.
Quitete, C. P., R. C. P. Bittencourt and M. M. Souza (2014). "Steam reforming of tar using toluene as a model compound with nickel catalysts supported on hexaaluminates." Applied Catalysis A: General **478**: 234-240.
Quitete, C. P., R. C. P. Bittencourt and M. M. Souza (2015). "Coking resistance evaluation of tar removal catalysts." Catalysis Communications **71**: 79-83.
Rönkkönen, H., P. Simell, M. Reinikainen, O. Krause and M. V. Niemelä (2010). "Catalytic clean-up of gasification gas with precious metal catalysts – A novel catalytic reformer development." Fuel **89**(11): 3272-3277.

Ruiz, J. A., M. Juárez, M. Morales, P. Muñoz and M. Mendívil (2013). "Biomass gasification for electricity generation: Review of current technology barriers." Renewable and Sustainable Energy Reviews **18**: 174-183.
Sehested, J., N. W. Larsen, H. Falsig and B. Hinnemann (2014). "Sintering of nickel steam reforming catalysts: Effective mass diffusion constant for Ni-OH at nickel surfaces." Catalysis Today **228**: 22-31.
Shen, Y. and K. Yoshikawa (2013). "Recent progresses in catalytic tar elimination during biomass gasification or pyrolysis—A review." Renewable and Sustainable Energy Reviews **21**: 371-392.
Shen, Y., P. Zhao, Q. Shao, D. Ma, F. Takahashi and K. Yoshikawa (2014). "In-situ catalytic conversion of tar using rice husk char-supported nickel-iron catalysts for biomass pyrolysis/gasification." Applied Catalysis B: Environmental **152**: 140-151.
Shozi, M. L., V. D. Dasireddy, S. Singh, A. Govender, P. Mohlala and H. B. Friedrich (2019). "The effect of rhenium on the conversion of glycerol to mono-alcohols over nickel catalysts under continuous flow conditions." Sustainable Energy & Fuels **3**(8): 2038-2047.
Sieminski, A. (2014). "International energy outlook." Energy information administration (EIA) **18**.
Silveira, E., R. Rabelo-Neto and F. Noronha (2017). "Steam reforming of toluene, methane and mixtures over Ni/ZrO2 catalysts." Catalysis Today **289**: 289-301.
Smisek, M. and S. Cerny (1970). "New books-Active carbon: Manufacture, properties, and applications." Analytical Chemistry **42**(14): 81A-81A.
Stroud, T., T. Smith, E. Le Saché, J. Santos, M. Centeno, H. Arellano-Garcia, J. Odriozola and T. R. Reina (2018). "Chemical CO2 recycling via dry and bi reforming of methane using Ni-Sn/Al2O3 and Ni-Sn/CeO2-Al2O3 catalysts." Applied Catalysis B: Environmental **224**: 125-135.
Studies—Energy, O. O. G. G. (2011). OECD: Paris, France.
Sutton, D., B. Kelleher and J. R. Ross (2001). "Review of literature on catalysts for biomass gasification." Fuel processing technology **73**(3): 155-173.
Sutton, D., B. Kelleher and J. R. H. Ross (2001). "Review of literature on catalysts for biomass gasification." Fuel Processing Technology **73**(3): 155-173.
Świerczyński, D., S. Libs, C. Courson and A. Kiennemann (2007). "Steam reforming of tar from a biomass gasification process over Ni/olivine catalyst using toluene as a model compound." Applied Catalysis B: Environmental **74**(3-4): 211-222.
Tan, R. S., T. A. T. Abdullah, A. Johari and K. M. Isa (2020). "Catalytic steam reforming of tar for enhancing hydrogen production from biomass gasification: a review." Frontiers in Energy: 1-25.
Tao, J., L. Zhao, C. Dong, Q. Lu, X. Du and E. Dahlquist (2013). "Catalytic steam reforming of toluene as a model compound of biomass gasification tar using Ni-CeO2/SBA-15 catalysts." Energies **6**(7): 3284-3296.
Tomishige, K., T. Miyazawa, M. Asadullah, S.-i. Ito and K. Kunimori (2003). "Catalyst performance in reforming of tar derived from biomass over noble metal catalysts."

Green chemistry **5**(4): 399-403.
Trinh, Q. T., A. V. Nguyen, D. C. Huynh, T. H. Pham and S. H. Mushrif (2016). "Mechanistic insights into the catalytic elimination of tar and the promotional effect of boron on it: first-principles study using toluene as a model compound." Catalysis Science & Technology **6**(15): 5871-5883.
Veksha, A., A. Giannis, W.-D. Oh, V. W.-C. Chang, G. Lisak and T.-T. Lim (2018). "Catalytic activities and resistance to HCl poisoning of Ni-based catalysts during steam reforming of naphthalene." Applied Catalysis A: General **557**: 25-38.
Virginie, M., C. Courson, D. Niznansky, N. Chaoui and A. Kiennemann (2010). "Characterization and reactivity in toluene reforming of a Fe/olivine catalyst designed for gas cleanup in biomass gasification." Applied Catalysis B: Environmental **101**(1-2): 90-100.
Vivanpatarakij, S., D. Rulerk and S. Assabumrungrat (2014). "Removal of tar from biomass gasification process by steam reforming over nickel catalysts." Chemical Engineering Transactions **37**: 205-210.
Wang, S. and S. Wang (2015). "Impacts of wind energy on environment: A review." Renewable and Sustainable Energy Reviews **49**: 437-443.
Wu, Y.-m., Z.-l. Zhao, H.-b. Li and H. Fang (2009). "Low temperature pyrolysis characteristics of major components of biomass." Journal of Fuel Chemistry and Technology **37**(4): 427-432.
Yang, L., L. Pastor-Pérez, S. Gu, A. Sepúlveda-Escribano and T. Reina (2018). "Highly efficient Ni/CeO2-Al2O3 catalysts for CO2 upgrading via reverse water-gas shift: Effect of selected transition metal promoters." Applied Catalysis B: Environmental **232**: 464-471.
Yang, X., S. Xu, H. Xu, X. Liu and C. Liu (2010). "Nickel supported on modified olivine catalysts for steam reforming of biomass gasification tar." Catalysis Communications **11**(5): 383-386.
Yu, J., N. Paterson and M. Millan (2019). "The primary products of cellulose pyrolysis in the absence of extraparticle reactions." Fuel **237**: 911-915.
Zhang, R., H. Wang and X. Hou (2014). "Catalytic reforming of toluene as tar model compound: Effect of Ce and Ce–Mg promoter using Ni/olivine catalyst." Chemosphere **97**: 40-46.
Zhang, Z., X. Hu, L. Zhang, Y. Yang, Q. Li, H. Fan, Q. Liu, T. Wei and C.-Z. Li (2019). "Steam reforming of guaiacol over Ni/Al2O3 and Ni/SBA-15: Impacts of support on catalytic behaviors of nickel and properties of coke." Fuel Processing Technology **191**: 138-151.
Zhang, Z., Z. Ou, C. Qin, J. Ran and C. Wu (2019). "Roles of alkali/alkaline earth metals in steam reforming of biomass tar for hydrogen production over perovskite supported Ni catalysts." Fuel **257**: 116032.
Zhang, Z., X. Zhang, L. Zhang, Y. Wang, X. Li, S. Zhang, Q. Liu, T. Wei, G. Gao and X. Hu (2020). "Steam reforming of guaiacol over Ni/SiO2 catalyst modified with basic oxides: impacts of alkalinity on properties of coke." Energy Conversion and

Management **205**: 112301.
Zhao, B., X. Zhang, L. Chen, R. Qu, G. Meng, X. Yi and L. Sun (2010). "Steam reforming of toluene as model compound of biomass pyrolysis tar for hydrogen." Biomass and Bioenergy **34**(1): 140-144.
Zhao, X., Y. Xue, Z. Lu, Y. Huang, C. Guo and C. Yan (2017). "Encapsulating Ni/CeO2-ZrO2 with SiO2 layer to improve it catalytic activity for steam reforming of toluene." Catalysis Communications **101**: 138-141.
Zhu, H. L., Y. S. Zhang, M. Materazzi, G. Aranda, D. J. Brett, P. R. Shearing and G. Manos (2019). "Co-gasification of beech-wood and polyethylene in a fluidized-bed reactor." Fuel Processing Technology **190**: 29-37.

Appendices

Appendix 1 List of publication

Zhu, Hua Lun, Laura Pastor-Pérez, and Marcos Millan. "Catalytic Steam Reforming of Toluene: Understanding the Influence of the Main Reaction Parameters over a Reference Catalyst." *Energies* 13.4 (2020): 813 (doi: 10.3390/en13040813).

Zhu, Hua Lun, Laura Pastor-Pérez, and Marcos Millan. "Catalytic Steam Reforming of Toluene: Understanding the Influence of Reforming Gas Atmosphere." (In preparation)

Zhu, Hua Lun, Laura Pastor-Pérez, and Marcos Millan. "Effect of Biomass Ash on the Steam Reforming of Toluene in Simulated Gas Atmosphere over Ni/Al_2O_3." (In preparation)

Appendix 2 Calibration of H_2 analyser

The hydrogen analyser used in this project is based on the principle of thermal conductivity. Considering that the fuel gases CH_4 and CO_2 have a significant thermal conductivity factor, the analyser was calibrated to measure H_2 in CO_2 and the hydrogen reading when CO_2 in N_2 is passed through, to evaluate the influence of CO_2 in product gas. Although CH_4 conductivity factor has a significant influence, typical CH_4 concentration in our product gas is less than 1%, this concentration of CH_4 in the product stream for the experiments and H_2 analyser was insignificant. Therefore, the influence of CH_4 thermal conductivity on this H_2 analyser was neglected. Calibration curve for this H_2 analyser was produced using different gas mixtures and the correction factors were

investigated.

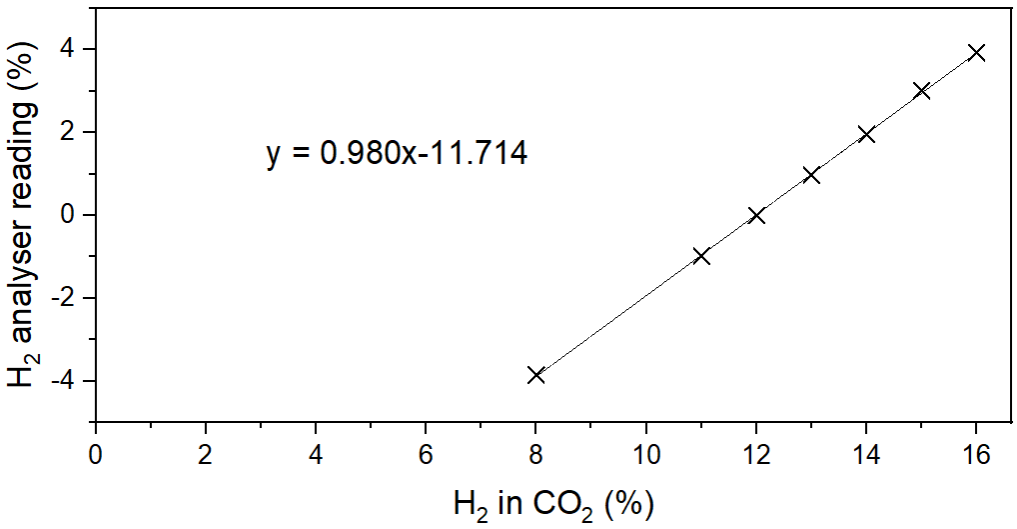

Figure 0.1 Calibration curve to estimate the hydrogen content in CO_2 gas of H_2 reading on H_2 analyser.

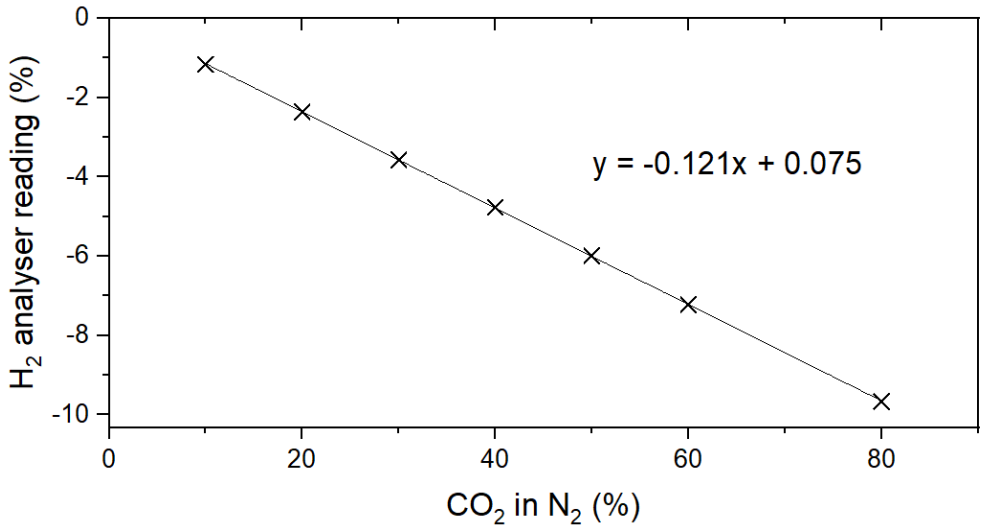

Figure 0.2 Calibration curve to estimate H_2 analyser reading when passing through CO_2 in N_2.

Appendix 3 Gas concentration data in Chapter 4

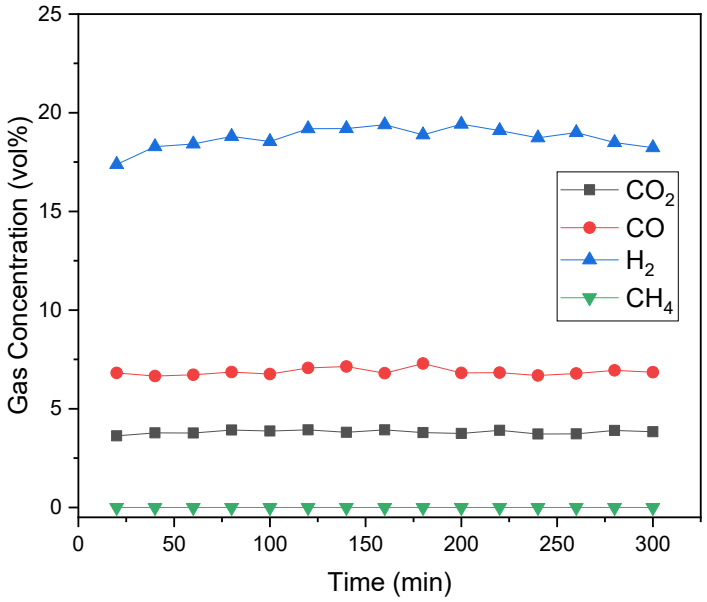

Figure 0.3 Gas concentration data of toluene steam reforming at 700 °C in 5-hour test (S/C ratio: 3, GHSV: 61,200 h^{-1}).

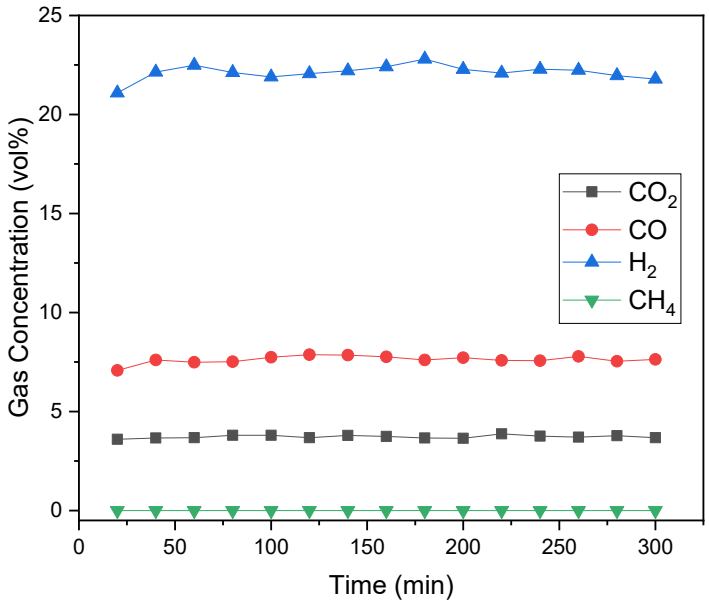

Figure 0.4 Gas concentration data of toluene steam reforming at 800 °C in 5-hour test (S/C ratio: 3, GHSV: 61,200 h^{-1}).

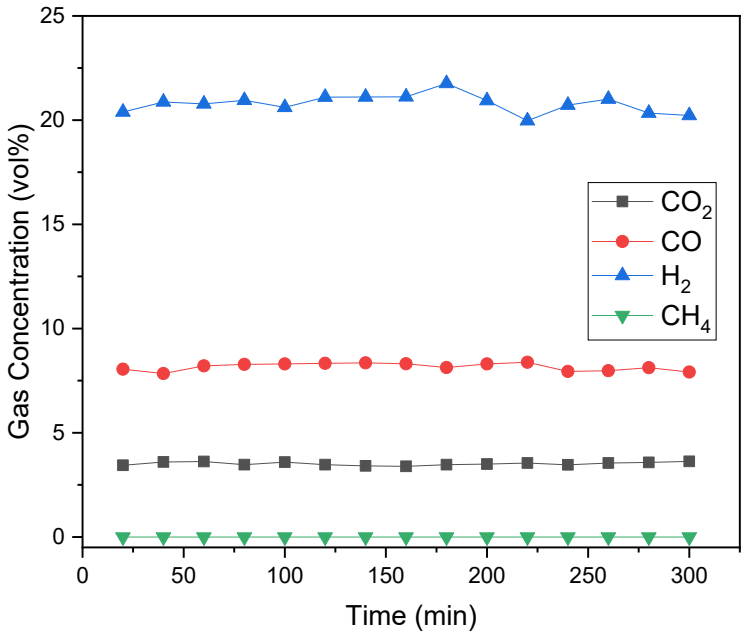

Figure 0.5 Gas concentration data of toluene steam reforming at 900 °C in 5-hour test (S/C ratio: 3, GHSV: 61,200 h^{-1}).

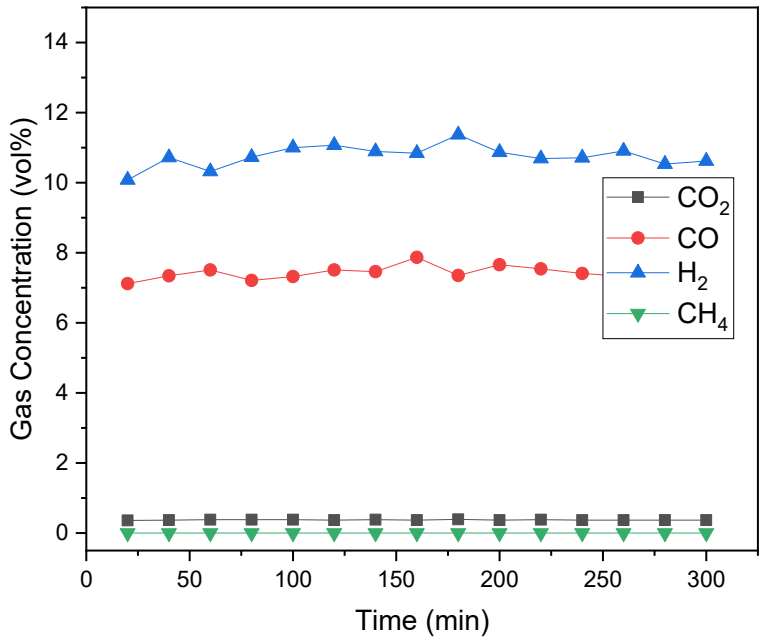

Figure 0.6 Gas concentration data of toluene steam reforming with S/C ratio 1 in 5-hour test (800 °C, GHSV: 61,200 h^{-1}).

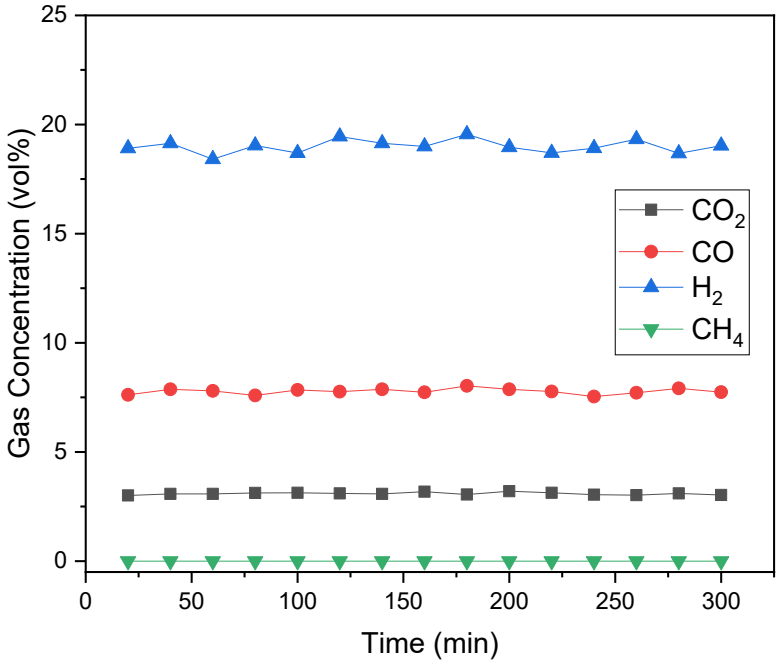

Figure 0.7 Gas concentration data of toluene steam reforming with S/C ratio 2 in 5-hour test (800 °C, GHSV: 61,200 h^{-1}).

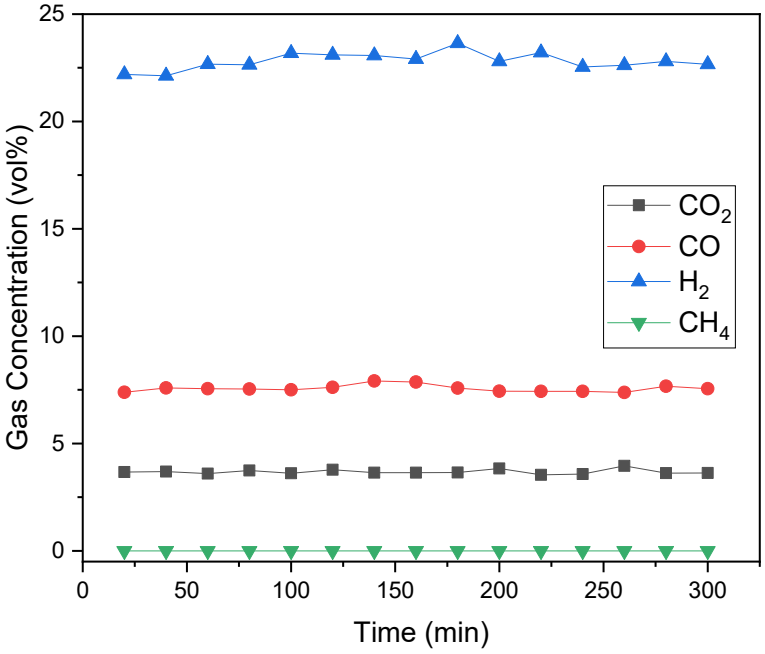

Figure 0.8 Gas concentration data of toluene steam reforming with S/C ratio 3 in 5-hour test (800 °C, GHSV: 61,200 h^{-1}).

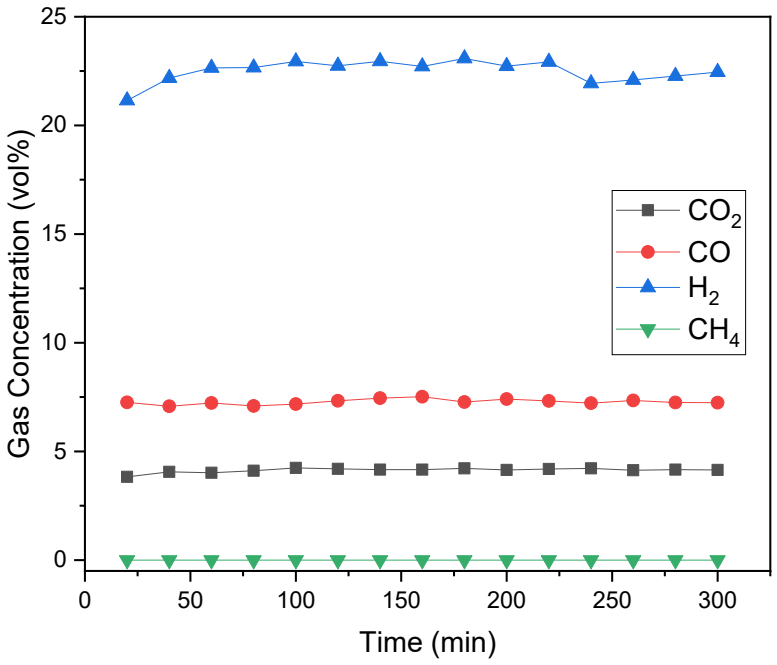

Figure 0.9 Gas concentration data of toluene steam reforming with GHSV 30,600 h^{-1} in 5-hour test (800 °C, S/C ratio 3).

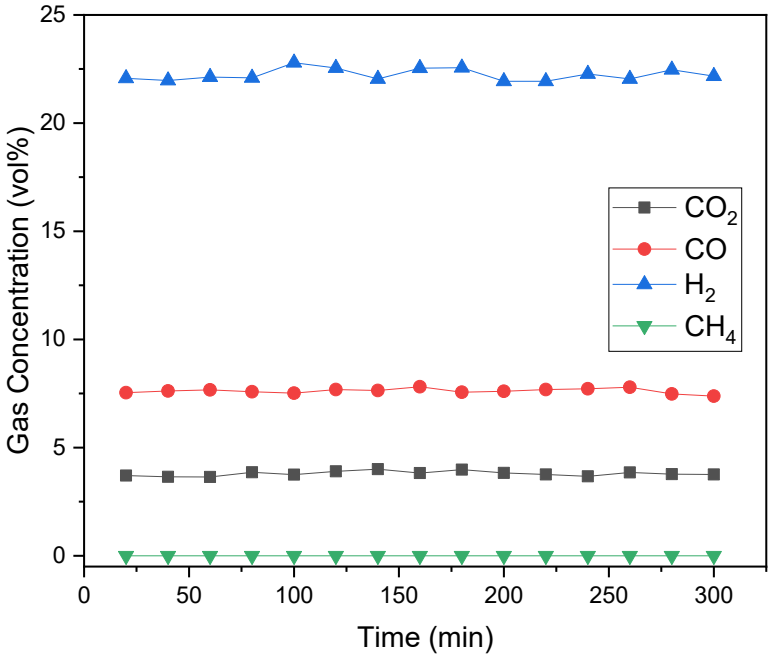

Figure 0.10 Gas concentration data of toluene steam reforming with GHSV 61,200 h^{-1} in 5-hour test (800 °C, S/C ratio 3).

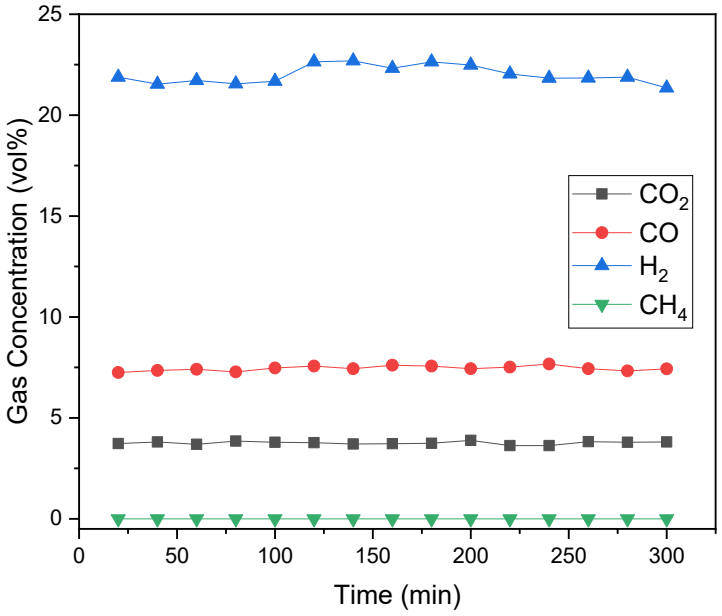

Figure 0.11 Gas concentration data of toluene steam reforming with GHSV 91,800 h^{-1} in 5-hour test (800 °C, S/C ratio 3).

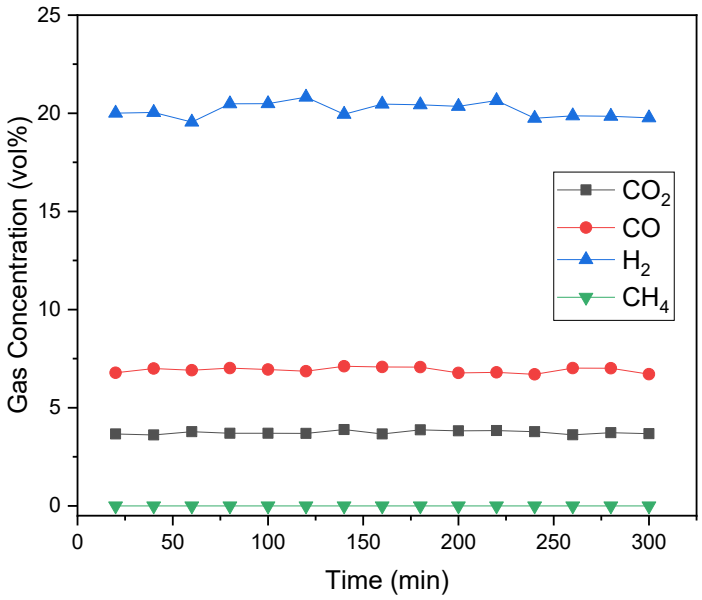

Figure 0.12 Gas concentration data of toluene steam reforming with GHSV 122,400 h^{-1} in 5-hour test (800 °C, S/C ratio 3).

Appendix 4 Gas concentration data in Chapter 5

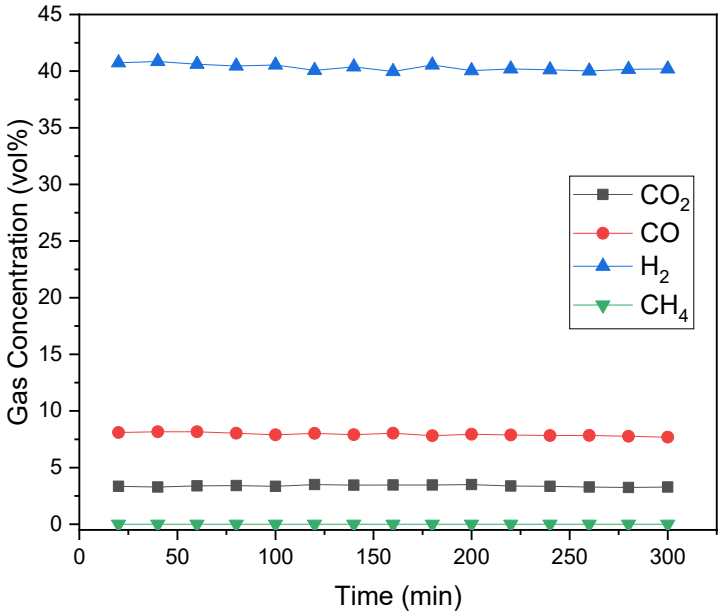

Figure 0.13 Gas concentration data of toluene steam reforming test in 30% H_2 balanced N_2 atmosphere (5-hour test, 800 °C, S/C ratio 3, GHSV: 91800 h^{-1})

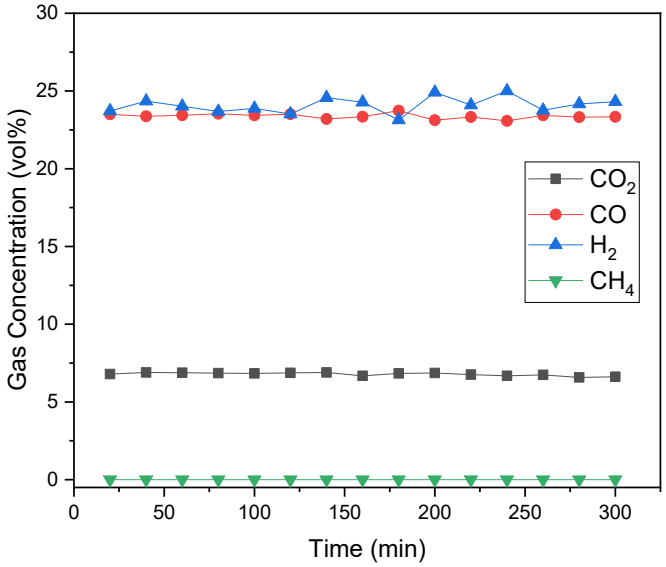

Figure 0.14 Gas concentration data of toluene steam reforming test in 30% CO balanced N_2 atmosphere (5-hour test, 800 °C, S/C ratio 3, GHSV: 91800 h^{-1})

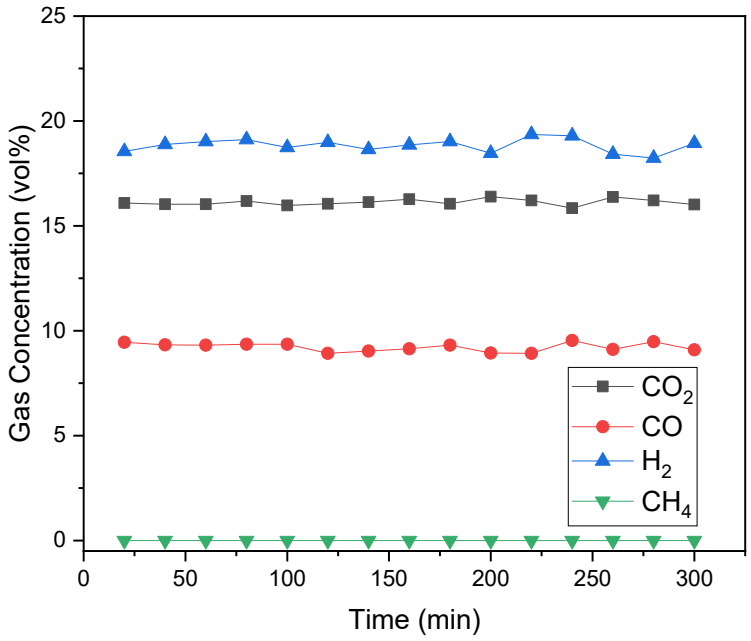

Figure 0.15 Gas concentration data of toluene steam reforming test in 20% CO_2 balanced N_2 atmosphere (5-hour test, 800 °C, S/C ratio 3, GHSV: 91800 h^{-1})

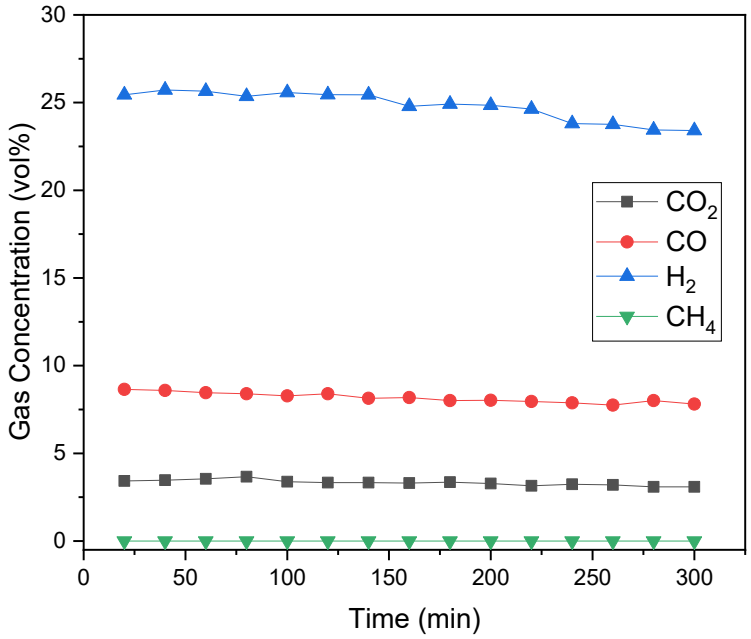

Figure 0.16 Gas concentration data of toluene steam reforming test in 3% CH_4 balanced N_2 atmosphere (5-hour test, 800 °C, S/C in toluene: 3, GHSV: 91800 h^{-1})

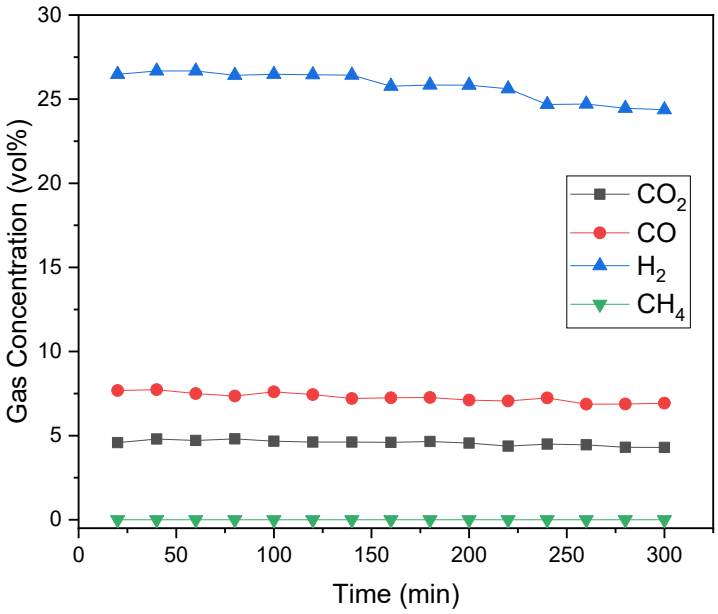

Figure 0.17 Gas concentration data of toluene steam reforming test in 3% CH_4 balanced N_2 atmosphere (5-hour test, 800 °C, S/C in toluene and methane: 3, GHSV: 91800 h^{-1})

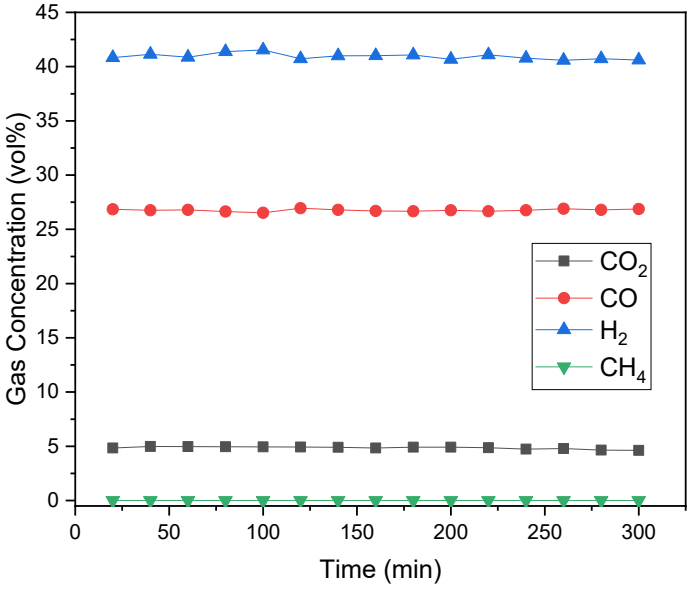

Figure 0.18 Gas concentration data of toluene steam reforming test in 30% CO and 30% H_2 balanced N_2 atmosphere (5-hour test, 800 °C, S/C in toluene and methane: 3, GHSV: 91800 h^{-1})

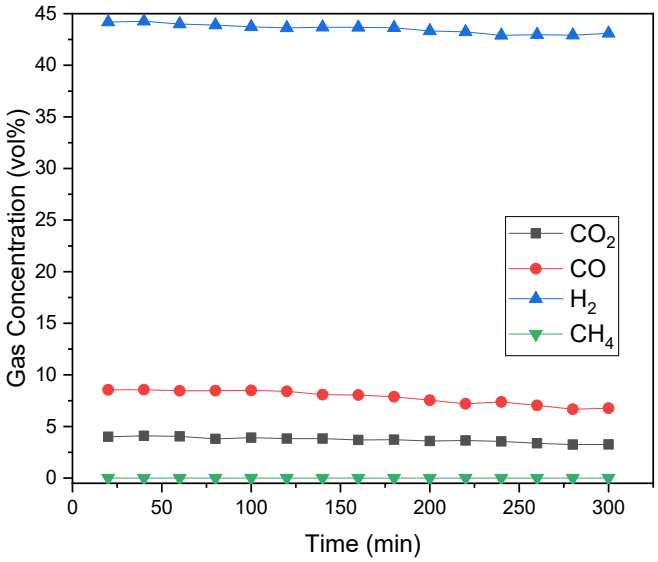

Figure 0.19 Gas concentration data of toluene steam reforming test in 30% H_2 and 3% CH_4 balanced N_2 atmosphere (5-hour test, 800 °C, S/C in toluene and methane: 3, GHSV: 91800 h^{-1})

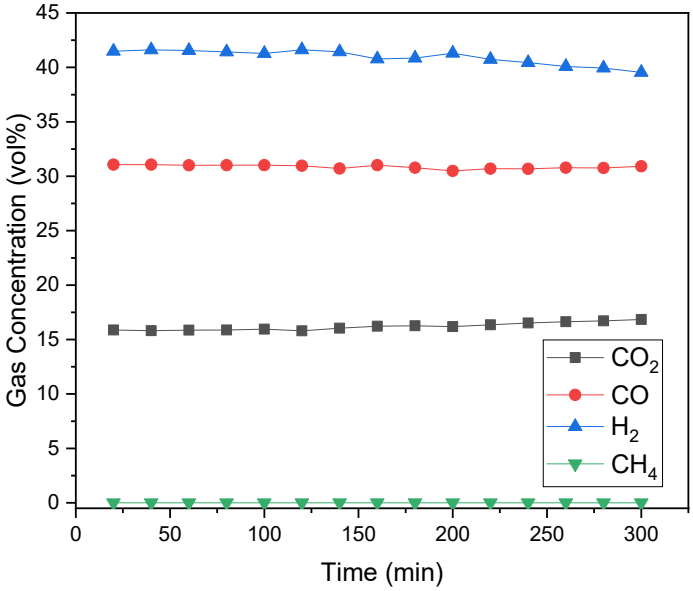

Figure 0.20 Gas concentration data of toluene steam reforming test in simulated gas atmosphere (5-hour test, 800 °C, S/C in toluene and methane: 3, GHSV: 91800 h^{-1})

Appendix 5 Gas concentration data in Chapter 6

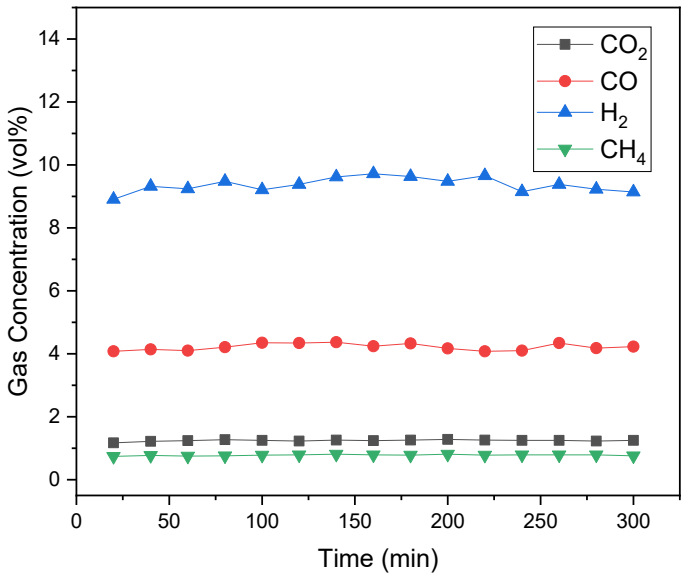

Figure 0.21 Gas concentration of toluene steam reforming test in N_2 atmosphere (5-hour test, biomass ash catalyst, 800 °C, S/C ratio 3, GHSV: 91800 h^{-1})

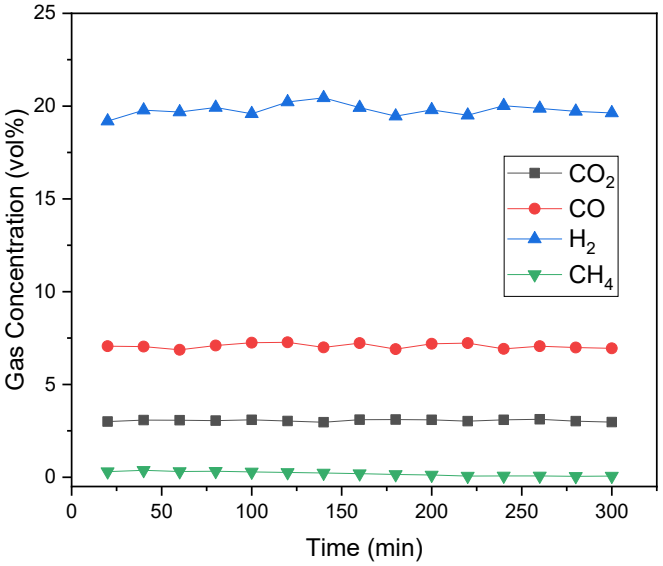

Figure 0.22 Gas concentration of toluene steam reforming test in N_2 atmosphere (5-hour test, biomass ash and Ni/Al_2O_3 mixture catalyst bed, 800 °C, S/C ratio 3, GHSV: 91800 h^{-1})

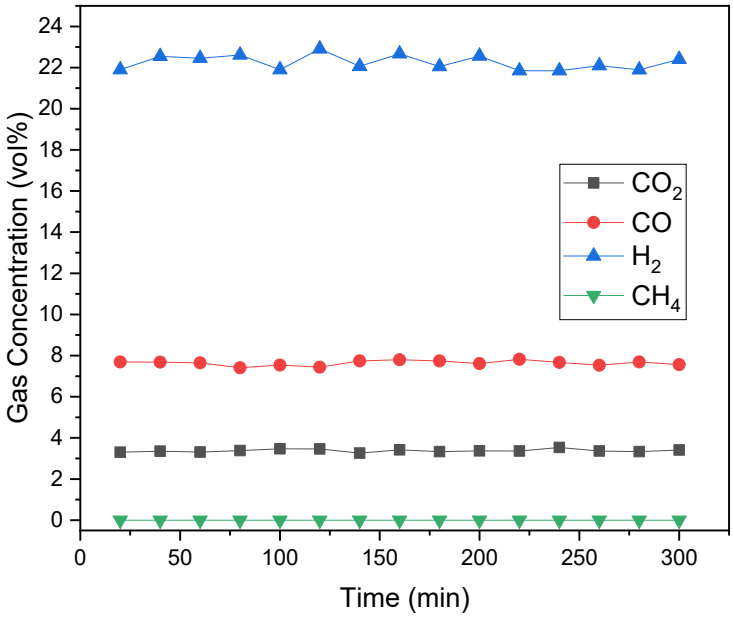

Figure 0.23 Gas concentration of toluene steam reforming test in N_2 atmosphere (5-hour test, 2-layer biomass ash and Ni/Al_2O_3 catalyst bed, 800 °C, S/C ratio 3, GHSV: 91800 h^{-1})

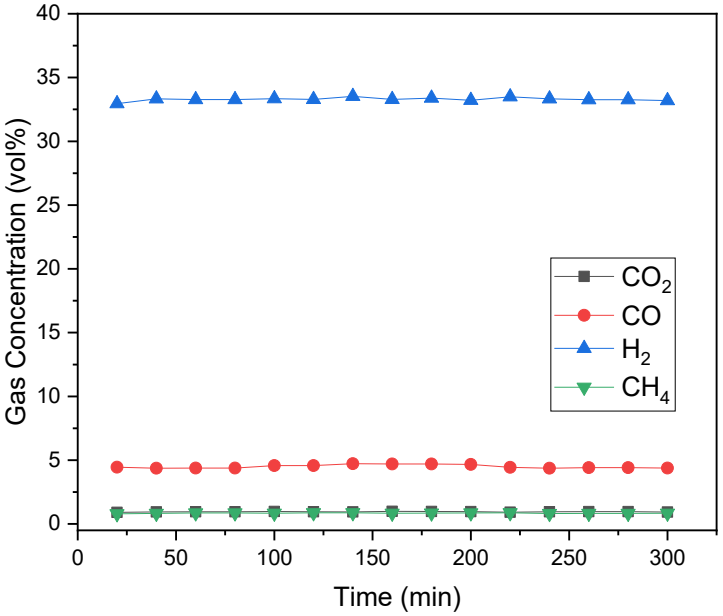

Figure 0.24 Gas concentration data of toluene steam reforming test in 30% H_2 atmosphere (5-hour test, biomass ash catalyst, 800 °C, S/C ratio 3, GHSV: 91800 h^{-1})

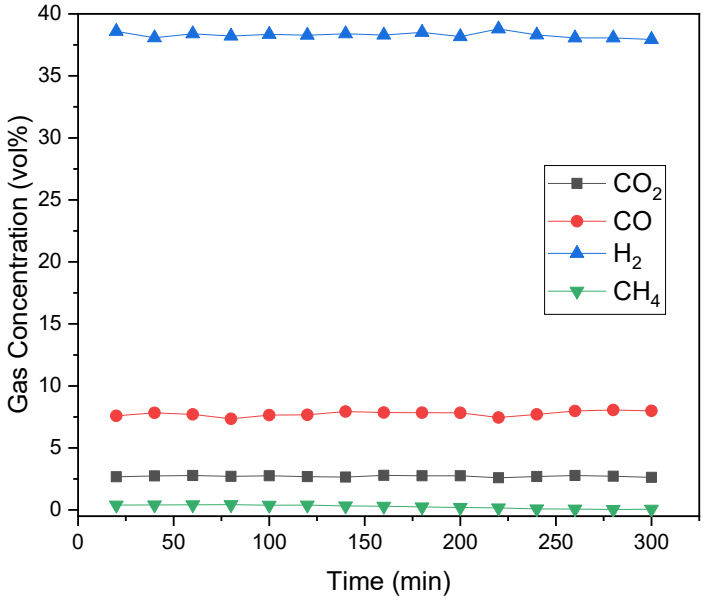

Figure 0.25 Gas concentration data of toluene steam reforming test in 30% H_2 atmosphere (5-hour test, biomass ash and Ni/Al_2O_3 mixture catalyst bed, 800 °C, S/C ratio 3, GHSV: 91800 h^{-1})

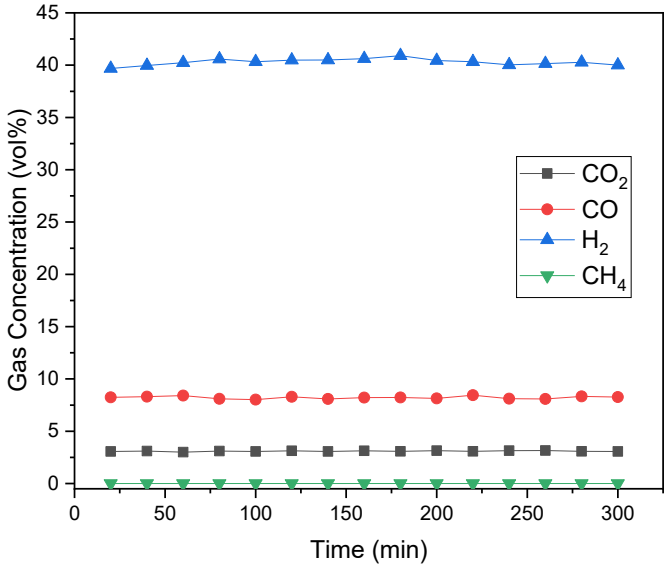

Figure 0.26 Gas concentration data of toluene steam reforming test in 30% H_2 atmosphere (5-hour test, 2-layer biomass ash and Ni/Al_2O_3 catalyst bed, 800 °C, S/C ratio 3, GHSV: 91800 h^{-1})

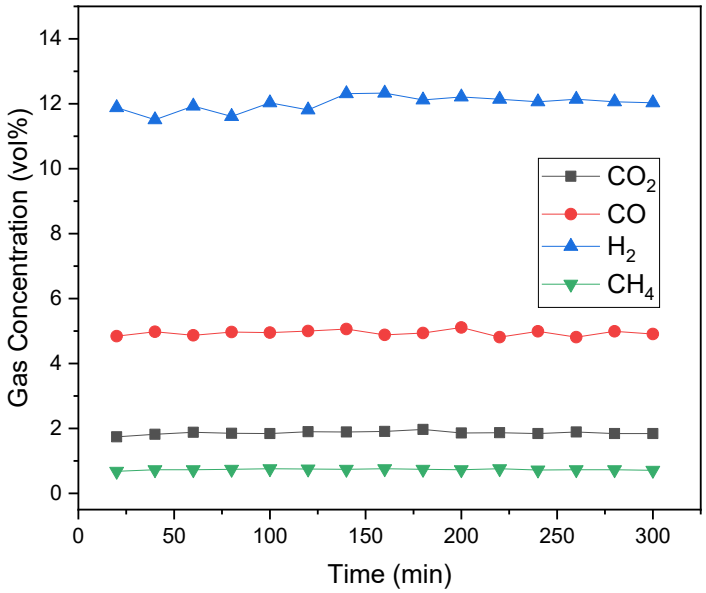

Figure 0.27 Gas concentration data of toluene steam reforming test in 3% CH_4 atmosphere (5-hour test, biomass ash catalyst, 800 °C, S/C ratio 3, GHSV: 91800 h^{-1})

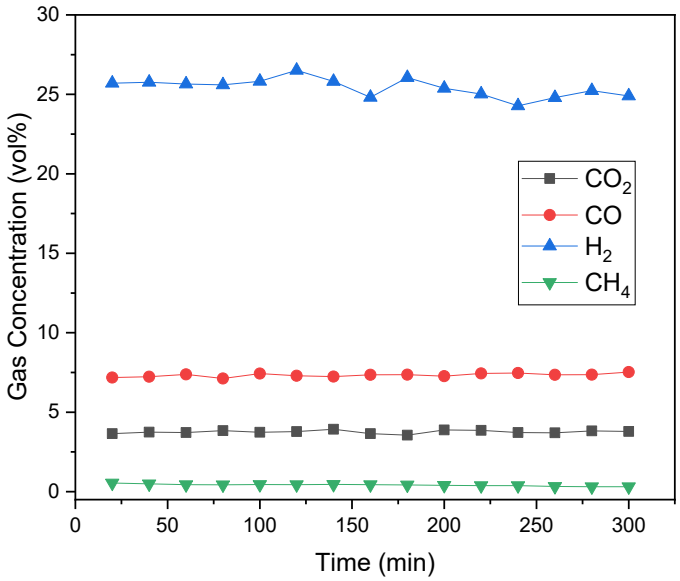

Figure 0.28 Gas concentration data of toluene steam reforming test in 3% CH_4 atmosphere (5-hour test, biomass ash and Ni/Al_2O_3 mixture catalyst bed, 800 °C, S/C ratio 3, GHSV: 91800 h^{-1})

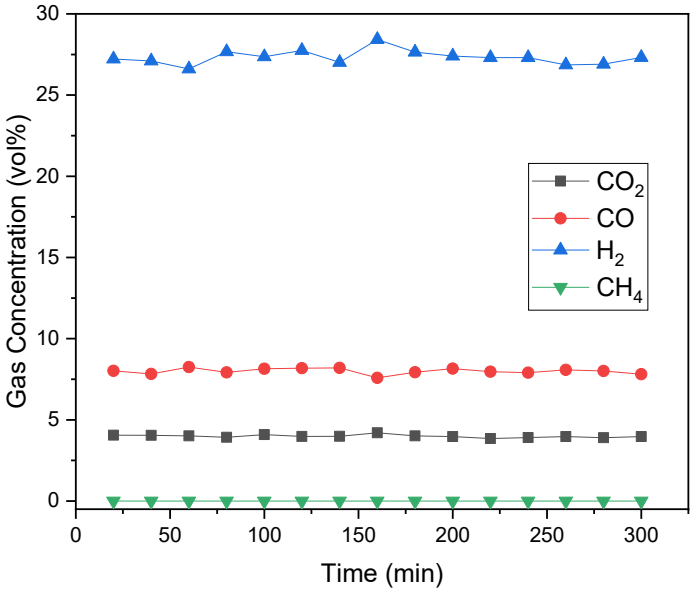

Figure 0.29 Gas concentration data of toluene steam reforming test in 3% CH_4 atmosphere (5-hour test, 2-layer biomass ash and Ni/Al_2O_3 catalyst bed, 800 °C, S/C ratio 3, GHSV: 91800 h^{-1})

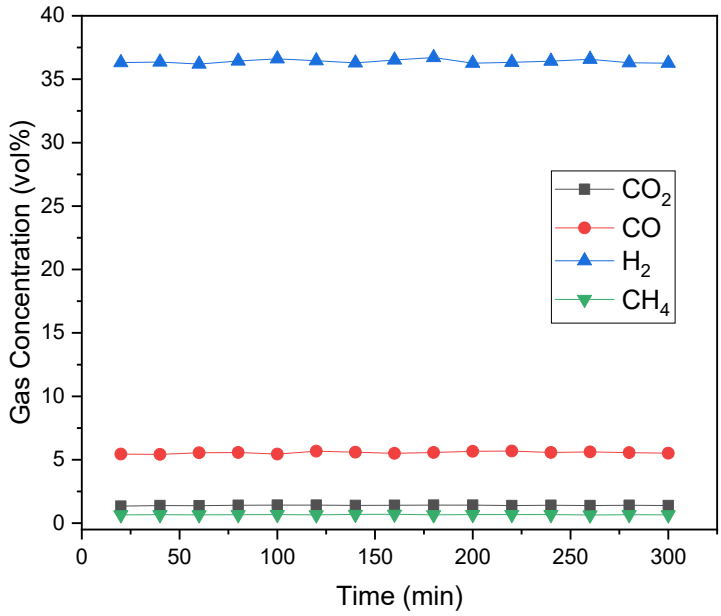

Figure 0.30 Gas concentration data of toluene steam reforming test in 3% CH_4 and 30% H_2 atmosphere (5-hour test, biomass ash catalyst, 800 °C, S/C ratio 3, GHSV: 91800 h^{-1})

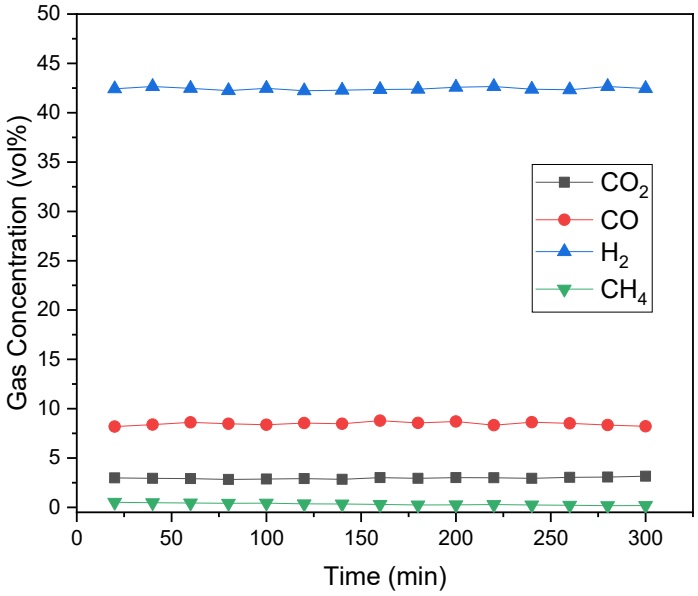

Figure 0.31 Gas concentration data of toluene steam reforming test in 3% CH_4 and 30% H_2 atmosphere (5-hour test, biomass ash and Ni/Al_2O_3 mixture catalyst bed, 800 °C, S/C ratio 3, GHSV: 91800 h^{-1})

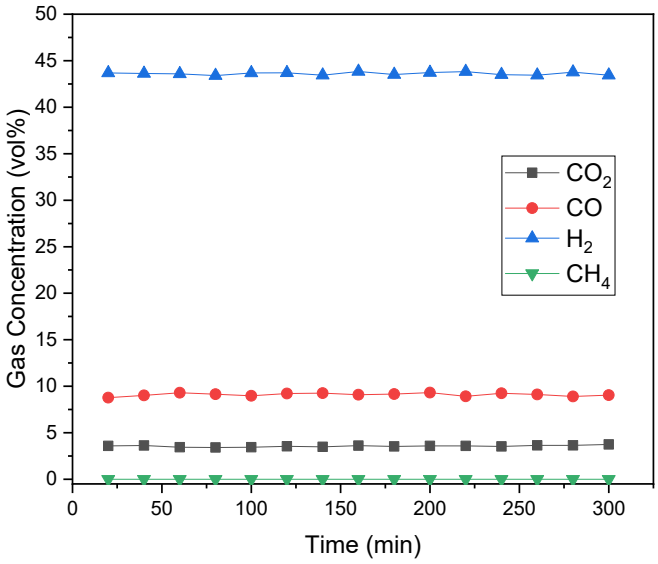

Figure 0.32 Gas concentration data of toluene steam reforming test in 3% CH_4 and 30% H_2 atmosphere (5-hour test, 2-layer biomass ash and Ni/Al_2O_3 catalyst bed, 800 °C, S/C ratio 3, GHSV: 91800 h^{-1})

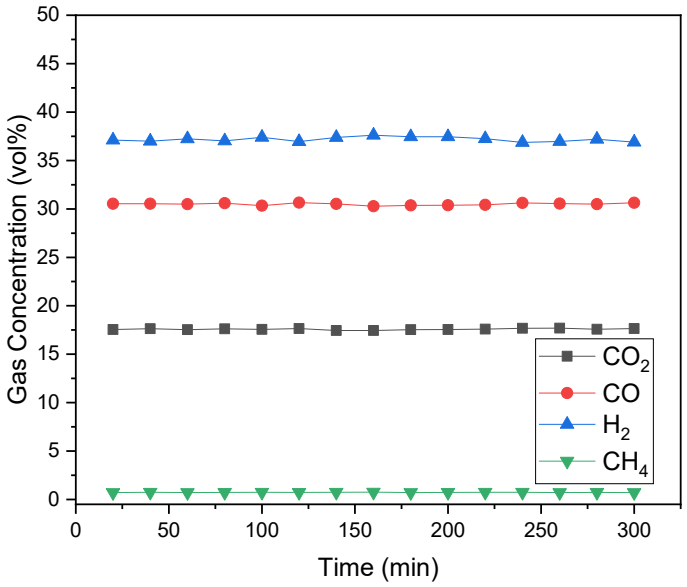

Figure 0.33 Gas concentration data of toluene steam reforming test in 3% CH_4, 30% H_2, 30% CO and 20% CO_2 atmosphere (5-hour test, biomass ash catalyst, 800 °C, S/C ratio 3, GHSV: 91800 h^{-1})

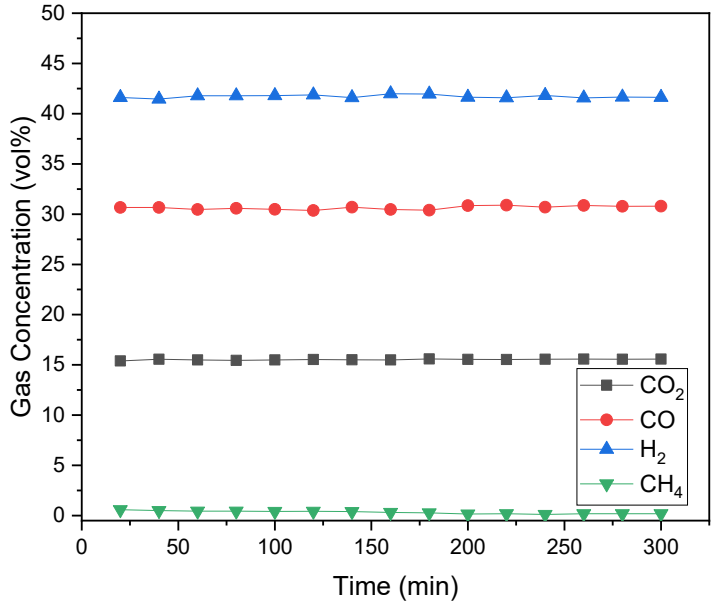

Figure 0.34 Gas concentration data of toluene steam reforming test in 3% CH_4, 30% H_2, 30% CO and 20% CO_2 atmosphere (5-hour test, biomass ash and Ni/Al_2O_3 mixture catalyst bed, 800 °C, S/C ratio 3, GHSV: 91800 h^{-1})

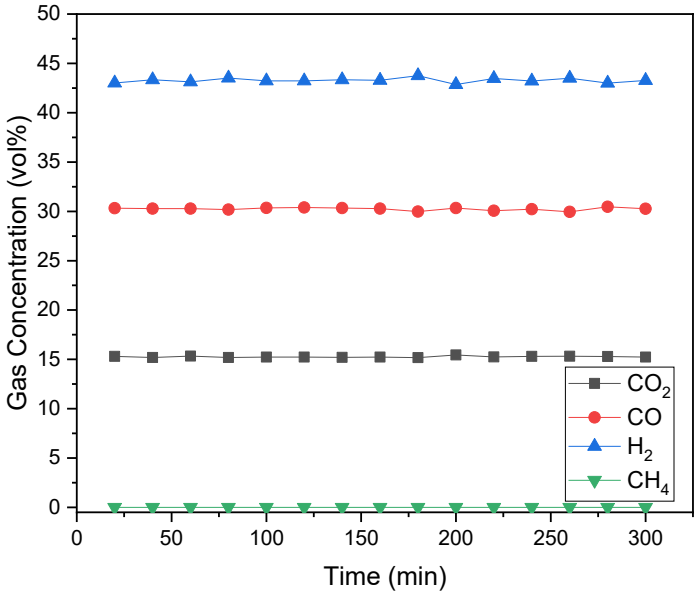

Figure 0.35 Gas concentration data of toluene steam reforming test in 3% CH_4, 30% H_2, 30% CO and 20% CO_2 atmosphere (5-hour test, 2-layer biomass ash and Ni/Al_2O_3 catalyst bed, 800 °C, S/C ratio 3, GHSV: 91800 h^{-1})